MCGILL UNIVERSITY

Inhibition of the Proprotein Convertase Subtilisin/Kexin type 9 (PCSK9) for the treatment of familial hypercholesterolemia

by Elodie Weider

Supervisor: Dr. Nabil G. Seidah

Department of Medicine
Division of Experimental Medicine
McGill University
Montreal, Canada
August 2017

A thesis submitted to McGill University in partial fulfillment of the requirements of the degree of Doctor of Philosophy

Abstract

A significant reduction of the levels of plasma low density lipoprotein cholesterol (LDLc) is highly recommended to decrease the incidence of cardiovascular disease (CVD). This is particularly important for high risk patients, including those suffering from familial hypercholesterolemia (FH). One of the proteins involved in this inherited disorder is the hepatic secreted Proprotein Convertase Subtilisin/Kexin type 9 (PCSK9), which triggers the degradation of the low density lipoprotein receptor (LDLR), thereby increasing LDLc levels. PCSK9 inhibition is now used as a strategy to prevent hypercholesterolemia and consequently CVD. This discovery constituted a major breakthrough since the widely prescribed cholesterol-lowering agents statins. The latter present limitations for patients suffering from adverse events or who do not reach target LDLc levels. The injection of monoclonal antibodies (mAbs) targeting the catalytic domain of PCSK9 prevents PCSK9 binding to the LDLR and reduces LDLc by ~60% in patients. Although these new agents are efficient and safe, they also present limitations.

We proposed the use of single domain antibodies (sdAbs) as an alternative approach to inhibit PCSK9. After a llama immunization with human PCSK9 (hPCSK9), four sdAbs binding the Cys- and His-rich domain (CHRD) of PCSK9 with nanomolar-range affinities were selected and synthesized as fusion proteins with a mouse Fc (mFc). We demonstrated that the latter efficiently blocked PCSK9-mediated LDLR degradation in various cell-based assays, including hepatocarcinoma cell lines, human hepatocytes and mouse primary hepatocytes. As expected, since these sdAb-mFcs do not bind the catalytic domain of PCSK9, they did not affect its binding to the LDLR, but rather block the PCSK9-induced intracellular degradation of the LDLR.

To assess the *in vivo* efficacy of PCSK9 inhibitors, we used a bacterial artificial chromosome to develop mice deficient in mouse PCSK9 and expressing exclusively hPCSK9 under the control of its own promoter. Four transgenic lines expressing 95 to ~5,000 ng/mL hPCSK9 were selected. Whole body *in situ* hybridization revealed that the hPCSK9 expression recapitulated that of endogenous mouse PCSK9 in control WT mice. Compared to transgene negative littermates, the transgenic mice exhibited increased levels of total cholesterol (TC) and decreased levels of hepatic

LDLR levels, in correlation with their hPCSK9 expression levels. We characterized their response to a single injection of the mAb evolocumab. One line expressing physiological levels of hPCSK9 (~370 ng/mL) was then selected for the short-term study of the sdAb P1.40-mFc. Four days post-injection, P1.40-mFc reduced 66% of the TC increase resulting from the expression of hPCSK9 in KO mice and increased liver LDLR levels. A long-term study of another sdAb, PKF8-mFc, and of evolocumab showed 58% and 116% TC decrease, respectively. It also enabled us to show that TC decreased in a reversible way upon injection of each inhibitor and a second injection yielded the same TC decrease.

The work performed during this PhD thesis enabled the establishment of the *in vitro* and *in vivo* proof-of-principle for the use of PCSK9-targeting sdAbs as LDLc-lowering drugs and as tools to elucidate the role of the CHRD in the trafficking of the PCSK9-LDLR complex to lysosomes. Besides, we validated the newly developed humanized transgenic mice as a model to analyze PCSK9 inhibitors, which will facilitate the research for new hPCSK9 inhibitors.

Résumé

Une réduction significative des niveaux plasmatiques du cholestérol lié à la lipoprotéine de basse densité (LDLc) est recommandée dans le but de réduire l'incidence des maladies cardiovasculaires (MCV). Cela est particulièrement important pour les patients à haut risque, dont ceux souffrant d'hypercholestérolémie familiale (HF). Une des protéines impliquée dans cette maladie est la Proprotéine Convertase Subtilisine/Kexine de type 9 (PCSK9) sécrétée par le foie, qui entraîne la dégradation du récepteur à la lipoprotéine de basse densité (LDLR), provoquant une augmentation de LDLc. L'inhibition de PCSK9 est dorénavant utilisée pour prévenir l'hypercholestérolémie et par conséquence les MCV. Cette découverte a constitué une avancée majeure depuis les statines, agents réducteurs de cholestérol largement prescrits. Ces derniers possèdent des limites pour les patients souffrant d'effets secondaires ou ne parvenant pas à atteindre les niveaux cibles de LDLc. L'injection d'anticorps monoclonaux (Acm) ciblant le domaine catalytique de PCSK9 prévient la fixation de PCSK9 au LDLR et réduit le LDLc ~60% chez les patients. Bien que ces nouveaux agents soient efficaces et sécuritaires, ils possèdent également des limites.

Nous avons proposé l'utilisation d'anticorps simple domaine (Acsd) comme alternative pour inhiber PCSK9. Après avoir immunisé un lama avec PCSK9 humaine (PCSK9h), quatre anticorps fixant le domaine riche en Cys et His (DRCH) de PCSK9 avec des affinités de l'ordre du nanomolaire ont été sélectionnés et synthétisés en tant que protéines de fusion avec un Fc murin (Fcm). Nous avons démontré que ces derniers bloquent de manière efficace la dégradation de LDLR médiée par PCSK9 dans divers tests cellulaires, dont des lignées cellulaires d'hépatocarcinome, des hépatocytes humains et des hépatocytes primaires murins. Tel qu'attendu, comme ces Acsd-Fcms ne fixent pas le domaine catalytique de PCSK9, ils n'affectent pas sa fixation au LDLR, mais semblent bloquer la dégradation intracellulaire du LDLR induite par PCSK9.

Pour évaluer l'efficacité *in vivo* des inhibiteurs de PCSK9, nous avons utilisé un chromosome artificiel bactérien pour développer des souris déficientes en PCSK9 murin exprimant exclusivement PCSK9h sous le contrôle de son propre promoteur. Quatre lignées transgéniques

exprimant entre 95 et ~5,000 ng/mL de PCSK9h ont été sélectionnées. L'hybridation *in situ* sur le corps entier a révélé que l'expression de la PCSK9h reproduisait celle de la PCSK9 murine endogène dans les souris WT contrôles. Comparées à leurs souris frères ou sœurs ne possédant pas le transgène, les souris transgéniques ont montré des niveaux de cholestérol total (CT) élevés et des niveaux de LDLR hépatiques diminués, corrélés avec leurs niveaux d'expression de PCSK9h. Nous avons caractérisé leur réponse à une injection unique de l'Acm evolocumab. Une lignée exprimant des niveaux physiologiques de PCSK9h (~370 ng/mL) a ensuite été sélectionnée pour l'étude à court terme de l'Acsd P1.40-Fcm. Quatre jours post-injection, P1.40-Fcm a réduit de 66% l'augmentation de CT résultant de l'expression de PCSK9h dans les souris KO et augmenté les niveaux hépatiques de LDLR. Une étude à long terme d'un autre Acsd, PKF8-Fcm, et d'evolocumab a montré 58% et 116% de diminution de CT, respectivement. Cela nous a également permis de montrer que le CT diminuait de manière réversible après l'injection de chaque inhibiteur, et une seconde injection a provoqué la même diminution de CT.

Le travail effectué lors de cette thèse de doctorat a permis d'établir la preuve de principe *in vitro* et *in vivo* de l'utilisation d'Acsd ciblant PCSK9 en tant que médicaments réducteurs de LDLc et en tant qu'outils pour élucider le rôle du DRCH dans le transport du complexe PCSK9-LDLR aux lysosomes. De plus, nous avons validé de nouvelles souris transgéniques humanisées comme un modèle pour analyser des inhibiteurs de PCSK9 et qui faciliteront la recherche de nouveaux inhibiteurs de PCSK9h.

Acknowledgements

First of all, I would like to thank Dr. Nabil G. Seidah for accepting me in his laboratory. It was really nice to work with such a high-level scientist. Your passion for research is communicative and very encouraging. Thanks Nabil for your guidance, your constant support and everything I learned from you. I feel really lucky that I got the opportunity to work in your stimulating lab. Second, I thank Dr. Annik Prat for being an excellent mentor complementing Nabil's mentoring very well. Thanks Annik for your patience, your help and your advice.

I also would like to thank particularly both research associates Dr. Delia Susan-Resiga and Dr. Rachid Essalmani. Delia, thanks for guiding me in the beginning of my PhD thesis and for entrusting me with the "llama project". You were always supportive and I really appreciated to work with you. Rachid, thanks for accepting me in the "mice project" and for all your help concerning mice work. You were always positive, patient and very helpful and I really liked working with you, even in the small surgery room.

I thank all the Seidah lab members for being excellent colleagues and friends: Josée Hamelin for your constant and extraordinary kindness, support and little attentions including cloning and maple syrup candies among others; Ann Chamberland for your constant enthusiasm and support; Edwige Marcinkiewicz for our (long) discussions and your (very long) time spent cutting my mice liver pieces; Marie-Claude Asselin and Valérie Menier for your exceptional kindness and support in the cell culture room; Dr. Anna Roubtsova Stepanova for your humor, support and advice concerning mice; Brigitte Mary for your secretary work and support; and the former lab member Suzanne Benjannet for your help.

I also address all my friendship and gratitude to all current Masters, PhD or post-doctoral students from the Seidah lab. First of all, Lorelei Durand, whom I wish to graduate soon, for your warm welcoming and our direct friendship and shared passions for zumba, sushis and other foods; Emmanuelle Girard for sharing your bench with me and so much more; Julie Cruanes for your good mood and support; Yahya Ashraf for your advice on antibodies; Stéphanie Duval for your

energy; Vatsal Sachan for your kindness and super powers as Batsal; Ali Ben Djoudi Ouadda for your help and advice; Mahshid Malakootian and Sepideh Mikaeeli for your kindness. I wish you all good luck for your studies, keep it up!
I do not forget very nice former students: Chutikarn Butkinaree (Pui) for your excellent mood, help and advice; Johann Guillemot for your humor and friendship; WooJin Kim for your jokes and support; as well as Grisel Luna, Erin Zekas, Zuhier Awan and Maryssa Canuel.
I also thank all the members of the IRCM "plateaux technologiques", especially Manon Laprise for your huge help in the mice projects and Suzie Riverin for maintaining the mice colonies.

I express my appreciation to all my annual thesis committee members: Dr. Jacques Genest Jr., Dr. David Hipfner, Dr. Marlene Oeffinger, Dr. Robert Day, Dr. Yves Durocher, Dr. Robert S. Kiss and Dr. Marc Prentki. I also thank my thesis examiners and defense committee members Dr. Jennifer Estall, Dr. Valérie Legendre-Guillemin, Dr. Loydie A. Jerome-Majewska and Dr. Christian F. Deschepper.
I also would like to thank all the participants of the Fondation Leducq in which I had the chance to be part of. We met every 6 months and our discussions always brought me excellent advice in order to advance my projects further. I am also very grateful to our collaborators in Belgium, Dr. Serge Muyldermans and Dr. Cécile Vincke. I also thank Elizabeth Douville, Kathryn Skorey and John Clement from Amorchem who supported the project financially and with whom we had many meetings at the beginning of my PhD project.

Finally, I would like to thank my friends from Canada, who always supported me, as well as my friends and my family from France who encouraged me despite the distance. I am especially grateful to one of my best friends who also happens to be my brother, Brice Weider, for his extraordinary humor and support although he did not get to learn what moles are…
I would like to thank particularly my parents, Claudia and Raymond Weider, who supported me throughout my studies. You taught me to be passionate about what I am doing and to do things throughout, and I will never thank you enough for that because this made who I am. I can now confirm that when you do want something, you can do it! Thanks for being here for me in every moments and for your unconditional love. I dedicate this PhD thesis to you two.

To finish, I thank my boyfriend, Florian Mauffrey, for his constant support in the day-to-day life and his love. You always knew how to cheer me up in the tough moments and I am really grateful for that. I could not have dreamt of a better life partner during this intensive period of my PhD studies and I hope that our future adventures will continue to keep us happy.

Table of contents

List of figures

List of tables

List of abbreviations

β-LPH: β-lipotropin

β-MSH: β-melanocyte-stimulating hormone

γ-LPH: γ-lipotropin

^{68}Ga: Gallium 68

^{99m}Tc: Technetium 99m

Aβ: amyloid beta-peptide

aa: amino acids

ABCG5/G8: ATP-binding cassette containing a heterodimer of G5 and G8 subunits

ACAT: acyl coenzyme A cholesterol acyltransferase

ACLY: ATP-citrate lyase

AD: Alzheimer's disease

ADH: autosomal dominant hypercholesterolemia

APLP2: amyloid precursor protein-like protein-2

apoB: apolipoprotein B

apoER2: apolipoprotein E receptor 2

ARH: autosomal recessive hypercholesterolemia

ASO: antisense oligonucleotide

BAC: bacterial artificial chromosome

BACE1: beta-site amyloid precursor protein-cleaving enzyme 1

BNA: bridged nucleic acid

bp: base pairs

BSND: Barttin CLCNK type accessory β-subunit

cDNA: complementary deoxyribonucleic acid

CDR: complementarity-determining region

CE: cholesterol esters

CETP: cholesteryl ester transfer protein

C_H: constant domain of the heavy chain

CHD: coronary heart disease

CHRD: Cys- and His-rich domain

C_L: constant domain of the light chain

CR: chylomicron remnants

CRD: Cys-rich domain

CT: cytosolic tail

CVD: cardiovascular diseases

DNA: deoxyribonucleic acid

ECL: enhanced chemiluminescence kit

EGF-A: epidermal growth factor-like repeat A

EGF-B: epidermal growth factor-like repeat B

EGF-C: epidermal growth factor-like repeat C

EGFP: epidermal growth factor precursor

endoF: endoglycosidase F

endoH: endoglycosidase H

ENaC: amiloride-sensitive epithelial Na^+ channel

ER: endoplasmic reticulum

Fab: antigen-binding fragment

FACS: fluorescence-associated cell sorting

FBS: fetal bovine serum

Fc: fragment, crystallisable

FcγR: Fc-γ-receptor

FcRn: neonatal Fc receptor

FDA: food and drug administration

FFA: free fatty acids

FH: familial hypercholesterolemia

FHS: Framingham Heart Study

GOF: gain-of-function

HAT: hypoxanthine-aminopterin-thymidine

HCD: heavy chain diseases

HCHOLA4: hypercholesterolemia, autosomal dominant 4

HCV: hepatitis C virus

HDL: high density lipoprotein

HDLc: high density lipoprotein-cholesterol

HeFH: heterozygous FH

HER2: human epidermal growth factor receptor 2

HGMCR: HMG-CoA reductase

HGPRT: hypoxanthine-guanine-phosphoribosyltransferase

HL: hepatic lipase

HMG-CoA: 3-hydroxy-3-methylglutaryl-CoA

HNF1α: hepatocyte nuclear factor-1α

HoFH: homozygous FH

hPCSK9: human PCSK9

hpf: hours post-fertilization

HSA: human serum albumin

IDL: intermediate density lipoprotein

IDOL: inducible degrader of the LDLR

Ig: immunoglobulin

IgNAR: Ig new antigen receptor

ISH: *in situ* hybridization

KO: knockout

LA: LDLR type A

LCAT: lecithin cholesterol acyltransferase

LDL: low density lipoprotein

LDLc: low density lipoprotein-cholesterol

LDLR: low density lipoprotein receptor

LNA: locked nucleic acid

LNO: lipidoid nanoparticle

LOF: loss-of-function

Lp(a): lipoprotein a

LPL: lipoprotein lipase

LRP: LDLR-related proteins

LRP1: LDLR-related protein 1

LPS: lipopolysaccharide

LXR: liver X receptor

miRNAs: microRNAs

mFc: mouse Fc domain

mLDLR: mouse LDLR

mPCSK9: mouse PCSK9

MTP: microsomal triglyceride transfer protein

NARC-1: neural apoptosis-regulated convertase 1

NPC1: Niemann-Pick type C protein 1

NPC2: Niemann-Pick type C protein 2

NPC1L1: Niemann-Pick disease type C1-like 1

PBS: phosphate-buffered saline

PC: proprotein convertase

PCR : polymerase chain reaction

PCSK9: proprotein convertase subtilisin/kexin type 9

PEG: polyethylene glycol

PHx: partial hepatectomy

POMC: pro-opiomelanocortin

PP: isopentenyl-5-pyrophosphate

PPAR: proliferator-activated receptors

PTM: post-translational modifications

QPCR: quantitative real-time polymerase chain reaction

RES: reticuloendothelial system

RIPA: RadioImmunoPrecipitation Assay

RNAi: RNA interference

RT: room temperature

S1P: site-1-protease

SCAP: SREBP cleavage-activating protein

scFv: single chain variable fragment

SDS: sodium dodecyl sulfate

SDS-PAGE: SDS polyacrylamide gel electrophoresis

SEM: standard error to the mean

siRNA: small interfering RNA

SKI-1: subtilisin kexin isoenzyme-1

SNP: single nucleotide polymorphism

SPECT: single-photon emission computed tomography

SR-B1: scavenger receptor class B type 1

SRE: sterol responsive elements

SREBPs: sterol regulatory element binding proteins

STAP1: signal transducing adaptor family member 1

T1D: type 1 diabetes

T2D: type 2 diabetes

TC: total cholesterol

Tg: transgene

TG: triglycerides

TGN: trans-Golgi network

TICE: transintestinal cholesterol excretion

TMEM61: transmembrane protein 61

USP24: ubiquitin carboxyl-terminal hydrolase 24

V_H: variable domain of the heavy chain

V_L: variable domain of the light chain

VLDL: very low density lipoprotein

VLDLc: very low density lipoprotein-cholesterol

WB: Western Blot

WHO: World Health Organization

WT: wild type

Preface

This PhD thesis is presented in accordance with the manuscript-based thesis guidelines. The thesis consists of an introductory literature review (Chapter I), two research articles including a published article (Chapter II) and an article that is in review (Chapter III), as well as discussion and perspectives (Chapter IV). Each article chapter contains sections covering preface, abstract, introduction, methodology, results, discussion, additional information (including the contributions of myself and of the co-authors which are also described in the next section), as well as a chapter discussion.

The work related in this PhD thesis contributed to gain knowledge in single domain antibodies by describing a new application of this relatively new technology, namely single domain antibodies targeting the human proprotein convertase subtilisin/kexin type 9 (PCSK9) for the study and treatment of cardiovascular diseases. It also provided a new tool for the research of PCSK9 inhibitors by outlining an innovative mouse model expressing exclusively human PCSK9. This mouse model was shown to be very advantageous in the analysis of the pharmacological effects of PCSK9 inhibitors.

List of publications:

- Manuscript 1 “Proprotein Convertase Subtilisin/Kexin type 9 (PCSK9) single domain antibodies are potent inhibitors of LDL receptor degradation” was published in 2016 in The Journal of Biological Chemistry (1).
- Manuscript 2 “Human PCSK9 transgenic mice for PCSK9 inhibitors screening” is in the process for submission in The Journal of Biological Chemistry.

Contribution of authors

Unless otherwise stated below (see sections II.7.4. and III.7.4.), I performed experiments, designed and coordinated the experiments not directly conducted by myself, performed analysis of results and wrote the manuscripts that constitute this thesis with guidance from my supervisor Dr. Nabil G Seidah, and Dr. Annik Prat.

Chapter II is reproduced from my manuscript published in The Journal of Biological Chemistry in which I am first author.

Chapter III is reproduced from my manuscript which will be submitted to The Journal of Biological Chemistry in which I am co-first author with my colleague Dr. Rachid Essalmani who designed and generated the human PCSK9 mouse model.

I. Chapter I: Introduction: literature review

The main subject of this PhD thesis was to study the inhibition of the function of the proprotein convertase subtilisin/kexin type 9 using single domain antibodies *in vitro* and *in vivo*, as a new therapeutic approach for the treatment of familial hypercholesterolemia.

First, biological and clinical aspects of familial hypercholesterolemia will be described.

Second, the proprotein convertase subtilisin/kexin type 9 will be presented in order to understand its role in familial hypercholesterolemia. In this part, emphasis will be put on the importance of animal models.

In a third part, the therapeutic approaches currently used to treat familial hypercholesterolemia and reduce cardiovascular diseases will be detailed.

Finally, antibodies will be presented to introduce single domain antibodies and their differences compared to monoclonal antibodies in order to bring up our working hypothesis.

I.1 Familial hypercholesterolemia and cardiovascular diseases

Cardiovascular diseases (CVD) are a group of disorders of the heart and blood vessels including coronary heart disease (CHD), cerebrovascular disease, peripheral arterial disease, rheumatic heart disease, congenital heart disease, deep vein thrombosis and pulmonary embolism.

According to the World Health Organization (WHO), CVD are the first cause of death worldwide. In 2012, deaths from CVD represented 31% of all global deaths, namely affecting 17.5 million people. From these deaths, an estimated 7.4 million were due to CHD and 6.7 million were due to stroke. The causes of heart attacks and strokes are multifactorial and include tobacco, unhealthy diet, obesity, physical inactivity, chronic alcohol use, hypertension, diabetes and hyperlipidemia.

Hypercholesterolemia is a form of dyslipidemia characterized by an excess of plasma low density lipoprotein-cholesterol (LDLc) levels that can lead to CVD.

I.1.1 Cholesterol

To understand why excess LDLc is harmful and why it should be controlled, it is important to grasp how cholesterol, a major lipid component of low density lipoprotein (LDL), is synthesized, regulated and distributed in the human body. Cholesterol is a very important molecule for all animal life and has been studied for over one century by many chemists and biologists. It is one of the main components of cell membranes, maintaining their motility and fluidity, and regulating their functions. Cholesterol is also a metabolic precursor for bile acids, vitamin D and all steroid hormones (2, 3).

I.1.1.1 Chemical structure of cholesterol

The structure of cholesterol was resolved by Heinrich Wieland and Adolf Windaus, awarded the Nobel Prize in Chemistry in 1928 for that discovery. Cholesterol is a lipid belonging to the sterols family. It is composed of four linked hydrocarbon rings that form a bulky steroid structure as indicated in Figure 1. One end of the steroid is composed of an aliphatic tail, whereas there is a hydroxyl group at the other end, classifying cholesterol as an amphipathic molecule.

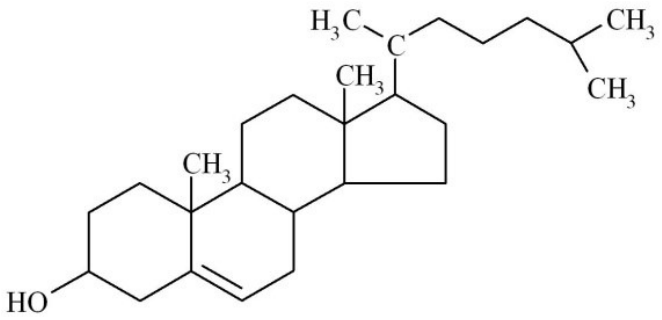

Figure 1. Chemical structure of cholesterol

I.1.1.2 Cholesterol de novo biosynthesis (endogenous cholesterol supply)

For their studies establishing the biosynthetic pathway of cholesterol, Konrad Bloch and Feodor Lynen received the Nobel Prize in Physiology and Medicine in 1964. This complex pathway implicates more than 40 enzymes and is regulated by a feedback of its end products: cholesterol and its oxidized forms named oxysterols. As indicated in Figure 2, cholesterol is synthesized from

acetyl-CoA that is condensed to 3-hydroxy-3-methylglutaryl-CoA (HMG-CoA) by HMG-CoA synthase. HMG-CoA reductase (HGMCR) then reduces HMG-CoA to mevalonate. This constitutes the rate-limiting step in cholesterol biosynthesis that is targeted by the HMGCR inhibitors cholesterol-lowering drugs known as “statins”, which will be detailed in part I.3.1.8. Mevalonate is then phosphorylated and decarboxylated to form isopentenyl-5-pyrophosphate (PP) (4). Condensation of 6 PPs results in squalene, which gives lanosterol after cyclization. Several oxidation, reduction and demethylation reactions finally occur to convert lanosterol into cholesterol.

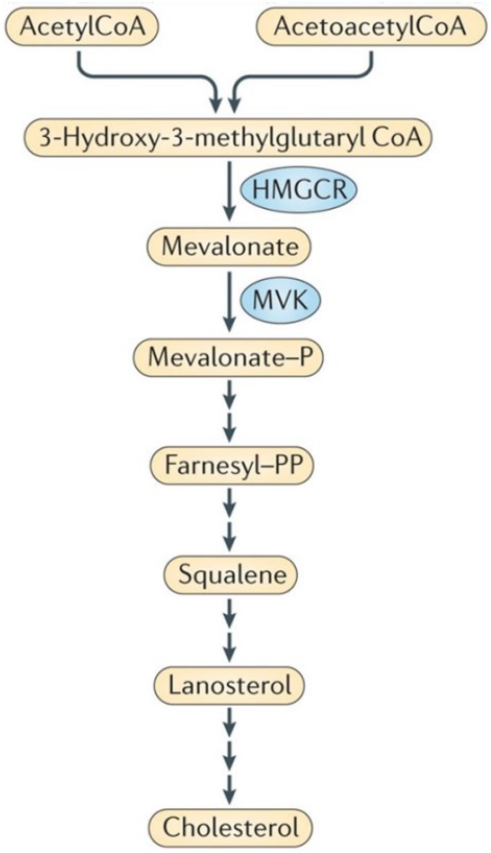

Figure 2. Cholesterol biosynthesis pathway adapted from (5)

This cholesterol *de novo* synthesis is found in all cells, but its bulk synthesis mostly takes place in the liver, intestine and adrenal glands. Humans synthesize ~900 mg cholesterol per day and it is estimated that the human body contains ~35g of cholesterol, which is mainly located in the cell membranes. The *de novo* synthesized cholesterol constitutes ~70% of total body cholesterol (6). Cholesterol can be esterified by acyl coenzyme A cholesterol acyltransferase (ACAT) in the endoplasmic reticulum (ER) and by lecithin cholesterol acyltransferase (LCAT) in plasma, allowing cholesterol esters (CE) to be transported throughout the circulation via specialized transport molecules called lipoproteins that will be detailed in the next section.

I.1.1.3 Regulation of cholesterol biosynthesis

Early animal experiments showed that a cholesterol-rich diet led to severe atherosclerosis (7). It was also demonstrated that human atherosclerotic plaque was loaded with cholesterol and fatty acids. Thus, cholesterol homeostasis is very important to maintain a healthy body. Michael Brown and Joseph Goldstein detailed the mechanistic feedback regulation implicated in cholesterol metabolism and were awarded the Nobel Prize in Physiology and Medicine in 1985. A large amount of genes participate in cholesterol metabolism and biosynthesis. Cholesterol contents directly regulate the transcription of these genes. The most important transcription factor genes involved in the regulation of cholesterol homeostasis are the ones encoding the sterol regulatory element binding proteins (SREBPs) (8). Those include two genes SREBP-1 (isoforms: SREBP-1a, SREBP-1c) and SREBP-2 (9, 10). The two transmembrane-containing SREBPs are first synthesized as inactive forms and then inserted in the ER membrane in a hairpin-like fashion. They subsequently form a complex with the SREBP cleavage-activating protein (SCAP), which contains a sterol sensing domain (11). SCAP acts differently depending on the cellular sterol concentrations: when cholesterol levels are high, SCAP maintains SREBPs in the ER membranes preventing its exit from the ER (12, 13). When sterol concentrations are low, SCAP escorts SREBPs to the cis/medial Golgi where their luminal segment is cleaved consecutively by the serine protease SKI-1/S1P and then by the metalloprotease site-2-protease (S2P), thereby releasing into the cytosol their N-terminal domain, which is then translocated into the nucleus as indicated in Figure 3 (14-17). This nuclear SREBP (nSREBP) then binds to sterol responsive elements (SRE) in the promoter/enhancer regions of target genes, thereby enhancing their transcription. As an

example, nSREBP-2 binds and activates SREs needed for the synthesis of 30 mRNAs, including those coding for HMGCR, low density lipoprotein receptor (LDLR) and proprotein convertase subtilisin/kexin type 9 (PCSK9) (8). Note that LDLR and PCSK9, that are two major actors of cholesterol metabolism, will be detailed in further sections.

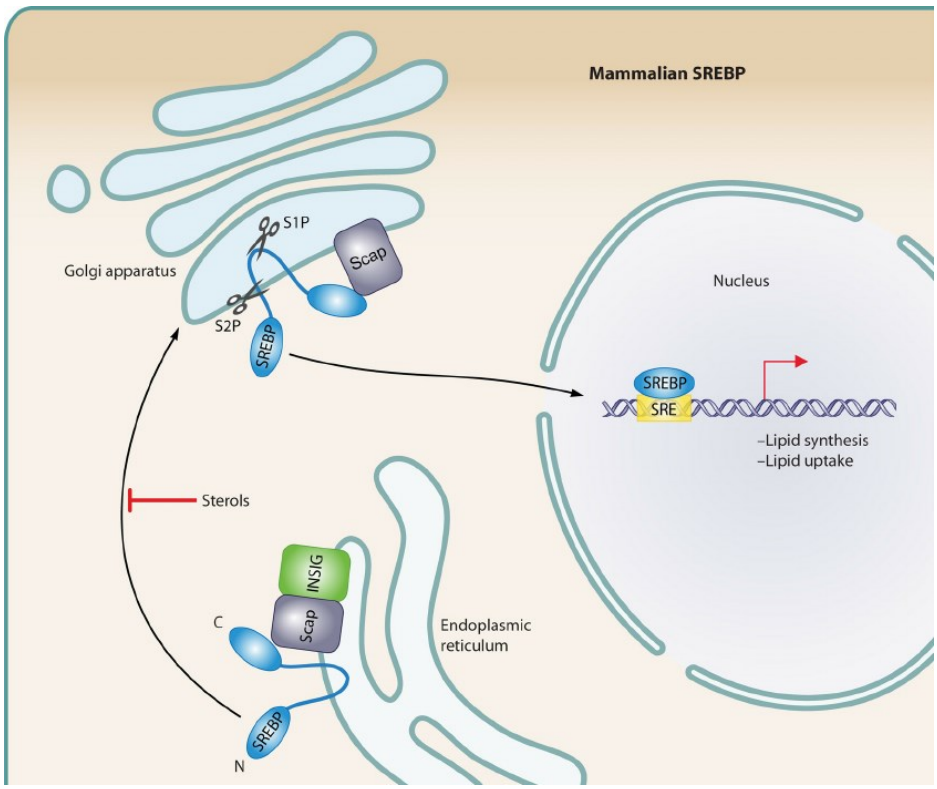

Figure 3. Illustration of the mammalian SREBP pathway (18)

I.1.1.4 Dietary cholesterol (exogenous cholesterol supply) and its absorption

As stated previously, 70% of the total cholesterol (TC) contained in our body originates from *de novo* synthesis. The remaining ~30% comes from the diet. Human dietary cholesterol intake is ~400 mg per day which is rapidly esterified and therefore poorly absorbed (~50%). Each day ~650 mg cholesterol are eliminated by the gastro-intestinal tract and by skin and ~450 mg are converted to bile acids and steroid hormones, which will be secreted in bile and urine (6).

Cells internalize exogenous cholesterol from circulating lipoproteins via the LDLR (see section I.1.2.3).

I.1.2 Lipoproteins

Since cholesterol and triglycerides (TG), esters derived from one glycerol and three fatty acids are not soluble in water, they need to be transported by specific proteins called lipoproteins.

I.1.2.1 Lipoproteins classification and composition

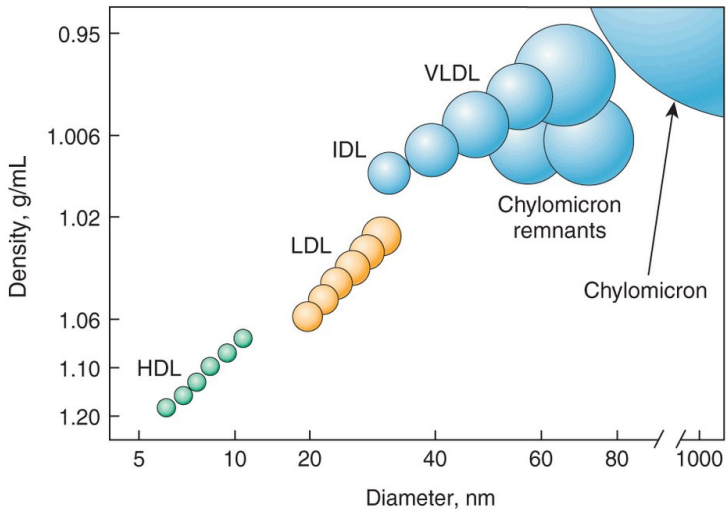

Figure 4. Density and size distribution of the major classes of lipoproteins (https://thoracickey.com/disorders-of-lipoprotein-metabolism/)

All lipoproteins contain a central core of TG and CE surrounded by free cholesterol, phospholipids and apolipoproteins (19). The seven types of lipoproteins are classified according to their increasing density as shown on Figure 4: chylomicrons, chylomicron remnants (CR), very low density lipoprotein (VLDL), intermediate density lipoprotein (IDL), low density lipoprotein (LDL), high density lipoprotein (HDL) and lipoprotein a (Lp(a), not shown on Figure 4). Except for HDL, high plasma concentrations of all other lipoproteins lead to atherosclerosis.

Each lipoprotein contains a specific set of apolipoproteins that constitute the protein building blocks of lipoproteins. Apolipoproteins, like phospholipids, can surround lipids because they are amphipathic. They are thus able to create water-soluble lipoproteins that can be transported in

water-based circulation such as blood or lymph. Apolipoproteins are also important because they allow lipoproteins to be recognized by specific receptors at different sites in the body. For example, apoB-100 enables LDL to bind LDLR, as will be detailed later. Apolipoproteins can also serve as enzyme cofactors and lipid transfer carriers, thus playing a major role in lipoproteins and lipids metabolism and their uptake by various tissues. For example, apoA-IV is involved in intestinal lipid absorption and exerts an anorectic action in the hypothalamus (20).

	ApoLIPOPROTEINS	
LIPOPROTEIN	**MAJOR**	**OTHER**
Chylomicrons	ApoB-48	A-I, A-IV, C-I, C-II, C-III, E
Chylomicron remnants	ApoB-48	A-I, A-IV, C-I, C-II, C-III, E
VLDL	ApoB-100	A-I, A-II, A-V, C-I, C-II, C-III, E
IDL	ApoB-100	C-I, C-II, C-III, E
LDL	ApoB-100	
HDL	ApoA-I	A-II, A-IV, A-V, C-III, E
Lp(a)	ApoB-100	Apo(a)

Table 1. Lipoproteins composition (https://thoracickey.com/disorders-of-lipoprotein-metabolism/)

The density, size and composition of each lipoprotein (21) are detailed in Table 1. Briefly:

- Chylomicrons contain mostly TG and many apolipoproteins
- CR contain TG and cholesterol and only apoB-48 and apoE
- VLDL contain mostly TG and apoB-100, apoE and apoC
- IDL contain apoB and both TG and cholesterol
- LDL contains mostly cholesterol and apoB-100
- HDL contains cholesterol and apo A-I, A-II, apoC and apoE
- Lp(a) is composed of an LDL and an apo(a) glycoprotein which is attached by a disulfide bond to the apoB-100 of the LDL. Apo(a) contains multiple copies of the plasminogen-like kringle IV domain, which can vary between 3 to >40, resulting in a size heterogeneity in the general population.

I.1.2.2 Lipoproteins metabolism: exogenous and endogenous pathways

A general scheme illustrating lipoproteins metabolism is presented in Figure 5.

The exogenous lipoprotein pathway takes place in the intestine where dietary lipids are taken up by specific receptors at the surface of enterocytes (22). The transmembrane protein Niemann-Pick disease type C1-like 1 (NPC1L1) transports cholesterol and plant sterols from the brush border enterocytes (intestinal lumen) into the enterocytes (23). The ATP-binding cassette containing a heterodimer of G5 and G8 subunits (ABCG5/G8) is also expressed at the enterocytes surface and transports cholesterol in the opposite direction when there is excess cholesterol (24). Inside the enterocytes, CE can be incorporated to chylomicrons and the microsomal triglyceride transfer protein (MTP) transfers TG to chylomicrons. Chylomicrons will then be metabolized by lipoprotein lipase (LPL), generating free fatty acids (FFA) that can cross the enterocytes membranes directly or be transported by proteins such as FATP4 or FAT/CD36, constituting energy for peripheral tissues. CR are then formed, which are hydrolyzed by hepatic lipase (HL) and taken up into liver by LDLR and LDLR-related protein 1 (LRP1).

The endogenous pathway is implicated in lipoproteins formation, distribution and homeostasis and mostly takes place in liver hepatocytes (6). First, sterols absorbed by the intestine or by the liver serve as building blocks of nascent HDL using apoA-I and ABCA1 to get into the circulation. Second, MTP transfers liver TG and CE to nascent apoB-100 and apoE in the hepatocytes ER in order to form VLDL. The amount of available TG determines if newly synthesized apoB-100 are secreted or degraded. If there is not a big amount of TG, apoB-100 will be rapidly degraded after its secretion. Thus, mutations in apoB-100 or MTP lead to an inability to produce VLDL, resulting in low plasma TG and cholesterol (familial hypobetalipoproteinemia or abetalipoproteinemia). VLDLs are then transported to muscle and adipose tissue, where their TG are metabolized by LPL, resulting in FFA release. This VLDL clearance mechanism can be inhibited by high levels of chylomicrons. When TG is removed from VLDL, this gives raise to VLDL remnants (IDL) that acquire apoE from HDL. About half of these IDL are removed from circulation by the binding to hepatic LDLR and LRP1 via their apoE. The other half of IDL will be further hydrolyzed by HL, leading to the formation of LDL. LDL particles are an important source of cholesterol for peripheral tissues.

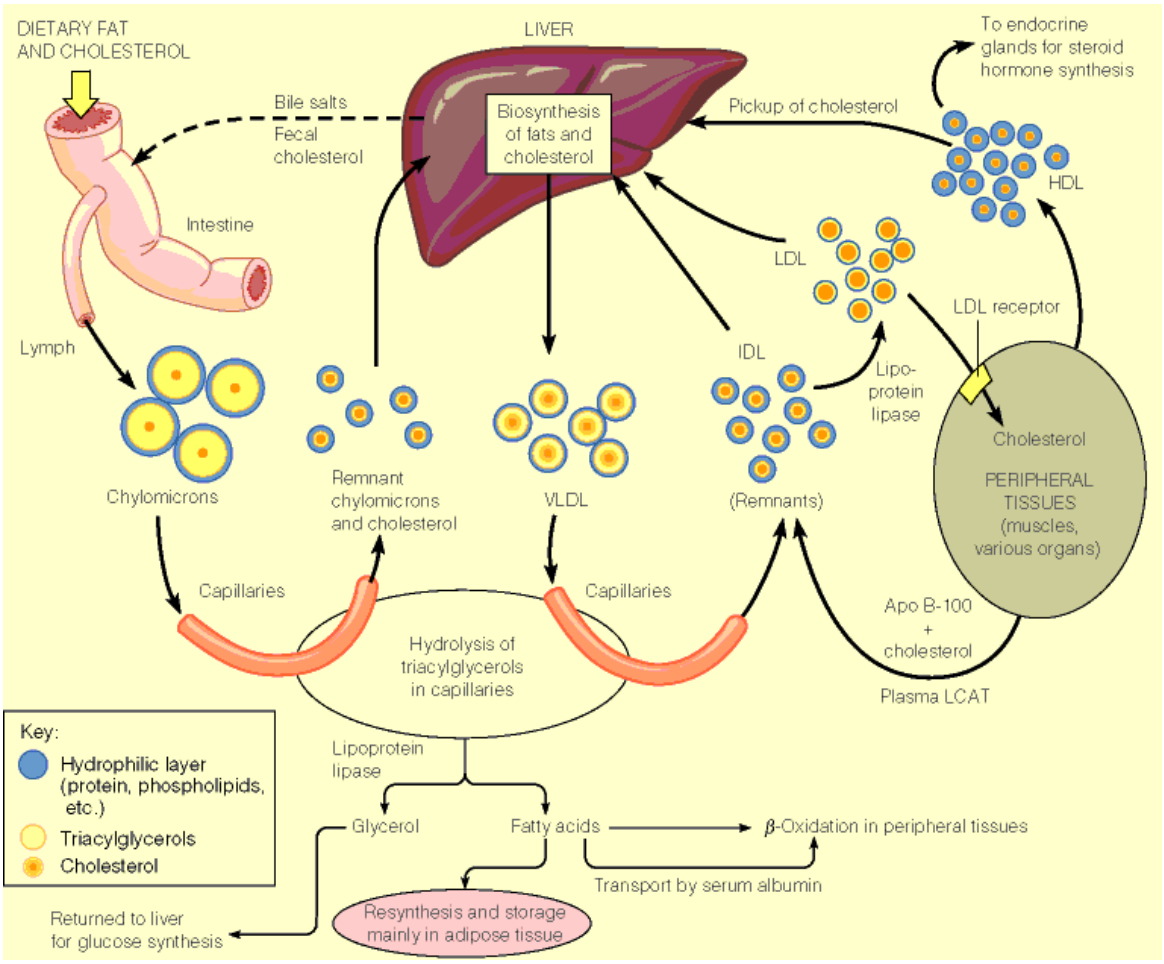

Figure 5. Illustration of lipoproteins metabolism (http://www.apsubiology.org/anatomy/2020/2020_Exam_Reviews/Exam_4/CH24_Lipid_Metabolism.htm)

I.1.2.3 The importance of the LDLR and its regulation

The LDLR is responsible for LDL uptake in many tissues, the most important one being the liver in which 70% of LDL is cleared (25, 26).

The LDL particles bind the LDLR via their unique apoB-100 and the complex LDLR-LDL gets inside of the cells by clathrin-mediated endocytosis. In late endosomes or lysosomes, the low pH triggers a dissociation of the complex (27). The LDLR is then recycled back at the cell surface, while the LDL is directed to lysosomal degradation (25). Lysosomal enzymes then degrade apoB into amino acids (28), while CE are hydrolyzed by acid lysosomal lipase (29). The subsequent release of free cholesterol can either be used by cells directly or be re-esterified by ACAT in order

to be stored (30). Free cholesterol is then linked to Niemann-Pick type C proteins 1 and 2 (NPC1 and NPC2), two proteins implicated in Niemann-Pick disease, a lethal disease in which LDL-derived cholesterol efflux is not functional (31). Briefly, cholesterol first binds NPC2 and then NPC1 (32). Subsequently, cholesterol redistribution from lysosomes is triggered by NPC1 to different cellular compartments such as membranes, mitochondria and ER (33).

Note that the levels of hepatic LDLR as well as lysosomal NPC1 and NPC2 are regulated by cells cholesterol contents and by SREBPs, similar to the regulation of HMGCR. Besides, oxidized sterols activate the nuclear hormone receptor liver X receptor (LXR) that is a transcription factor mediating the transcription of the inducible degrader of the LDLR (IDOL), leading to the ubiquitination and degradation of LDLR. Depending on the levels of cholesterol sensed by the cells, they can regulate both cholesterol synthesis and LDLR activity to maintain appropriate cholesterol contents. Accordingly, if the cell needs cholesterol, LDLR activity will be enhanced in order to increase the cholesterol uptake and vice versa.

I.1.2.4 Reverse cholesterol transport

Since most cells cannot catabolize cholesterol, there is a need for a mechanism enabling them to eliminate excess cholesterol, which is done by reverse cholesterol transport. This process is very important in atherosclerosis prevention because it enables macrophages to efflux their cholesterol. Small nascent HDL formed in hepatocytes and enterocytes trigger the reverse cholesterol transport. They get cholesterol and phospholipids that are effluxed from cells, which results in mature HDL formation. Once in circulation, mature HDL can then be lipidated and acquire more cholesterol from cells via binding of their apoA-1 to ABCA1/G1 (34). LCAT then esterifies the cholesterol in HDL, which is an important step in HDL maturation. The cholesterol from HDL is then transported to the liver, where it is either directly degraded via the scavenger receptor class B type 1 (SR-B1) or indirectly degraded after transfer to VLDL or LDL by cholesteryl ester transfer protein (CETP). Inhibition of CETP activity leads to higher cholesterol efflux by HDL, resulting in an increase in HDL-cholesterol (HDLc) and a decrease in LDL LDLc.

I.1.2.5 Lipoproteins, cholesterol and atherosclerosis formation

The LDL particles carrying cholesterol can be oxidized and taken up by macrophages, which become engorged and form foam cells, contributing to the atherosclerotic plaque formation. In presence of high LDLc levels, an excess of cholesterol can be deposited on the artery wall. HDL has the opposite function and triggers the transport of cholesterol away from the artery wall. Therefore, patients having high levels of LDLc and low levels of HDLc have a high risk of developing atherosclerosis, which is a chronic inflammation disease of the artery wall (35).

I.1.3 The importance of lipid homeostasis and epidemiological studies

By the 1940s, death due to CVD was already important in America, responsible for about half of the deaths. At that time, very little was known about prevention and risk factors for CVD. Following premature death of the American President Franklin D. Roosevelt due to his poor cardiovascular health (hypertension and stroke) in 1945, a need for epidemiological studies identifying risk factors and biomarkers of CVD was encouraged. Accordingly, the Framingham Heart Study (FHS) study was created in 1948. A presumably healthy population of 5,209 men and women aged 30 to 62 years old, inhabitants from the city of Framingham, Massachusetts, USA, was analyzed and followed on long-term in order to determine factors leading to CVD development (36, 37). Today, the FHS is still collecting data on the third generation of the initial cohort, namely their grandchildren. Importantly, the FHS enabled the discovery of the main risk factors leading to CVD: high blood pressure, high cholesterol levels, smoking, obesity, diabetes, and physical inactivity. More recently identified biomarkers for CVD are homocysteine (38), chronic kidney disease (39), high-sensitivity C-reactive protein (40) and air pollution (41, 42).

Thereafter, other studies have shown that lowering LDLc reduces CVD risk (43). However, it has to be noted that a lipid paradox is sometimes observed, in which the direct correlation between LDLc levels or saturated fat consumption and death by CVD is lost or even inverse: this is the case of patients recovering from an acute myocardial infection (44), elderly patients (45), and some European countries such as France (46).

Maintaining adequate levels of all atherogenic lipoproteins by controlling their synthesis and uptake, as well as by absorbing adequate levels of dietary fats is crucial to maintain a healthy

functional body. Evidences for this are genetic disorders in which lipoproteins levels are unbalanced. The major disorder observed is dyslipidemia, which can be either hyper- or hypolipidemia. Frequently, hyperlipidemia is observed in people who have no genetic disorder but lack a healthy way of life because of unhealthy diet and physical inactivity. Therefore, their symptoms can be treated by a lifestyle modification. However, for patients suffering from a genetic disorder, although the same lifestyle modifications need to be applied, there is a need for therapeutic approaches in order to help them treat their symptoms and decrease their CVD risk.

I.1.4 Familial hypercholesterolemia clinical aspects

The first reports relating a hereditary disease giving rise to CVD appeared in 1938. Norwegian physicians observed that patients who presented multiple xantonomas or xantehelesmas often presented CVD (either early death due to heart failure or later death following angina pectoris) and that those clinical characteristics seemed to be hereditary (47). Initially named lipidose or xanthomatosis, this genetic disorder was first named familial hypercholesterolemia (FH) in 1948 after a study of 159 patients with high or normal cholesterol levels (48).

In the general populations, 1 in 20 people suffer from monogenic or multifactorial hypercholesterolemia. Although some apoE isoforms have been linked to multifactorial forms of hypercholesterolemia (49), the genes associated with FH are the only ones that have been identified so far for being responsible for hypercholesterolemia. FH can be inherited in an autosomal recessive way (autosomal recessive hypercholesterolemia; ARH) or in an autosomal dominant way (autosomal dominant hypercholesterolemia; ADH). ARH (OMIM#603813) is a very rare disease worldwide, except on Sardinia Island in Italy because of a founder effect due to geographical isolation (50). It is caused by mutations in the adaptor protein called ARH which interacts with LDLR, clathrin and AP2 adaptor complex and leads to a defect in LDLR hepatic internalization (51). In contrast, ADH (OMIM#143890) is the most common autosomal dominant disorder in man and is thus usually referred to as FH. Homozygous FH patients (HoFH) present the most severe clinical symptoms and are present in 1 in 1,000,000. Heterozygous FH (HeFH) is a common disorder with frequencies of 1:500 to 1:200 in the general population. Some regions characterized by a founder effect present much higher frequencies up to 1:217 such as in Denmark (52), in Ashkenazi Jew populations (53), in Lebanon (54) and in French Canada (55).

The major clinical characteristic of FH patients is an extreme hypercholesterolemia defined by levels of circulating LDLc >5 mM or ~190 mg/dL in adults and >3.4 or ~130 mg/dL in children (56, 57). FH patients also present a history and/or family history of premature (<50 years old) CVD such as peripheral vascular disease, angina pectoris or myocardial infarction. They also present xanthomas that are physical evidences of cholesterol accumulation located around the eyelids (xanthelasmas, Figure 6A) (58) or the tendons of the elbows, hands, knees and feet, notably the Achilles tendon (xanthomas, Figure 6B) (59). Only HoFH present interdigital xanthomas (Figure 6C). The presence of corneal arcus, that are white, blue or grey opaque rings in the corneal margin (Figure 6A) is a FH diagnostic only in patients <45 years old since they are commonly developed in aging healthy subjects (57). All these types of xanthomas were initially observed in ~40% FH patients but this frequency is estimated to be lower nowadays with the use of cholesterol-lowering treatments such as statins that reduce their incidence as well as the size of existing xanthomas (60).

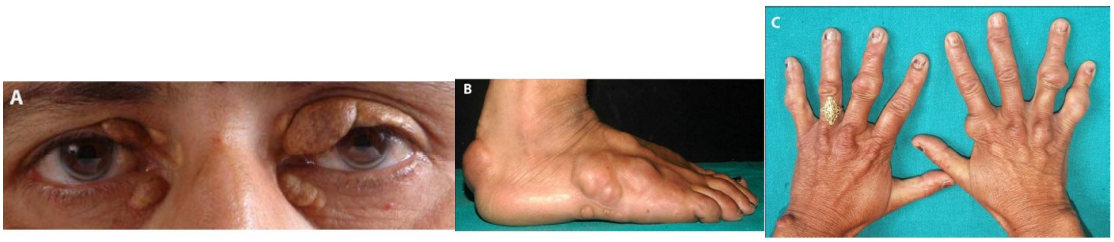

Figure 6. Physical evidences of cholesterol accumulation. Xanthelasma and corneal arcus (*A*), tendon xanthomas of the Achilles tendons and extensor tendons of feet (*B*), tendon xanthomas of the extensor tendons of hands (*C*)

Most FH patients harbor mutations in the genes encoding the LDLR (FH1; ~67%) or APOB (FH2; ~14%) that hamper LDL binding to its receptor or internalization of the lipoprotein, leading to LDL accumulation in the plasma (61). FH patients thus suffer from 3.5- to 16- fold higher CVD risk than non-FH patients (62). More recently, the gene encoding the PCSK9 (63) was identified as a third locus of FH (*PCSK9*; FH3; ~2%) (64). Note that some FH patients do not have mutations in *LDLR*, *APOB* or *PCSK9* genes (~17%). Their mutations are thus located in so far unknown genes. However, mutations were identified in *APOE* (65-67), in the signal transducing adaptor family member 1 (*STAP1*) encoding signal transducing adaptor family member 1 (68, 69) and in hypercholesterolemia, autosomal dominant 4 (*HCHOLA4*) (70).

I.1.5 Role of LDLR and its mutations

I.1.5.1 The discovery of the LDLR

In 1973, Joseph Goldstein and Michael Brown investigated the molecular basis of FH and observed that skin fibroblasts from HoFH patients presented higher HMGCR activity compared to control non-FH patients (71). Three years later, the LDLR was discovered as well as its control of cellular cholesterol contents (25). Importantly, the discovery of the LDLR also brought the fundamental concept of receptor-mediated endocytosis. The same year, LDLR were shown to be located at the surface of fibroblast plasma membranes in healthy patients. Interestingly, LDLR could not be observed in fibroblasts from HoFH patients, indicating that a defect in LDLR could be the genetic cause of FH (72). The LDLR was then purified from bovine adrenals (73), its human complementary deoxyribonucleic acid (cDNA) cloned (74) and its gene identified in 1985 (75).

I.1.5.2 The structure of the LDLR

The LDLR founded and is a member of the LDLR-related proteins (LRP) which is composed of eight structurally distinct transmembrane proteins (Figure 7B): α-macroglobulin/LRP1, LRP1b, megalin/LRP2, LDLR, VLDLR, ME GF7/LRP4, LRP5/LRP6 and LRP8/apolipoprotein E receptor 2 (apoER2).

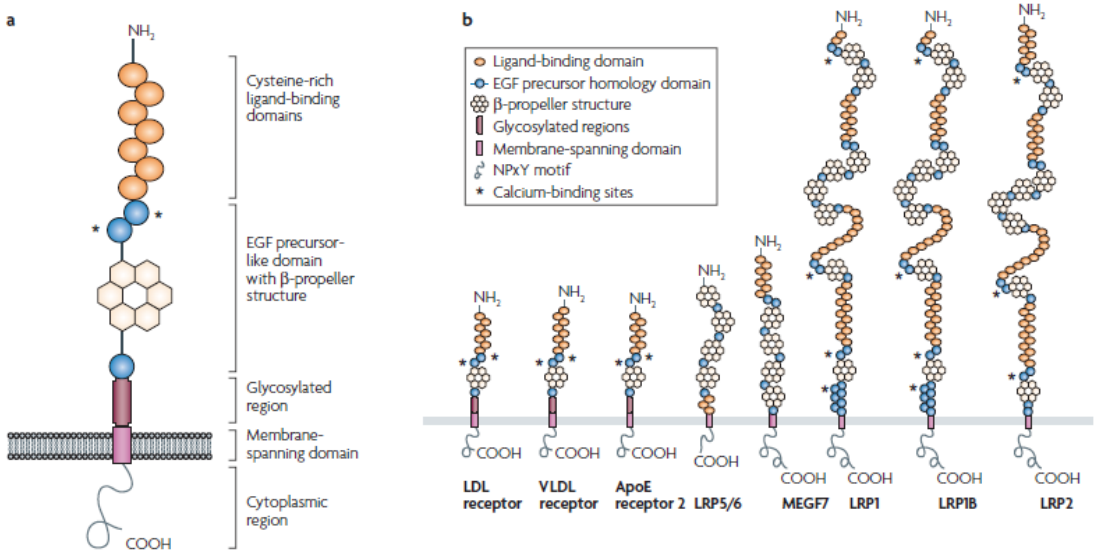

Figure 7. LDLR structure and LRP family (76)

The *LDLR* gene is found on human chromosome 19p13.2 and contains 18 exons. The LDLR is a modular type I transmembrane receptor composed of 839 amino acids (aa) /160 kDa when mature (74, 75). LDLR encompasses three different extracellular protein modules (Figure 7A).

- The first one is named LDLR type A (LA) and consists of seven cysteine-rich ligand binding domains (~40 amino acids (aa) each).
- The second one (~400 aa) is a region with 35% homology to the epidermal growth factor precursor (EGFP) containing two EGF-like repeats A and B (EGF-A and EGF-B) followed by a YWTD domain (named by the conserved residues tyrosine, tryptophan, threonine and aspartate) and a third EGF-like repeat C (EGF-C).
- The third extracellular module (58 aa) is rich in serine and threonine and thus undergoes O-glycosylation (77).

These three extracellular modules are followed by the transmembrane domain of LDLR and a cytoplasmic tail (~50 aa) containing the NPXY sequence (where X is any aa), which is known to direct receptors to clathrin-coated pits (78).

I.1.5.3 The ligands of the LDLR

The LDLR naturally binds the single copy of apoB-100 of the LDL particles (79) that will be detailed in the next section.

ApoE-containing particles such as VLDL can also be recognized by LDLR, as well as VLDLR, apoER2, LRP1 and LRP2 (80).

I.1.5.4 Mutations in LDLR leading to FH

Since the cloning of its human cDNA, the *LDLR* gene abnormalities could be studied. Molecular biology quickly led to the identification of mutations in *LDLR* causing FH by cloning its genomic DNA (54, 81-85). Today, more than 1,700 mutations in *LDLR* gene were identified (86). Those mutations are classified in up to 8 classes depending on the mutation location in LDLR and on its phenotypic effect. LDLR mutations can lead to a defect in LDLR synthesis (class 1) like in the case of the occurrence of a stop codon at the aa 167 (61). In the second class, the transport of the LDLR from the ER is completely (class 2a) or partially (class 2b) blocked such as in the case of

the substitution mutation G565V (87). Defects can also occur in LDL binding (class 3) like the D227E mutation (61) or in the clustering in clathrin-coated pits (class 4) like Y828C (88). LDLR mutations can also lead to recycling defects (class 5) like T454N (89), sorting defects in polarized epithelial cells (class 6) like G844D (90) or to a higher degradation by extracellular PCSK9 (class 7) like H327Y (91). The recently published R410S mutation led to a proposed novel class of mutations (class 8) showing defective LDL delivery to lysosomes as well as resistance to extracellular PCSK9 degradation (92).

Interestingly, these different mutation classes can be associated with patients variability in phenotypes, response to statins and risk of premature CVD (89).

I.1.6 Role of apoB and its mutations

I.1.6.1 The functions of apoB

The apoB-100 is the protein component of the LDL particles and the most abundant apolipoprotein in human plasma. Like apoE, apoB can interact with lipoprotein receptors at the cell surface (93). It is very important in TG-rich lipoprotein formation and is unique because it is the only apolipoprotein that is not exchangeable on lipoproteins. In contrast, apo A-I, A-II and E can transfer easily among various lipoproteins. Therefore, apoB remains attached to lipoproteins from their synthesis in the intestine or liver until their uptake by cell surface receptors. There are two apoB types: apoB-100 and apoB-48 (94). In the liver, the full-length apoB-100 is synthesized and assembles VLDL particles. An mRNA editing process occurring exclusively in the intestine transforms the Gln^{2153} codon of apoB-100 into a stop codon, resulting in apoB-48, which consists of the N-terminal 48% of apoB-100 (95). The role of apoB-48 is to assemble chylomicrons.

I.1.6.2 Structure of APOB

Although the clinical importance of apoB-100 was known, its insolubility and large size made it difficult to study (96) before its gene was cloned in 1986 (97-99). The *APOB* gene is located on human chromosome 2p24.1 and contains 29 exons. Interestingly, more than half of the protein is coded by the exon 26, which is one of the largest one reported with its 7,572 base pairs (bp) (100). The apoB-100 protein is 4,536 aa long (97, 98, 101). The N-terminal 89% of apo-B100 wraps the LDL particle like a belt, whereas the C-terminal 11% forms a bow crossing over the belt, bringing the C-terminal portion of apo-B100 close to aa 3,500 (see Figure 8). A cluster of positively charged residues called site B at aa 3,359–3,369 has been identified as the only or primary apoB-100 binding domain to the LDLR (102). It is hypothesized that the bow modulates the affinity of site B for LDLR.

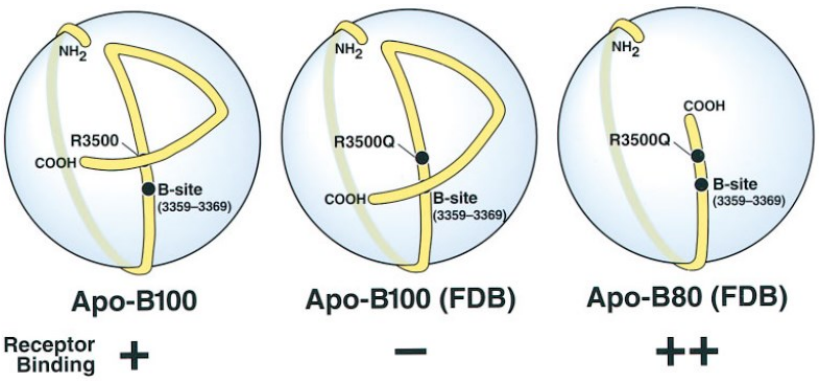

Figure 8. Schematic of the carboxyl-tail modulator model for apo-B100 binding to the LDL receptor (102)

I.1.6.3 Ligands of apoB

The apoB-100 protein binds to lipids and corresponds to the structural component of LDL and VDL. It is also the ligand of LDLR, as stated previously. Since apoB-100 binds LDLR only after VLDL conversion to LDL, two parameters are essential for its role as a ligand for LDLR: its lipid composition and its conformation. Basic amino acids in apoB-100 also interact with heparin and negatively charged sulfate groups of proteoglycans in the artery wall, leading to atherosclerosis (103-105).

I.1.6.4 ApoB mutations

Patients with truncation mutations of the *APOB* gene present a rare codominant disorder of lipoprotein metabolism, familial hypobetalipoproteinemia (FHBL, OMIM#615558), characterized by low levels of LDLc and apoB and leading to neurological disorders, liver diseases and fat malabsorption (106, 107).

ApoB-100 mutations leading to a defective binding to LDLR, such as the substitution mutation R3500E, lead to an autosomal dominant genetic disorder called familial defective apoB-100 (FDB, OMIM#144010) (108), although the residue R3500 is not directly involved in apoB-100 binding to LDLR (102). Since the LDL is not able to bind its receptor because of its defective apoB-100, it accumulates in plasma, leading to hypercholesterolemia. *APOB* mutations are thus also associated with FH (109). FDB patients suffer from 2.7-fold higher CVD risk compared to healthy patients, while FH patients suffer from 8.5-fold higher risk (110). The mutation R3500Q decreases

the affinity of apoB for LDLR (109, 111) and is predominant in Europe, accounting for up to 10% of all FH patients (112). Other FH mutations impairing LDLR binding capacity and decreasing LDL uptake were reported in *APOB* such as R23W, R1137T and Q422del (113, 114). Besides, some *APOB* variants such as R3531C showed reduced LDLR binding but are not clearly linked to FH. They are thus considered as "susceptibility" variants increasing hypercholesterolemia risk (115).

I.2 PCSK9

In order to fully understand the biology and the functions of PCSK9, which stands for Proprotein Convertase Subtilisin/Kexin type 9, and which is the last and 9th family member of the Proprotein Convertase (PC) family, it is important to know how the eight other PCs were discovered and operate.

I.2.1 The discovery of the Proprotein Convertases

The number of genes constituting the mammalian genome has been estimated to be ~20,000. Today, more than 200 post-translational modifications (PTM) are known to increase the diversity of proteins encoded by these genes. Those include notably asparagine and serine/threonine glycosylation; serine, threonine or tyrosine phosphorylation; tyrosine sulphation; protein lipidation; cholesterol attachment; lysine methylation and ubiquitination. PTM can be classified into two different types: reversible PTM providing a feedback mechanism guaranteeing the good working of cells; irreversible PTM such as limited protein proteolysis at specific sites generating multiple products. The latter is mediated by proteases acting by cleaving specific peptide bonds and constitutes one of the most drastic irreversible PTM. A large part of secreted proteins, which are encoded by nearly one fifth of the genome, are synthesized as precursors that need to be cleaved in order to become either mature bioactive products or inactive ones. Processing of secretory proteins occur in various subcellular locations such as the trans-Golgi network (TGN), endosomes, immature secretory granules or cell surface.

The prohormone theory stated that a peptide hormone could be derived from the cleavage of a larger polypeptide. It originated from the late 60's when Michel Chrétien and Choh H. Li observed that β-lipotropin (β-LPH; 91 aa) and γ-lipotropin (γ-LPH; 58 first aa of β-LPH) contained the sequence of the pituitary gland (hypophysis) octadecapeptide β-melanocyte-stimulating hormone (β-MSH; aa 41 to 58 of β-LPH and γ-LPH) (116). It was hypothesized that β-LPH could be proteolytically cleaved; pairs of basic aa (KK and KR) flanking β-MSH/γ-LPH were pointed as potential cleavage sites. The subsequent sequencing of β-LPH (117, 118) brought the new concept of a single precursor containing several active molecules, which was subsequently named pro-opiomelanocortin (POMC) (119). Similar studies were performed on pro-insulin, showing similar

results. This important discovery brought the idea that many active peptides could also be synthesized as large precursor molecules containing pairs of basic aa as cleavage sites. This implicated the existence of specific proteases involved in the proteolytic cleavage of the precursors, which were named PCs. Although the hypothesis of a PTM cleaving precursor molecules into smaller entities was rapidly established, the identification of the nature of the enzymes responsible for this maturation took many years (120). Today, around 600 proteases have been identified in mouse and human genomes and can be divided into five major classes: metalloproteases and cysteine, serine, threonine or glutamic acid proteases (121).

Methods such as classical biochemical tissues purification and enzyme assays enabled the first hint of the presence of two calcium-dependent endoproteinases as the first mammalian PCs implicated in pro-insulin processing in 1987 by Howard W. Davidson *et al*. (122). In the 80's, another important discovery was the fact that the yeast *Saccharomyces cerevisiae* contained a PC belonging to the subtilisin-like serine protease family, namely kexin encoded by the *Kex2* gene and showing similar specificity towards paired basic residues, calcium-dependent activity and POMC processing (123-125). In 1989, Robert S. Fuller *et al*. observed that like kexin, the predicted cDNA sequence of furin, a type 1 transmembrane protein thought to be a receptor, carried the signature of the catalytic domain of *subtilases* (126), namely subtilisin/kexin like serine proteases (127). This breakthrough led to an intensive period of race for homologs to this cDNA from endocrine tissue mRNA. To that end, scientists used polymerase chain reaction (PCR) with degenerate oligonucleotides designed to overlap the codons corresponding to residues of the active triad found in the catalytic pocket of kexin and furin. This led to a series of PCs cDNA characterization studies from 1989: PC2 from a human insulinoma, which is a pancreatic tumor overproducing insulin (128); PC1 and PC2 from murine pituitary gland (129); PC1 (named PC3 or PC1/3) from human insulinoma (130). It then took thirteen years to identify the six other PC-encoding cDNAs structurally similar to furin, PC1/3 and PC2: namely PC4, PC5/6, PACE4, PC7, SKI-1/S1P and PCSK9. This completed the identification of the nine Proprotein Convertase Subtilisin/Kexin Types 1-9 (PCSK1-9) forming the complete PC family. All their human genes are named *PCSK1* to *PCSK9*, except for PCSK3 (furin) which is named *FURIN* and for PCSK8 (SKI-1/S1P) that is named *MBTPS1*.

I.2.2 The seven first members of the Proprotein Convertases family: the kexin-like PCs

After their discovery, the biochemistry, biological and physiological functions of each PC have been extensively studied and are reviewed in many scientific publications (131-135). Importantly, a wide body of knowledge was gained from *in vivo* studies using knockout (KO) animals, mostly in mice (136, 137). Focus will be put on the *in vivo* discoveries because they clearly demonstrate the crucial physiological roles that each PC plays. However, more detailed information on other aspects of individual PCs can be found in the cited articles.

I.2.2.1 Structure

The protein structure of all PCs begins with a signal peptide followed by a prosegment and a catalytic domain, which contains the typical catalytic triad residues Asp (D), His (H) and Ser (S) as well as the Asn (N) comprising the oxyanion hole (which is replaced by Asp for PC2), as indicated in Figure 9. The first seven PCs also harbor a β‑ barrel-containing P domain downstream of the catalytic domain, which is thought to stabilize the catalytic pocket and regulate the calcium and pH dependence of the PCs (138). The C-terminal domain of each PC harbors a specific sequence dictating their cellular localization and trafficking. For example, PC5 and PACE4 contain a C-terminal Cys-rich domain (CRD) allowing them to bind to heparin sulphate proteoglycans both at the cell surface and in the extracellular matrix.

I.2.2.2 Function

The first seven PCs, namely PC1/3, PC2, furin, PC4, PC5/6, PACE4 and PC7, cleave at paired or single basic residues, recognizing the following pattern: (K,R)-2X_n-(K,R)↓ where X is any residue and n=0, 1, 2 or 3.

PC1/3 and PC2 were found to be mostly located within immature or dense core secretory granules. They constitute the PCs of the regulated secretory pathway of endocrine and neuronal cells and are often both expressed in the same tissues and cells (139) where they perform proteolytic activation of polypeptide hormones and neuropeptides precursors (140). Mice lacking PC1/3 (*PCSK1* gene) are normal at birth but present a dwarfism phenotype (at 10 weeks, they are only ~60% of normal size) accompanied by several neuroendocrine peptide processing defects (141).

PC2 (*PCSK2*)-defective mice also seem normal at birth but present severely impaired pancreatic processing of proglucagon, prosomatostatin, and proinsulin; altered pancreatic islet morphology as well as a small decrease in growth rate (142).

PC4, furin, PC5/6, PACE4 and PC7 cleave and activate/inactivate secretory precursor proteins in the TGN, cell surface or endosomes.

PC4 is a membrane-bound PC which has a reproductive function. Indeed, its transcripts have been localized exclusively in round spermatids in mice (143, 144). Pcsk4-deficient mice present fertility impairment (145, 146).

In contrast, furin, PC5/6, PACE4 and PC7 are widely or even ubiquitously expressed and are implicated in processing events occurring in the constitutive secretory pathway. They thus activate or inactivate receptors, ligands, enzymes, growth factors or viral glycoproteins (147). Interestingly, these four PCs showed some functional redundancy when they were transfected in cell lines. However, their inactivation in mice resulted in specific phenotypes. This revealed that each PC has unique *in vivo* functions during embryonic development and/or in the adult. Furin KO mice present many embryonic malformations, including the absence of axial rotation and heart looping, which results in death around embryonic day 11 (148, 149). The particularity of PC5 is that it is the only PC to exhibit two validated alternatively spliced forms, namely soluble PC5A and transmembrane PC5B. PC5 KO mice die at birth and present anteroposterior pattern disorders including extra vertebrae, lack of a tail, kidney agenesis, smaller size, hemorrhages, collapsed alveoli and retarded ossification (150).

PACE4 KO mice present an altered left-right patterning including cyclopism, craniofacial and cardiac malformations in some embryos (151). These mice were also hypertensive, indicating a role of PACE4 in blood pressure regulation, which is in agreement with the link of *PCSK6* gene to hypertension (152).

Silencing the expression of the membrane-bound PC7 (153) in mice results in anxiolytic and novelty-seeking phenotypes (154). In cellular studies and in human genome-wide association studies, it was demonstrated that PC7 regulates iron metabolism by shedding transferrin receptor-1 (155). PC7 loss-of-function (LOF) was also associated with high HDL levels, low TG, low atherogenic small dense LDL and insulin resistance reduction, indicating a decreased CVD risk (156-160).

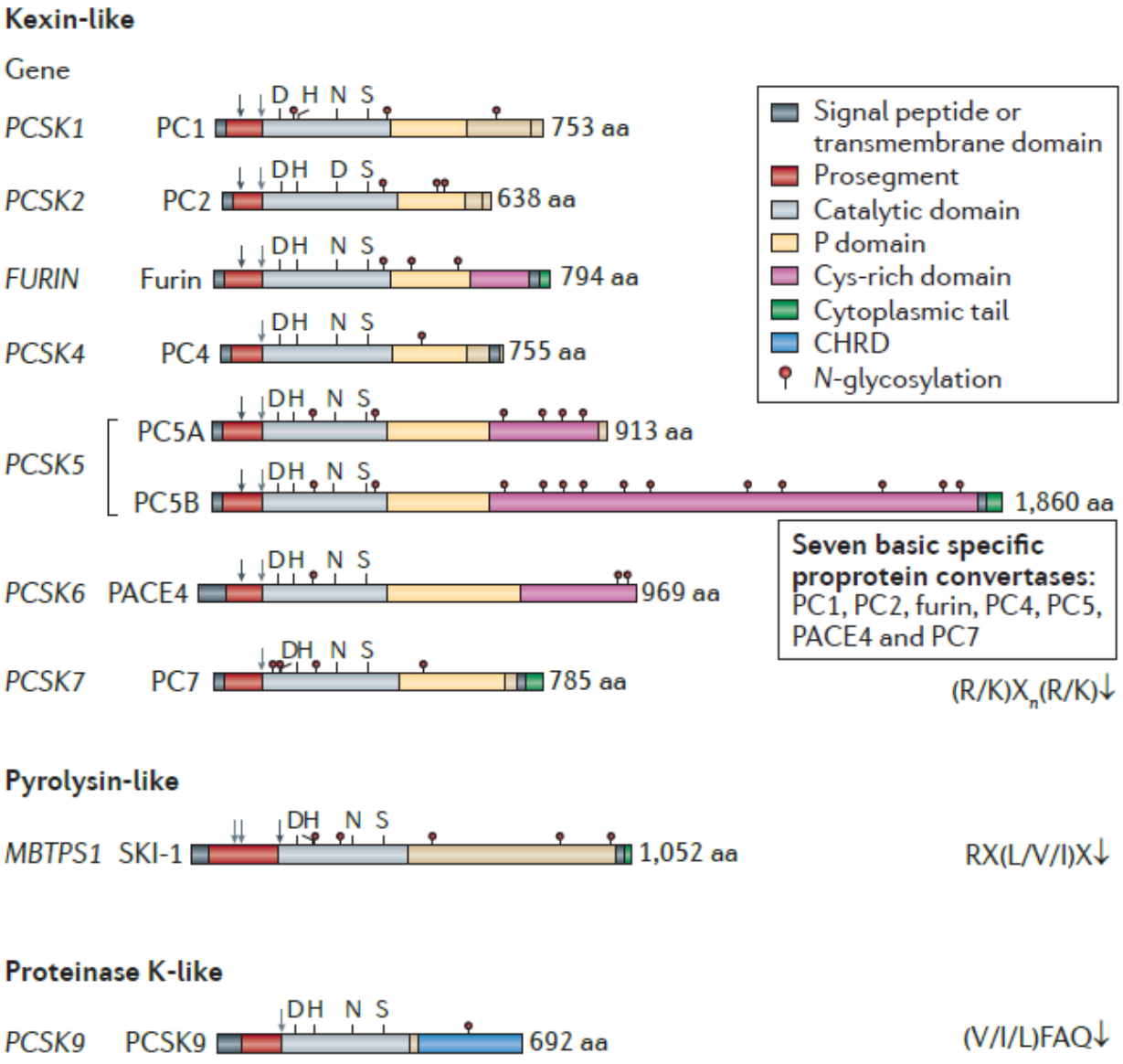

Figure 9. Schematic representation of the primary structures of the human proprotein convertases. The various domains and N‐glycosylation sites are indicated, as well as their primary (light grey arrows, and a light grey double arrow for SKI‐1) and secondary autocatalytic processing sites (dark grey arrows) (132)

I.2.3 The eighth member of the Proprotein Convertases family: the pyrolysin-like SKI-1

The Subtilisin Kexin Isoenzyme-1 (SKI-1) (17), also known as site-1-protease (S1P) (161, 162) is a PC related to pyrolysin and cleaving proproteins at non- basic residues according to the motif R- X- (aliphatic)- X↓. It is a membrane-bound PC that is also expressed ubiquitously. It activates precursors of membrane-bound transcription factors such as SREBP1 and SREBP2 in the *cis*/*medial* Golgi network. A second luminal cleavage by the protease S2P often follows S1P processing, releasing an N-terminal cytosolic domain acting as a transcription factor upon its translocation into the nucleus (161). SKI-1/S1P was thus the first PC reported to regulate lipid metabolism. When 80-90% inactivated in the liver, lipid synthesis is decreased by 75% (163). In contrast, complete *Mbtps1* gene inactivation leads to early embryonic death with an absence of epiblast formation (163). SKI-1 is the first PC that does not contain a P domain, which is common to the first seven PCs (17), as indicated in Figure 9.

I.2.4 The ninth member of the Proprotein Convertases family: the proteinase K-like PCSK9

I.2.4.1 The discovery of NARC-1/PCSK9

By 1999, the eight members of the PC family have been discovered. However, researchers knew that there could be more PCs to discover since some processing sites were known not to be recognized by the eight PCs identified so far (164). This led them to look for other family members using bioinformatics tools. The BLAST program (www.ncbi.nlm.nih.gov/BLAST) was used to search for a protein containing SKI-1 catalytic subunit short conserved segments. This enabled Nabil G. Seidah and his team to identify a putative convertase called neural apoptosis-regulated convertase 1 (NARC-1) (63) or LP251 in a patented database. This protein has been previously identified and cloned by two pharmaceutical companies, Millennium Pharmaceuticals (NARC1: patent no. WO 01/57081 A2) and Eli Lilly (LP251: patent no. WO 02/14358 A2). Millennium Pharmaceuticals identified NARC-1 as an upregulated gene in primary cerebellar neurons upon apoptosis induction by serum deprivation, while Eli Lilly identified LP251 by global cloning of secretory proteins. The information on NARC-1 was limited at that time: it was known that its

gene was located on human chromosome 1p33-p34.3 and that its mRNA was mostly expressed in liver and less importantly in testis and kidney (63) .

In 2003, NARC-1 was shown to belong to the proteinase K subfamily of subtilases because of the ~42% identity of their catalytic domains (63).

Like all the other PC family members, pro-NARC-1 is synthesized as a zymogen, which gets autocatalytically processed in the ER. This results in the cleavage of its prodomain which remains attached with secreted NARC-1, constituting a particularity of NARC-1 compared to the eight other PC family members (63). Another particularity is that NARC-1, like SKI-1/S1P, does not have a P domain, as indicated on Figure 9.

The tissue distribution of NARC-1 was studied in embryonic and adult mouse and rats using Northern blot and *in situ* hybridization (ISH) histochemistry. These studies revealed that in the adult NARC-1 mRNA is expressed exclusively in the liver, kidney, cerebellum, and small intestine; and transiently expressed during development in kidney epithelial and brain telencephalon cells (63). Interestingly, a partial hepatectomy (PHx) was conducted in rat in order to induce liver regeneration and showed a peak of NARC-1 mRNA 2 days post-PHx (63). In primary embryonic telencephalon cells obtained from embryonic day 13.5 (E13.5) mice, NARC-1 transfection resulted in an increased percentage of differentiated neurons (63). Similarly, NARC-1 expression was studied in various cell lines and shown to be particularly high in neuroepithelioma SK-N-MCIXC, hepatic BRL-3A, and in colon carcinoma cell lines (63). This data, together with the fact that NARC-1 was located in tissues that have the capacity to proliferate and differentiate, suggested that NARC-1 is involved in cortical neurons differentiation (63).The discovery of NARC-1 constituted the discovery of the last PC in 2003.

I.2.4.2 The link between NARC-1/PCSK9 and FH

It was noticed earlier that the human chromosomal localization of NARC-1 (initially estimated on chromosome 1p33–34.3 (63) and finally established on chromosome 1p32) was close to a locus associated with an increase in the hepatic secretion of LDLc, but not HDLc or TG (165, 166). This locus was identified in FH families from France (165) and Utah (166) in which mutations in *LDLR* or *APOB* were absent.

Note that the gene encoding the protein NARC-1 was first named *PCSK9* (on recommendation of the Nature editor, Annik Prat, personal communication) in the short communication by Marianne Abifadel *et al.* linking mutations of the *PCSK9* gene to FH (64). Since then, PCSK9 was almost never referred to as NARC-1 anymore. Human *PCSK9* gene encodes 12 exons transcribed into a 3,710 bp mRNA encoding a 692 amino-acid PCSK9 protein.

In this publication, the 12 exons of *PCSK9* were sequenced and enabled the identification of a T→A mutation at nucleotide 625 in exon 2, predicting a substitution of a conserved serine into an arginine at codon 127 (S127R) in 12 ADH patients and in a patient with TC levels in the 90th percentile, for whom the implication of mutations in *LDLR* and *APOB* had been excluded (64). This mutation was absent in 100 control patients, the authors thus concluded that is not a polymorphism (64). Another mutation, T→C at nucleotide 890, predicting a substitution of a conserved phenylalanine at codon 216 to leucine (F216L) was identified in 22 probands with ADH, one of whom died from myocardial infarction at 49 years of age. Strikingly, these two missense *PCSK9* mutations (S127R and F216L) have been found in 12.5% of the tested ADH families, and 25 polymorphisms were also identified (64).

This study clearly established *PCSK9* as the third locus for FH. Hence, it is denoted as the FH3 gene critical for LDLc regulation.

I.2.4.3 How was PCSK9 related to cholesterol metabolism?

In 2003, PCSK9 mRNA was shown to be downregulated by dietary cholesterol like a cholesterogenic target of SREBP2 *in vivo* (167). However, HepG2 cells (hepatocarcinoma human cell line) stably overexpressing PCSK9 or its natural S127R mutant presented decreased LDLR levels (168), indicating a direct link between PCSK9 activity and LDLR regulation. This reduction was abrogated upon incubation of cells with 5 mM ammonium chloride, suggesting that PCSK9 overexpression might increase the turnover rate of the LDLR by enhancing its intracellular degradation in acidic compartments (168).

Importantly, several *in vivo* studies demonstrated that adenoviral-mediated expression of murine (169) or human (168, 170) PCSK9 induced a post-transcriptional degradation of the LDLR. Accordingly, mouse models lacking PCSK9 presented decreased cholesterol levels as well as increased hepatic LDLR protein levels (171, 172).

I.2.4.4 Structure / function and mechanism of action of PCSK9

As indicated on Figures 9 and 10, PCSK9 primary structure is composed of a signal peptide (aa 1-30), a prodomain (pro; aa 31-152), a catalytic domain (aa 153-404), a hinge (H; aa 405-452) and a Cys- and His-rich domain (CHRD; aa 453-692) (63), which comprises three modules M1, M2 and M3 (173).

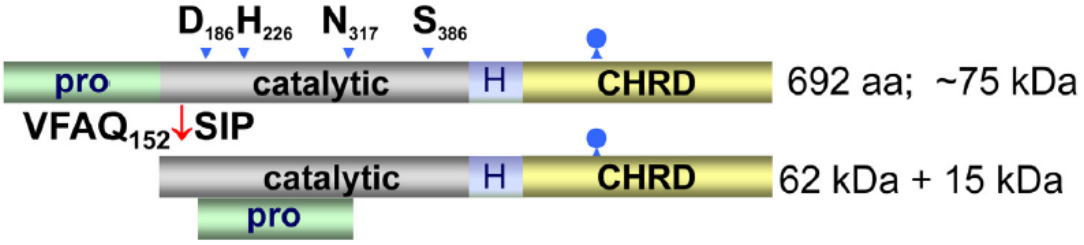

Figure 10. Schematic representation of PCSK9. proPCSK9 and its processed form PCSK9 that is non-covalently bound to the autocatalytically processed prodomain (pro; 15 kDa) at $VFAQ_{152}$-SIP. Note the active site residues Asp, His, and Ser and the oxyanion hole Asn as well as the single N-glycosylation site (blue). (174)

PCSK9 is a unique PC belonging to the proteinase K family. Like SKI-1, PCSK9 also cleaves at non-basic residues, albeit only once upon its autocatalytic activation in the ER. PCSK9 catalytic domain presents 25% sequence identity with that of SKI-1/S1P (63). PCSK9 cleaves at $VFAQ_{152}$↓SIP (168, 175). The residue Q_{152} is critical since only a few residues can replace it without loss of function, unfavorable residues creating a dominant negative zymogen retaining native pro-PCSK9 intracellularly (176). Unlike other PCs, PCSK9 does not require basic residues close to its cleavage site.

While the prodomain acts as an intramolecular chaperone and a potent but transient inhibitor for the other PCs, PCSK9 prodomain remains non-covalently bound to the catalytic domain of mature PCSK9 (63). Secreted PCSK9 is thus an inactive protease, any catalytic activity of the enzyme being prevented by the prodomain (173) as shown in crystal structures such as in Figure 11. Therefore, the only proteolytic activity of PCSK9 is on itself during the zymogen processing of proPCSK9 into PCSK9 in the ER.

PCSK9 binds several receptors and escorts them to endosomes and/or lysosomes for degradation.

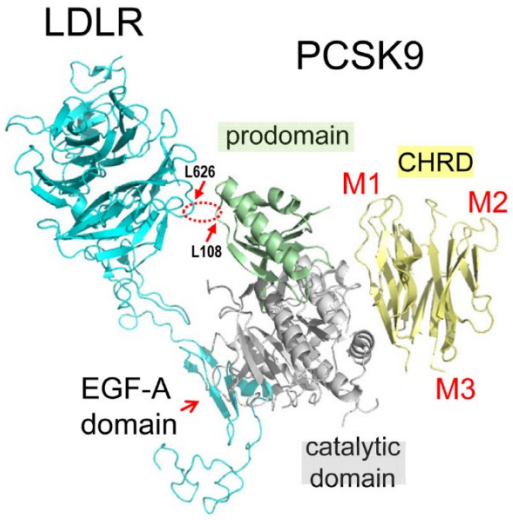

Figure 11. Crystal structure of PCSK9 with LDLR (174)

The first reported and most studied receptor that PCSK9 binds to is the LDLR, enabling PCSK9 to indirectly regulate circulating LDLc levels. PCSK9 binds the EGF-A domain of the LDLR through its catalytic domain (177, 178), as indicated on Figure 11 representing the crystal structure of PCSK9 in complex with LDLR. This binding is crucial for PCSK9 to trigger LDLR degradation (179, 180). The prodomain of PCSK9 has been shown to interact with the β-barrel domain of the LDLR (178). This evidence was strengthened by the discovery of the L108R mutation which increases the ability of PCSK9 to trigger LDLR degradation (181). Unfortunately, the structure of the N-terminal aa 31-59 of the prodomain could not be determined by various crystal studies of PCSK9 (173, 178), suggesting that this highly acidic segment is mobile and might need a stabilizing partner which could be apoB-100 (182). Interestingly, the deletion of segment 31-51 of PCSK9 led to an increase of >7-fold of the affinity of this truncated PCSK9 for LDLR (183).

In Figure 12, the extracellular pathway of PCSK9-induced degradation of the LDLR is represented. Briefly, in presence of low levels of PCSK9 (right part of the graph), the LDL-LDLR complex gets endocytosed *via* heavy-chain clathrin-coated vesicles that fuse with early endosomes, where the acidic pH causes conformational changes driving LDL release, and the subsequent recycling of the LDLR to the cell surface as well as the sorting of LDL to lysosomes for cholesterol recovery and distribution in the cell (27), as mentioned previously. This leads to high cell surface LDLR levels and low circulating LDLc levels. In contrast, in presence of high PCSK9 levels (left part of

the graph), the PCSK9-LDLR complex also gets endocytosed via clathrin-coated vesicles (184, 185). Nevertheless, the acidic pH enhances the affinity of PCSK9 for the LDLR (173), resulting in the degradation of the complex in late endosomes/lysosomes, independently of LDL binding to LDLR. This prevents the recycling of LDLR, leading to low cell surface LDLR levels and subsequently increased levels of circulating LDLc.

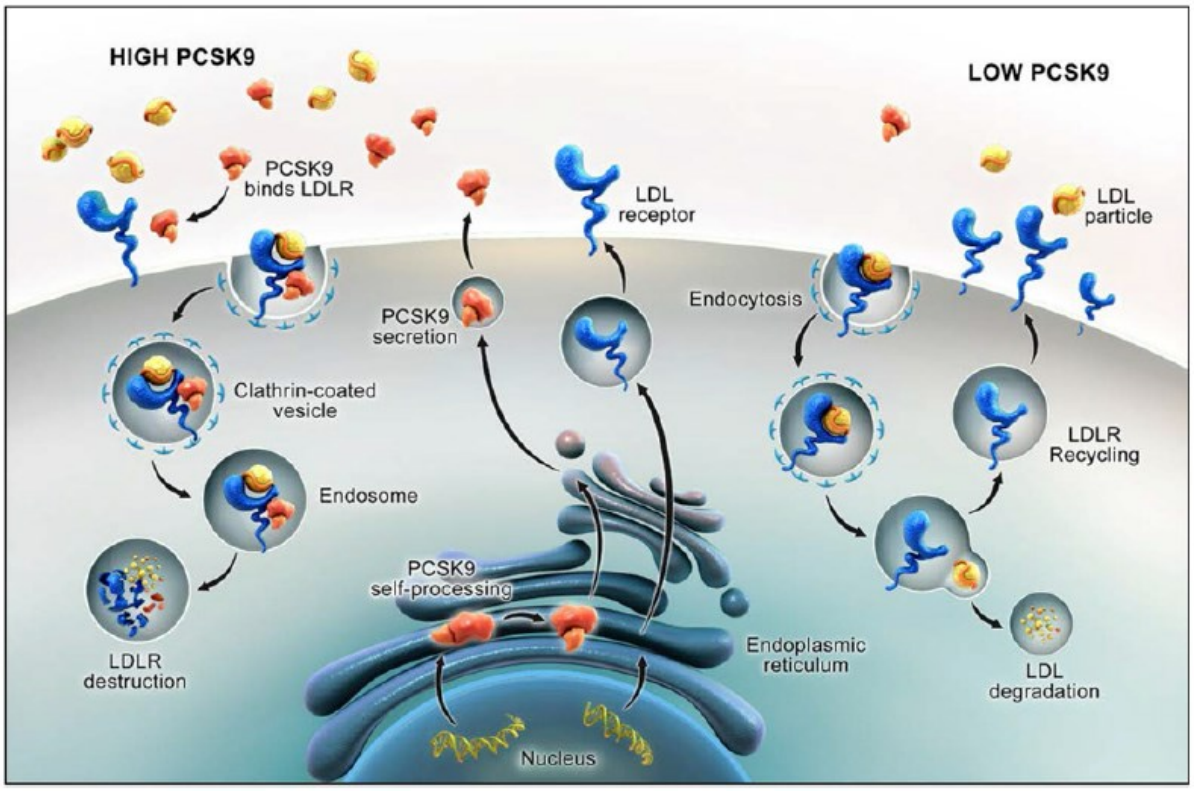

Figure 12. Schematic of the extracellular pathway of PCSK9-induced degradation of the LDLR (135)

Interestingly, *ex vivo* studies on HepG2 cells and mouse primary hepatocytes have demonstrated that PCSK9 also triggers the intracellular degradation of the LDLR following its exit from the TGN (186). However, both extra- and intracellular LDLR degradation pathways seem to occur in parallel in cell lines, while in liver the extracellular pathway is predominant. More work is needed to define the tissue(s) where the intracellular pathway is predominant *in vivo*.

I.2.4.5 The importance of the CHRD and the search for protein X

Although it has now been 14 years since the discovery of PCSK9, the precise molecular mechanisms leading it to enhance the degradation of the LDLR in late endosomes/lysosomes has not been identified yet (135, 174).

One important structural determinant in this process seems to be the CHRD of PCSK9. Indeed, a truncated version of PCSK9 lacking the CHRD bound LDLR but did not lead to LDLR degradation in cells (179, 184). The M2 module of the CHRD was demonstrated to be particularly important for LDLR degradation (180). Interestingly, domains in both PCSK9 and LDLR that are not required for binding (or internalization) are essential for PCSK9-dependent LDLR degradation (179). Accordingly, monoclonal antibodies (mAbs, see section I.4.2.) targeting the CHRD of PCSK9 have been designed: while they did not block the interaction of PCSK9 with LDLR, they decreased PCSK9 activity from 50-75% (187, 188). In contrast, mAbs targeting the catalytic domain of PCSK9 inhibit 100% of its activity since they prevent the binding of PCSK9 to the LDLR (189). This difference could be rationalized by the fact that blocking the CHRD by a mAb results in a partial prevention of the cellular internalization and/or lysosomal targeting of the PCSK9-LDLR complex (190). More studies are needed to fully elucidate the role of the CHRD in the degradation of the PCSK9-LDLR complex. For example, PTM of PCSK9 CHRD such as Asn_{533} glycosylation (63) or Ser_{688} phosphorylation (191, 192) could play a role in this process. Finally, the CHRD may influence differently the intracellular and extracellular pathways of PCSK9-induced LDLR degradation (171).

Many potential CHRD binding partners have been proposed, denoted “protein X”, which would direct the PCSK9-LDLR complex to late endosomes/lysosomes (174, 190). One of the proposed partners is the ligand binding domain of LDLR (193) but this was not corroborated by PCSK9-LDLR crystal structure (178). It was also suggested that the CHRD may displace a protein required for LDLR recycling at the cell surface (135). Given that the cytosolic tail (CT) of the LDLR contains an NPXY motif that binds the adaptor protein ARH, which in turn binds clathrin (51), it was proposed that the CT of the LDLR controls the endocytosis of the PCSK9-LDLR complex. Nevertheless, this hypothesis was rejected by several studies showing that PCSK9 can degrade a construct of LDLR lacking its CT (194, 195). Protein X was also

proposed to be another membrane-bound protein containing the NPXY motif in its CT such as LRP1, which was upregulated in livers of PCSK9 KO mice but was not essential for LDLR degradation (194). The *SORT1* gene, known to be linked to hypercholesterolemia, has been proposed to be a critical regulator of PCSK9 activity *in vivo* (196). Similarly, another group demonstrated that PCSK9 CHRD interacts with amyloid precursor protein-like protein-2 (APLP2), which could be involved in PCSK9 trafficking to endosomes/lysosomes (197). However, another study showed that the two protein X candidates, SORT1 and APLP2, are not necessary for the *in vivo* PCSK9-dependent LDLR degradation and that hepatic LDLR levels were not different in mice lacking sortilin or APLP2 (190). Others identified Sec24A, a cytosolic adaptor protein involved in the ER-Golgi trafficking of the coat protein complex COPII vesicles, as critical for PCSK9 exit from the ER and hence secretion (198). Finally, the chaperone like-protein GRP94 was shown to bind PCSK9 and to prevent LDLR degradation within the ER (199).

Taken together, a number of candidates have been proposed as protein X, but many of them were not validated in *in vivo* studies, and some still need confirmation. More studies will be necessary in the future to elucidate the precise mechanism underlying PCSK9-driven LDLR degradation and the role of the CHRD in this process both in the intracellular and extracellular pathways.

I.2.4.6 Human mutations in PCSK9

Mutations can be found in all four structural components of PCSK9 and these tremendously helped to understand the importance of each domain, even though a lot of research is still ongoing.

Gain-of-function (GOF) mutations resulting in higher PCSK9 activity or levels were expected to lower hepatic LDLR levels and hence raise circulating LDLc, due to its decreased clearance by the small number of LDLR. In humans, the discovery of *PCSK9* as FH3 was rapidly followed by the identification of the D374Y mutation, the most drastic one, in Utah, USA (200) and in Norway (201). The affinity of this GOF PCSK9 for the LDLR is increased ~10-fold compared to WT PCSK9 (173), leading to ~4-fold higher LDLc levels associated to early death due to CVD (200). Many other mutations causing FH were identified in consecutive years and were reviewed (202, 203) and some of them are shown on Figure 13. Interestingly, in 2015 a study found 16 different PCSK9 GOF mutations in 164 patients originating from 8 countries (204).

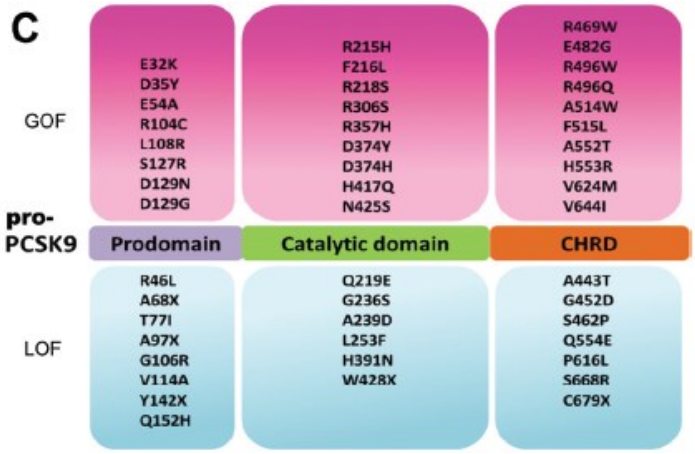

Figure 13. Schematic representation of the main GOF and LOF mutations in *PCSK9* (205).

The demonstration that, on the opposite, LOF mutations led to higher LDLR concentrations and hence decreased LDLc levels was first published in 2005 (206). Two heterozygote nonsense mutations, Y142X and C679X, were identified in 2% of an African American population by screening 32 patients having the lowest LDLc levels from the Dallas Heart study (207). Patients harboring one of these mutations had ~40% less LDLc and ~60% lower PCSK9, associated with ~88% reduction in CVD risk (207). The mutated forms of *PCSK9* can lead to decreased plasma LDLc by preventing the secretion of mature PCSK9 by various mechanisms such as disruption of the synthesis (Y142X), cleavage (L253F), or folding (C679X) of PCSK9 (208). Y142X is located in PCSK9 prodomain and leads to an early truncation and thus no PCSK9 production, while the C-terminal C679X mutation causes the retention of the autocatalytically cleaved PCSK9 in the ER, likely because of defective folding.

A spectrum of *PCSK9* alleles variations associated with LDLc was shown to span a wide range of allele frequencies (0.2 – 34%) as well as magnitude of phenotypic effects (from 3% increase to 49% decrease in LDLc), thereby contributing to inter-individual LDLc differences (209).

More than 100 single nucleotide polymorphisms (SNP) with diverse consequences were identified in PCSK9. Common polymorphisms such as R46L lead to partial PCSK9 LOF characterized by lower LDLc (209), an anti-atherogenic lipoprotein profile (210) and reduced CVD risk (211, 212). The frequency of this polymorphism varies between 4.8% in French Canadian and 2.4% in Caucasian (213).

The mutations evoked in this thesis are only a small sample of all the existing mutations. In Figure 13, a list of the main GOF (in pink) and LOF (in blue) in each PCSK9 domain is presented.

Three people presenting a complete LOF of PCSK9 have been reported, in whom no immunodetectable circulating PCSK9 was identified. All three present strikingly low plasma LDLc levels ~0.4 mM or ~15 mg/dL.

The first studied individual was a healthy, fertile, college graduate 32-year-old woman from the Dallas Heart Study who was found to be a compound heterozygote for the two inactivating PCSK9 mutations Y142X and ΔR97 that disrupt the synthesis and processing/secretion of PCSK9, respectively (208).

In another study meant to determine the frequency of the two LOF mutations Y142X and C679X in an African population in Zimbabwe, a 21-year-old woman who was homozygote for the C679X variant was identified as the second patient lacking PCSK9 (214). Not much information is available on this patient but it can be speculated that she went to a doctor because she was pregnant.

The third patient is a French 49-year-old diabetic man who had profound familial hypobetalipoproteinemia (FHBL; OMIM 107730). He was initially hospitalized for the rapid-onset of an insulin-requiring diabetes which etiology is still uncertain and presented moderate liver steatosis. A mono-allelic PCSK9 double-mutant R104C/V114A was identified, which processing and secretion was severely impaired when transfected in hepatocytes, thereby showing that this double mutant PCSK9 acts as a dominant negative to the secretion of WT PCSK9 (215). Importantly, this study also constituted the first direct evidence in human that decrease of LDLc associated to PCSK9 LOF mutations are attributable to an increased clearance rate of LDL (215).

Another LOF mutation, Q152H, was shown to reduce circulating PCSK9 up to 80% in patients (216). It was identified in a French Canadian family and co-transfection of equal amounts of mutated PCSK9 and WT PCSK9 decreased WT PCSK9 secretion by approximately 80%. Similarly to R104C/V114A double mutant, PCSK9 Q152H has a dominant negative effect on WT PCSK9 secretion (216).

Importantly, the identification of these specific patients brought the proof-of-principle that hypercholesterolemia and CVD could be treated by targeting PCSK9 (217, 218).

I.2.4.7 Physiological factors related to PCSK9

In human, plasma PCSK9 concentrations measured by a sandwich ELISA vary up to 100-fold as demonstrated by a study on >3,100 patients from a large and ethnically diverse population (219). PCSK9 levels were higher in women (510 ng/mL) than in men (450 ng/ml) and in postmenopausal women compared to premenopausal women, irrespective of estrogen status (219). Although there was a correlation between PCSK9 and LDLc levels, only 8% of LDLc variations could be explained by PCSK9 levels, indicating that multiple metabolic and genetic factors contribute to variation of PCSK9 plasma levels in the general population (219).

A similar study was conducted on 1,739 French Canadian children aged 9, 13, and 16 years and a mean plasma PCSK9 concentration ~85 ng/mL was found using another ELISA (220). Plasma PCSK9 decreased with age in boys whereas it increased in girls, confirming that PCSK9 plasma concentrations are strongly associated with **age** and **sex** (220).

Researchers also performed studies in order to determine whether PCSK9 circulating levels are influenced by diurnal changes and fasting (221). To that end, circulating PCSK9 was monitored in patients and enabled to demonstrate that serum PCSK9 levels show a diurnal rhythm that is closely related to that of cholesterol synthesis, whereas LDLc were stable. Circulating PCSK9 peaks around 4:30 am in healthy subjects. The diurnal rhythms of both PCSK9 and cholesterol synthesis could be abolished by depletion of liver cholesterol via treatment with the bile acid-binding resin cholestyramine. Fasting highly decreased both PCSK9 and cholesterol levels, without changing LDLc levels (222).

The impact of diet and exercise will be described in sections I.3.1.1.and I.3.1.2.

I.2.4.8 Ligands of PCSK9

Aside from LDLR, PCSK9 has been shown to bind other members of the LDLR superfamily through its interaction with EGF-A such as VLDLR and ApoER2 *in vivo*, which roles will be described in the next section, and LRP1 *in vitro* (194).

PCSK9 was also shown to interact with apoB in mouse hepatocytes, leading to an increased apoB production which could be explained by the inhibition of intracellular apoB degradation via the autophagosome/lysosome pathway (223).

It was also demonstrated that >40% of total plasma PCSK9 from normolipidemic patients was associated with LDL with a $K_D \sim 325$ nM and competition binding curves were consistent with a one-site binding model (182). An N-terminal region of the PCSK9 prodomain (aa 31-52) was determined to be necessary for binding to LDL *in vitro*, and the study proposed that PCSK9 association with LDL particles reduces the PCSK9 binding to LDLR, suggesting an inhibition of the PCSK9-mediated LDLR degradation (182).

It was demonstrated in patients and in mice that plasma PCSK9 is found associated to Lp(a) but does not bind apo(a) alone (224). Interestingly, a preferential association of PCSK9 with Lp(a) versus LDL (1.7-fold increase) was seen in subjects with high Lp(a) and normal LDLc (224), suggesting that variations in Lp(a) and its levels may modify its affinity to PCSK9. Besides, the same association was found in type 2 diabetes (T2D) patients (225). Interestingly, this data is contradictory to a previous study that demonstrated that PCSK9 does not bind Lp(a) directly *in vitro* but that its catabolism is regulated by PCSK9 *via* the LDLR (226). Therefore, it is not clear whether this association between PCSK9 and Lp(a) is direct or requires an additional protein.

The 33 kDa pleiotropic protein annexin A2 was discovered to bind PCSK9 and to be a natural inhibitor of its extracellular activity (227). It has been demonstrated that the N-terminal R1 domain of annexin A2 interacts with M1 and M2 modules of PCSK9 CHRD and inhibits PCSK9 mRNA translation (227, 228). The importance of this molecule was proven *in vivo* in annexin A2-deficient mice harboring ~1.4-fold higher LDLc, ~2-fold higher plasma PCSK9 and ~2-fold less LDLR protein levels in adrenals and colon (229). An annexin A2 polymorphism, V98L, correlated with lower plasma PCSK9 (229), while two recently identified SNP were found to reduce *ANXA2* gene

expression and to be associated with ~19% higher LDLc and higher CVD risk in patients (230), thereby confirming the physiological role of annexin A2 in humans.

I.2.4.9 The importance of animal models to study PCSK9

Like for all other PCs and for biological studies in general, PCSK9 animal models have exerted and are still playing a crucial role in our understanding of the *in vivo* roles of PCSK9.

Interestingly, in 2004, the year following the discovery of PCSK9, three teams reported animal models overexpressing PCSK9 by using adenoviruses. The first one reported that murine PCSK9 overexpression led to a 2-fold increase in plasma TC and a 5-fold increase in non-HDL cholesterol due to an increase in LDLc compared with mice infected with a control adenovirus. Since *Ldlr*$^{-/-}$ mice infected with the PCSK9 adenovirus had the same lipid profile, the *in vivo* link with the LDLR was established. It was also observed that LDLR mRNA levels remained unchanged upon PCSK9 overexpression whereas hepatic LDLR protein levels were nearly absent (169). The second one overexpressed human PCSK9 (hPCSK9) and observed an ~9-fold increased LDLc that they compared to the ~2-fold increased LDLc in *Ldlr*$^{-/-}$ mice, confirming the results with hPCSK9 (168). The third one reported that overexpression of human WT or GOF mutant S127R, F216L or S386A PCSK9 led to hypercholesterolemia by increasing TC ~2-fold, confirming again that PCSK9 regulates LDLR protein levels by a post-transcriptional mechanism, thereby also regulating LDLc levels (170).

An intriguing observation was that although mice overexpressing PCSK9 led to very low hepatic LDLR levels, their TC levels were still ~1.5-fold lower than *Ldlr*$^{-/-}$ mice (172). However, equivalent cholesterol levels obtained in *Ldlr*$^{-/-}$ and *Ldlr*$^{-/-}$*Pcsk9*$^{-/-}$ mice demonstrated that the cholesterol regulation of PCSK9 is entirely LDLR-dependent (172).

Alternatively, mouse models lacking PCSK9 were also developed from 2005.

Livers of *Pcsk9*$^{-/-}$ mice showed 2- to 3-fold higher LDLR protein levels but constant LDLR mRNA compared to WT mice (171, 172). Although WT mice presented 96 mg/dL TC, *Pcsk9*$^{-/-}$ mice only had 46 mg/dL, leading to an enhanced response to statin treatment (171).

Another very important study is the one relating total and hepatocyte-specific *Pcsk9*$^{-/-}$ mice presenting 42% and 27% less TC, respectively (172). This shows that hepatic PCSK9 is

responsible for two thirds of the phenotype (172). It also enabled to show that PCSK9 originates exclusively from hepatocytes (172). An intriguing discovery was that PCSK9 deficiency does not lead to cholesterol accumulation or bile acid production in the liver, although 80% of total LDLR is expressed in the liver (171, 172, 231). It remains unclear why such high levels of LDLR do not trigger a cholesterol accumulation in the liver or in pancreatic islets (232). The only possible explanation to date would be that cholesterol could be excreted through the transintestinal cholesterol excretion (TICE) pathway (233). Further studies will need to be performed to elucidate the mechanisms underlying cholesterol metabolism under those specific conditions.

Interestingly, the dramatic hepatic and pancreatic islets cell surface LDLR increase observed in *Pcsk9*$^{-/-}$ male mice was not observed in female mice (234). The latter demonstrated increases in cell surface LDLR in enterocytes and VLDLR in adipocytes, showing that PCSK9 deficiency may result in a sex- and tissue-specific subcellular distribution of both LDLR and VLDLR (234). This study is very relevant in the use of PCSK9 inhibitors, which dosage might have to be adjusted depending on sex. Indeed, a clinical trial study related a lower response to a PCSK9 mAb in women compared to men (235).

In parallel, the capacity of circulating PCSK9 to target hepatic LDLR for degradation was demonstrated in a parabiosis experiment between WT mice and transgenic mice expressing 1,000-fold endogenous levels of hPCSK9 (236). It was later established that intravenously administered PCSK9 preferentially reduces hepatic LDLR protein levels (237). However, further studies demonstrated that circulating PCSK9 can be active on peripheral tissues such as VLDLR in adipose tissue, which does not express PCSK9 (238). Interestingly, it was shown that LDLR constitutes the main elimination route of PCSK9, LDLR and PCSK9 regulations being reciprocal and controlling plasma levels of PCSK9 and LDLc as well as hepatic LDLR levels (239).

Note that in all these *in vivo* studies, mice were mostly used. However, mice don't possess the *CETP* gene (240) and thereby carry most of their cholesterol on HDL. In that sense, they are not a good model of human lipoprotein metabolism. Nevertheless, they are widely used in biological studies because they are the easiest, quickest and cheapest way to implement animal models in a laboratory setting. Interestingly, in order to determine the ideal animal models to study human dyslipidemia, a research group measured the lipid profiles of several mouse strains, non-primate species, non-human primates and humans and compared them across species (241). The measures

were performed in both healthy animals and animals with metabolic disorders, and their response to statin treatment was evaluated. They found out that the models closest to humans were non-human primates followed by dogs, while the majority of traditionally used mouse models were not similar to dyslipidemic humans (241). While cynomolgus monkeys are widely used in animal clinical trials before drugs are tested on humans, to our knowledge the only PCSK9 transgenic animal that is not a mouse is a pig (242). Interestingly, a recent study proposed a single intravenous injection of an adenovirus containing PCSK9 as an easy, fast and cheap approach to rapidly induce a sustained hypercholesterolemia in adult mice (243). This would allow avoiding the complex and time-consuming mice backcrosses, and we could imagine that this technique might be applicable to other animal models. Note that a research group recently compared the correlation between PCSK9 expression and LDLc levels in the SPRET/EiJ and C57BL/6J mice strains that are known for their polymorphic differences (244). Although SPRET/EiJ and C57BL/6J mice presented similar TC levels, the SPRET/EiJ mice expressed less PCSK9 and more hepatic LDLR. This suggests that the SPRET/EiJ mouse may be an example where genetic variations lead to an absence of direct correlation between PCSK9 and cholesterol levels, and highlights the importance of the selection of an adequate animal model.

Since adenoviruses direct the expression of their transgene (Tg) exclusively to the liver, mouse models with adenoviral expression of hPCSK9 are not ideal models because PCSK9 expression is not present in all the other tissues such as small intestine and pancreas. Transgenic PCSK9 mice have to be the closest possible to human in order to study PCSK9 or when PCSK9 inhibitors need to be screened. The models reported so far present limitations as such models. One of them expresses hPCSK9 under the control of the albumin promoter but unexpectedly led to PCSK9 overexpression in kidney (245). Another approach was the use of a bacterial artificial chromosome (BAC) fragment containing the WT or D374Y *PCSK9* gene (246). However, the WT strain is unavailable and the D374Y leads to a drastic human GOF phenotype, new mouse models are thus needed for the study of PCSK9 and its inhibition.

I.2.4.10 Role of PCSK9 in tissues other than liver

PCSK9 is mostly known for its role in hepatic LDLR levels modulation, but it has additional roles in various tissues and organs. The extensive role of PCSK9 has been described in several reviews (135, 247, 248).

- PCSK9 was shown to be expressed in the small intestine, especially in the ileum which is the final section of the small intestine (63). It is important to study the role of PCSK9 in the intestine, especially since PCSK9 was shown to modulate TICE, an important cholesterol excretion pathway, in an LDLR-dependent manner (233). In intestinal cell lines, LDLR levels are regulated by PCSK9 (249, 250). In mouse, a homogeneous PCSK9 expression along the intestinal cephalo-caudal axis was demonstrated at similar levels to that of the liver (251). In the enterocyte Caco-2 cell line and in human jejunum and ileum biopsies, immunohistochemistry analysis showed that PCSK9 is localized in enterocytes and goblet cells, which secrete mucus components (251). However, the specificity of the mouse PCSK9 (mPCSK9) antibody is questioned. Moreover, there were some contradictory studies concerning PCSK9 intestinal expression: although the ability of differentiated Caco-2 cells to secrete PCSK9 was demonstrated (250), no circulating PCSK9 could be detected in liver-specific *Pcsk9*$^{-/-}$ mice (172). Thus, a significant *in vivo* intestinal PCSK9 secretion is excluded. Although the precise molecular mechanisms leading to these effects are still unknown, several cell-based studies have shown a positive relation between intestinal PCSK9 expression level and apoB secretion (250-252).
- PCSK9 was observed to be highly expressed in β- and δ-cells from pancreas (63, 232). A group showed that in *Pcsk9*$^{-/-}$ mice, a 2-fold increase in LDLR protein content was observed in isolated islets compared to WT mice, mainly in β -cells. Conversely, incubation of islets with recombinant PCSK9 almost abolished pancreatic LDLR expression (232). Despite these findings, PCSK9 did not alter insulin secretion in mice (232). In contrast, another group demonstrated that older male *Pcsk9*$^{-/-}$ mice expressed more LDLR in pancreatic islet cells and are glucose-intolerant compared to controls (253). Although this discrepancy can be explained by the distinct mouse backgrounds and ages used in the two studies, it remains to be established whether circulating PCSK9 affects LDLR and other receptors at the surface of pancreatic islets

and whether the upregulation of these in the absence of PCSK9 results in lipotoxicity or impairment of pancreatic functions.

- PCSK9 expression was detected in the kidney (63) where it regulates murine LDLR levels (237, 254). Studies on widely used HEK293 cells suggested an interaction of PCSK9 with the amiloride-sensitive epithelial Na^+ channel (ENaC), an important pathway for the urinary Na^+ reabsorption (255), leading to its proteasomal degradation (256). However, in mice models of hypertension, PCSK9 deficiency was shown not to alter blood pressure nor ENac activity (257). The latter data is consistent with hPCSK9 genetics given that Black American carrying the PCSK9 nonsense mutation Y142X or C679X are less hypertensive than non-carriers (258).
- As stated previously, PCSK9 was cloned in apoptotic primary cerebellar neurons (63), suggesting a role in neurogenesis. This hypothesis was supported by the neural progenitor cells differentiation stimulation following PCSK9 overexpression in primary cultures of embryonic neural progenitor cells (63). Interestingly, PCSK9 inhibition in zebrafish eggs tremendously impaired the early central nervous system development as soon as 24h post-fertilization (hpf) compared to controls, and led to embryonic lethality from 48 hpf (259). However, *Pcsk9*$^{-/-}$ mice presented no signs of impaired central nervous system (171). Nevertheless, PCSK9 is implicated in mouse brain development since it was shown to downregulate LDLR levels during mice brain development (260). In human, PCSK9 could be detected in cerebrospinal fluid at levels up to 20-fold lower than in the plasma and did not show any correlation with plasma levels or diurnal variations (261). Through its interaction with apoER2 (262), PCSK9 has been demonstrated to potentiate neuronal apoptosis (263).
- PCSK9 interacts with VLDLR (238, 262, 264). Circulating PCSK9 originating from the liver regulates VLDLR protein levels in adipose tissue *in vivo*. PCSK9 is thus also implicated in fat metabolism but limits visceral adipogenesis via VLDLR regulation (238).

I.2.4.11 Role of PCSK9 in disease

Many studies demonstrated that loss of PCSK9 reduces the incidence of several physiological disorders:

- Compared to nondiabetic patients, those with T2D are exposed to >5-fold higher CVD-related mortality (265). This risk can be treated by lowering excess LDLc characterized by this T2D-associated dyslipidemia, also known as diabetic or atherogenic dyslipidemia, using statins (266). Nonetheless, statin treatment has also been associated with a higher incidence of new-onset of T2D (267-269). Many researchers thus tried to study the link between PCSK9 and T2D in several *in vitro* and *in vivo* experiments and clinical trials, resulting in conflicting data that have been reviewed by several authors (247, 248, 270, 271).

  First, several groups have conducted epidemiological studies in order to determine if there is an association between PCSK9 and T2D, presenting contradictory results. While four studies showed that PCSK9 circulating levels were up to 17% higher in T2D patients compared to healthy or type 1 diabetes (T1D) patients (219, 225, 272, 273), one study did not observe any difference in PCSK9 between T2D and healthy patients (274). Note that in the latter study, 55% of T2D patients have been newly diagnosed (274), which might explain the observed discrepancy. Besides, it should be reminded that all these studies may be biased by the use of cholesterol-lowering therapies that are known to increase circulating levels of PCSK9 (see section I.3.1.16). Despite these contradictions, it is thought that there is a positive correlation between PCSK9 levels and T2D (270). This is comforted by various *in vitro*, animal and human studies investigating the effect of insulin on hepatic PCSK9 expression in different models (275, 276) as well as hepatic PCSK9 expression in insulin resistance (275, 277) or insulin deficiency (278) models. Together, these studies demonstrated that both PCSK9 expression and plasma levels are positively associated with insulin and T2D glycemic parameters, suggesting a link between PCSK9 and insulin resistance.
- The study of WT, *Pcsk9*$^{-/-}$ or transgenic mice fed a Western diet during one year enabled to establish that PCSK9 modulates atherosclerosis via LDLR: PCSK9 overexpression is pro-atherogenic, whereas its absence is anti-atherogenic (279). Recently, it has been demonstrated in mice that PCSK9 inhibition could decrease vascular inflammation and inhibit the TLR4/NF-

κB signaling pathway, thus suppressing atherosclerosis without affecting TC levels (280). Hence, PCSK9 is suspected to be an inflammatory mediator in atherosclerosis pathogenesis.

- The R46L variant has been demonstrated to be protective against myocardial infarction (281).
- Sepsis is a complex disease in which in response to bacterial infection, systemic activation of inflammation and coagulation takes place. Severe sepsis is accompanied by at least one organ dysfunction and affects 0.3–1% Americans per year, from which ~30% die (282). Since clearance of lipids from pathogens is related to endogenous lipid clearance, it was hypothesized that PCSK9 may also regulate removal of pathogen lipids such as lipopolysaccharide (LPS). In mouse and human, several studies demonstrated that decreased PCSK9 function is associated with increased LDLR-mediated pathogen lipid clearance, decreased inflammatory response and improved septic shock outcome, while PCSK9 overexpression exacerbates multi-organ pathology as well as the hypercoagulable and pro-inflammatory states in early sepsis (283-286). It was also demonstrated that LPS is cleared from the circulation via hepatic LDLR (287), establishing the direct link to PCSK9. PCSK9 is thus also a therapeutic target for sepsis, adding an application to the cholesterol-lowering PCSK9 inhibitors (288, 289). However, recently a role of LDLR and PCSK9 in regulating LPS-induced septic shock was challenged, at least in mice (290). Indeed, in PCSK9 KO mice or in WT mice treated with a PCSK9 mAb, no reduction in LPS-induced death was observed (290).
- Since liver is both one of the most common sites for metastatic disease and the major tissue expressing PCSK9, the role of PCSK9 was investigated in liver metastasis. It was observed that after melanoma cells injection to induce liver metastasis, *Pcsk9*$^{-/-}$ mice presented 2-fold less liver metastases than WT mice. This decrease is linked to cholesterol because a 2-week high cholesterol diet in *Pcsk9*$^{-/-}$ mice deleted this protection, and high cholesterol levels were shown to promote metastasis progression in both groups. An LDLR-independent TNFα regulation was also observed. Thus, PCSK9 deficiency decreases liver metastasis by its cholesterol-lowering effect and possibly by TNFα-mediated apoptosis enhancement (291).

- The role of PCSK9 in Alzheimer's disease (AD) is controversial. A first group showed that *Pcsk9*$^{-/-}$ mice presented less beta-site amyloid precursor protein-cleaving enzyme 1 (BACE1) and amyloid beta-peptide (Aβ) than control mice (292). BACE1 is the rate-limiting enzyme in the generation of Aβ that are the main components of the amyloid plaques found in AD patients brains. This data indicates that the absence or therapeutic inhibition of PCSK9 might increase the risk of AD development in human. However, two years later a second group published that PCSK9 was not involved in LDLR, VLDLR or ApoER2 degradation nor BACE1 degradation in adult mouse brain (293). A recent study of >111,000 patients from the Danish general population showed that low LDLc due to PCSK9 and HMGCR variants were not linked to higher risk of AD (294). Strikingly, they even discovered that low LDLc levels may reduce AD risk (294). Although there is a "need for more robust evidence" (295), the onset of AD and other neurocognitive diseases is closely followed by clinical trials testing PCSK9 inhibitors. For now, the inhibiting agents seem safe but this needs to be assessed in long-term studies. Nevertheless, further studies need to be achieved in order to better understand the role of PCSK9 in AD.

In contrast, some studies highlighted that loss of PCSK9 favored some disorders:

- Given that LDLR is suspected to be involved in hepatitis C virus (HCV) entry, some researchers established that PCSK9 modulates CD81, a major HCV liver receptor, in an LDLR-independent manner in HuH7 cells (296, 297). Note that HuH7 cells are another human hepatocarcinoma cell line very similar to HepG2 (298). Interestingly, cells expressing PCSK9 were resistant to HCV infection (296, 297). Mouse liver CD81 expression was also down-regulated by PCSK9 *in vivo*, thus PCSK9 plasma levels and activity may influence HCV infectivity in humans (296). These studies highlight an antiviral role for PCSK9. However, it also raised concerns about the pharmacological inhibition of PCSK9 that would increase patients HCV susceptibility. Other researchers showed contradictory data: in their cell-based and *in vivo* studies, neither PCSK9 overexpression nor PCSK9 inhibition with a PCSK9 mAb had any effect on CD81 or HCV entry (299). This study is supported by clinical data that do not relate PCSK9 inhibition to HCV susceptibility so far. However, long-term studies on a

large number of patients will have to confirm the safety of PCSK9 inhibition towards HCV infection, especially for genotype 3 HCV patients (300).

- Since PCSK9 was shown to be upregulated in regenerating rat liver (63), the *in vivo* role of PCSK9 in liver regeneration was investigated by performing PHx on WT and *Pcsk9*$^{-/-}$ mice (172). PCSK9 mRNA peaked 3 days post-PHx in mice, whereas it peaked at day 2 in the rat. While the livers of WT mice regenerated well 3 days post-PHx and had a normal morphology, livers from KO mice presented a compromised regeneration as well as necrotic lesions. Interestingly, this difference between WT and KO mice could be prevented by a high cholesterol diet. Therefore, patients lacking PCSK9 naturally or following a PCSK9-lowering treatment might be at risk upon hepatic damage (172).

I.2.4.12 PCSK9 regulation

Similar to any gene, *PCSK9* gene expression is first regulated transcriptionally. PCSK9 was shown to be regulated by SREBP1a (167), SREBP1c (276) and SREBP2 (167, 301). SREBP activation of *PCSK9* gene promoter is potentiated by the hepatocyte nuclear factor-1α (HNF1α). *PCSK9* is also regulated by ligand-activated nuclear receptors such as the Farnesoid X receptor and peroxisome proliferator-activated receptors (PPAR) α or γ (302). Note that SREBP2 and HNF1α are mostly downstream targets of other factors. Taken together, the transcriptional up- or downregulation of *PCSK9* is determined by the relative abundance and activity of a variety of nuclear factors cooperatively or competitively acting on *cis* regulatory elements (174). To date, the physiological importance of these regulatory pathways is still unknown.

The post-transcriptional regulation of PCSK9 expression have been less studied but might include microRNAs (miRNAs) such as miR-27a (303) or miR-30c (304).

Once secreted, an important regulation of PCSK9 is its cleavage and inactivation by the PC furin, which is reduced by the two GOF mutations F216L and R218S (305). The processing site of furin on PCSK9 is at $R_{218}\downarrow$ and was shown to inactivate PCSK9 in mice (306) and human (307), cleaving up to 40% of total circulating PCSK9. Interestingly, a mAb named LY3015014 binding a narrow epitope in the N-terminal part of PCSK9 catalytic domain (aa 160-181), which does not include the furin cleavage site, was developed (308). Different from the other available mAbs (see

I.3.2.1), the latter binds intact but not truncated PCSK9, thereby extending the LDLc lowering durability relative to mAbs that block the furin processing site (308).

I.2.4.13 PCSK9 and evolution

Interestingly, PCSK9 is neither found in all vertebrates nor in all primates (309). It has been demonstrated that the bovine PCSK9 genome contains a stop codon in exon 10 (310), leading to undetectable PCSK9. The latter constitutes very important information, given that fetal bovine serum (FBS) is routinely used in cell culture. Besides, the primary protein sequence of PCSK9 has been shown to be very conserved within the years that separate modern humans from either Denisovans (estimated separation ~380,000–473,000 years ago) or Neanderthals (estimated separation ~550,000–765,000 years ago) (311). However, one amino acid change, H449L, was recently detected in Denisovans that may result in a LOF of PCSK9 (135).

I.2.5 PCs as therapeutic targets

Given their largely demonstrated important roles in many vital biological processes, many PCs have been considered as therapeutic targets in order to treat some of their related diseases as illustrated by Figure 14.

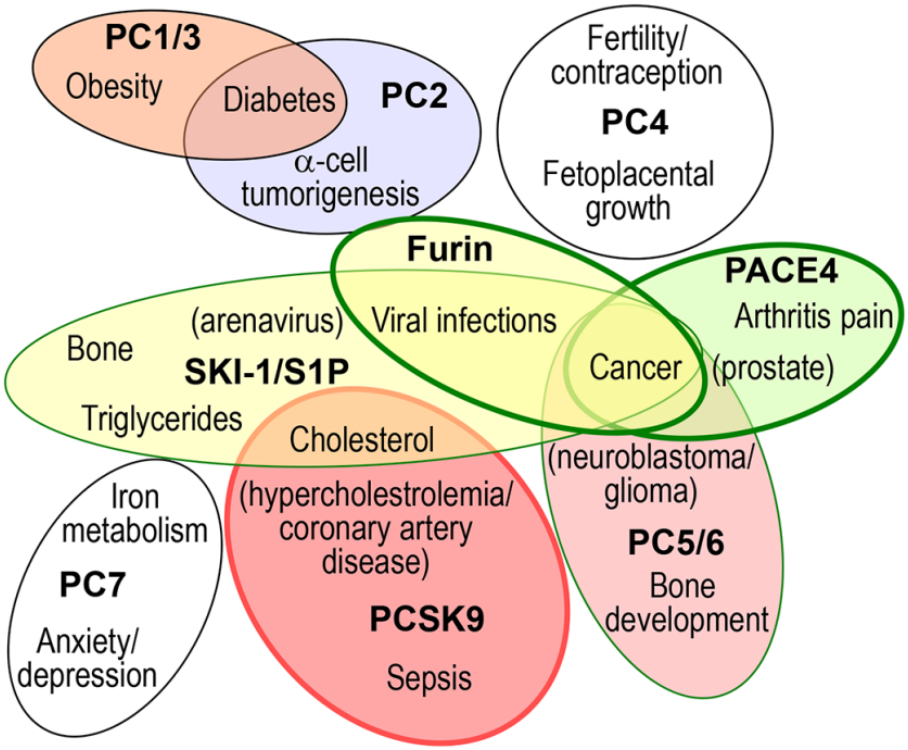

Figure 14. Scheme representing all proprotein convertases in health and diseases (135)

PACE4 is an established therapeutic target in order to treat ovarian and prostate cancer using peptide inhibitors (312, 313). It shows promising results in mice and has potential to be tested in humans. It is also indicated to inhibit PACE4 for the management of arthritis pain (314, 315).
PC4 could be targeted to create a male contraceptive (132).
It was also suggested that small-molecule inhibitors to PC7 able to cross the blood–brain barrier might be used to manage anxiety (132).
The use of a small molecule inhibitor of SKI-1, PF-429242, showed efficient inhibition of SREBP processing and decreases of SREBP target genes expression and cholesterol synthesis in cell lines (316). In treated mice, expression of hepatic SREBP was suppressed and thus the rates of

cholesterol and fatty acids synthesis were reduced (316). Short-term treatments with this inhibitor were suggested for management of viral infections such as arenavirus (317, 318), HCV (319) and Dengue virus (320). Interestingly, osteocytes-specific *MBTPS1* inactivation has been shown to stimulate soleus muscle regeneration and to increase muscle size and contractile force with age, making SKI-1 a potential target for prevention of age-related muscle loss (321).

Furin inhibition can target a wide range of therapeutic applications, including cancer, virus infections or rheumatoid arthritis. In a phase 1 clinical trial, a vaccine named FANG or "bi-shRNAi^{furin}/GMCSF DNA/Autologous Tumor Cell" containing a bi-functional short hairpin RNA interference (RNAi) targeting furin and a plasmid encoding granulocyte-macrophage colony-stimulating factor was injected to advanced cancer patients and prolonged their survival (322). Similarly, luteolin, a natural product, limits dengue virus replication by inhibiting furin (323). Inhibitors to furin and PC5A have also shown promising results in limiting Chikungunya virus infection (324). In contrast, it has been shown that upregulating furin may be beneficial in the treatment of rheumatoid arthritis (325).

Finally, PCSK9 can be considered as the therapeutic target amongst all PCs with the most specific physiological functions. Indeed, although it was the last PC family member to be discovered, therapeutic approaches to inhibit PCSK9 are the most numerous as well as the most advanced. They will be detailed in the next section I.3.2. Overall, although therapeutic targeting of the eight other PCs might be beneficial, it might lead to many off-target effects.

I.3 How to treat hypercholesterolemia?

Various strategies have been used in order to decrease TC or at least decrease LDLc and/or increase HDLc, the main goal being the reduction of CVD risk. The Canadian Cardiovascular Society Guidelines recommended LDLc levels < 77 mg/dL (2.0 mM) or a > 50% reduction from baseline (326). Similarly, European guidelines fixed target LDLc levels ~100 mg/dL (2.6 mM) or 50% reduction from baseline for very high risk patients (327). In contrast, the American Heart Association recommended high- or moderate intensity statin therapy for all patient groups in which they expect LDLc reductions ≥50% or 30%-50%, respectively (328). Note that interestingly, guidelines differ in each country (329).

First, classical therapies to reduce hypercholesterolemia will be presented. In a second part, the different approaches that have been used to decrease CVD by targeting PCSK9 will be detailed.

I.3.1 Available treatments to prevent CVD

I.3.1.1 Benefits of a healthy diet

In order to reduce circulating cholesterol levels, it was first thought that reducing dietary cholesterol intake would be enough. Importantly, dietary cholesterol is not the only factor acting on our cholesterol levels. The total caloric intake as well as the amount of saturated versus unsaturated fatty acids and soluble fiber are factors that also contribute to TC. A combination of changes needs to be achieved and maintained on the long-term in order to maximize the cholesterol reduction and thus CVD risk (330).

It has been shown that a Mediterranean-style diet reduces LDLc and PCSK9 levels up to 10% and 11%, respectively (331, 332). Although the precise mechanisms of diet-induced LDLc decrease are not fully understood yet, it was hypothesized that the high phytosterols (see section I.3.1.4) intake might decrease LDLc levels by inhibiting cholesterol intestinal absorption (333). Similarly, a diet rich in vegetable n-6 polyunsaturated fatty acids versus saturated fatty acids showed reduction in both LDLc and PCSK9 (334). Besides, some specific foods such as tree nuts (335) and flavonoids from dark chocolate (336) also exhibit potential benefits in CVD reduction,

although they should be further studied in larger groups of patients. Interestingly, those effects were mostly observed independently of body weight loss. Fasting has been shown to decrease circulating levels of PCSK9 in human (222, 337). In contrast, an increase in PCSK9 was observed after a short-term high fructose diet (277).

I.3.1.2 Benefits of exercise

It has been demonstrated that exercising regularly has a beneficial effect on human lipoprotein profile. However, except in a group of patients exercising a lot and with a high intensity, there was no decrease in LDLc levels but rather an increase in LDL particle size and a decrease in IDL (338). The benefits of exercise have also been demonstrated to reduce circulating levels of PCSK9 (339).

I.3.1.3 Challenges of lifestyle modifications and new approaches

The drawback of lifestyle modification such as a healthier diet and more exercise is that it is sometimes difficult to implement for patients (Dr. Robert Dufour, IRCM clinic, personal communication). While it works for some patients, it is a challenge for others, especially when hypercholesterolemia is discovered late in the life of patients, at a time when "old habits" need a high determination and motivation to be changed drastically. Therefore, other approaches are necessary when lifestyle modification is not followed seriously or when it is not sufficient to reduce CVD risk.

Mobile applications on smartphones are promising tools to help patients perform lifestyle modifications or adhere to treatment. A recent study showed that this type of technological tool helped patients to exercise more and to be more aware of diet, although it was not useful to help patients reach target LDLc levels (340). Another study demonstrated modest benefit of application-based interventions to improve diet, physical activity and sedentary lifestyles (341). More studies need to be done in the future to know if these tools could be helpful.

I.3.1.4 Phytosterols

One of the approaches to reduce circulating cholesterol is to reduce its absorption by the intestine. This can be achieved naturally by the addition of phytosterols to the diet and can reach 10% LDLc

reduction (342). Phytosterols include plant sterols and stanols and constitute the structural and functional components of the plants cellular membranes. Their structure is very close to cholesterol and they are found at high concentrations in plant oils and nuts and less concentrated in cereals, legumes, fruits and vegetables (343). Briefly, since phytosterols are more hydrophobic than cholesterol, they displace cholesterol from mixed micelles (344). This replacement leads to a decrease of micellar cholesterol concentration, which is followed by a lower cholesterol absorption (345). The unabsorbed cholesterol is then eliminated from the body via excretion in faeces (346). More recently, the mechanism of cholesterol absorption decrease was shown to be more complex and to influence cholesterol metabolism: notably, phytosterols also increase hepatic LDLR levels (347, 348). An important advantage of this approach is that it is easy to implement: an intake of 2-2.5 g/day of phytosterols-enriched products can reduce LDLc up to 14% without any reported side effects (347). A study on 46 healthy hyperlipidemic patients demonstrated that a "dietary portfolio" rich in plant sterols, soy proteins, viscous fibers and almonds reduced LDLc by up to ~30% (349). Interestingly, this decrease was similar to the one observed in the group treated with statins under a diet composed of whole-wheat cereals, low fat dairies and very low intake of saturated fats (349). Finally, phytosterols do not seem to influence PCSK9 levels (www.pcsk9forum.org/phytosterols-do-not-influence-pcsk9-levels/).

I.3.1.5 Ezetimibe

Another approach is the use of ezetimibe, which blocks cholesterol absorption by selectively inhibiting NPC1L1 in the small intestine (350). NPC1L1 expression and promoter activity are modulated by cholesterol in a SREBP2-dependent mechanism (351). NPC1L1-defficient mice present ~80% less cholesterol absorption compared to WT mice (352). In humans, ezetimibe can decrease cholesterol absorption up to 50% (353) and LDLc up to 20% (354). The crucial role of NPC1L1 was demonstrated in a study showing that patients presenting a mutation in *NPC1L1* gene have nearly 90% less CVD risk compared to patients without mutation (355), which was similar to WT mice or rats treated with ezetimibe (356, 357).

The Improved Reduction of Outcomes : Vytorin Efficacy International Trial (IMPROVE-IT) clinical trial showed that the addition of ezetimibe to statin therapy led to a 24% incremental

lowering of LDLc and improved CVD outcomes (358). No adverse events or toxic effects were reported, underlining the excellent safety of ezetimibe.
However, ezetimibe has been shown to rapidly increase PCSK9 levels within 3 days by 124% in rats (359) and by 29% at day 1 and 39% at day 3 in human (360).

I.3.1.6 Fibrates

Fibrates are used to reduce TG and increase HDLc (361). Briefly, their mechanism of action is based on their ability to alter the transcription of genes encoding proteins controlling lipoprotein metabolism. Fibrates are agonists of the PPAR, which is involved in the transcription and synthesis of apoA-I and A-II, the major HDL apo. Fibrates also increase LPL and decrease apo-CIII synthesis. They also lead to enhanced fatty acids uptake which reduces TG synthesis and results in less VLDL secretion (362, 363).
The beneficial effects of fibrates are controversial. On one hand, a clinical study showed that the addition of fenofibrate to statin treatment in 5,518 patients with T2D did not decrease the number of CVD (364). On the other hand, a systematic review and meta-analysis of 18 trials providing data for 45,058 patients showed that fibrates reduce major CVD events by preventing coronary events (365). Fibrates influence PCSK9 expression indirectly via cholesterol levels control. Treatment with fibrates in 19 patients has shown decreases of TC and LDLc by 11% and ~4%, respectively and increases of HDLc and PCSK9 by ~16% and 17%, respectively (366). Their drawback is their side effects, notably their risk of rhabdomyolysis (367, 368).

I.3.1.7 Chinese traditional drugs

Xuezhikang is an extract of red yeast rice containing a lovastatin-like compound and other compounds. Its long term use (~4.5 years) has been shown to reduce all causes of CVD-linked mortality by ~36%, with reductions in TC, LDLc and TG of ~11%, ~17% and ~11 %, respectively as well as HDLc increase ~5% (369, 370). The drawback of this drug is that it is still in the process of Food and Drug Administration (FDA) approval (371) and that adverse events are similar to those with statins. Thus, it increases PCSK9 levels in rats and humans by up to 55%, 3 days post-treatment. Interestingly, the combination of xuezhikang with ezetimibe did not further increase PCSK9 levels compared to either monotherapy (359, 360).

Berberine is a natural isoquinoline alkaloid widely used in Chinese medicine and isolated from medicinal plants such as *Coptis chinensis*, *Berberis aquifolium* and *Berberis aristata*. Its pharmacological applications are numerous and include LDLc reduction (372). Interestingly, berberine decreased both PCSK9 mRNA and protein levels in HepG2 cells (373), which has been shown to be mediated by HNF1α and SREBP2 (374). In clinical trials, berberine displayed TC, LDLc and TG decreases as well as HDLc slight increase (375).

I.3.1.8 Statins

Statins are the most largely used cholesterol-lowering drugs. They inhibit HMGCR competitively by mimicking HMG and hence prevent the binding of HMGCR to HMG-CoA. This drug was extracted from fungi and is used since 1987 and improved quality of life by decreasing CVD (376-380). There are many types of statins: in USA, seven statins are approved for use: atorvastatin (Lipitor), fluvastatin (Lescol, Lescol XL), lovastatin (Mevacor, Altoprev), pravastatin (Pravachol), rosuvastatin (Crestor), simvastatin (Zocor) and pitavastatin (Livalo). Overall, they are considered to be similar. After one year statin treatment, LDLc levels were reduced from 143 to 102 mg/dL (3.70 to 2.63 mM) in more than 129,000 patients from 21 clinical trials, and this lowered CVD risk by >20% (43). However, statin therapy presents some drawbacks.

First, they present many adverse events leading some patients to discontinue the treatment. A large part of statin adverse events (72%) is related to muscle-related symptoms (381), which can lead to rhabdomyolysis, which is characterized by muscle necrosis and release of creatine kinase in

plasma and of myoglobin in urine (382). It is accompanied by symptoms such as muscle weakness, fatigue and pain. Various factors such as age, body mass index, renal, hepatic or thyroid dysfunction, hypertriglyceridemia and alcohol or drugs consumption may predispose some patients to develop statin-induced rhabdomyolysis (383). These adverse events are present in statin monotherapy and even more in combinational therapies in which the efficiency of statins is ameliorated. However, for some patients, muscle pain is attributed to statin treatment because of psychosomatic reasons or misattribution of the pain source (384). This highlights the importance of differentiating statin-related muscle pain from symptoms caused by concomitant factors.

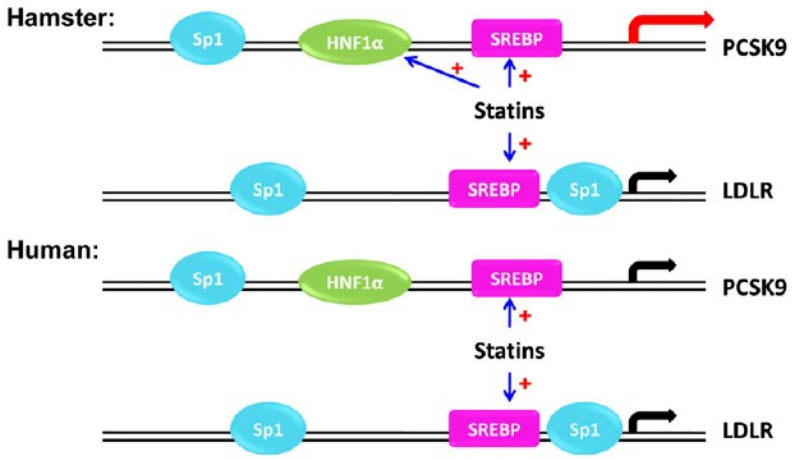

Figure 15. Mechanism of PCSK9 upregulation upon statin treatment (385)

Second, even with maximal dosage of statins, some high risk patients cannot reach optimal LDLc levels. This could be explained by the fact that statins directly increase PCSK9 expression. In HepG2 cells and human primary hepatocytes, five different statins upregulated the mRNA levels of PCSK9 (386). In dyslipidemic hamsters, the same was shown and the mechanism elucidated: this upregulation takes place through HNFα and SREBP2 in hamsters and through SREBP2 only in humans, as indicated on Figure 15 (385). Treatment with atorvastatin in 19 patients has shown decreases of TC and LDLc by 25% and 38%, respectively and increases of HDLc and PCSK9 by ~8% and 7%, respectively (366). These upregulations have been demonstrated to occur rapidly, namely already within one day of treatment (360, 387). This suggests that SREBP2 activation

increases PCSK9 synthesis. Accordingly, LOF mutations in PCSK9 were associated with increased responsiveness to statins (388, 389).

I.3.1.9 CETP inhibitors

CETP has been a popular drug target in order to increase HDLc and thus decrease LDLc levels. However, the fate of CETP inhibitors is quite unsuccessful. Torcetrapib reduced LDLc as expected, but presented the off-target effect of blood pressure increase, raising CVD events and mortality (390). Dalcetrapib only had a slight decreasing effect on HDL and did not affect LDLc. Its clinical use was thus interrupted (391). Evacetrapib seemed to be more potent than previous CETP inhibitors with 128% HDLc increase and 35% LDLc decrease. However, its phase 3 clinical trial showed no significant reduction in CVD events or mortality (392). The drug will thus not be marketed. One other CETP inhibitor, anacetrapib, seems safe and promising so far and is under active investigation (393, 394). A phase 3 clinical trials was recently published and showed LDLc reductions of 37% and HDLc increase of 118% (395). Studies showing the effect of anacetrapib on clinical outcomes such as CVD events are ongoing (NCT01252953) and their results should be known in 2019.

I.3.1.10 Bile acid sequestrants

Bile acid sequestrants have the ability to bind bile acids in the intestine and thus to deviate them from the enterohepatic circulation. Hence, the liver is deleted of bile, upregulating the conversion of cholesterol to bile acids. The hepatic cholesterol pool is therefore depleted, enhancing LDLR activity and reducing LDLc (396). When administered daily at doses of 24 g cholestyramine, 20 g colestipol or 4.5 g colesevelam, LDLc reduction of up to 25% can be reached (397). Bile acid sequestrants can be used as monotherapy for low risk patients or in combination with statins to enhance its potency (398) to reduce CVD. Unfortunately, their use is limited because of gastro-intestinal side effects and drug interactions.

I.3.1.11 ApoB antisense

Another strategy to reduce hypercholesterolemia is to directly inhibit the synthesis of apoB. This can be achieved by antisense oligonucleotide (ASO) such as mipomersen which concentrates in the liver and binds to apoB mRNA (399). The aim is to block the synthesis of apoB-containing lipoproteins by preventing apoB mRNA translation, the bound mRNA being degraded by hepatic RNAse. Subcutaneous injection of mipomersen every week reduced apoB and Lp(a) by ~30% (400). An advantage of this technique is that it does not require LDLR and can thus be used in HoFH (401). However, its side effects are numerous and longer-term studies are needed to evaluate them. For now, mipomersen is approved in the USA only in HoFH (402). Antisense technology is also promising in the inhibition of apoC-III to treat hypertriglyceridemic patients (403) .

I.3.1.12 Lomitapide

MTP has been targeted in order to reduce the synthesis of apoB-containing lipoproteins (400). Lomitapide is an oral MTP inhibitor able to reduce LDLc by up to 50% in HoFH (404, 405). It is approved for HoFH in addition to diet and drug therapy. However, elevated liver enzymes and hepatic steatosis raise concerns about its long-term use (406). A recent study is contradictory to this and showed very good safety profile for lomitapide (407).

I.3.1.13 LDL apheresis

For some patients, such as HoFH, more aggressive measures are needed if target LDLc levels are not reached despite maximal dosage of lipid-lowering drugs such as statins. In those cases, LDL apheresis can be performed. It consists in separating patients plasmas in order to selectively remove apoB-containing lipoproteins, yielding LDLc decrease between 25 to 60% (408-410). The drawback of this technique is that LDLc levels come back to pre-treatment levels 12 to 14 days later (411). However, the advantage is that LDL is selectively removed, while HDL is unchanged and adverse events are rare (410, 412, 413). Long-term effect of LDL apheresis in FH patients has shown a ~4-fold decrease in relative risk for CVD and a 20-fold decrease in relative risk for cardiac interventions (414).

I.3.1.14 Niacin

Niacin (nicotinic acid or water-soluble vitamin B_3) can be found in foods such as turkey or peanuts and was initially used as a therapeutic agent to prevent its deficiency disorder, pellagra, in the 19th century. Its administration showed several beneficial lipid-modifying effects, including lowering of all apoB-containing lipoproteins known to cause atherosclerosis (415). Its administration led to decreases in LDLc, TG, VLDLc and Lp(a) of 13%, 24%, 45% and 35%, respectively and HDLc increase of 44% (416). These reductions were accompanied by reductions in CVD, including atherosclerosis (417). Although these results look promising, the routine use of niacin is limited because of its several adverse effects including flushing, gastrointestinal and metabolic adverse effects (418). However, niacin therapy should be further studied because it has a unique advantage: it is the only lipid-lowering drug that decreases PCSK9 levels ~15% when used in combination with statin and fibrate that increase PCSK9 levels. Thus, the LDLc decrease might be due partially to the PCSK9 decrease (419).

I.3.1.15 Inhibitors of ATP-citrate lyase

A more recent approach to reduce LDLc using oral small molecules is the inhibition of ATP-citrate lyase (ACLY) (420). The cytoplasmic ACLY produces acetyl-coA for *de novo* synthesis of fatty acids and cholesterol. Therefore, ACLY inhibition leads to reductions in acetyl-coA synthesis and thus in substrates for both cholesterol and fatty acid synthesis. Bempedoic acid (ETC-1002 or 8-hydroxy-2,2,14,14-tetramethylpentadecanedioic acid) (421) is the only ACLY inhibitor that is currently in clinical trials. When administered to hypercholesteraemic patients who are statin intolerant or have T2D in phase 2 clinical trials, LDLc reductions from 28% to 43% were obtained (422-424). Although results from phase 3 clinical trials are waited to assess the long-term efficacy on CVD outcome, this new approach seems promising and can be used in combination with other lipid-lowering agents, for example ezetimibe (425).

I.3.1.16 Limitations of lipid-lowering treatments

In this section, the effect of various lipid-lowering drugs on PCSK9 levels has been described. This topic has also been reviewed by several authors (359, 360, 426, 427). This upregulation is a factor limiting the efficiency of statins, fibrates, ezetimibe, xuezhikang and berberine. Therefore, many of these therapies could largely benefit from PCSK9 inhibition.

I.3.2 Targeting PCSK9 to reduce CVD

Since PCSK9 was considered a valid and safe therapeutic target to treat FH and prevent CVD, many different techniques have been used in order to reduce PCSK9 levels, inhibit its action towards LDLR or suppress its expression. The majority of these approaches are described in this section and more details can be found in several reviews (428-431).

I.3.2.1 Monoclonal antibodies targeting PCSK9

The first approach developed to inhibit PCSK9 is also the only one marketed so far: mAbs preventing its binding to LDLR and its subsequent degradation. In 2009, just 6 years following the discovery of PCSK9, both *in vitro* (432) and an *in vivo* (189) studies demonstrated that it is possible to disrupt PCSK9 binding to LDLR and hence to reduce circulating LDLc levels. In the *in vitro* study, surface plasmon resonance assays showed that three polyclonal antibodies to mature PCSK9 or PCSK9 peptide sequences known to be crucial for LDLR binding could prevent the binding of PCSK9 to LDLR. In HepG2 cells either exposed to exogenous PCSK9 or overexpressing it, those antibodies could restore LDL uptake, demonstrating their inhibition of PCSK9 activity. Interestingly, these antibodies also prevented the interaction of the GOF D374Y PCSK9 with LDLR (432). Two of these antibodies were shown to bind regions of PCSK9 catalytic domain involved in its binding to LDLR, while a control antibody which did not alter PCSK9 binding to LDLR bound PCSK9 CHRD (432). This study constitutes the first proof-of-concept that PCSK9 inhibition can be used to lower LDLc levels. It was very rapidly followed by an *in vivo* study reporting a mAb binding an epitope on PCSK9 close to the region involved in LDLR binding (189). The latter mAb, which is fully humanized and directed against hPCSK9, was obtained after immunization of mice engineered to express fully human IgG antibodies (189). It was also shown to disrupt PCSK9 binding to LDLR and to decrease PCSK9-dependent LDLR degradation as assessed by LDLR protein levels estimation and LDL uptake (189). Cell-based assays in HepG2 evaluating the effect of this mAb in combination with a statin showed higher LDLR levels than either treatment alone. The mAb was injected in WT mice and increased ~2-fold liver LDLR levels, while reducing TC up to 36%. *Ldlr*$^{-/-}$ mice were also injected with the mAb as controls and did not show any effect (189). When injected to cynomolgus monkeys, an LDLc reduction of 80%

was observed and maintained for 10 days (189). This study constituted the first *in vivo* proof-of-concept that mAbs targeting PCSK9 catalytic domain can reduce hypercholesterolemia.

These two studies were rapidly followed by the development of mAbs targeting PCSK9 catalytic domain in order to inhibit the extracellular activity of PCSK9. Many pharmaceutical companies simultaneously competed to bring such mAbs to clinical trials in humans. The first results of a phase 1 clinical trial with a PCSK9 mAb were published in 2012 by the company Sanofi/Regeneron with their mAb REGN727 (alirocumab) (433). It demonstrated that LDLc reductions up to 60% could be reached upon intravenous or subcutaneous injection of REGN727 in healthy, FH and non-FH patients (433). Note that there was no treatment discontinuation due to adverse events, indicating the safety of the mAb.

Other companies developed mAbs, such as evolocumab from Amgen and bococizumab from Pfizer, that were the most advanced ones.

Since 2015, two mAbs, evolocumab and alirocumab, which tradenames are Repatha and Praluent, respectively, are commercially available in the United States and in Europe (434). Injected subcutaneously every 2 or 4 weeks at a dose of 140 mg, they achieve a ~60% LDLc decrease for up to 4 years treatment (see Figure 16), which resulted in 10 to 15% reduced CVD according to very recent reports (435-437). Unexpectedly, mAbs to PCSK9 also decrease Lp(a) (438). Note that in a vast majority of clinical studies, mAb therapy was added to statin therapy.

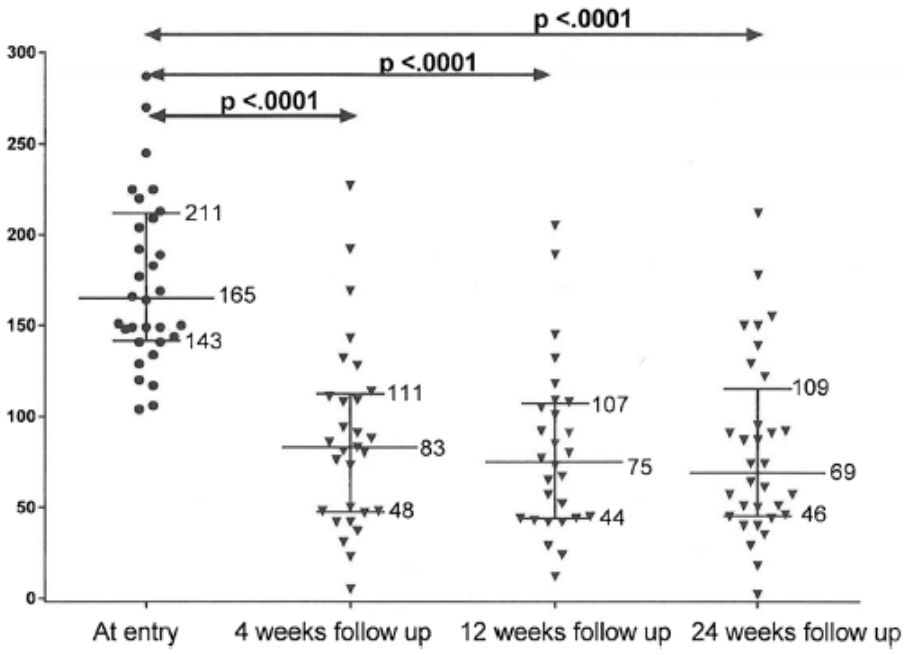

Figure 16. Median, 25th and 75th percentile LDLc (mg/dL) at study entry and 4, 12 and 24 weeks follow-up on evolocumab 140 mg every two weeks (437)

Bococizumab was supposed to be the third mAb to be marketed but it was discontinued in November 2016 because of anti-mAb antibodies formation that led to both reduced efficiency and side effects (439). This is probably due to the fact that bococizumab is a humanized antibody, whereas evolocumab or alirocumab are fully human.

Another humanized mAb, LY3015014 from Eli Lily, mentioned earlier for its ability to bind to intact but not truncated PCSK9 (308) is also advanced in clinical trials. Its phase 2 was published in 2016 and showed that subcutaneous injections of 300 mg every 4 or 8 weeks led to LDLc reductions of ~50% and ~37%, respectively (440). Although its efficiency in terms of LDLc decrease is slightly lower than evolocumab and alirocumab, LY3015014 presents an advantage compared to the two other mAbs in that it can be injected every 4 or 8 weeks versus 2 or 4 weeks. However, although LY3015014 looks promising and has no reported safety issues so far, long-term effects on CVD still need to be determined in large phase 3 clinical trials which, to our knowledge, were not reported yet and are not in recruitment period (https://clinicaltrials.gov). Given that LY3015014 is also a humanized mAb, the formation of auto-antibodies will need to be carefully followed in order to avoid the repetition of bococizumab fate.

Note the exceptionally rapid "bench to bedside" transition of PCSK9 inhibition: only 14 years after PCSK9 discovery, patients suffering from FH and high CVD risk can already benefit from PCSK9 inhibitors that efficiently decrease their LDLc levels and have the potential to lengthen their average life expectancy, although further studies are still ongoing to assess the long-term benefits of this new type of therapy (437, 441, 442). This huge scientific advancement is the result of a very big amount of work by many research teams worldwide, both in academia and in the pharmaceutical industry and would not have been possible without the collaborative spirit many scientists have demonstrated.

Some concerns about PCSK9 mAbs include notably the risk of developing neurological disorders (295) or diabetes (443). The limitations of these mAbs are that the FDA allowed their use in patients with FH and with CVD who receive maximally tolerated statin therapy and require further LDLc lowering. Although PCSK9 mAbs are very valuable therapeutics, their high costs remain a drawback and means that their use will be restricted to specific patient populations (444, 445). Therefore, there is a need for more accessible therapies targeting PCSK9.

I.3.2.2 Adnectins targeting PCSK9

In 2014, another way to neutralize plasma PCSK9 extracellular activity was the use of injectable adnectins as small protein biologics alternative to PCSK9 mAbs. Adnectins are a relatively new family of therapeutic proteins based on the 10th fibronectin type III domain that bind targets with the same affinity and specificity as mAbs, are easier to genetically engineer and compatible with bacterial expression systems (446). PCSK9-binding adnectin (BMS-962476) is a ~11 kDa polypeptide conjugated to polyethylene glycol (PEG) to enhance its pharmacokinetics. BMS-962476 showed up to 35% TC decrease in transgenic mice overexpressing 500 µg/mL hPCSK9, which was accompanied by a rapid decrease to near zero in circulating PCSK9 after 3 and 6 hours injection, returning to baseline after 24 hours (447). When injected to cynomolgus monkeys, BMS-962476 reduced LDLc ~35% and circulating PCSK9 >99%, which was followed by a 6-fold increase in PCSK9, indicating a slow clearance of BMS-962476 - PCSK9 complex (447). A phase 1 clinical trial was completed in 2013 (https://clinicaltrials.gov/) but no results were published.

I.3.2.3 PCSK9 expression inhibitors

Another proposed approach is to directly inhibit PCSK9 mRNA expression. To that end, several PCSK9 ASO and small interfering RNA (siRNA) have been developed.

Administration of a PCSK9 ASO (ISIS 394814 from Isis Pharmaceuticals) was reported in 2007 in hyperlipidemic mice fed a high fat diet and reduced TC by 53% and LDLc by 38%, while increasing liver LDLR protein levels 2-fold after 6 weeks of treatment (448). The use of anti-PCSK9 bridged nucleic acids (BNA), which are modified RNA nucleotides, showed reduction in hepatic PCSK9 mRNA and 43% reduction in LDLc after 6 weeks of bi-weekly injections in mice (449). In 2012, several locked nucleic acid ASO (LNA ASO) to PCSK9, another form of modified RNA nucleotides, have also been developed. One of them led to ~ 60% decrease in PCSK9 mRNA levels associated with an up to 3-fold increase in liver LDLR levels in mice (450). Two other ones, SPC5001 and SPC4061 from Santaris Pharma, were injected in nonhuman primates and led to 85% reduction in circulating PCSK9 and PCSK9 mRNA as well as 50% reduction in LDLc and TC (451). The agents presented no toxicology issues, making PCSK9 LNA ASO a viable therapeutic approach which brought it to clinical trials. In 2011, a phase 1 was conducted with SPC5001, which results were reported in 2015 (452). Unfortunately, although SPC5001 led to efficient PCSK9 and LDLc decreases, the study had to be terminated because of injection site reactions and renal tubular toxicity (452). This suggests that further studies need to be conducted on the side effects of such compounds.

In parallel, the use of siRNA targeting PCSK9 was proposed and its first report published in 2008 by the company Alnylam Pharmaceuticals (453). They developed a siRNA formulated in a lipidoid nanoparticle (LNP) (454) named ALN-PCSsc or inclisiran, which achieved liver-specific PCSK9 silencing by decreasing PCSK9 mRNA up to 70% and TC by 60% during 3 weeks after a single injection in mice and rats. In nonhuman primates, injection of 3 mg/kg inclisiran resulted in >80% lower circulating PCSK9 and 60% lower LDLc levels lasting more than 30 days, with a slow return to baseline up to 120 days after administration (453). Recently, another group reported a similar compound which showed a 2-month lasting 90% PCSK9 silencing and 50% LDLc decrease after a single injection in cynomolgus monkeys (455). Subcutaneous injections of inclisiran was then tested in human in a phase 1 clinical trial and led to 70% and 40% lower circulating PCSK9 and

LDLc, respectively, without safety issues (456). Recently published phase 1 and phase 2 clinical trials showed that single or double doses ≥300 mg inclisiran led to >70% or ~50% LDLc reduction and 60% or ~55% PCSK9 reduction lasting 84 or 240 days, respectively (457, 458). The phase 3 clinical trial of inclisiran was announced in April 2017 (https://www.dddmag.com). Importantly, although inclisiran presents similar LDLc-lowering effects to mAbs, it could be administered every 3 to 6 months, which would present a net advantage over mAbs.

I.3.2.4 PCSK9 functional activity blockers

Another proposed approach is to block PCSK9 binding to LDLR by using LDLR EGF-A mimetics. Four studies reported such strategies. In 2008, it was shown for the first time that the interaction between PCSK9 and LDLR or VLDLR can be inhibited by an EGF-A peptide, which limits LDLR degradation in HepG2 cells (264). In 2011, the second study reported the development of a fully human antibody, 1D05-IgG2, that structurally mimics the EGF-A in order to bind PCSK9 catalytic domain (459). After injection in mice, 1D05-IgG2 lowered LDLc by 40% and raised liver LDLR up to 5-fold. When injected in rhesus monkeys, LDLc and PCSK9 levels were reduced up to 50% for >2 weeks, although 1D05-IgG2 half-life was only ~3 days (459). In 2012, others identified an EGF-A variant, EGF66, that bound to PCSK9 with a high affinity as an Fc protein fusion and demonstrated increased LDLR levels *in vitro* and *in vivo* (460). In 2013, another study presented a truncated 26 aa EGF-A peptide analog which presented a higher affinity to PCSK9 than WT EGF-A and enhanced LDLR levels in cell-based assays (461). Taken together, this approach seems promising but did not reach clinical trials yet, probably mostly due to the difficulty of developing stable peptide-based drugs.

I.3.2.5 Small molecule inhibitors

The use of small molecules inhibiting PCSK9 would be promising because they could be delivered orally in contrast to injected mAbs or siRNA. However, it has been very challenging given that the stability and potency of small molecule inhibitors in plasma is very poor and need specific strategies to increase their bioavailability and safety. Moreover, the interaction site between LDLR and PCSK9 is a large-flat interface spanning over ~600 Å, thereby making the design of small molecules inhibitors binding such a large surface difficult. Despite these drawbacks, many

companies are currently racing to develop such a compound. The company Shifa Biomedical developed molecules inhibiting either PCSK9 binding to LDLR or its autocatalytic processing / secretion. Both compounds are currently tested in preclinical trials. As an example of the difficulties in this field, Pfizer was working on the development of an oral PCSK9 inhibitor, but decided not to move forward because it was not as efficient as mAbs. Kowa reported that a CETP inhibitor, K-312, inhibits PCSK9 expression (462). Following a high-throughput screen assay, a small molecule named R-IMPP for (R)-*N*-(isoquinolin-1-yl)-3-(4-methoxyphenyl)-*N*-(piperidin-3-yl) propanamide was identified as a transcript-dependent inhibitor of PCSK9 translation, resulting in increased LDLR levels and LDLc uptake in HuH7 cells (463). It acts through the targeting of 80S ribosome that inhibits the translation of PCSK9, but was not specific for PCSK9.

I.3.2.6 Vaccine

A more recent approach that would allow a long-term cholesterol management without the need of frequent injections is anti-PCSK9 vaccines (464). In 2014, a study from a company named AFFiRiS demonstrated that injection of a peptide-based vaccine to PCSK9 led to 30% and 50% TC and LDLc decreases, respectively, that were maintained up to one year in WT and *Ldlr*$^{+/-}$ mice and rats thanks to the formation of anti-PCSK9 antibodies (465). A phase 1 clinical trial is currently ongoing with this peptide-based PCSK9 vaccine. Another proposed vaccine approach is a virus-like particle-based vaccine targeting PCSK9 which showed reduced levels of TC up to 55% and of circulating PCSK9 by 50% in mice (466). The results of the phase 1 clinical trial are expected to give information about the long-term effects and safety of a PCSK9 vaccine. If it is safe and efficient, it would be a valuable therapeutic tool because it allows for an annual injection.

I.3.2.7 CRISPR/Cas9

More recently, targeting PCSK9 via genome editing using CRISPR/Cas9 has been proposed (467). In mice, this technique enabled an efficient disruption of the *PCSK9* gene and led to a reduction of TC up to 40%, ~90% decreased plasma PCSK9 and increased hepatic LDLR (468).

I.3.2.8 Less explored possible therapeutic approaches

Another possibility to target PCSK9 is to mimic its natural inhibitors such as annexin A2. A synthetic peptide derived from annexin A2 was developed and enabled to block the binding of PCSK9 to LDLR *in vitro* (229).

It was proposed in 2013 to use PCSK9 prodomain to block the activity of PCSK9 on the LDLR (469). To that end, a chimeric protein named Fcpro containing the Fc domain of human IgG1 and PCSK9 prodomain was engineered. When secreted from HepG2 or HEK293 cells or added extracellularly, Fcpro prevented PCSK9 activity on LDLR (469).

Other possible targets to treat FH are microRNAs (470) because they have been shown to modulate LDLc metabolism (471). Thus, miRNAs targeting LDLR, apoB or PCSK9 have been identified. Not many miRNAs regulating *PCSK9* have been verified so far, but some have been suggested, such as mIR-224 (472), mIR-27a (303) and mIR-195 (473).

I.3.2.9 Drawbacks of PCSK9 inhibition

Although PCSK9 mAbs are already prescribed and seem safe so far, and the three individuals with complete PCSK9 LOF are apparently healthy, some long-term issues due to very low PCSK9 or LDLc levels could still exist. Concerns about PCSK9 inhibition are to enhance HCV susceptibility by increasing LDLR and VLDLR cell surface levels (296, 297). This is especially important for genotype 3 HCV (300). Other concerns are for patients who would need to be subjected to hepatectomy since PCSK9 is involved in liver regeneration (172). The reduction of LDLc to very low levels has also been discussed (474-476).

I.4 Monoclonal or single domain antibodies as therapeutic tools

I.4.1 Antibodies

I.4.1.1 Antibodies general structure and classes

In mammalians, antibodies, also named immunoglobulins (Ig), are all composed of two identical pairs of chains: the heavy (H) and light (L) chains. Heavy chains are glycosylated, while light chains are not. Those two chains are linked together covalently by disulfide bonds.

Mammals produce five different classes (or isotypes) of antibodies, determined by the isotype of the heavy chain: α for IgA, δ for IgD, ε for IgE, γ for IgG and μ for IgM. The light chains can be just of two types: κ or λ and determine the subclass of Ig, thus there are ten types of antibodies. IgG is found in tissues and in blood stream and constitutes the most abundant antibody with its four different subclasses: IgG1, IgG2, IgG3 and IgG4 in humans. All antibodies possess antigen binding sites named paratopes that are specific for particular antigens designated as epitopes (477, 478).

More precisely, each pair or heavy or light chain is composed of three types of regions: the C-terminal constant regions C_H and C_L (constant domains, heavy and light chain, respectively), the variable regions V_H and V_L (variable domains, heavy and light chain, respectively) and the N-terminal hypervariable regions that consitute the antigen-binding site, as shown in Figure 17. This hypervariable region is actually composed of three hypervariable regions HV1, 2 and 3 which are sandwiched between framework regions that are less variable. These hypervariable regions are also named complementarity-determining regions (CDR). Generally, a single disulfide bond links each C_H to C_L and a double disulfide bond links the two pairs of heavy chains in the flexible hinge region. Note that the number of disulfide bonds can differ for each isotype.

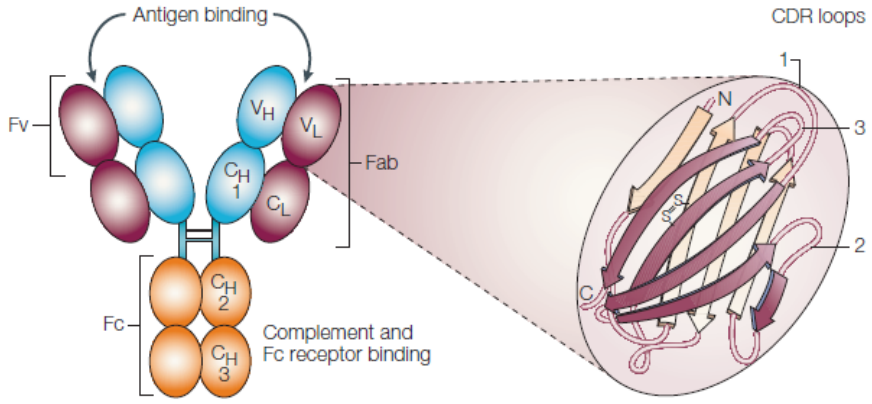

Figure 17. Schematic representation of the structure of an antibody (479)

Following proteolytic cleavage using the enzyme papain, an IgG gets cut at two places in the hinge region, giving rise to three fragments of similar size: two antigen-binding fragments (Fab: fragment, antigen-binding) and one crystallizable fragment (Fc: fragment, crystallizable, named so because of its ease of crystallization). Similarly, following proteolytic cleavage using the enzyme pepsin, the IgG is cut at one place at the C-terminal of the double disulfide bond in the hinge region, giving rise to two fragments: the Fc and a divalent fragment called F(ab')2 composed of two Fabs joined by disulfide bonds. The repeating domains making up antibodies have a characteristic three-dimensional structure: the Ig fold, consisting of two beta pleated sheets held together by a disulfide bond, as shown in Figure 17. This particular structure is evolutionarily widespread and is found in many proteins other than antibodies, including some cell-adhesion molecules.

I.4.1.2 The neonatal Fc receptor

Since the immune system of the newborn is immature, his immunity relies exclusively on his mother's one. In 1964, Rogers Brambell *et al.* (480) first came with the idea of a system able to transfer γ-globulins from a mother to her infant. In mice, they identified the neonatal Fc receptor (FcRn) on intestinal epithelial cells as a receptor enabling the capture of maternal IgGs from ingested breast milk by transcytosis through the intestine to the blood (481, 482). This enables the transfer of protective antibodies from the mother to the infant, conferring him a passive immunity after birth. In humans, the transmission of passive immunity already occurs before birth (482):

fetal cells that are in contact with the maternal circulation carry the FcRn, enabling the delivery of IgG from the mother circulation to the fetus through transcytosis across the placenta. Maternal antibodies thus protect the newborn until its own immune system is sufficiently mature to produce antibodies on its own (483).

Following this discovery, the FcRn has been extensively studied and reviewed (484-486). Briefly, FcRn is a membrane-bound glycoprotein that belongs to the Ig supergene family (487). It is distributed through a variety of tissues and transports IgG through their Fc domain in a pH-dependant manner (488). FcRn transports IgG through polarized epithelial barriers (489), conferring passive immunity to fetus and newborn, and helps them developing adaptive immunity (490). FcRn is also responsible for the intracellular trafficking of IgG and antigen-containing IgG-immune complexes through the endolysosomal system (491, 492). It has been shown that it binds independently to both sites of the IgG homodimer with equal affinities (493). Importantly, FcRn protects IgG and albumin, which is a natural ligand of FcRn, from catabolism by endocytic salvage through pH-dependant recycling and transcytosis pathway (494-497). FcRn is thus crucial in IgG and albumin biodistribution (498). As an example, mice lacking FcRn showed an IgG clearance increase up to 10-fold (499). FcRn is thus crucial for the long serum half-life of these abundant proteins, and this specific property is a useful asset that can be exploited for delivery of therapeutic antibodies or proteins (500). As an example, nanoparticles targeting the FcRn and administered orally in mice have been shown to cross the intestinal epithelium and reach circulation (501). Since FcRn is also expressed on mucosal cells, FcRn transcytotic pathway has also been considered for transmucosal delivery of nanoparticule systems that could act as carriers of a range of biotherapeutics (502).

The use of Fc fusion in order to increase a drug half-life was first used in 1989 in a pioneer study with an Fc-fused protein and showed promising results in terms of functionality and half-life of the drug (503). The first Fc-fused protein appeared on the market in 1998 (504). Today, 11 Fc-fused proteins have been approved by the FDA (505).

Although less studied, the Fc-γ-receptor (FcγR) may also be involved in the elimination of therapeutic antibodies (506).

I.4.1.3 Antibodies fragment engineering

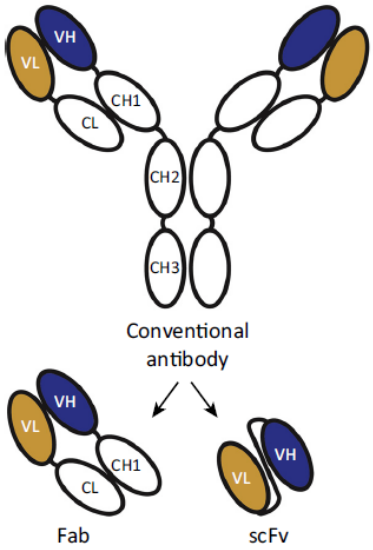

Figure 18. Schematic of the main engineered antibodies fragments (507)

Although therapeutic mAbs were initially complete IgGs (~150 kDa), it was realized that smaller fragments retaining their antigen-binding properties could also be used as efficient therapeutic proteins. Indeed, in some cases such as radio-immunotherapy, the long half-life of mAbs is not advantageous. Moreover, mAbs present a limited tumor and tissue penetration.

As depicted on Figure 18, the two most used formats of antibodies fragments are "antigen-binding fragments" (Fab) or "single chain variable fragment (scFv).

Fabs (~50 kDa) are an attractive and cheaper alternative to mAbs because they are monovalent, but they are rapidly eliminated by renal clearance. Several Fabs can be linked to enhance the size of the final molecule. Many therapeutic Fabs have been approved and are efficient in therapy, such as the PEGylated Fab certolizumab pegol (Cimzia) which is indicated for the treatment of numerous autoimmune diseases (508).

The advantage of scFvs (25 kDa) over Fabs is that they are more customizable. Their half-life being just 2 h, diabodies composed of two scFvs were engineered by decreasing the length of the linker between the two scFv domains (509). These bivalent molecules are ~60 kDa and can be designed to be bispecific (510). scFvs are mostly used for imaging techniques. However, their production yield is quite low (511).

I.4.1.4 Affinity maturation

Mammalian antibodies naturally undergo affinity maturation. Besides, when developing memory lymphocytes, antibody repertoires are created. This is what scientists are trying to reproduce *in vitro* by ameliorating the affinity of antibodies for specific antigens (512). This is achieved by using stringent selective conditions in the assays such as harsh washing conditions or antigen concentration reduction. Antibodies affinity maturation consists in modifying the antibody variable domains without altering its specificity. Given that most of the crucial binding parts of antibodies are located in the V_H and especially within the CDR3 loops of V_H and V_L, some techniques are based on chain-shuffling. Another approach is the randomization of CDR. Alternative approaches will be described in the section I.4.2.4 describing the phage display technology.

I.4.2 Monoclonal antibodies

I.4.2.1 From the discovery of antibodies to the creation of monoclonal antibodies

In 1901, the first Nobel Prize in Medicine and Physiology was awarded to Emil von Behring, a German physiologist, for his work with the Japanese physician Shibasaburo Kitasato on serum therapy and its use in diphtheria (513). The German physician Paul Ehrlich collaborated with Emil von Behring and developed a method for standardized production of therapeutic serums to treat diphtheria. Paul Ehrlich is also known for putting the idea of a "magic bullet" that could neutralize disease-causing agents in the body without harming the patient (514). He also had theories about protective antibodies termed "side chains" and their ability to target chemical groups on specific molecules, which led him to be awarded the 1908 Nobel Prize in Physiology or Medicine, alongside with Ilya Mechnikov, a Russian zoologist. Thus, antibodies were discovered in the 1890s. However, it was not until the 1960s that scientist discovered that only lymphocytes could produce them. The human immune system possesses ~1×10^{12} lymphocytes that constitute ~1% of our body weight.

I.4.2.2 Production of monoclonal antibodies

This historical context led to the development of mAbs, which discovery deeply modified biomedicine. Since lymphocytes were difficult to culture *in vitro*, in 1975 three scientists named Niels Jerne, Georges Köhler and César Milstein had the idea to fuse spleen cells from an immunized mouse with myeloma cells, thereby obtaining a hybrid cell line named hybridoma (515). The latter is able to produce large quantities of identical antibodies coming from a unique clone and therefore named mAbs as the first "real" magic bullets. The three scientists were rewarded the Nobel Prize in 1984 for this discovery (516).

The breakthrough of the hybridoma technology (see Figure 19) is the use of myeloma cells that are deficient in an enzyme called hypoxanthine-guanine-phosphoribosyltransferase (HGPRT) which is essential for cell growth and renders them sensitive to hypoxanthine-aminopterin-thymidine (HAT) medium. Those HGPRT-deficient myeloma cells are fused to spleen cells from an immunized mouse using PEG and cultured for more than one week on HAT medium. Given that on one side, spleen cells only survive in culture less than one week, and on the other side, the HGPRT-deficient myeloma cells are unable to grow in presence of HAT, only the hybrid myeloma cells which obtained the *HGPRT* gene from the spleen cells can grow and secrete antibodies. Subsequent steps are the screening of clones secreting the mAb of interest and the expansion of the latter to obtain sufficient quantities of mAbs that can then be purified.

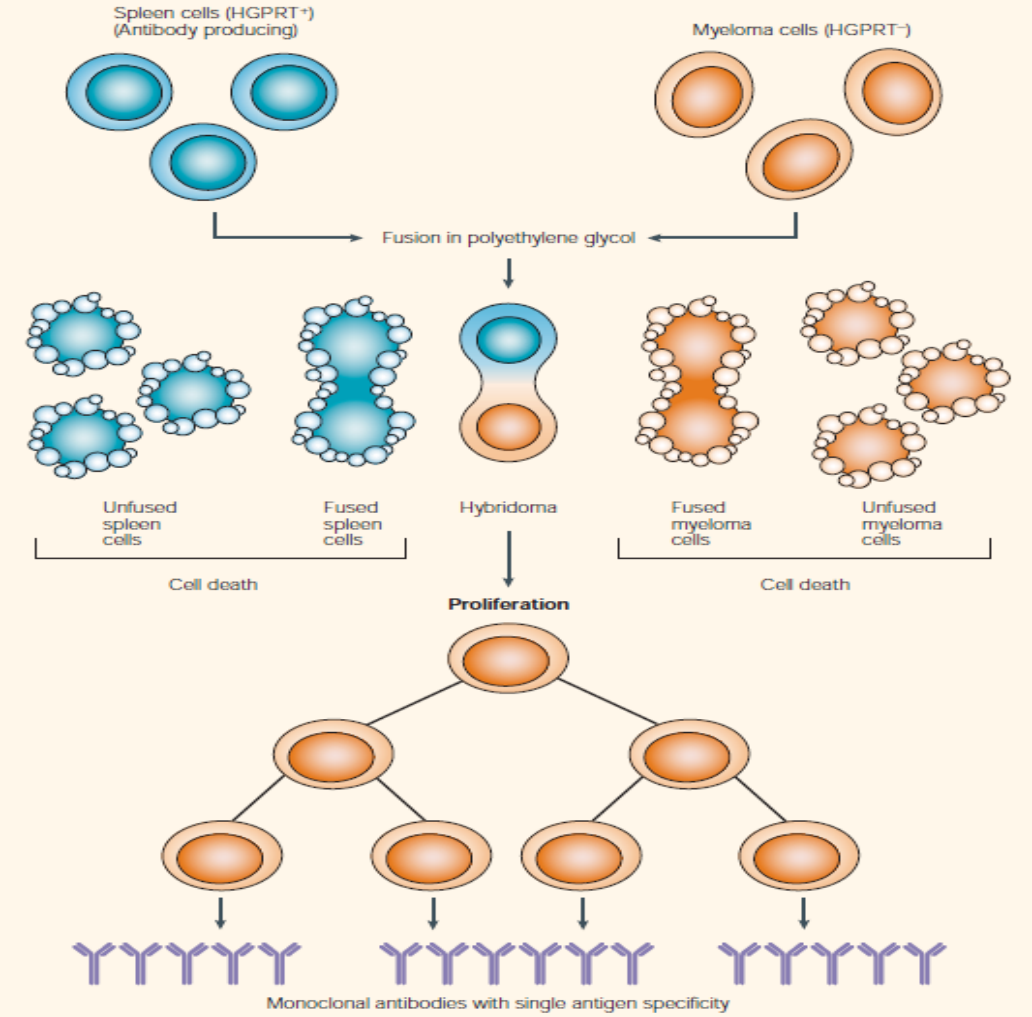

Figure 19. Illustration of the hybridoma technique to produce mAbs (516)

The first therapeutic mAb, muromomab (OKT-3), entirely murine (suffix –omab), was approved by the FDA in 1986 and was indicated in the treatment of organ transplant rejection (517). It was followed by several other therapeutic murine mAbs. Although they were efficient in some cases, they presented some issues such as their immunogenicity (518) and their short half-life <20h due to their lack of interaction with human FcRn (519).

I.4.2.3 Synthetic or humanized antibodies

New techniques thus needed to be investigated in order to reduce immunogenicity of mouse antibodies. From 1984, chimeric mouse-human mAbs (suffix –ximab, see Figure 20) were engineered by fusing murine variable regions on human constant regions, resulting in up to 75% human mAbs that presented reduced immunogenicity and improved half-life (520). Abciximab (Reopro) was the first chimeric mAb approved by the FDA in 1994 for prevention of blood clots (521).

Then, humanized mAbs (suffix –zumab, see Figure 20) were engineered by grafting mouse hypervariable regions to human antibodies, named CDR grafting and leading to ~95% human mAbs (522). The drawback of this technique is that the affinity of the humanized mAb can be up to 230-fold lower than the original murine one (523). However, techniques have been developed to overcome this shortcoming such as mutagenesis of the CDR using various molecular biology techniques including site-specific mutagenesis (524, 525). Daclizumab (Zenapax) was the first humanized mAb approved by the FDA in 1997 for reversal of transplantation rejection (526). Since then, a large portion of therapeutic mAbs are humanized. Although they generally present low immunogenicity, some patients still develop anti-mAb antibodies (527).

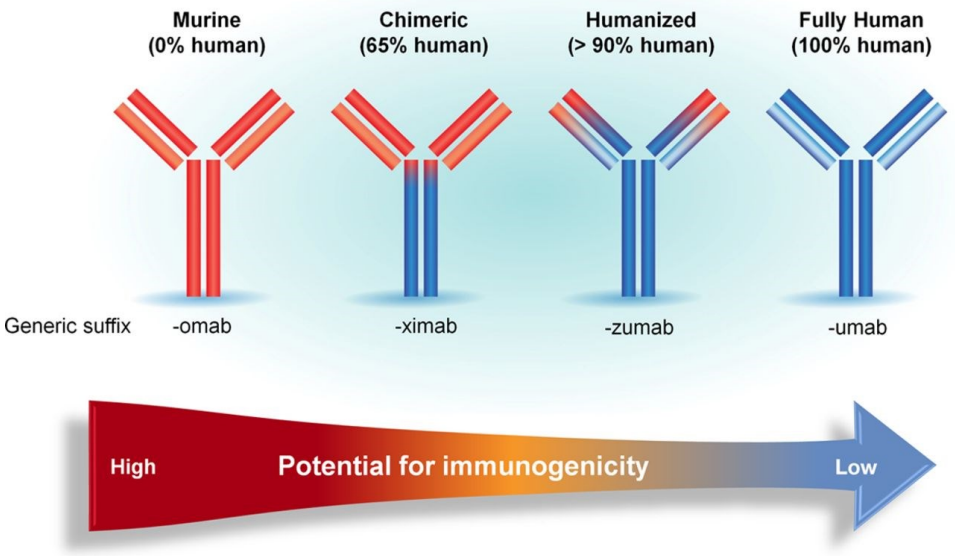

Figure 20. Schematic representation of the different types of therapeutic antibodies (528)

I.4.2.4 Fully human antibodies

To further increase the human portion on therapeutic mAbs, fully human mAbs (suffix -umab) were then engineered using various techniques, as indicated on Figure 20. From 1981, techniques were already used to try to replicate hybridoma with human cells by using viruses such as Epstein-Bar to immortalize human lymphocytes so that they produce mAbs continuously (529). However, this technique presented some limitations mainly due to the low yield of synthesis of mAbs.
Later, scientific advancements such as the isolation of genes encoding human variable regions and their successful expression in *Escherichia coli* (530, 531), together with the introduction of the phage display technique (532-534), allowed the selection of fully human variable domains more easily. Briefly, phage display uses viruses infecting bacteria that are called bacteriophages (mostly M13 filamentous phage). Genes encoding antibodies are fused to the phage genes encoding coat proteins (pIII protein in the M13 phage). This will lead each phage to display a specific antibody (or mostly an antibody fragment such as Fab or scFv) on its surface. The phages library can then be screened against a chosen antigen in order to select only the phages presenting antibodies with high affinity for the antigen, namely the phages able to bind the surface coated with the antigen (generally a 96-well plate), the other being washed away. These steps, called biopanning, can be repeated several times in order to increase the affinity of the selected antibodies for the antigen. The phages present in the last step can then be used to infect bacteria in order to amplify them and excise and collect their DNA sequence, especially the DNA sequence of the antigen-binding antibodies. Phage libraries can be made from human naïve repertoires (IgM and IgD), from pre-immunized donors or from totally synthetic variable genes that are diversified by using notably random gene combination or PCR to introduce mutations in V_H and V_L. In either case, the use of such diverse libraries enables to reproduce the natural diversity and immune selection. The other advantage of phage display is that it can be used for any type of antigen, even those that would be toxic to a mouse. There are also mRNA-display technologies such as ribosomal display that are used for affinity maturation and stability engineering of antibodies (535). This technique allows large human antibodies libraries to be screened, amplified and their corresponding coding sequence to be recovered rapidly *in vitro*. It constitutes the most used technology for new fully human mAbs discovery.

Alternatively, transgenic mice possessing the human Ig locus (XenoMouse) were created in the late 1990s and are able to produce human Ig. They can be immunized and their spleen cells used to create hybridomas directly producing human mAbs (536). They are still used today and constitute a very valuable platform for novel mAbs discovery (537).

Adalimumab (Humira) was the first human mAb approved in 2008 by the FDA for use in a large panel of autoimmune diseases including rheumatoid arthritis. Crohn's disease and plaque psoriasis (538).

I.4.2.5 Monoclonal antibodies therapeutic applications

According to data from January 2017, the FDA already approved 68 mAbs for therapeutic uses (539). Interestingly, in 2015 and 2016, the FDA approved 10 new mAbs each year, which is historically high (540). Thus, mAbs are currently considered to be the fastest growing group of biologics in clinical trials (541), with increasing rates of approvals and sales that are expected to grow even more in the coming years. In 2013, the global sales revenue for all mAbs was ~75 billion $, which represents nearly half of the total biopharmaceutical products sales (542). Note that mAbs are also very valuable tools that are widely used in research and diagnostic.

mAbs present many advantages such as their specificity and affinity for their targets and their wide therapeutic applicability. Some bispecific mAbs can be developed and generally mAbs can be used to treat various forms of cancer, autoimmune diseases, transplant rejection or even AD. However, their main drawback is their high cost due to the large-scale production of these large (~150 kDa) proteins in mammalian cells, which limits their wide use, especially for life-long diseases. Besides, they are very rarely curative in cancer treatments and lead to side effects, mainly infusion reactions.

I.4.2.6 Monoclonal antibodies clearance mechanisms

Since mAbs are widely used drugs, the complex processes involved in their clearance were extensively studied. mAbs can be cleared by mechanisms being either target-specific or unspecific. Most marketed mAbs have shown a dose-dependent clearance consistent with target-mediated elimination, which is related to their high target specificity (543). In these cases, mAbs bind antigens and are then cleared via endocytosis and subsequent lysosomal degradation (544).
Unspecific mAbs clearance is similar to endogenous human IgGs clearance and is mainly governed by the reticuloendothelial system (RES) (543, 544) and the FcRn-mediated recycling (481, 545) that was described previously in section I.4.1.2.
The RES is part of the immune system and is composed of phagocytic cells located in the reticular connective tissue, which is composed of primary monocytes and macrophages. The main role of this system is to conduct phagocytosis and thus clear immune complexes. The RES eliminates both antigen-bound and free mAbs (544). Note that FcRn and RES are linked in that the FcRn is thought to rescue mAbs from endosomes, thus decreasing the metabolism and elimination rates *via* the RES. This is achieved through binding of the mAbs to phagocytes and endothelial cells, thereby limiting their clearance by recycling mAbs from the endosomes to the serum by pH-dependent binding (506).

I.4.3 Single domain antibodies

I.4.3.1 Heavy chain disease, a disease of the B cells

Heavy chain diseases (HCDs) are rare B-cell proliferative disorders presenting with varying degrees of malignancy. HCD was first described in 1968, when pathological Ig were found in serum, urine and saliva of a young Arab patient with abdominal lymphoma and diffuse lymphoplasmacytic infiltration of the small intestine (546). Maxime Seligmann *et al.* found out that this new type of protein was devoid of light chains and characterized by electrophoretic heterogeneity, tendency to polymerize and high carbohydrate content. Since they detected no intracellular synthesis of light chains, they assumed that this antibody was not due to an absence of light chain assembly but to a lack of light chains synthesis in the proliferating cells (546). This constituted the first evidence of human antibodies lacking their light chains.

Since then, more than 400 cases of α-HCD (first described in 1968, structurally abnormal IgA, rare), 33 cases of μ-HCDs (first described in 1969, structurally abnormal IgM, very rare) and 120 cases of γ-HCDs (first described in 1964, structurally abnormal IgG) have been described. The prognosis of HCDs is variable and no treatment is available for γ- and μ-HCDs. However, early-stage α-HCD may respond to antibiotics, as chronic antigenic stimulation by intestinal organisms is thought to play a role in the development of α-HCD (547). In most of γ- and μ-HCDs, an underlying autoimmune disorder such as rheumatoid arthritis has been reported (548, 549). Although HCDs are very diverse, all HCD proteins possibly derive from a common normal precursor, which could be a rare B cell undergoing gene somatic hypermutation within the germinal center.

I.4.3.2 The discovery of camelid sdAbs

In 1993, by performing affinity chromatography using proteins A and G or gel filtration to study camelids serum, Cécile Hamers-Casterman and her colleagues realized that on top of conventional antibodies, camelids also possessed a class of antibodies devoid of light chains (550). This was the case for old world camelids (*Camelus bactrianus and Camelus dromedarius*) and new world camelids (*Lama pacos, Lama glama and Lama vicugna*): heavy chain antibodies (hcAbs) were abundant (up to 75%) in all sera (550). They also demonstrated that the hcAbs are able to produce a repertoire of antibodies against a given antigen. This questioned the contribution of the light chain to antibodies repertoires. Clones representing different V_H sequence were isolated and sequenced from camel spleen. This enabled to demonstrate the complete lack of the CH1 domain. Therefore, the last framework residues (FR4) of the V_H region are immediately followed by the hinge (550).

It was later demonstrated by sequencing the alpaca genome that conventional antibodies and hcAbs genes reside in same locus (551).

These antibodies are thus composed of two heavy chains, each including an antigen binding domain followed by two constant domains CH2 and CH3 as shown on Figure 21. The ~15 kDa antigen binding domain of hcAbs is named variable of the heavy chain (VHH), single domain antibody (sdAb) or nanobody (tradename from the company Ablynx).

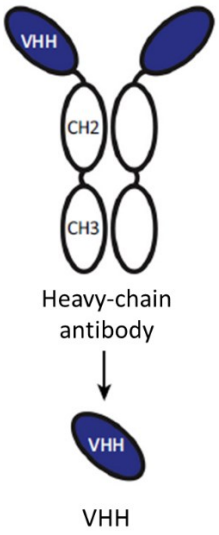

Figure 21. Schematic of a heavy-chain antibody and its VHH fragment (507)

The resolution of the crystal structure of a sdAb in complex with its antigen (lysozyme) revealed that half of the CDR3 protrudes from the antigen binding site and penetrates deeply into the active site of lysozyme, while the other half is linked to the V_H region instead of the V_L in conventional antibodies (552). The fact that sdAbs prefer to interact with cavities on the surface of their antigen, such as the catalytic site of enzymes or the ligand-binding site of receptors represents a net advantage over mAbs.

In 1995 it was discovered that cartilaginous fishes such as sharks, skates and rays also present an uncommon antibody isotype named Ig new antigen receptor (IgNAR) that is formed of a heavy chain homodimer lacking light chains (553). The equivalents of their sdAbs are called VNARs and are ~13 kDa. Their crystal structure is similar to camelid sdAbs (554). Although clinically less advanced than camelid sdAbs, they have the potential to be used as biologics (555).

The discovery of naturally occurring hcAbs in camelids inspired researchers in their quest for Ig-based recognition units of minimum size (556, 557).

I.4.3.3 The camelization of human antibodies

In 1995 Julian Davies *et al.* introduced mutations in a human V_H in order to mimic the camelid hcAbs, creating camelized antibodies (558). Then, they randomized the CDR3 of the V_H in order to yield a repertoire of $2x10^8$ independent clones. The latter library was displayed on phages and

selected for antigen binding. They were able to identify V_H clones specific for haptens (small molecules which, when combined with a larger protein, can lead to the production of specific anti-hapten antibodies) with affinities of 100-400 nM, similar to scFv, Fab or whole mAb but with a lower specificity. This was a nice technique, which presented some limitations, since no good binders against proteins could be retrieved from their synthetic library. Nevertheless, they could conclude that these camelized human V_H domains were highly specific, stable and well expressed in *E. coli*.

I.4.3.4 The direct use of camelids single domain antibodies

In 1997 Mehdi Arbabi Gharoudi *et al.* showed for the first time that it is possible to immunize a dromedary with proteins to clone the repertoire of the variable domains of its hcAbs and to use phage display to screen them in order to identify antigen-specific sdAbs (559). They also related that these binders were well expressed in *E. coli*, were extremely stable, very soluble, specific and presented high affinities (low nM range) for antigens (559). A similar study was performed on llama and was also promising (560). Llama sdAbs were compared to mouse mAbs and showed the same affinity and specificity to antigens. Interestingly, sdAbs were more resistant to high temperatures than mAbs (561).

Although these first studies were successful, the wide applicability of these approaches was limited because it is long, requires access to camelids and does not always yield affine enough antibodies. Therefore, since then many techniques were developed in order to improve the identification of potent sdAbs following llamas or camels immunization, including a mass spectrometry-based approach enabling the generation of large repertoires of readily expressible recombinant sdAbs with high specificities and subnanomolar affinities (562). More recently, an approach based on *in vitro* immunization of naïve alpaca B lymphocytes was proposed as a rapid and cheap way to develop sdAbs (563). sdAbs libraries can also be created using phage display or ribosome display, like it is done for mAbs development.

Importantly, sdAbs can be efficiently produced from bacteria (564), yeast (565) or plants (566), and are thus expected to be cheaper and easier to manufacture compared to mAbs that need to be synthesized in mammalian cells.

sdAbs constitute valuable tools for crystallization (567), cell biology (568, 569), research and diagnostic (507). In some applications, their small size and short half-life resulting from a rapid clearance from blood is an advantage. In other applications such as therapeutics, sdAbs can be fused to another moiety or linked with other sdAbs in order to increase the size of the therapeutic agent and thus increase their clearance rate. This technique also enables bispecific sdAbs to be engineered.

Several authors reviewed the importance of sdAbs as therapeutics (556, 570). Interestingly, they can be used as an inhaled drug to treat lung diseases (571) or as an orally-delivered drug in specific cases such as gastrointestinal disorders (565). The particularity of sdAbs is their low immunogenicity. This is notably due to the high degree of identity sdAbs share with human V_H. Importantly, no immune response was observed in sdAb-injected mice or humans (see next section). Besides, a strategy to humanize 12 out of the 14 aa differing between human V_H and camelid sdAbs was developed and seems relatively easy to implement (572).

I.4.3.5 Current clinical applications of sdAbs

The first proof-of-concept of sdAb *in vivo* efficacy was shown by tumor-targeting sdAbs nine years after the sdAbs discovery (573). Although no sdAb is commercialized yet, many of them are currently tested in clinical trials. Given their wide applicability, sdAbs are used to target various diseases.

Four sdAbs are currently in phase 2 or more advanced:

- The most advanced sdAb (caplacizumab or ALX-0081, proprietary of the company Ablynx), which is the unique sdAb in an ongoing phase 3, is a bivalent sdAb directed towards von Willebrand factor used to treat thrombotic thrombocytopenic purpura. The studies in phase 1 and 2 demonstrated that the sdAb is well tolerated and effectively acts on the tested pharmacological markers (574-576).
- Albuferon (ozoralizumab or ATN-103) is a trivalent drug composed by two sdAbs targeting TNFα fused to one sdAb targeting human serum albumin (HSA) (577, 578). It is indicated in the treatment of rheumatoid arthritis for which phase 2 is completed, and in cases of HCV for which several phase 3 studies have been completed. All clinical trial studies have shown

promising outcomes (Roy M. Fleischmann, Ablynx poster) and the drug was licensed for development in Japan in 2015.

- Auto-immune diseases such as rheumatoid arthritis or systemic lupus erythematosus can also be targeted by sdAbs, as shown by ALX-0061 (vobarilizumab), a bispecific drug targeting both the pro-inflammatory cytokine IL-6 receptor and HSA. This drug showed potency *in vitro* and *in vivo* (579) and seems promising in the phase 1/2 trial in rheumatoid arthritis (576). A phase 2 study is ongoing and results are expected in 2018.
- ALX-0171 is a trivalent sdAb towards the glycoprotein F of the respiratory syncytial virus, which is a leading cause of infant hospitalization. Its efficiency has been proven *in vivo* (580), and several phase 1 studies were performed in both infants and adults and showed a good response to the treatment and limited side effects (Ablynx report, Erik Delpa, May 6, 2015). The phase 2 is ongoing. The advantage of this drug is that it can be inhaled and thus be delivered directly to the infection site.

Besides, several phase 1 clinical studies are going on with sdAbs:

- ALX-0761 (M1095), targeting both IL-17A and IL-17F, is indicated for psoriasis. The phase 1 is ongoing and some recent results showed that it was safe and efficient (Danka Svecova, March 2017, Ablynx website).
- ALX-0141 is directed towards RANKL for treatment of bone-loss related disorders including osteoporosis and bone metastasis. A phase 1 was completed and demonstrated the safety of this drug in post-menopausal women.
- Another sdAb targeting the rotavirus protein has been shown to reduce stool output in infants with diarrhea upon oral administration of the sdAb. No side effects were observed (565).

Only three clinical trials testing sdAbs have been terminated:

- ALX-0651, a sdAb targeting the GPCR CXCR4 and indicated for lymphoma, myeloma and HIV seemed promising *in vitro* (581) but has been terminated during phase 1 for unknown reasons (www.clinicaltrials.gov).
- The phase 1 study of TAS266, a tetravalent sdAb targeting the death receptor 5 and involved in advanced cancer with solid tumors, was terminated because of unexpected hepatotoxicity

(582). This was probably due to the presence of auto-antibodies to TAS266 in the patients showing these side effects. However, this hepatotoxicity was rapidly reversible.

- The injection of a sdAb aiming at treating AD, BI1034020, led to a drug-related serious adverse event that terminated the study. Note that the drug target was unknown.

Overall, the use of sdAbs as therapeutics seems to be a flexible innovative technology, enabling the coupling of the small sdAb to any moiety, depending of the intended use. Importantly, they do not seem to be immunogenic and are very well tolerated in human. It is reasonable to expect that at least one sdAb will be marketed in the next few years.

I.5 Working hypothesis and research objectives

The role of PCSK9 in cholesterol regulation was described in my thesis introduction. I also emphasized the importance of maintaining healthy cholesterol, and more importantly LDLc levels in patients, especially those who have FH, as well as the currently available therapeutic options that were also described and discussed. It is clear that PCSK9 is a very promising therapeutic target for dyslipidemia management. However, PCSK9 inhibitors that are marketed so far are pricy and are only prescribed to very high risk patients. Hence, this leads to an unmet need for cheaper and more accessible inhibitory molecules.

This is why, as an alternative, we proposed the use of sdAbs to target PCSK9. In order to screen and characterize extensively the selected sdAbs *in vivo*, we developed new *Pcsk9*$^{-/-}$ mouse lines carrying a human BAC Tg directing hPCSK9 expression under the control of its own promoter. Those mice constitute a precious tool to test PCSK9 inhibitors, which was not feasible with the available mouse models. In the interest of comparing our innovative approach to the available therapies, we compared the therapeutic potency of our sdAbs to that of a commercial PCSK9 mAb.

To summarize, the aim of my thesis work was to:

1. Generate sdAbs directed against PCSK9 as an alternative therapeutic approach to the mAbs (Chapter II)
2. Select the best sdAbs and characterize their effects on LDLR, PCSK9, LDLc and other parameters in various assays and settings (Chapter II), including *in vivo* assays in a newly developed mouse line which is now a very useful tool for the *in vivo* screening of hPCSK9 inhibitors (Chapter III)

II. Chapter II: Manuscript 1 (The Journal of Biological Chemistry, 2016)

Title: Proprotein Convertase Subtilisin/Kexin type 9 (PCSK9) single domain antibodies are potent inhibitors of LDL receptor degradation

Authors: Elodie Weider, Delia Susan-Resiga, Rachid Essalmani, Josée Hamelin, Marie-Claude Asselin, Yahya Ashraf, Keith L. Wycoff, Jianbing Zhang, Annik Prat, and Nabil G. Seidah

Journal: The Journal of Biological Chemistry. 2016, volume 291, issue 32: p 16659-71.

II.1 Preface

PCSK9 is clearly an established therapeutic target. However, since the most advanced therapeutic approaches are the expensive mAbs, we conceived the idea of developing sdAbs against PCSK9 as a cheaper alternative. A llama was chosen as a camelid source of hcAbs in order to get its PCSK9-specific sdAbs. The aim of this study was to obtain sdAbs with a high affinity to PCSK9 that are able to prevent LDLR degradation by immunizing a llama with PCSK9. We then selected a few sdAbs among the most promising ones in order to fuse them to a mouse Fc domain (mFc) and to produce them in larger quantities. This choice was made in order to extend the *in vivo* half-life of the sdAbs that would be too short for sdAbs alone. The potency of these fusion proteins "sdAb-mFcs" was then evaluated in various cell-based assays in order to establish the *in vitro* proof-of-concept that they regulate cell surface and total LDLR levels as well as LDL uptake. In these experiments, sdAbs were compared to mAbs that became commercially available in between and to EGF-A mimicking peptides. The cholesterol-lowering effect of a selected sdAb, P1.40-mFc was then confirmed *in vivo* in a newly developed transgenic mouse model that was tested for the first time. Note that concentrations of PCSK9 and sdAb-Fcs used throughout this study had to be adjusted for each assay in order to get the largest window possible between the negative control (absence of PCSK9) and the positive control (presence of PCSK9). This allowed optimal evaluation of the inhibitory potencies of the sdAb-Fcs.

Proprotein Convertase Subtilisin/Kexin type 9 (PCSK9) single domain antibodies are potent inhibitors of LDL receptor degradation

Elodie Weider*, Delia Susan-Resiga*, Rachid Essalmani*, Josée Hamelin*, Marie-Claude Asselin*, Surendra Nimesh*, Yahya Ashraf*, Keith L. Wycoff[§], Jianbing Zhang[†], Annik Prat*, and Nabil G. Seidah*[¶]**

*Laboratory of Biochemical Neuroendocrinology, Institut de Recherches Cliniques de Montréal, affiliated to the University of Montreal; 110 Pine Ave. West, Montreal, QC H2W 1R7, Canada.

[§]Planet Biotechnology Inc., Hayward, CA 94545-2740, USA.

**Institute for Biological Sciences, National Research Council of Canada, 100 Sussex Drive, Ottawa, K1A 0R6, ON, Canada.

[¶]Corresponding author: Nabil G. Seidah, Laboratory of Biochemical Neuroendocrinology, Institut de Recherches Cliniques de Montréal, 110 Pine Ave. West, Montréal, QC H2W 1R7, Canada. Tel: (514) 987-5609; E-mail: seidahn@ircm.qc.ca

[†]Present address: Xiangxue Pharma, Jinfengyuan Road 2, Guangzhou, China

Keywords: cholesterol regulation, inhibitor, LDL, PCSK9, sdAb, nanobody, FH, LDLR, CHRD

II.2 Abstract

sdAbs correspond to the antigen-binding domains of camelid antibodies. They have the same antigen-binding properties and specificity as mAbs, but are easier and cheaper to produce. We report here the development of sdAbs targeting hPCSK9 as an alternative to anti-PCSK9 mAbs. After immunizing a llama with hPCSK9, we selected four sdAbs that bind PCSK9 with a high affinity, and produced them as fusion proteins with a mFc. All four sdAb-Fcs recognize the C-terminal CHRD of PCSK9. We performed multiple cellular assays, and demonstrated that the selected sdAbs efficiently blocked PCSK9-mediated LDLR degradation in cell lines, in human hepatocytes and in mouse primary hepatocytes. We further showed that the sdAb-Fcs do not affect binding of PCSK9 to the LDLR, but rather block its induced cellular LDLR degradation. Pcsk9 KO mice expressing a human BAC Tg were generated, resulting in plasma levels of ~300 ng/ml of hPCSK9. Mice were singly or doubly injected with the best sdAb-Fc and analyzed at day 4 or 11, respectively. After 4 days mice exhibited a 32% and 44% decrease in the levels of TC and apolipoprotein B (apoB), and ~1.8-fold higher liver LDLR protein levels. At 11 days, the equivalent values were 24%, 46% and ~2.3-fold higher LDLR protein. These data constitute a proof-of-principle for the future usage of sdAbs as PCSK9-targeting drugs that can efficiently reduce LDL-cholesterol, and as tools to study the CHRD-dependent sorting the PCSK9-LDLR complex to lysosomes.

II.3 Introduction

For over 30 years, a large number of clinical trials have firmly consolidated the importance of lowering LDLc in the prevention of CVD and its associated devastating sequelae (43). Healthy diets and exercise are highly recommended to lower LDLc in patients with high baseline levels. However, many individuals, including those suffering from FH, cannot reach the recommended LDLc levels to prevent cardiovascular complications. With an overall incidence of ~1:200, FH is a common inherited disease that affects at least 30 million people, of whom ≤ 1% have been diagnosed. It is characterized by plasma LDLc levels greater that the 95th percentile, which result in tendon xanthomas, xanthelasmas, corneal arcus, and premature atherosclerosis, leading to premature ischaemic vascular disease and mortality if left untreated. In most cases, FH subjects exhibit mutations in the LDLR (*LDLR*; 67%) and its ligand apoB (*APOB*; 14%), hampering LDL clearance from the circulation (61). In 2003, merging biological studies with Hum Genet led to the discovery of PCSK9, the 9th and last member of the family of PCs related to Subtilisin and Kexin (63), and the demonstration that the PCSK9 gene represents the 3rd locus of ADH (64).

PCSK9 is a serine protease first synthesized as a zymogen that auto-catalytically cleaves itself in the ER to excise its N-terminal prodomain (63), which acts as a chaperone and a potent inhibitor. However, different from all other convertases (132), PCSK9 is secreted as an enzymatically inactive non-covalent complex with its inhibitory prodomain tightly bound to the catalytic subunit of mature PCSK9 (173). Thus, PCSK9 has no substrate other than itself. Rather, it binds to specific cell-surface receptors and escorts them towards intracellular acidic endosome/lysosome degradation compartments (177, 184). A schematic diagram of PCSK9's primary structure and its domains (prodomain; catalytic domain; hinge; CHRD) is shown in Figure 22A. The crystal structure of PCSK9 revealed that the CHRD is composed of three distinct Cys/His-rich modules, denoted M1, M2 and M3 (173).

The first PCSK9 target that was identified is the LDLR at the surface of hepatocytes (168, 170, 583). The catalytic subunit of PCSK9 was shown to bind the LDLR through its EGF-A domain (177, 178), as well as the LDLR superfamily members VLDLR, ApoER2 (262, 264) and LRP1 (194). Upon LDL binding to cell surface LDLR the complex is internalized into the cell within heavy-chain clathrin-coated vesicles that fuse with early endosomes. Herein, the acidic pH causes conformational changes driving LDL release, and the subsequent recycling of the LDLR to the cell surface, and the sorting of LDL to lysosomes for cholesterol recovery and distribution in the cell (27). The PCSK9-LDLR complex also enters the cell via clathrin-coated vesicles (184, 185). However, the acidic pH enhances the affinity of PCSK9 for the LDLR (173) and, through some unknown mechanism requiring the CHRD (179, 184, 262), favors its ability to escort the LDLR to late endosomes/lysosomes for degradation by as yet undefined proteases (168, 184).

The rare PCSK9 mutations identified in FH patients result in a GOF, *i.e.*, an increased potency of PCSK9 to promote LDLR degradation, with ensuing higher circulating LDLc levels (64, 168). The most dramatic GOF D374Y mutation increases ~10-fold the affinity of PCSK9 for the LDLR (173) and results in ~4-fold higher LDLc levels (~10 mM), as well as early death due to CVD (200). LOF PCSK9 mutations were also identified. Namely, two non-sense mutations Y142X and C679X found in ~2% of black Africans were associated with ~40% decrease in LDLc, and ~88% reduction in the risk of CVD (206, 584). This provided a proof-of-principle that PCSK9 inhibition may be safe and represents a promising approach to treat hypercholesterolemia and prevent CVD (174, 585).

Accordingly, PCSK9 mAbs blocking its interaction with the LDLR were developed and are presently prescribed in clinics to patients suffering from severe hypercholesterolemia, who are statin-resistant and/or cannot reach target LDLc using available drugs. Such subcutaneously injected mAbs every 2 or 4 weeks result in a sustained ~60% reduction in LDLc (132, 174, 586) and thus represent a powerful drug against heart disease that is superior to statins. Over the past 30 years, mAbs became established as effective medicines for several serious diseases (587-589). However, their high molecular mass (~150 kDa) require large amounts to be injected in order to reach efficacy (e.g., 150 mg/14 days), and their high cost limits their wide applicability. The mAbs targeting PCSK9 cost ~14,000 US$/year/patient (590), likely making them the most costly class

of medications marketed so far. This definitely restricts their use to high risk patients not reaching LDLc target levels despite maximal doses of statins (591). Thus, there is an unmet need for cheaper, more accessible inhibitory molecules.

Camelid sdAbs, also known as nanobodies, were first discovered in 1993 (550). Different from conventional antibodies, up to 75% of camelid antibodies are devoid of light chains. They are made of two hcAbs, each comprising an antigen binding domain (VHH or sdAb), followed by two constant domains CH2 and CH3 (556). Although 10-fold smaller (~13 kDa) than conventional IgGs, sdAbs bind antigen targets with equivalent specificity, affinity and low toxicity (560), and show enhanced tissue penetration. Importantly, sdAbs can be produced from recombinant bacteria, and are thus expected to be cheaper and easier to manufacture. They can also easily be engineered to achieve high potency by affinity maturation and can be humanized for pre-clinical studies in non-human primates and in human (556, 572). Therefore, they constitute an attractive alternative to mAbs (565, 577, 592).

In the present study, following llama injections of full length hPCSK9, we isolated a number of sdAbs that inhibit the function of PCSK9 on LDLR degradation in various cell lines and primary hepatocytes. The validation of a selected sdAb called P1.40 was performed in Pcsk9 KO mice carrying a 67.5 kb human BAC Tg that results in the expression of hPCSK9 under its own promoter.

II.4 Methodology

II.4.1 Generation of anti-PCSK9 single domain antibodies

hPCSK9 carrying a C-terminal His-tag was purified to homogeneity from the media of baculovirus-infected High Five cells (593). A male llama (*Lama glana*) was immunized with 80 µg of PCSK9 on day 1, and with 20 µg on days 21, 36, 50 and 64. Complete Freund's adjuvant (Sigma) was used for the primary immunization and incomplete Freund's adjuvant was used for immunizations 2–5. Leukocytes were isolated from the last bleed at day 71 post-immunization. Total RNA was then isolated, reverse-transcribed and used to produce an immune V_HH library as previously described (594). Briefly, the cDNAs encoding V_HH domains were amplified using specific sense (MJ1, 5-GCCCAGCCGGCCATGGCCSMKGTGCAGCTGGTGGAKTCTGGGGGA-3; MJ2, 5-CAGCCGGCCATGGCCCAGGTAAAGCTGGAGGAGTCTGGGGGA-3; and MJ3, 5-GCCCAGCCGGCCATGGCCCAGGCTCAGGTACAGCTGGTGGAGTCT-3) and antisense (CH2, 5-CGCCATCAAGGTACCAGTTGA-3 and CH2b3, 5-GGTACCTGTCATCCACGGACCAGCTGA-3) primers for V_HH and CH2 domains (S:C or G; M: A or C; K: G or T), respectively, and cloned into the phagemid pMED1 vector. The size of the library was measured as 2.3 x 10^8 independent transformants, greatly exceeding the number of leukocytes used for library construction. Exponentially growing *E. coli* expressing the phagemid library were infected with helper phages to "rescue" the phage particle auto-assembly, and grown overnight for phage production. Isolation of PCSK9-specific sdAbs was performed by phage display. Using PCSK9-coated 96-well plates, four rounds of panning were performed, with each round comprising steps of phage binding to PCSK9, washes, phage elution and amplification. In a last step, the phages produced by 45 individual clones were tested for their ability to bind PCSK9, and the 10 strongest binders were selected. Corresponding sdAbs were sequenced and subcloned in a pSJF2H vector comprising an *OmpA* signal peptide that targets the protein to the periplasmic space of *E. coli*, and a C-terminal hexa-His tag that allowed sdAb purification by an automated procedure using a KingFisher Flex (Thermo Scientific).

II.4.2 Co-immunoprecipitation

HEK293 cells were plated in 100 mm^2-plates and transiently transfected using jetPRIME (Polyplus transfection) with 10 µg of vectors (168, 184) coding for various PCSK9 constructs or each of the four sdAbs. The sdAb conditioned media were incubated with those containing PCSK9 variants (Figure 22A), and immmunoprecipitated with TALON Metal Affinity Resin (Clontech) overnight at 4°C. The following day, the samples were washed 4 times with Radio ImmunoPrecipitation Assay (RIPA) buffer (50 mM Tris-HCl, pH 8.0, 1% (v/v) Nonidet P-40, 0.5% sodium deoxycholate, 150 mM NaCl, and 0.1% (v/v) sodium dodecyl sulfate (SDS)), and lastly with phosphate-buffered saline (PBS). The immunoprecipitates were then resolved on a 12% Tris-glycine SDS polyacrylamide gel electrophoresis (SDS-PAGE) and revealed by a V5-HRP antibody (Invitrogen).

II.4.3 PCSK9-sdAb complex binding to the LDLR

The ability of sdAbs to prevent the interaction of PCSK9 with the EGF-A domain of LDLR was assessed using a PCSK9-LDLR *in vitro* binding assay kit (Circulex).

II.4.4 Purification of sdAb-Fc fusion proteins

Four selected sdAbs (P1.40, PKF8, PKE9, P2.57) were fused through their C-terminus to a mouse IgG2a Fc domain carrying a C-terminal V5 tag. Chimeric proteins were expressed in modified proprietary HEK293 cells and purified to homogeneity with a yield of 80-100 mg per 600 ml of medium (National Research Council Canada, Biotechnology Research Institute).

II.4.5 sdAb-Fcs affinity measurements to PCSK9

Affinity measurements were performed by the XTAL BioStructures, Inc. Briefly, PCSK9 carrying a C-terminal His-tag was captured on a NiHC1000M chip non-covalently at various low densities to determine kinetic binding parameters of the four different sdAb-Fcs. All binding experiments were performed at 25°C on a BiOptix 404pi Enhanced Surface Plasmon Resonance (E-SPR) instrument. A 7-point, 3-fold dilution of sdAbs starting at 200 nM were injected over each of three PCSK9 densities and the sensorgrams were globally fitted with a floating Rmax using Scrubber2

software. Fits across all three ligand densities matched well, suggesting little influence from avidity due to bivalency of the antibodies to the calculated binding parameters.

II.4.6 Cell culture

Human hepatocellular carcinoma HepG2 cells from the American Type Culture Collection (ATCC) were grown in Eagle's Minimal Essential Medium (EMEM, Wisent). Cells were stably transfected with either wild type (WT) or D374Y GOF PCSK9 using the FuGENE HD transfection reagent (Promega) and grown with 600 µg/ml of G418 (Wisent) for selection of cells stably expressing the cDNA coding for PCSK9. Immortalized human primary hepatocytes (IHH) were generously provided by Dr. H. Moshage from the University Hospital Groningen, the Netherlands (595), and were grown in William's E Medium (Wisent). HEK293 cells were grown in DMEM. All cells were maintained at 37°C under 5% CO_2.

II.4.7 sdAb-Fc assays

Purified PCSK9 (69) or conditioned media from HEK293 cells overexpressing either WT or D374Y PCSK9 were pre-incubated for 1h at 37ºC with various amounts of purified sdAb-Fcs. The mix was then applied onto cells for 4h to 24h. For experiments with HepG2 cells stably overexpressing WT or D374Y PCSK9, sdAb-Fcs were diluted in the culture medium and directly added to cells. In separate experiments we also incubated the above cells with various concentrations of the inhibitory mAb evolocumab, originally denoted as Amgen's AMG-145 (49), kindly supplied by Dr. Robert Dufour from our institute (IRCM).

II.4.8 DiI-LDL uptake assay

HepG2 cells were plated at a density of 25,000 cells/well in 96-well plates (Corning) in EMEM medium containing 10% FBS. After 18-20h, cells were washed and switched to serum-free medium (SFM) containing 5% lipoprotein-deficient serum for 24h. Purified PCSK9 and sdAb-Fcs were pre-incubated at 37°C in the same medium and added on cells (3 wells/condition). After 3h at 37°C, 10 µL of DiI-LDL (Biomedical Technologies) were added to the cell medium (5 µg/ml), and cells were further incubated for 2h. After 3 washes in D-PBS (without calcium and magnesium; Wisent), plates were scanned on a SpectraMax i3 Multi-Mode Detection Platform

(Molecular Devices). DiI-LDL uptake was measured in each well as an average fluorescence intensity. Plates were then frozen overnight (-80°C) and used the next day to perform a CyQuant cell assay (Invitrogen) for normalizing the DiI-LDL uptake to the number of cells in each well.

II.4.9 Immunofluorescence

About 70,000 HepG2 cells/well were seeded in 24-well plates containing coverslips (Fisher) coated with poly-lysine (Sigma), and cultured overnight in complete medium, and in SFM containing 5% lipoprotein-deficient serum for the following 24h. Following a 4h incubation with PCSK9 (3 μg/ml) alone or in combination with each sdAb-Fc (1.2 μM), cells were rinsed with cold PBS, incubated 10 min on ice with LDLR antibody (1:200 in SFM; mouse, R&D systems), rinsed twice with cold PBS and finally fixed with 4% paraformaldehyde for 10 min on ice and 5 min at room temperature (RT). After 2 washes in PBS at RT and a 30 min incubation with PBS containing 1% BSA, LDLR-antibody complexes were revealed by a 5 min incubation with anti-mouse Alexa Fluor 555-tagged antibody (1:200; goat, Molecular Probes). Cells were then rinsed twice with PBS and nuclei were stained with DAPI during the final mounting step (ProLong Gold Antifade Reagent with DAPI, Life Technologies). Immunofluorescence analyses were performed with a confocal microscope (Zeiss LSM-710) and the Volocity software (x64, Perkin Elmer). Because the parameters remained unchanged throughout image acquisition, the values obtained were proportional to LDLR levels (47).

II.4.10 Western blotting

Cells were washed twice with ice-cold PBS and lysed 40 min on ice with RIPA buffer supplemented with 1x complete protease inhibitor mixture (Roche Applied Science). The cell lysates were then subjected to 8% Tris-glycine SDS-PAGE. The gels were transferred overnight on PVDF membranes (Millipore) that were blocked for 1h at RT in TBST (50 mM Tris-HCl, pH 7.5, 150 mM NaCl, 0.1% Tween 20) containing 5% non-fat dry milk. Membranes were then incubated overnight at 4°C in 5% milk-TBST with human (goat, R&D systems) or mouse (goat, Novus Biologicals) LDLR antibody (1:1,000) and human β-actin antibody (mouse, Sigma; 1:2,500) for normalization. After incubation with secondary antibodies coupled to horseradish peroxidase (HRP) at 1:10,000 in 5% milk-TBST, immunoreactive bands were revealed by

chemiluminescence using the ECL plus kit (GE Healthcare). Quantification was performed with the ImageJ software or using a Biorad ChemiDoc MP imaging system.

II.4.11 Mouse primary hepatocytes

Primary hepatocytes were isolated from the liver of 6- to 14-week old mice using a two-step collagenase perfusion method as described previously (306). Fibronectin-coated (0.5 mg/ml, Sigma) plates (24-well) were seeded with ~10^5 cells/well in Williams' medium E (Wisent) containing 10% FBS. After 2h, the medium was replaced with HepatoZYME medium (Gibco) for 12h prior to treatment.

II.4.12 LDLR ELISA assay

Cells were lysed for 40 min on ice at 4°C with ice-cold, non-denaturing cell lysis buffer (20 mM Tris-HCl, pH 8, 137 mM NaCl, 2mM Na2EDTA, 1% NP-40, 10% glycerol,4% protease inhibitor cocktail without EDTA). Cell lysates were pooled for each experiment, total human LDLR was measured by ELISA (human LDLR DuoeSet ELISA Development kit, R&D Systems) and protein levels by a protein assay (Bio-Rad DC). Briefly, a high-binding 96-well plate was coated and incubated overnight at RT with mouse anti-human LDLR antibody (4 μg/ml) diluted in PBS. The next day, the plate washed four times with PBS/0.05% Tween-20 and blocking was carried out with PBS/1% + BSA/0.05% + Tween-20/0.01% sodium azide for 1.5h at RT. Following four washes, standards (7 points, 2-fold serial dilutions starting at 8 ng/ml, and a zero point) and pooled cell lysates (5-fold dilution in PBS/1% BSA) were added to the plate and incubated for 2h at RT. After four washes, detection was carried out with biotinylated goat anti-human LDLR antibody (0.4 μg/ml, diluted in ELISA buffer: 20 mM Tris-HCl, pH 7.2-7.4, 137 mM NaCl, 0.05% Tween-20, 0.1% BSA) for 2h at RT. Following four washes, streptavidin-HRP diluted in ELISA buffer (1:200) was added and incubated for 20 min at RT, protected from direct light. After four washes, substrate solution containing a 1:1 mixture of H_2O_2 and tetramethylbenzidine (R&D Systems) was added to the wells and incubated in the dark for 20 min at RT. The reaction was stopped with 2N sulfuric acid (R&D Systems). The optical density of the yellow colored product was determined using a SpectraMax i3 plate reader (Molecular Devices) set to 450 nm, from each the readings at

540 nm were subtracted to correct for any plate imperfections. The total amount of LDLR was normalized to the quantity of total protein measured in each cell lysate.

II.4.13 Expression of sdAb-Fc fusion proteins carrying a KDEL C-terminal tag

The pIRES2-EGFP vector expressing the sdAb-Fc fusion protein carrying a KDEL ER-retention signal at the C-terminus of the protein, downstream of the V5 tag, was obtained as described previously (184). HEK293 cells (~300,000 cells/well) were seeded in 12-well plates in complete media, transfected overnight with various constructs using FuGENE HD and switched to SFM for another 24h.

II.4.14 Expression of EGFs-Fc fusion proteins

A DNA sequence encoding amino acids 314-393 of Genbank accession no. P01130 (the epidermal growth factor-like repeat AB domain (EGF-AB) of human LDLR) was synthesized by GeneArt (Thermo Fisher). Both sequences were ligated between a signal peptide and the sequence of human IgG1 Fc in the plant expression/transformation vector pTRAkc (596). The clones were transformed into *Agrobacterium tumefaciens*, which was then used for transient expression in *Nicotiana benthamiana* (597). The recombinant proteins were purified by Protein A affinity chromatography.

II.4.15 Fluorescence-associated cell sorting (FACS) analysis

About 500,000 HepG2 cells/well were seeded in 12-well plates in complete media overnight and in SFM for 24h. Cells were then incubated with PCSK9 (15 μg/ml) for 4h alone, with sdAb-Fc (0.04 μM), with increasing concentrations of EGF-AB-Fc (Planet Biotechnology Inc.) or their Fc control. Cells were rinsed in FACS buffer (D-PBS containing 0.5% BSA and 1 g/L glucose (Wisent)), then in 2.5 mM EDTA-2Na-2H_2O (Bioshop), and incubated for 20 min at 37°C in 0.5 ml of EDTA-2Na-2H_2O. Detached cells were collected, centrifuged for 5 min at 72 g at 4°C, re-suspended in 0.5 ml of FACS buffer containing 1:250 of human LDLR antibody (R&D Systems) and incubated for 10 min on ice. Cells were then washed with 5 ml of FACS buffer, centrifuged, re-suspended in 0.5 ml FACS buffer containing 1:500 of goat Alexa Fluor 647-labeled anti-mouse antibody (Molecular Probes) and incubated for 5 min. Cells were washed again, re-suspended in

0.3 ml of FACS buffer containing 1.67 µg/ml propidium iodide (Sigma) and finally analyzed by FACS using a CyAn flow cytometer (Beckman Coulter).

II.4.16 Animal studies

The RPCI human BAC library 11 was screened by PCR for the presence of the *PCSK9* gene and the clone 55M23 identified. A 67.5 kb fragment of the BAC was injected into B6C3F1 fertilized eggs. Mice were then backcrossed to *Pcsk9* KO mice in C57BL/6J background for 5 generations. Thus, these mice only express hPCSK9 and no mouse orthologue. Male mice (Tg+ and Tg- littermates) were injected in the tail vein with vehicle (PBS) or 10 mg/kg of sdAb-Fc. For single injections mice were analyzed 4 days post-injection, whereas for double injections, mice were injected at day 0 and 7 and sacrificed at day 11. In both cases blood samples and livers were collected. TC levels were determined by the colorimetric assay Infinity (Thermo Scientific) and apoB levels by ELISA (Cloud-Clone Corp.). Liver LDLR levels were measured by Western blot (WB) using a mouse LDLR (mLDLR) antibody, as for primary hepatocytes.

II.4.17 Statistics

Two-tail Student's *t* test was performed in order to assess the statistical significance of the data sets. For the DiI-LDL uptake assay, a two-way ANOVA was performed when triplicates were repeated more than once.

II.5 Results

II.5.1 Inhibitory PCSK9 sdAbs

We obtained sdAbs directed against hPCSK9 by llama immunization and screening of an immune phage display library (Figure 22B). The cDNAs of 10 selected sdAbs that bind PCSK9 efficiently were sequenced. Alignment of their corresponding protein sequences revealed that they belong to distinct sub-families (Figure 22C). A member of each of family was selected to favor sdAb diversity. P1.40, PKE9, PKF8 and P2.57 sdAb cDNAs were then subcloned in an expression vector for production in *E. coli* and purified by His-affinity chromatography.

To define the recognition domains within PCSK9, each sdAb carrying N-terminal V5 and C-terminal hexa-His tags was separately expressed in HEK293 cells. The conditioned media were then mixed with those containing different forms of PCSK9: the full-length protein harboring a C-terminal V5 tag (PCSK9), the CHRD alone, and the C-terminally truncated L455X mutant lacking the CHRD (168, 184) (Figure 22D). The sdAb-PCSK9 complexes were then immunoprecipitated using a hexa-His-binding resin and resolved by SDS-PAGE and analyzed by WB using a mAb-V5. As expected, all sdAbs interacted with full-length PCSK9, but surprisingly all four sdAbs best recognized the CHRD as indicated by the very efficient immunoprecipitation of this domain (Figure 22A, D). In comparison, only traces of the L455X mutant (Figure 22D) were observed. Here we only show the results for P1.40, as all other sdAbs gave similar data (*not shown*). To define which module(s) in the CHRD are recognized by the sdAbs, we performed similar experiments with PCSK9 variants lacking the CHRD modules M2 alone (ΔM2), M2 and M1 (ΔM1M2) or M2 and M3 (ΔM2M3). We could only use the above deletants as PCSK9 ΔM1, ΔM3 or ΔM1M3 are not secreted (180). The data showed that P1.40 does not recognize the M2 module (45% of the ΔM2 input bound by P1.40), but the presence of both M1 and M3 is needed for optimal recognition, as only 18% of ΔM1M2 and 14% of ΔM2M3 inputs were immunoprecipitated with P1.40 (Figure 22E). The three other sdAbs also predominantly recognize ΔM2 (*not shown*).

Chimeric sdAbs were then fused to a mouse IgG2a Fc domain, known to increase the half-life of sdAbs in plasma (598), followed by a C-terminal V5 tag (Figure 22F). Each chimeric protein was

produced in HEK293 cells and purified from 600 ml of spent media. The purity of each preparation was assessed by Coomassie staining of an SDS gel run under reducing (+DTT) or non-reducing (-DTT) conditions. All sdAb-Fcs have an apparent molecular mass of ~42 kDa as monomers under reducing conditions (+DTT) and of ~85 kDa as disulfide-linked dimers under non-reducing conditions (-DTT) (Figure 22G). The estimated molecular masses of the dimeric chimeras using MALDI mass spectral analysis were as expected from theoretical calculations, i.e., ~89 kDa for P1.40, ~85 kDa for PKE9 and PKF8, and ~87 kDa for P2.57.

We next used Enhanced Surface Plasmon resonance to estimate the binding constants (K_d) of each sdAb-Fc to PCSK9. The rank order of binding constants were : PKF8 (5.6 nM) > P2.57 (9.8 nM) > PKE9 (37 nM) > P1.40 (49 nM). However, as will be shown later, the above *in vitro* binding affinities do not necessarily correlate with the most active sdAb-Fc to inhibit the PCSK9-enhanced cellular degradation of the LDLR.

Although these four sdAb-Fcs interact with the CHRD M1/M3 modules (Figures 22D, E), we assessed their ability to disrupt the PCSK9 interaction to the EGF-AB domains of the LDLR in an *in vitro* binding assay (Figure 22H). The data show that the sdAb-Fcs did not decrease PCSK9 binding to LDLR, demonstrating that none of the sdAbs interferes with the ability of PCSK9 to bind the EGF-AB domain of the LDLR. Surprisingly, almost 2-fold higher PCSK9 binding was observed with all sdAb-Fc, except for P2.57. The doubling of PCSK9 levels bound to EGF-AB is likely due to the fact that sdAb-Fcs are homodimers (Figure 22G) and hence could conceptually bind up to two PCSK9 molecules.

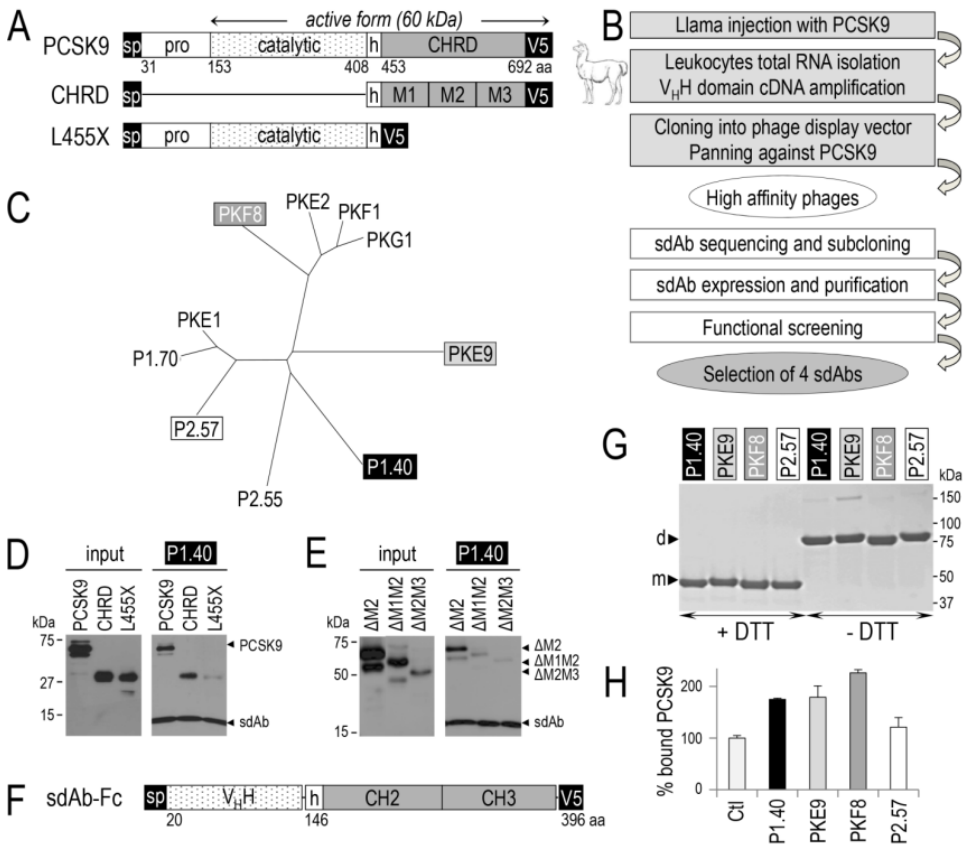

Figure 22. Generation of llama PCSK9-specific sdAbs, PCSK9 binding to sdAb, effect of the sdAb on LDLR binding. The primary structure of PCSK9 and its deletants are shown: aa, amino acid; sp, signal peptide; pro, prodomain; h, hinge domain; CHRD, Cys/His-rich domain and its modules M1, M2 and M3 (*A*). Flow chart of the steps for llama sdAb selection (*B*). Phylogenetic tree deduced from the alignment of the full protein sequences of 10 selected sdAbs (*C*). The media of HEK293 transiently expressing PCSK9 or its deletants lacking either the pro- and catalytic domains (CHRD) or the CHRD (L455X) and the sdAb P1.40 were mixed and immunoprecipitated with TALON Metal Affinity Resin. The input (conditioned media containing the different PCSK9 variants) and pellets were analyzed by WB with mAb-V5 antibody after SDS-PAGE on 12% Tris-glycine gels (*D*). Similar experiments were performed on PCSK9 variants lacking the CHRD modules M2 alone (ΔM2), M2 and M1 (ΔM1M2) or M2 and M3 (ΔM2M3) (*E*). Panels (*D*) and (*E*) are representative of three independent experiments. Schematic of the representative fusion of P1.40 with a mFc comprising the hinge (h), CH2 and CH3 domains (*F*). Purified sdAb-Fcs (2 µg) were separated by SDS-PAGE in the presence (+) or absence (-) of DTT, and revealed by Coomassie staining (*G*). The four sdAb-Fcs were incubated with PCSK9 and tested for their ability to prevent binding of PCSK9 to the LDLR EGF-AB coated on a binding assay plate (*H*). This assay is an average of three technical replicates.

II.5.2 Effect of sdAb-Fcs on DiI-LDL uptake and cell surface LDLR levels in HepG2 cells

To assess the ability of each sdAb-Fc to inhibit the PCSK9-mediated degradation of the LDLR, we pre-incubated purified PCSK9 (0.08 μM) with increasing concentrations of sdAb-Fcs (0 to 1 μM) for 1h and applied these media onto HepG2 cells for a further 5h incubation. PCSK9 alone resulted in a ~60% decrease of the DiI-LDL uptake, reflecting the reduced levels of functional LDLR at the cell surface (first two bars in Figures 23A, B). All sdAb-Fcs except P2.57 exhibited a dose-dependent inhibitory effect, with the P1.40 being the most potent, giving a ~80% inhibition at 0.1 μM, and 100% at 1 μM (Figure 23A). In a separate experiment, we also showed that the mAb evolocumab gave a similar ~80% inhibition between 0.04 and 0.1 μM and a 100% inhibition at 1 μM (Figure 23B).

We also tested by immunofluorescence the ability of each sdAb-Fc to rescue the LDLR cell surface labeling of HepG2 cells. PCSK9 (0.05 μM) and the sdAb-Fcs (1.2 μM) were pre-incubated as above and applied onto cells for 4h (Figure 23C). LDLR labeling was quantified by confocal microscopy and expressed as a percentage of that in control cells not exposed to PCSK9. All four sdAb-Fcs were able to enhance the levels of immunoreactive LDLR, proving their inhibitory potential, but could not completely rescue the LDLR signal in this assay. Again, P1.40 seemed the most potent sdAb-Fc with ~50% rescue of immunoreactive cell-surface LDLR.

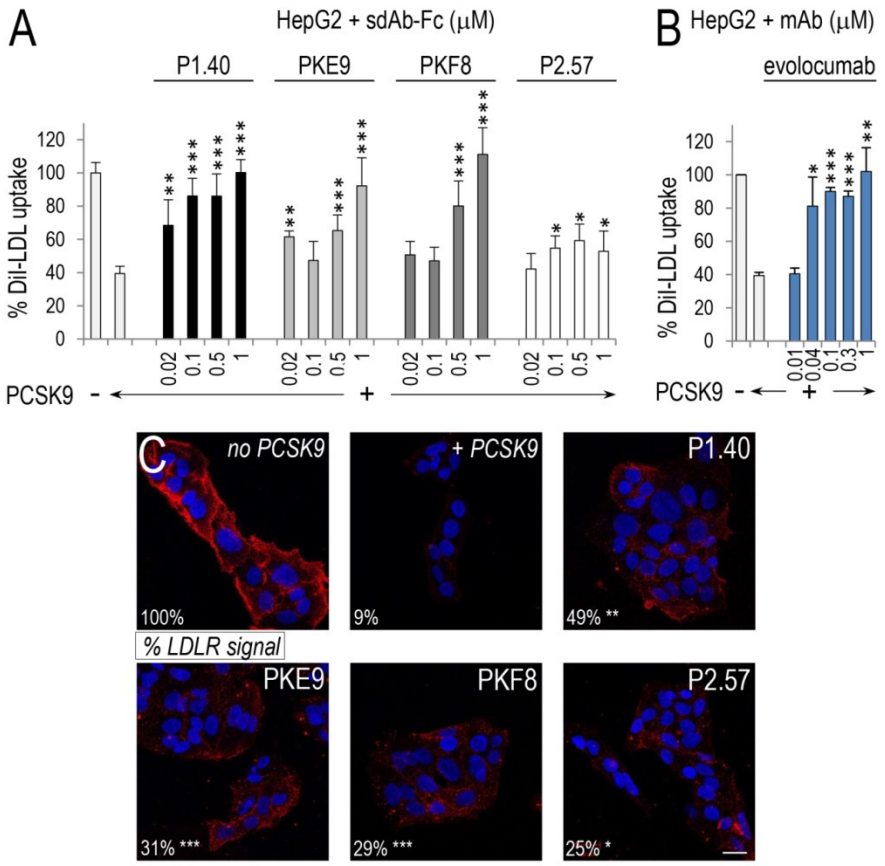

Figure 23. Effect of sdAb-Fcs on DiI-LDL uptake by HepG2 cells and their LDLR cell surface levels. HepG2 cells were incubated for 5h in the absence or presence of 0.08 μM (5 μg/ml) PCSK9 mixed with increasing concentrations of sdAb-Fcs. DiI-LDL (5 μg/ml final) was added during the last 2h of incubation. The % DiI-LDL uptake shown here is normalized to the number of cells per well and calibrated to the % uptake in control cells (in absence of PCSK9) (*A*). A similar experiment was performed with evolocumab (*B*). In both (A) and (B) the data represent averaged values ± standard error of the mean (SEM) for at least three independent experiments, with each comprising three independent samples per condition. HepG2 cells were incubated for 4h without (*no PCSK9*) or with 0.05 μM (3 μg/ml) of PCSK9 (+*PCSK9*) in the absence or presence of each sdAb-Fc (1.2 μM). LDLR immunocytochemistry with Alexa 555-labeled secondary antibodies was performed, and nuclei were stained with DAPI. Scale bar indicates 20 μm (*C*). In two separate experiments, LDLR labeling was quantified based on the average pixel values of 10 fields calibrated to the number of nuclei per field as determined by DAPI staining. The numbers (bottom left corner) are expressed as % of the value obtained in absence of PCSK9 (*no PCSK9*), and represent averaged pixel values of the two independent experiments. *, $P < 0.05$, **, $P < 0.005$, ***, $P < 0.0005$. *P* values were obtained from Student's *t* tests, except for some conditions in (*A*), for which a two-way ANOVA test was more appropriate.

II.5.3 Effect of sdAb-Fcs on total LDLR levels in hepatocytes

The inhibitory effect of sdAb-Fcs was then analyzed in mouse primary hepatocytes, which are closer to an *in vivo* model than HepG2 cells. The latter were isolated from PCSK9-deficient mice (172, 306) and used to test the sdAb activity towards hPCSK9 (in absence of endogenous mouse Pcsk9) and to maximize LDLR levels, which were reported to increase by ~3-fold in KO *versus* WT mice (172, 306). Notably, hPCSK9 acts similarly on both human and mLDLR (228). HepatoZYME media control (Figure 24A, upper panel) or containing 0.08 μM of PCSK9 and 0 to 1.2 μM of each sdAb-Fc were pre-incubated for 1h and then incubated with mouse primary hepatocytes for 24h. Normalized WB analyses of mLDLR levels revealed that P1.40 did not affect the levels of endogenous LDLR in the absence of PCSK9 (Figure 24A, upper panel), demonstrating the PCSK9 specificity for the inhibitory effect. In addition, in the presence of extracellular PCSK9 only P1.40 was able to totally rescue LDLR levels, while P2.57 had no effect (Figure 24A, lower panels). PKF8 and PKE9 led to a partial LDLR rescue at 1.2 μM, with relative levels of 0.7 and 0.6, respectively *versus* maximal 1.1 with P1.40. The above conclusions were confirmed in the IHH cell line. Indeed, incubation with the three sdAb-Fcs PKE9, PKF8 and P2.57 (*not shown*) showed low to good efficiency, whereas P1.40 showed the highest potency. Thus, the presented WB data only depict the results for P1.40 (Figure 24B), and all the rest of our studies will be conducted with P1.40.

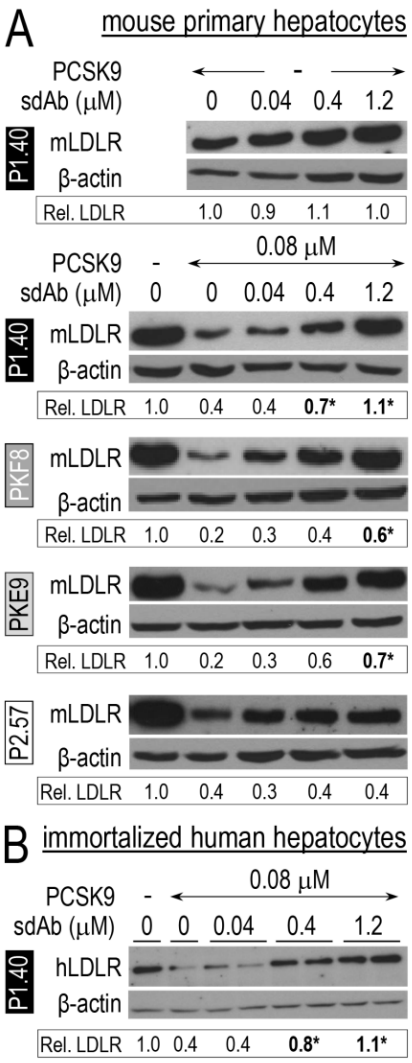

Figure 24. Effect of sdAb-Fcs on total LDLR levels in hepatocytes. Primary hepatocytes isolated from PCSK9-deficient mice (*A*) or immortalized human hepatocytes (IHH; *B*) were incubated for 24h in the absence (-) or presence of 0.08 μM (5 μg/ml) WT PCSK9 and increasing concentrations of sdAb-Fc. Cell lysates were subjected to WB analysis of LDLR and β-actin levels after separation by SDS-PAGE on 8% Tris-glycine gels. LDLR signals were calibrated to β-actin ones and were normalized to the values obtained in the absence of sdAb-Fc. The blots shown are representative of at least five independent experiments, each run as one biological sample per condition. The averaged normalized LDLR values are indicated below each blot. *, $P < 0.05$, (Student's *t* test).

II.5.4 Inhibitory effect of P1.40 on WT and D374Y PCSK9

The inhibitory properties of P1.40 towards WT PCSK9 or its GOF mutant D374Y, which has a >10-fold higher affinity for the LDLR (173), was examined in naïve HepG2 cells (Figure 25A) or HepG2 cells stably expressing PCSK9 (Figure 25B) (176). Note that the LDLR appears as a doublet consisting of LDLR that is not O-glycosylated (110 kDa) and that is fully mature and O-glycosylated (150 kDa) (599). Unexpectedly, in both cases, the strongest recovery of the LDLR signal was obtained in the presence of D374Y PCSK9, suggesting that P1.40 neutralized the activity of this mutant form of PCSK9 with a higher efficacy. Indeed, the inhibition of PCSK9 activity at 1.2 μM was estimated at 93% for D374Y PCSK9 *versus* ~50% for WT PCSK9 (Figure 25A). As expected, upon stable PCSK9 expression, the LDLR signal was more efficiently reduced by the D374Y mutant. However, P1.40 incubation of D374Y PCSK9 stably expressing cells significantly increased the LDLR signal by a maximal 2.7-fold, whereas cells expressing the WT PCSK9 showed a more modest 1.7-fold increase obtained at all concentrations, revealing that the best effect was obtained at 0.04 μM P1.40 sdAb-Fc on cells stably expressing WT PCSK9 (Figure 25B).

In order to compare the efficacies of P1.40 to the mAb evolocumab, we performed similar experiments with WT PCSK9 added extracellularly to HepG2 cells (Figure 25C) and with HepG2 cells stably expressing D374Y PCSK9 (Figure 25D). WB analysis of the lysates revealed a ~90% recovery of the LDLR with 1.2 μM P1.40, whereas 150% were recovered with evolocumab at this concentration (Figure 25C), suggesting that in this WB assay evolocumab was more active than P1.40. Similarly, in HepG2 cells expressing D374Y PCSK9, evolocumab was more active that P1.40, as evidenced by a ~3-fold increase in LDLR with P1.40 *versus* ~6-fold with evolocumab at 1.2 μM (Figure 25D). Finally, these conclusions were supported by an LDLR ELISA assay performed on a pool of cell lysates obtained from experiments in Figures 25C, D, which also revealed the higher efficacy of evolocumab compared to P1.40, especially using the D374Y PCSK9 (Figures 25C, D, lower sections).

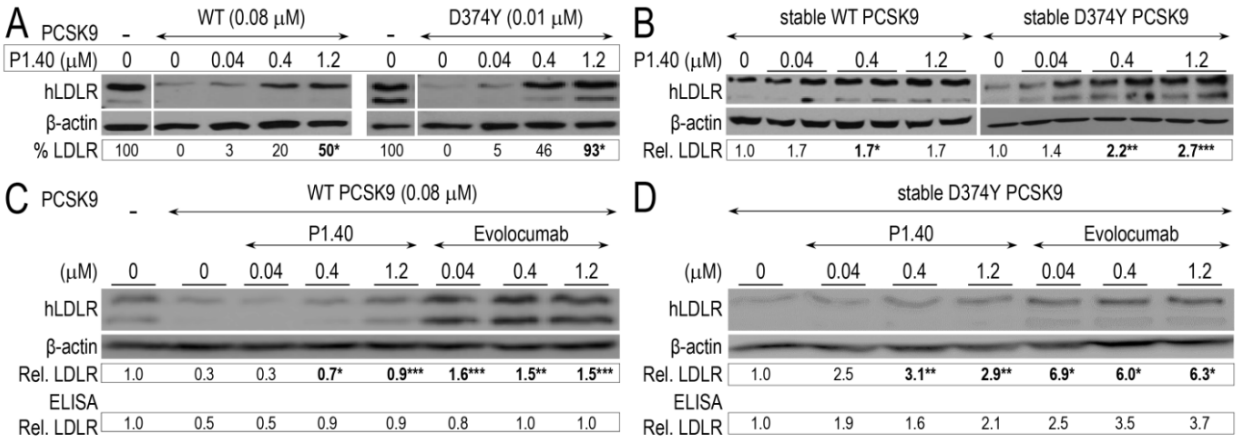

Figure 25. Inhibitory effect of P1.40 on WT and D374Y PCSK9. HepG2 cells were incubated 24h with media lacking PCSK9 or containing 0.08 μM (5 μg/ml) of WT PCSK9 or 0.01 μM (0.7 μg/ml) of D374Y PCSK9, and 0 to 1.2 μM sdAb P1.40 (*A*). The LDLR signal (% LDLR) was calibrated to that of β-actin levels and expressed in percentage of the difference between the first lane (no PCSK9) and second (+PCSK9) lane. Stably transfected HepG2 cells that expressed ~300 ng/ml/24h of WT or D374Y PCSK9 were incubated 24h with increasing concentrations of the sdAb P1.40 (*B*). HepG2 cells were incubated 24h with media lacking PCSK9 or containing 0.08 μM (5 μg/ml) of WT PCSK9, and 0 to 1.2 μM sdAb P1.40 or evolocumab (*C*). Stably transfected HepG2 cells that expressed ~300 ng/ml/24h of D374Y PCSK9 were incubated 24h with increasing concentrations of the sdAb P1.40 or evolocumab (*D*). The blots shown are representative of at least two independent experiments consisting of one (*A*), two (*B*), and three (*C, D*) biological samples per condition. In both (*C*) and (*D*) we also quantified the total levels of cellular LDLR using an ELISA assay on pooled cell lysates. The calibrated LDLR signals were normalized to that of the first lane (no sdAb). The averaged normalized LDLR values are indicated below each blot. *, $P < 0.05$, **, $P < 0.005$, ***, $P < 0.0005$ (Student's *t* test).

II.5.5 Effect of ER-localized sdAb-Fcs on PCSK9 secretion and activity

We next evaluated the ability of intracellular P1.40 to effectively retain PCSK9 within the ER, and hence block the PCSK9 activity. Accordingly, since addition of a C-terminal KDEL motif retains efficiently secretory proteins in the ER (600), we fused a KDEL retention signal to the C-terminus of P1.40-Fc-V5. Thus, P1.40 ± KDEL forms were co-expressed in HEK293 cells with PCSK9 or its D374Y mutant, and the LDLR levels assessed by WB analysis (Figures 26A, B). The data demonstrated that P1.40-KDEL was efficiently retained in the ER, as only traces of this protein were observed in the media (lanes 3, 6 and 10). Neither P1.40 nor P1.40-KDEL had an impact on LDLR levels (lanes 2 and 3), likely due to the quasi-absence of PCSK9 expression in HEK293 cells (mRNAs are 10,000-fold lower than in HepG2 cells). As expected, LDLR levels were reduced significantly (70%) upon expression of D374Y or WT PCSK9, respectively (lanes 4 and 8). The ER-retention of P1.40-KDEL clearly increased LDLR levels in cells expressing WT or D374Y PCSK9 (lanes 4-6 *versus* 8-10). Note that the inhibitory potency of P1.40 and P1.40-KDEL is almost similar (lanes 9, 10), possibly related to the high luminal concentrations of P1.40 attained during its transit through the Golgi, such that most of the intracellular PCSK9 activity is inhibited. However, higher levels of ER-retained WT PCSK9 by P1.40-KDEL had no effect on LDLR recovery above that of P1.40 alone (0.8 and 0.9; lanes 9 and 10), while higher intracellular levels of D374Y PCSK9 significantly increased LDLR levels (0.6 and 0.9; lanes 5 and 6).

In order to assess the subcellular localization of the intracellular forms of PCSK9 and LDLR, the above cell lysates were digested with endoglycosidases H (endoH) and F (endoF). As previously reported, most of the overexpressed PCSK9 found in cells is endoH and endoF sensitive, suggesting it is in the ER (63, 168). However, in the above cell lysates the LDLR is always endoH resistant, but endoF sensitive, even the lower 110 kDa form (*not shown*). This suggests that while P1.40 KDEL prevents the secretion of PCSK9, it does not result in the retention of the LDLR in the ER. This is very likely due to a recent discovery that LDLR does not bind efficiently to PCSK9 in the ER because of the presence of a competitive chaperone like-protein GRP94 that prevents such ER-interaction (199).

It was shown previously that PCSK9 can induce the degradation of the LDLR by distinct intracellular and extracellular pathways, and that cellular overexpression of WT PCSK9 mostly reflects the intracellular pathway, whereas expression of the ~10-fold more potent GOF D374Y PCSK9 affects both pathways (180, 186). Accordingly, the above data demonstrate that retention of PCSK9 in the ER by P1.40-KDEL, has a bigger effect on the inhibition of the D374Y activity than that of WT PCSK9 (Figure 26A, lanes 4-6 *versus* Figure 26B, lanes 8-10), likely due to the elimination of both pathways by P1.40-KDEL.

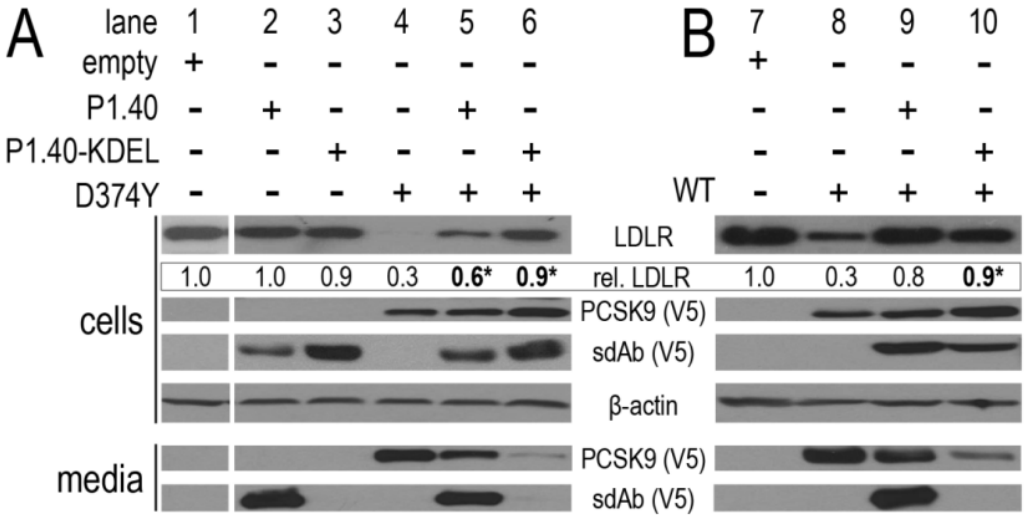

Figure 26. ER retention of the sdAb P1.40 via a C-terminal KDEL motif. P1.40-V5 ± KDEL and PCSK9-V5 mutant D374Y (*A*) or WT (*B*) were co-expressed in HEK293 cells. Lysates and media were then analyzed by Western blotting using LDLR, β-actin and V5 antibodies. These results are representative of at least two independent experiments run as a single biological sample per condition. The averaged normalized LDLR values are indicated below the LDLR blots.

II.5.6 PCSK9 inhibition by P1.40 versus EGF-AB domains from the LDLR

Because PCSK9 and LDLR interact essentially through the EGF-A domain of the LDLR (177), we compared the potency of P1.40 (sdAb-Fc) and the chimera consisting of the EGF-AB domains, mimicking the LDLR binding site to PCSK9, fused to a human Fc (EGFs-Fc). HepG2 cells were incubated for 4h in the absence or presence of PCSK9 pre-incubated with the Fc alone as a control, or its binding proteins P1.40 and EGFs-Fc (Figure 27). LDLR levels at the cell surface were then quantified by FACS. At 4h post-incubation, cell surface LDLR levels were reduced by ~60% in the presence of 0.2 μM PCSK9. A high concentration of Fc alone (7 μM) had no effect, whereas 0.04 μM P1.40 doubled the LDLR levels. In contrast, a 100-fold higher concentration of EGFs-Fc (4 μM) was required to obtain a similar effect. This suggests that P1.40 is between 10 to 100-fold more potent on a molar basis than the EGFs-Fc protein.

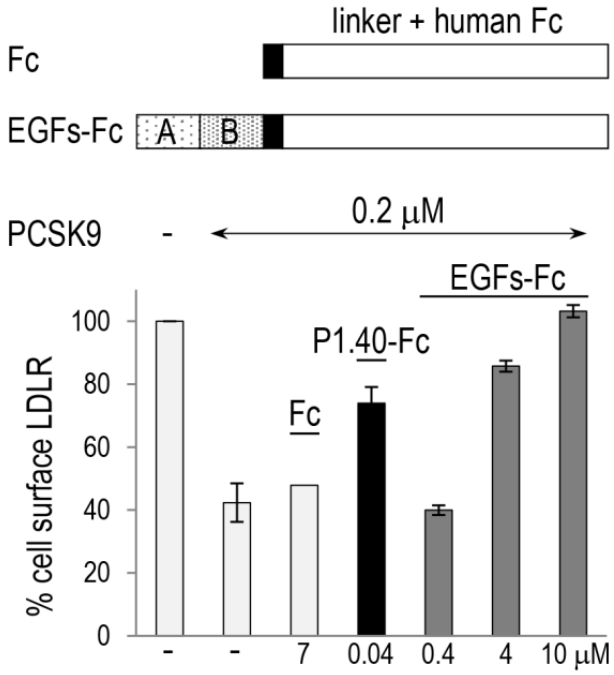

Figure 27. Comparison of the inhibitory activity of the sdAb P1.40 and EGF-AB fused to Fc domains. The primary structure of the Fc alone or EGF-AB fusion is shown. HepG2 cells were incubated for 4h in the absence (-) or presence of 0.2 μM (15 μg/ml) WT PCSK9 mixed with 7 μM of control linker+Fc (Fc), 0.04 μM sdAb P1.40, or 0.4 - 10 μM of EGFs+Fc. Cells were then analyzed by FACS for cell surface LDLR levels. The average values of two independent experiments are shown, except for Fc (n = 1).

II.5.7 *In vivo* efficacy of sdAb-Fc P1.40

We next validated the activity of P1.40 *in vivo*. *Pcsk9* KO transgenic mice carrying a 67.5 kb fragment of the human chromosome 1p32 containing the *PCSK9* gene (Tg^+) were obtained. These transgenic mice (Tg^+) express exclusively human *PCSK9* under the control of its own promoter, resulting in circulating PCSK9 levels of ~300 ng/ml, which are ~2-fold higher than endogenous levels of WT mice (234, 238). These Tg^+ mice exhibited ~1.7-fold and ~2.9-fold higher levels of circulating TC and apoB, respectively, as compared to littermate transgene-negative (Tg^-) *Pcsk9* KO mice (Tg^+ PBS *versus* Tg^- PBS; Figure 28). Tg^- and Tg^+ male mice were injected with equivalent volumes (~ 150 µl) of PBS or PBS containing P1.40 (10 mg/kg). Mice were bled 10 days pre-injection, and 1h, 2 days and 4 days post-injection. After the last bleed, livers were collected, homogenized and total LDLR protein levels were estimated by WB (Figure 28, lower panel). As expected, Tg^+ mice exhibited lower LDLR levels than Tg^- mice (0.4 *versus* 1.0). P1.40-Fc had no effect in Tg^- mice, but led to ~50% recovery of LDLR levels in Tg^+ mice (0.7 *versus* 0.4). Moreover, 32% and 44% reductions were observed in circulating TC and apoB levels 4 days post-injection (Figure 28, upper panels). In conclusion, these data indicate that P1.40 neutralized 66% and 71% of the TC and apoB increases resulting from the expression of hPCSK9 in KO mice.

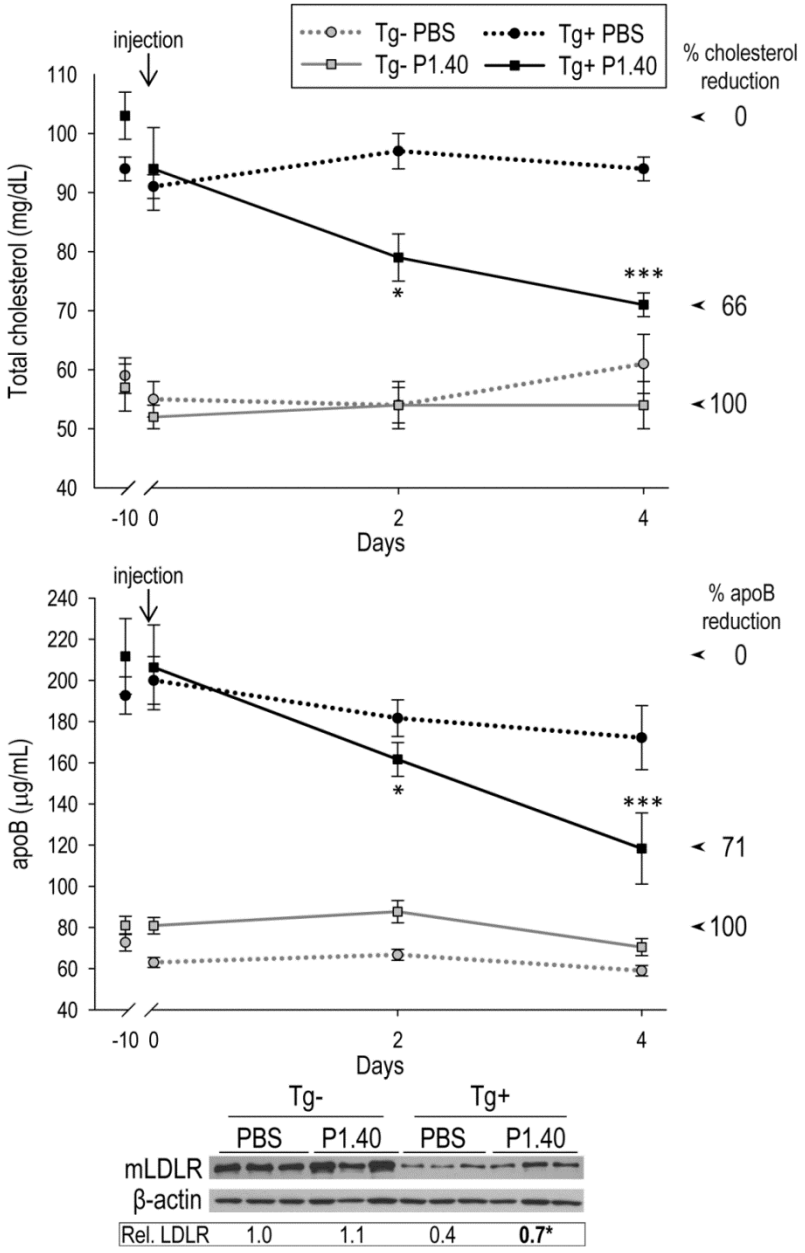

Figure 28. *In vivo* efficacy of the sdAb P1.40 after a single injection to mice. Plasma from Tg^- and Tg^+ that received PBS or P1.40 was collected before injection (-10 days) or 1h, 2 days and 4 days post-injection, and were analyzed for their cholesterol or apoB contents. The 0% reduction was fixed as the cholesterol or apoB levels in Tg^+ mice before P1.40 injection (highest levels), while the 100% reduction was given by the average levels observed in Tg^- mice (lacking PCSK9) receiving the same treatment. Liver LDLR levels were analyzed by WB, calibrated to β-actin ones, and normalized to the value obtained for Tg^- mice injected with PBS. A representative blot is shown and the averaged normalized LDLR values were obtained from 4-9 mice per group. *, $P < 0.05$, **, $P < 0.005$, ***, $P < 0.0005$ (Student's *t* test).

We next performed a similar experiment to test the possible advantage of a double injection at days 0 and 7 (Figure 29). Mice were bled 10 days pre-injection, and 1h, 2 days, 4 days, 7 days, 9 days and 11 days following the first injection. After the last bleed, LDLR protein levels were estimated by WB (Figure 29, lower panel). The data showed that P1.40 led to ~80% recovery of LDLR levels in Tg^+ mice (0.9 *versus* 0.4). In addition, 24% and 46% reductions were observed in circulating TC and apoB levels at 11 days after the first injection (Figure 29, upper panels). These data indicate that two injections of P1.40 resulted in the neutralization of the 44% and 100% of the TC and apoB increases resulting from the expression of hPCSK9 in KO mice.

In conclusion, compared to a single injection, two injections of P1.40 spaced by 7 days resulted in a more efficacious increase in hepatic LDLR and reduction in apoB levels, close to the ones seen in absence of PCSK9.

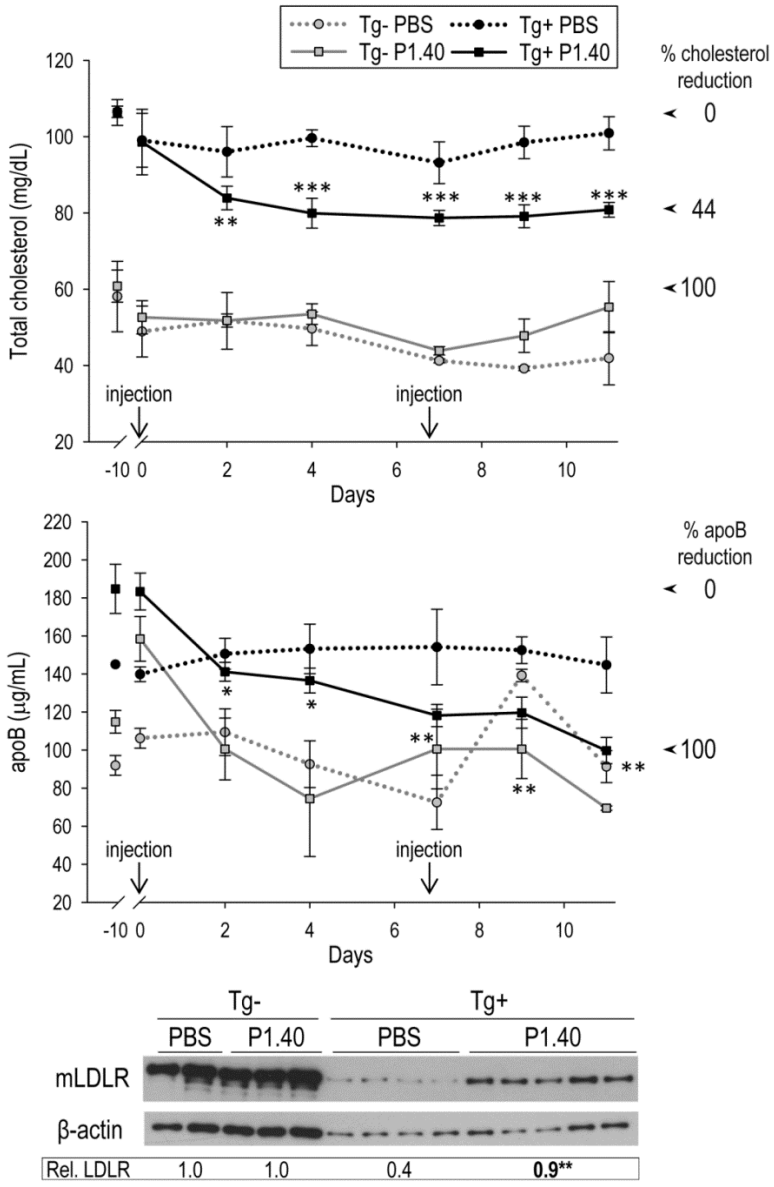

Figure 29. *In vivo* efficacy of the sdAb P1.40 after two injections to mice. Mice were injected at day 0, and then at day 7. Plasma from Tg^- and Tg^+ that received PBS or P1.40 was collected before injection (-10 days) or 1h, 2 days, 4 days, 7 days, 9 days, and 11 days following the first injection, and were analyzed for their cholesterol or apoB contents. The 0% reduction was fixed as the cholesterol or apoB levels in Tg^+ mice before P1.40 injection (highest levels), while the 100% reduction was given by the average levels observed in Tg^- mice (lacking PCSK9) receiving the same treatment. Liver LDLR levels were analyzed by WB, calibrated to β-actin ones, and normalized to the value obtained for Tg^- mice injected with PBS. A representative blot is shown and the averaged normalized LDLR values were obtained from 2-5 mice per group. *, $P < 0.05$, **, $P < 0.005$, ***, $P < 0.0005$ (Student's *t* test).

II.6 Discussion

In this work, we report the generation of four PCSK9 sdAbs with nM affinity against the CHRD (Figure 22). As sdAb-Fc fusion proteins, they efficiently inhibited PCSK9-induced LDLR degradation although they did not prevent the binding of PCSK9 to LDLR (Figure 22). In HepG2 cells, IHH cells, and/or primary hepatocytes, they restored LDL uptake, as well as cell surface and total LDLR levels (Figures 23-25). Even though P1.40 proved to be the most active sdAb candidate in our cell based assays, it was surprising to find that *in vitro* it bound the CHRD of PCSK9 with a ~5-fold lower K_d than P2.57, which has minimal inhibitory activity. Although this may not be the case in all functional sdAbs, it emphasizes the notion that a lack of correlation may exist between the binding affinity and functional inhibitory effect of PCSK9 sdAbs recognizing the CHRD.

Herein, we focused on the most promising sdAb-Fc, P1.40, and showed that its retention in the ER blocked PCSK9 secretion (Figure 26). We also showed that P1.40 was more potent than an EGF-AB-Fc fusion chimera (Figure 27). Finally, 4 and 11 days following a single/double injection, respectively, in transgenic mice expressing exclusively hPCSK9, P1.40 led to 32%/24% and 44%/46% lower circulating cholesterol and apoB levels respectively, and to 1.8-/2.3-fold higher levels of hepatic LDLR (Figures 28, 29).

The mAbs presently used in the clinic, e.g., evolocumab, bind the catalytic domain of PCSK9 and sterically hinder its binding to the LDLR (189). Although the four sdAbs analyzed in this study differed in their primary sequences (Figure 22C), they all bind the CHRD modules M1/M3 of PCSK9 (Figures 22D, E). It is important to note that all the other PCs (132) seem poorly immunogenic, as only for PC1 and PC2 do the available antibodies allow the detection of endogenous proteins in tissue extracts or by immunohistochemistry (601). Thus, the CHRD may be the most antigenic domain of PCSK9. Although this domain is not involved in LDLR binding (173), it is required for the PCSK9-induced LDLR degradation. Human LOF mutations are found in the CHRD, and PCSK9 lacking this domain cannot target the LDLR for degradation (174, 179, 184, 186, 262). In agreement, CHRD mAbs that do not block the LDLR interaction can reduce PCSK9 activity, albeit only partially (50-75% *versus* 100% for clinical mAbs) (187, 188). This

likely occurs through prevention of the cellular internalization and/or lysosomal targeting of the PCSK9-LDLR complex (190). Similarly, the four tested sdAb-Fcs did not sterically hinder PCSK9 binding to the LDLR (Figure 22H), suggesting a similar mode of action as the CHRD-specific mAbs. Future analysis of sdAb-PCSK9 complexes by X-ray crystallography should reveal their respective epitopes. Their degree of proximity to the catalytic domain will allow us to define the inhibitory mechanism of the corresponding sdAbs, and will possibly shed light on the better inhibition of D374Y than WT PCSK9 by P1.40 (Figure 25A). Whether any antibody targeting the CHRD may achieve a total PCSK9 inhibition, for example by interfering in PCSK9 binding to the LDLR, remains unknown.

Comparison of the potency of P1.40 to the mAb evolocumab that recognizes the catalytic domain of PCSK9 (189) revealed that at 1.2 μM the latter more efficiently inhibits LDLR degradation by WT and especially D374Y PCSK9 (Figures 25C, D).

Upon its ER localization *via* the addition of a C-terminal KDEL motif, P1.40-KDEL reduced PCSK9 secretion (by ~90%), and restored LDLR levels in cells expressing WT PCSK9 and more so D374Y PCSK9 (Figure 25). The potency of P1.40 was compared to that of a similar construct comprising the LDLR EGF-like domains A and B (EGFs-Fc) and was found to be between 10- and 100-fold higher with an EC_{50} ~0.04 μM *versus* 0.4 to 4 μM (Figure 27). In agreement with the above values, fusions containing EGF-A only or its improved form EGF66 exhibited EC_{50} of 11 μM and 1.6 μM, respectively, in the same HepG2 cells (460).

Mice lacking endogenous Pcsk9 and expressing human *PCSK9* gene under its own promoter exhibited higher TC and apoB levels than *Pcsk9* KO Tg^- mice. Single or double injections of P1.40 neutralized the increase in apoB levels after 4 days by ~70% and after 11 days by 100%, respectively (Figures 28, 29). In a "pioneer" experiment, the TC of WT mice was reduced by a PCSK9 mAb evolocumab injection by 26 and 28% after 3 and 6 days, respectively (189). In our study, we found that P1.40 can reduce TC by 32% and 24% at 4 or 11 days following P1.40 injections (Figures 28, 29), which is similar to the results obtained with evolocumab. Plasma PCSK9 remained quite stable at the different time points. However, when P1.40, which does not interfere with our *in house* ELISA, was immunoprecipitated from plasma obtained from the single

injection experiment, we found that ~50% of PCSK9 existed as a complex with P1.40 at day 4, indicating that no major clearance took place in this delay (*not shown*). Interestingly, a similar proportion of PCSK9 was captured by a human mAb recognizing the catalytic subunit causing a 40% reduction in LDLc in humanized CETP/LDLR-hemi mice (459). In another approach, the injection of a PCSK9 inhibitory "adnectin" conjugated to PEG in a similar mouse model led to a drastic reduction of free PCSK9 in the first 24h post-injection, but did not affect circulating cholesterol levels (447), suggesting a higher ability of adnectin to bind PCSK9 than to inhibit its activity towards LDLR. Although the molecular mass of our sdAb-Fc fusion protein is only 40 kDa *versus* ~50 kDa for conjugated adnectin, its dimerization (Figure 22G) may slow down its clearance.

Other proposed approaches to lower PCSK9 levels are based on ASO. In mice, they were shown to reduce PCSK9 mRNA levels and total and/or LDLc by ~50%, generally after several weeks of treatment (448-450, 453). Namely, LNP achieving liver-specific RNAi silencing of PCSK9 (453) are currently in Phase 2 and have a potential for bi-annual dosing (Alnylam pharmaceuticals). PCSK9 vaccines, peptide- or virus-like particle-based, were also developed, and achieved ~50% lower total and/or LDLc levels for up to one year in rodents and/or primates (465, 466).

Since their discovery in 1993 (560, 572), sdAbs have been studied extensively as new therapeutic tools. The first evidence of their *in vivo* efficacy was obtained in 2002 in a study showing that tumor growth in mice was inhibited by lysozyme sdAbs (573). Although no sdAb has yet been approved for clinical use, many of them are in clinical trials. For example, the sdAb caplacizumab targets von Willebrand factor (592) and is used to treat acquired thrombotic thrombocytopenic purpura in a Phase 3 clinical trial (Ablynx). Another advanced sdAb is ozoralizumab. It is directed against TNFα and fused to serum albumin, and is evaluated in a Phase 2 clinical trial for its efficacy in the treatment of rheumatoid arthritis (577). Finally, sdAbs neutralizing the respiratory syncytial- (Ablynx) or rota-virus (36) are currently in Phase 2 clinical trials.

In the present study, we developed the first sdAb that targets hPCSK9. This sdAb was shown to reduce PCSK9-mediated LDLR degradation *in vivo*, and therefore to increase hepatic LDLR and decrease TC and apoB levels. Further studies will be necessary to validate its therapeutic potential. Meanwhile, the P1.40 PCSK9 sdAb constitutes a precious tool to better define the mechanism underlying LDLR targeting to lysosomes, and thus to identify new PCSK9 partners. Biochemical, genetic and epidemiological studies revealed that loss of PCSK9 reduces the incidence of atherosclerosis (279), myocardial infarction (281), stroke (602), inflammation (174), sepsis (283), and tumor-associated metastasis (291). Because different domains of PCSK9 may be implicated in these processes, various inhibitory antibodies, including the present one that binds the CHRD and not the catalytic domain, may allow a fine tuning of PCSK9 inhibition.

II.7 Additional information

II.7.1 Funding

This work was supported by Canadian Institutes of Health Research Grants PP2-125775 and MOP 102741, Pfizer Cardiovasc Res awards, a grant from Amorchem, Canada Research Chair 216684, and Fondation Leducq Grant 13CVD03.

II.7.2 Acknowledgements

We are grateful to all the members of the Seidah laboratory for technical support and discussions. We are grateful to Suzanne Benjannet, who helped us with some experiments. We thank Drs. Rex Parker and Franck Duclos (Bristol Myers Squibb) for the donation of pure hPCSK9; Manon Laprise, Anna Roubtsova, and Jadwiga Marcinkiewicz for animal experimentation; and Dr. Dominic Filion for help in confocal imaging analysis. We also thank Shenghua Li for sdAb production in Dr. Zhang's laboratory, and Drs. Archana Belle and James Maclean from Planet Biotechnology who worked on the development of EGFs+Fc. Finally, we acknowledge the precious help of Dr. Robert Dufour from the Institut de Recherches Cliniques de Montréal for the generous gift of evolocumab.

II.7.3 Conflict of interest

The authors declare that they have no conflicts of interest with the contents of this article.

II.7.4 Author contributions

EW conducted most of the experiments and analyzed the results. DSR conducted several early experiments, including those on DiI-LDL uptake. RE prepared the primary hepatocytes and conceived the mouse model. JH did most of the cloning work, and MCA contributed to cell culture. YA performed one of the co-immunoprecipitations. KLW provided the EGFs-Fc proteins. JZ produced and screened the llama library. **AP analyzed the data and wrote the manuscript with EW and NGS, who also conceived and followed the project.** SN provided the original screen for the best sdAbs that bind PCSK9 from the llama library and their functional analysis in cell lines.

II.8 Chapter discussion

In this chapter, a thorough characterization of four selected sdAb-Fcs targeting PCSK9 was presented. Although the latter were selected because they belong to four distinct phylogenetic groups based on their protein sequence, note that in some assays, their efficacies were difficult to discriminate, especially in FACS assays (see Appendix A1). Except P2.57-mFc, which showed less promising results in most of the assays, which was confirmed in an *in vivo* assay, the three other sdAbs gave similar activities. In several tests, this was not facilitated by the narrow window of the assay, which had to be optimized by adjusting various parameters such as the concentration of PCSK9, the time of incubation of the sdAb-PCSK9 complexes on cells, the number of plated cells and the passage number of cell lines.

The fact that we only obtained sdAbs targeting the CHRD can be explained by the fact that the CHRD is the most antigenic domain of PCSK9 and/or by the fact that apoB or LDL bind to the injected hPCSK9 in the llama plasma. Note that in order to overcome this shortcoming, we performed two other camelid immunizations with hPCSK9 in collaboration with Dr. Serge Muyldermans, a Belgian scientist who participated in the discovery of sdAbs, and his scientist Dr. Cécile Vincke. We first injected an alpaca and then a dromedary (*data not shown*). On one hand, the alpaca injection yielded 7 sdAbs with K_d for hPCSK9 ranging between 9 and 220 nM. Unfortunately, only one sdAb showed a potency to increase LDLR levels that was much lower than the one obtained with llama sdAbs. On the other hand, the dromedary injection yielded 14 sdAbs with K_d for hPCSK9 ranging between 6.4 and 181 nM. The latter seemed more promising since three of them showed potencies similar to our llama sdAbs and three others were similar to evolocumab in a cell-based assay. These efficiencies suggesting that these sdAbs might bind the catalytic domain of PCSK9, their binding domains on PCSK9 were determined by immunoprecipitation. Unfortunately, the data indicated once again that all sdAbs bind the CHRD of PCSK9, with the exception of 5 sdAbs that might bind both the CHRD and the catalytic domain (*data not shown*). More cell-based assays will be needed in the future in order to confirm that the potency of these sdAbs is more important than llama sdAbs or evolocumab. *In vitro* assays will also need to be performed to determine if these sdAbs prevent PCSK9 binding to LDLR. Note that

the PCSK9-specific sdAbs were selected by phage display using immobilized PCSK9 on the plastic bottom of the assay plate. It can thus also be hypothesized that the CHRD is more exposed when PCSK9 is fixed on plastic, leading to the selection of CHRD-specific sdAbs. In order to avoid this shortcoming, we decided to repeat the screening of the dromedary sdAbs library by using conditioned media containing the PCSK9 construct L455X lacking the CHRD of PCSK9. Although this construct is properly secreted (180), its secretion levels are low. Therefore, in order to produce large quantities of PCSK9 L455X, we treated the transfected cell lines with sodium butyrate (603). Phage display assays are ongoing to screen the sdAbs library against PCSK9 L455X in solution and we hope that it will help identifying sdAbs directed against the catalytic domain of PCSK9.

Interestingly, although the four selected llama sdAbs did not prevent the *in vitro* binding of PCSK9 to LDLR, they still increased liver LDLR levels as well as LDL uptake and reduced circulating TC. This might be due to a steric hindrance provoked by the sdAb that could prevent sdAb-PCSK9-LDLR intracellular degradation. The sdAbs could also prevent the binding to the CHRD of one or several protein(s) X, of which role(s) would be to send the PCSK9-LDLR complex to lysosomal degradation. These mechanisms still need to be determined, as discussed in the first chapter of this thesis and in the second manuscript presented later (Chapter III). However, our studies confirmed the importance of the CHRD in LDLR degradation. A possible application of the identified llama sdAbs in order to study the role of the CHRD could be studies on the trafficking of PCSK9 and LDLR in presence or absence of anti-CHRD sdAbs in hepatic cell lines, primary hepatocytes or even in mice. This could be done by fluorescence microscopy using various markers of cellular localisation such as antibodies to the early endosome antigen (EEA1) enabling to localize early endosomes, pH-sensitive diazaoxatriangulene fluorescent probes to localize late endosomes or cytopainter lysosomal staining kit to mark lysosomes.

sdAbs targeting another PC, furin, were also developed since furin is a therapeutic target for many disorders (604). The issues encountered with furin inhibition are related to specificity. These sdAbs constitute non-competitive furin inhibitors with K_d in the nanomolar range and were shown to bind exclusively to furin but not to other PCs. They were able to prevent the cleavage of several furin

substrates by a mechanism likely based on steric hindrance. No information was available concerning the binding domain of sdAbs to furin, but it has to be kept in mind that PCSK9 is a particular PC since it only cleaves itself and no longer acts as a protease afterwards. Furin inhibition can thus not be entirely compared to PCSK9 inhibition. Although this study seemed promising, so far, these furin-specific sdAbs were never tested *in vivo* according to the literature.

The chosen fusion of our llama sdAbs can be discussed. We could have fused the sdAb with another entity than a mFc, for example PEG (605), HSA (606) or another sdAb targeting HSA like for the anti-TNFα sdAb ozoralizumab. It is also possible to couple several similar or different sdAbs to obtain a higher molecular weight like it was done for the von Willebrand factor-targeting sdAb caplacizumab, the most advanced sdAb in clinical trials. We tried to incubate cells with several combinations of the four selected sdAb-mFcs but it did not yield a further increase in LDLR levels. We could also speculate that if the sdAb would bind very fast to PCSK9, the size of the sdAb-PCSK9 complex would be large enough not to be filtered by the kidney through the glomerulus with the primary urine, which threshold is ~20 kDa.

Another point to be discussed is the price of mAbs. According to U.S. pharmacy benefits (www.health.usnews.com), although only 2% of the population uses biologics drugs, their sales account for >40% of prescription drugs sales. Biologics include drugs such as mAbs, vaccines, insulin and gene therapies. However, mAbs are the most expensive biologics. The only hope for the reduction of the price of biologics is to use of biosimilars that could reduce their price up to one third, which would still be expensive but more affordable. Note that raw materials needed for mAbs production are not expensive. Their high price is rather due to the expensive and complex large-scale mAbs production, the need for relatively high doses, and particularly to the research and development costs and the legal need for a return of investment to their shareholders (607, 608). Therefore, although sdAbs are attractive because their production costs are lower than mAbs, it could be speculated that their final price might not be so much cheaper than mAbs, since sdAbs-producing companies would also have to reimburse their research and development costs and their investments. The market price of sdAbs will be known once a sdAb will be approved by the FDA and marketed.

III.Chapter III: Manuscript 2 (to be submitted to The Journal of Biological Chemistry)

Title: Human PCSK9 transgenic mice for PCSK9 inhibitors screening

Authors: Elodie Weider and Rachid Essalmani, Jadwiga Marcinkiewicz, Ann Chamberland, Delia Susan-Resiga, Anna Roubtsova, Nabil G. Seidah and Annik Prat

Journal: The Journal of Biological Chemistry, *to be submitted*

III.1 Preface

The following manuscript was designed in the attempt to document the elaboration and the full characterization of the mouse model that was used in Chapter II to determine the *in vivo* efficacy of the sdAb P1.40-mFc. To that end, PCSK9 tissue distribution as well as liver and plasma characteristics were studied in four selected mouse lines expressing increasing levels of hPCSK9. Their response to an injection of the mAb evolocumab was studied and one mouse line was selected for a long-term study aiming at comparing the *in vivo* effects of PKF8-mFc, which is strongly related to P1.40-mFc, and evolocumab. This will assess the reversibility of the mouse model and the pharmacodynamics of both PCSK9 inhibitors, to possibly compare the efficacy of various PCSK9 inhibitors. Indeed, there is a need for a new transgenic mouse allowing these types of studies in conditions of physiological PCSK9 concentrations and in an animal model in which the tissue distribution of PCSK9 is similar to that of humans. Note that this study also allowed us to compare the *in vivo* efficacies of P140-mFc and PKF8-mFc, which were very similar in our cell-based assays.

Human PCSK9 transgenic mice for PCSK9 inhibitors screening

Elodie Weider* and Rachid Essalmani*, Jadwiga Marcinkiewicz*, Ann Chamberland*, Delia Susan-Resiga*, Anna Roubtsova*, Nabil G. Seidah* and Annik Prat*¶

*Laboratory of Biochemical Neuroendocrinology, Institut de Recherches Cliniques de Montréal, affiliated to the University of Montreal; 110 Pine Ave. West, Montreal, QC H2W 1R7, Canada.

¶Corresponding author: Annik Prat, Laboratory of Biochemical Neuroendocrinology, Institut de Recherches Cliniques de Montréal, 110 Pine Ave. West, Montréal, QC H2W 1R7, Canada. Tel: (514) 987-5738; E-mail: annik.prat@ircm.qc.ca

Keywords: cholesterol regulation, evolocumab, FH, LDL, PCSK9, mAb, sdAb, nanobody, LDLR, transgenic mouse

III.2 Abstract

Background: PCSK9 is a secreted protein promoting the degradation of the LDLR and hence implicated in LDLc regulation and familial hypercholesterolemia. Inhibition of PCSK9 is used as a strategy to decrease LDLc, and thereby cardiovascular disease risk. Efficient and so far well-tolerated mAbs are currently used to prevent the binding of extracellular PCSK9 to the LDLR. However, mAbs are expensive and cannot be administered to all patients. Therefore, other PCSK9 inhibitors are needed. To that end, we developed mice expressing hPCSK9 to facilitate the screening of PCSK9 inhibitors.

Methods: A fragment of the human chromosome containing the *PCSK9* gene was obtained from a human BAC library, and was injected into fertilized eggs to generate transgenic lines. Four of them were backcrossed to mice lacking endogenous mPCSK9 and harboring the C57BL/6J genetic background, generating mice expressing exclusively hPCSK9 under the control of its own promoter.

Results: Transgenic lines expressing 95 to ~5,000 ng/mL of plasma hPCSK9 were selected. Whole body ISH revealed that the expression of hPCSK9 recapitulated that of endogenous mPCSK9. Compared to Tg negative littermates, transgenic mice exhibited increased levels of TC and apoB and decreased levels of hepatic LDLR levels, in correlation with their hPCSK9 expression levels. We characterized their response to a single injection of the mAb evolocumab. One line expressing physiological levels of hPCSK9 was then selected for a long-term study of two PCSK9 inhibitors, evolocumab and PKF8-mFc, a previously described sdAb. TC levels decreased in a reversible way upon injection of each inhibitor and a second injection yielded the same TC decrease.

Conclusion: These newly developed transgenic mice responded adequately to the tested inhibitors in a reversible way. They are thus well suited to screen, analyze and compare hPCSK9 inhibitors. We predict that these powerful mouse models will be in demand in the search for innovative PCSK9 inhibitors that could complement the market of mAbs.

III.3 Introduction

Reducing LDLc levels is highly beneficial to decrease the incidence of heart attack, stroke and overall CVD. HMGCR inhibitors, known as statins, are traditionally prescribed to reduce LDLc and are associated with substantial clinical benefits (379, 380). After one year statin treatment, the LDLc levels were reduced from 143 to 102 mg/dL (3.70 to 2.63 mM) in more than 129,000 patients from 21 clinical trials, and this lowered CVD risk by >20% (43). However, statin-intolerant patients tend to discontinue their treatment, and some high CVD risk patients cannot reach optimal LDLc levels (~100 mg/dL) or 50% reduction from baseline fixed by European guidelines (327). Therefore, new therapies are needed, notably for high risk patients (609, 610) including those suffering from FH. FH is a common autosomal dominant disorder with frequencies of heterozygotes from 1:500 to 1:217, as in Denmark (52). Most FH patients harbor mutations in the genes encoding the LDLR (*LDLR*; FH1; 67%) or apoB (*APOB*; FH2; 14%) that hamper LDL binding to its receptor or internalization of the lipoprotein, leading to LDL accumulation in the plasma (61). FH patients thus suffer from 3.5- to 16- fold higher CVD risk than non-FH patients (62). More recently, the gene encoding the PCSK9 was identified as a third locus of FH (*PCSK9*; FH3; 2%) (64).

PCSK9 is the 9th member of the PCs family, which is related to subtilisin and kexin (63). PCSK9 is composed of a prodomain, a catalytic domain, a hinge and a CHRD, which comprises three modules (168, 173). PCSK9 is a serine protease initially produced as a zymogen. In the ER, it auto-catalytically cleaves itself to excise its prodomain, which acts first as a chaperone (63), and then as a potent inhibitor, since it remains tightly bound to the catalytic subunit of mature PCSK9 (173). PCSK9 has thus no substrate other than itself, unlike the eight other convertases (132). PCSK9 is mainly expressed in hepatocytes, which are the source of the circulating protein, but it is also synthesized in enterocytes, kidney, pancreatic islets and cerebellum (63, 172, 232, 251).

Shortly after its discovery, PCSK9 was shown to be downregulated by cholesterol via SREBP2, like the cholesterogenic targets of this transcription factor that regulates lipid homeostasis (167). However, and paradoxically, adenoviral-mediated expression of murine (583) or human (168, 170)

PCSK9 was found to induce the post-transcriptional degradation of the LDLR. Accordingly, mouse models lacking PCSK9 showed decreased cholesterol levels that were coupled to increased LDLR protein levels in liver (171). Finally, the ability of circulating PCSK9 to target liver LDLR for degradation was shown in a parabiosis experiment between WT mice and transgenic mice expressing 1,000-fold endogenous levels of hPCSK9 (236). PCSK9 binds the EGF-A domain of the LDLR through its catalytic domain (177, 178), as well as that of other members of the LDLR superfamily, VLDLR, ApoER2 (262, 264) and LRP1 (194). This binding was found to prevent LDLR recycling back to the cell surface after internalization of the LDL-LDLR complex, and to promote its degradation in late endosomes/lysosomes. However, the mechanism of this process that requires the presence of the CHRD has not yet been identified (179, 184).

The link between PCSK9 and LDLc was established by identifying two single point mutations (S127R and F216L) in French FH patients (64). On the other hand, non-sense mutations Y142X and C679X were found in ~2% of black Africans and were associated with a ~40% decrease in LDLc, and ~88% reduction in the risk of CVD (206, 207). Strikingly, the GOF D374Y mutation increases ~10-fold the affinity of PCSK9 for the LDLR (173), leading to ~4-fold higher LDLc levels that are associated to premature death due to CVD (200). Finally, the identification of individuals completely lacking functional PCSK9 constituted a proof-of-principle that hypercholesterolemia and CVD could be treated by targeting PCSK9 (218, 302, 611). mAbs targeting the catalytic domain of PCSK9 and thus preventing its binding to LDLR are commercially available since 2015 (434). Injected subcutaneously every 2 or 4 weeks, they achieve a ~60% LDLc decrease even after 2 to 4 years of treatment (435), and resulted in 15 to 20% reduced (435, 436) cardiovascular death, myocardial infarction, or stroke (436). However, these lipid-lowering agents are pricy and only prescribed to patients at very high risk or that are resistant to the LDL-lowering “statins”. Therefore, there is an unmet need for cheaper, more accessible inhibitory molecules.

As an alternative to mAbs, we proposed the use of sdAbs, known as nanobodies (1). Up to 75% of camelid antibodies are devoid of light chains: they are composed of two hcAbs, each including an antigen binding domain (VHH or sdAb) followed by two constant domains CH2 and CH3 (556).

Although sdAbs are 10-fold smaller (~13 kDa) than conventional antibodies, they bind antigens with the same affinity and specificity (560). Importantly, sdAbs can be produced from bacteria or yeast, and are thus expected to be cheaper and easier to manufacture (565, 577, 592). To screen selected sdAbs *in vivo*, we developed mouse lines that constitute a precious tool to test PCSK9 inhibitors. The transgenic PCSK9 mice reported to date present limitations as models for the screening of PCSK9 inhibitors. One of them expresses hPCSK9 under the control of the albumin promoter but led to PCSK9 overexpression in kidney (245). Other mice carrying a BAC fragment containing the WT or the GOF D374Y *PCSK9* gene were also reported (246). However, the D374Y strain exhibits ~14 μg/mL of highly active PCSK9, making thus any inhibitor screening very difficult. In the present report, we describe *Pcsk9*$^{-/-}$ mouse lines carrying a human BAC Tg directing hPCSK9 expression under the control of its own promoter, and their use in the comparative analysis of PCSK9 inhibition using evolocumab and one of our previously reported sdAb, PKF8-mFc (1).

III.4 Methodology

III.4.1 Generation of transgenic mice

The RPCI human BAC library 11 (Children's Hospital Oakland Research Institute) was screened for the presence of the *PCSK9* gene. The clone RP11-55M23 was selected and an *Abs*I fragment, verified by a PCR using oligonucleotides detailed in Table 2, was injected into B6C3F1 fertilized eggs. Transgenic founders were selected and backcrossed to our *Pcsk9*$^{-/-}$ (PCSK9 KO) mice in the C57BL/6J background (172) for 10 generations to generate C57BL/6J-*Pcsk9*$^{-/-}$ Tg(RP11-55M23-AbsI)$^{+/0}$ lines.

Table 2. Oligonucleotides used in PCR to validate the purity of the *Abs*I fragment

	Forward	Reverse
A	CCTGGCAAGGCAGAATAAAGTGAAC	CCTCACTCTCAGGCCTCCGGTCCC
B	GAGTAGTTACTATGTGCTGGGG	CATATGATGAAATACTATTCAGCC
C	CCCCACGGCAGCCTCAGAGCCCC	GGCCCTGAGTGCCATGGCCTCAAG
E1	CCGGCAGAACTTGGAGTCT	GCTAGCACCAGCTCCTCGTA
E7-8	AGTGGATCAGTCTCTGCCTCA	GTGTCACAGAGTGGGACATCAC
E11	TCCTTGACTTTGCATTCCAGA	CTGAGGCCACGAGGTCAG

III.4.2 Mice and Genotyping

Mice were housed in a 12h light/dark cycle and fed a standard diet (2018 Teklad global 18% protein rodent diet; Envigo). All procedures were approved by the committee for animal care of the Montreal Clinical Research Institute. Male mice were genotyped by PCR analysis of tail DNA using specific pairs of primers for human and mouse Pcsk9 (Table 3), and analyzed at 3 to 4 months of age.

III.4.3 Determination of the transgene copy number

Quantitative RT-PCR was performed on genomic DNA. The mouse *Dolt1* gene was used for normalization. Taqman probes (IDT) were used with the fluorescent dye FAM™ for h*PCSK9* (5′-GACGAGGACGGCGACTA *forward* and 5′-GGAAGGTGGCTGTGGTTC *reverse*) and VIC®

for mouse *DOLT1* (5′-GCCCCAGCACGACCATT *forward* and 5′-TAGTTGGCATCCTTATGCTTCATC *reverse*).

III.4.4 *In situ* hybridization

Frozen whole bodies of postnatal mice (P10) were cut into 12-µm thick sections that were mounted onto glass slides and fixed in fresh 4% formaldehyde. RNA sense and antisense riboprobes were synthesized *in vitro* from recombinant PCRII vectors (Invitrogen) using the T7 and SP6 RNA polymerase promoters in the presence of [^{35}S] UTP (>1,000 Ci/mmol; PerkinElmer), as previously reported (63). They covered the sequences encoding amino acids 352–648 and 221-377 in mouse and hPCSK9 mRNAs, respectively. Briefly, and as described previously (612), tissue sections were hybridized overnight with 50-80,000 cpm/µl of ^{35}S-labeled cRNA probe, washed at 65 °C, and treated with 20 µg/ml of RNase A at 37 °C. After washing, the slides were dehydrated, exposed for 4 days, dipped in Kodak NTB nuclear track emulsion, and finally exposed for 12 days at 4°C.

III.4.5 Quantitative RT-PCR (QPCR)

RNA from livers was extracted using TRIzol (Invitrogen). cDNA synthesis and QPCR were performed as previously described (386). Primers from neighboring exons were used to measure hPCSK9, and mLDLR and HGPRT mRNA levels (Table 3).

Table 3. Oligonucleotides used in QPCR

	Forward	Reverse
hPCSK9	TGGAGCTGGCCTTGAAGTTG	GATGCTCTGGGCAAAGACAGA
mLDLR	GGAGATGCACTTGCCATCCT	AGGCTGTCCCCCCAAGAC
mHPRT	CCGAGGATTTGGAAAAAGTGTT	CCTTCATGACATCTCGAGCAAGT

III.4.6 Western blotting

Liver protein extraction was performed in radioimmune precipitation assay buffer (50 mM Tris-HCl pH 7.8, 150 mM NaCl, 1% Nonidet P-40, 0.5% sodium deoxycholate, 0.1% SDS) containing protease inhibitors (Roche Applied Science). After centrifugation at 13,975 g during 10 min at 4°C and recovery of supernatants, total protein concentrations were quantified by using the DC Protein

assay (Bio-Rad). Mouse plasma, diluted or not with that of Tg negative littermates (Tg0), was directly loaded on gels. Proteins were analyzed by 8% SDS-PAGE and Western blotting using hPCSK9 (1:3,000 (184)), and mLDLR (1:1,000; R&D system) and β-actin (1:3,000; Sigma) primary antibodies, and corresponding secondary antibodies conjugated to horseradish peroxidase (1:10,000; Invitrogen). The antigen-antibody complexes were visualized using the enhanced chemiluminescence kit (ECL; Amersham or Pierce). Quantification was performed with a ChemiDoc MP imaging system (Bio-Rad).

III.4.7 Plasma measurements and ELISAs

TC levels were determined by the colorimetric assay Infinity (Thermo Scientific). Circulating hPCSK9 and apoB levels were measured with a home-based (613) and the Cloud-Clone Corp ELISAs, respectively. Liver proteins were extracted in a non-denaturing extraction buffer (20 mM Tris-HCl, pH 8, 137 mM NaCl, 2mM Na2EDTA, 1% NP-40, 10% glycerol, 4% protease inhibitor cocktail without EDTA) with a Dounce homogenizer. LDLR protein levels were measured with the mLDLR DuoSet ELISA Development kit (DY2255; R&D Systems) and normalized to protein content (Bio-Rad DC Protein assay). Optical densities were obtained on a SpectraMax i3 plate reader (Molecular Devices).

III.4.8 Animal injections

Mice were injected in the tail vein with vehicle (PBS, Wisent) or 10 mg/kg of evolocumab (Repatha®, Amgen) or PKF8-mFc, a llama sdAb targeting hPCSK9 previously described (1). Blood samples were collected from the cheek before the injection in heparin-coated CAPIJECT® collection tubes (Terumo) and from the tail at indicated time points following the injection using heparinized Fisherbrand™ Microhematocrit Capillary Tubes (Fisher Scientific). Plasma was obtained by blood centrifugation at 752 g for 15 min at 4°C.

III.4.9 PCSK9 binding/internalization by primary hepatocytes

Hepatocytes were isolated from 8 to 10 week-old male mice (Tg0) using the two-step collagenase perfusion method, as described previously (614). Briefly, the liver was successively perfused with calcium-free HEPES buffer I (142 mM NaCl, 6.7 mM KCl, 10 mM Hepes, pH 7.6) and calcium-supplemented HEPES buffer II (4.7 mM CaCl2, 66.7 mM NaCl, 6.7 mM KCl, 100 mM Hepes, pH 7.4) containing 0.5 mg/mL collagenase Type V (Sigma Aldrich). Hepatocytes were seeded in 12-well plates (250,000 cells/well) in Williams' medium E supplemented with 10% FBS (GIBCO BRL) for 2 h, and incubated in HepatoZYME-SFM (GIBCO BRL) for at least 12 h. Purified PCSK9 (PC9; 0.083 μM) and/or PKF8-mFc (PKF8; 2 μM) were pre-incubated for one hour at 37°C in HepatoZYME-SFM that was then added onto primary hepatocytes. After incubation for 1, 2, 4 or 6 hours at 4°C or 37°C, cells were washed twice in neutral (pH 7.4) or acidic (pH 2.5) PBS for 15 min, and were lysed in the above non-denaturing extraction buffer.

III.4.10 Statistics

Two-tail Student's *t* test was performed in order to assess the statistical significance of all data sets.

III.5 Results

III.5.1 Generation of transgenic mice

The RPCI-11 human BAC library was screened by PCR for the presence of the *PCSK9* gene and the clone RP11-55M23 was identified and characterized. We opted for using a 67.5 kb *Abs*I DNA fragment of this clone that contained the entire *PCSK9* gene (~25 kb, positive strand), but also ~35.5 and 7 kb of upstream and downstream sequences, respectively, to optimally preserve *in cis* transcriptional regulatory elements (Figure 30). The upstream *BSND* gene, which encodes the Barttin CLCNK type accessory β-subunit implicated in the antenatal Bartter's syndrome with sensorineural deafness, is located ~30 kb upstream of *PCSK9* exon 1, and the 67.5 kb fragment only contains the 3' half of it. The last exon of the neighboring downstream gene, *USP24* (negative strand), which codes for the ubiquitin carboxyl-terminal hydrolase 24, lays only 1.5 kb away of the *PCSK9* exon 22. Thus, the *Abs*I DNA fragment contained the two last *USP24* exons. The RP11-55M23 BAC clone was digested with *Abs*I restriction enzyme (Figure 30, lower left panel), and the purity of the 67.5 kb recovered fragment was confirmed by PCR (Figure 30, lower center panel). The latter was finally injected into mouse B6C3F1 fertilized eggs that were re-implanted into surrogate mothers. Four lines were selected based on preliminary hPCSK9 plasma concentrations measured after one or two backcrosses to C57BL/6J mice. To eliminate endogenous mPCSK9 expression, all lines were further backcrossed 9 times to *Pcsk9*$^{-/-}$ mice on the C57BL/6J genetic background. Thus, C57BL/6J-*Pcsk9*$^{-/-}$ Tg(RP11-55M23-AbsI)$^{+/0}$ mice express exclusively hPCSK9 under the control of its own promoter. Importantly, littermates are either lacking the Tg (Tg$^{0/0}$; control mice named Tg0 herein) or heterozygous for the Tg in order to avoid any phenotype linked to the insertion site in the mouse genome (Tg$^{+/0}$; and named Tg1, Tg2, Tg3 or Tg4 according to the mouse line).

After at least 5 backcrosses, all lines were further characterized. Plasma hPCSK9 levels were measured by a home-made ELISA (613) that estimates average human plasma levels at ~150 ng/mL. In Tg1, Tg2, Tg3 and Tg4, plasma PCSK9 values of 95, 369, 360, and 4,974 ng/mL were calculated, respectively. The stable expression of PCSK9 across the last backcrosses was in favor of unique or genetically linked insertion sites, in which one or several copies of the fragment may

be present. To determine the Tg copy number in each line, a genomic QPCR using Taqman probes and the mouse *Dolt1* gene as a normalizer was performed (Figure 30, lower right panel). No Tg could be detected in Tg0 mice and Tg1, Tg2, Tg3 and Tg4 lines had 1, 2, 2, and 32 copies of the fragment, respectively. Note the good correlation between these copy number values and hPCSK9 levels.

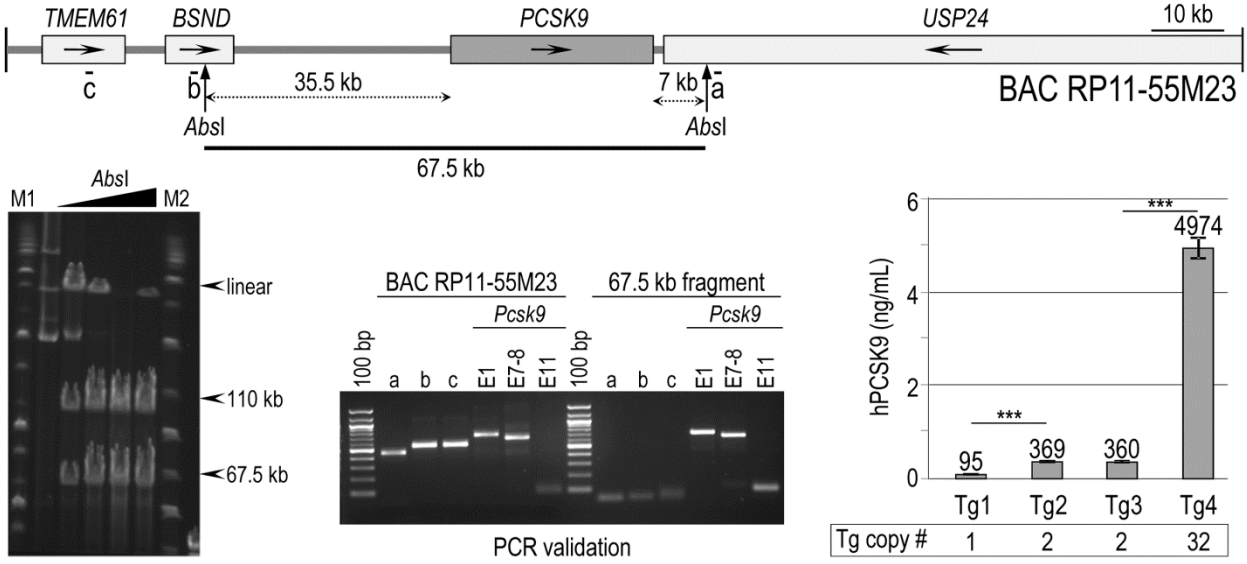

Figure 30. Generation of transgenic mice expressing human PCSK9 under the control of its endogenous promoter. Schematic representation of the RP11-55M23 BAC clone containing the *PCSK9* gene. A 67.5kb *Abs*I fragment comprising the entire *PCSK9* gene flanked with 35.5 kb and 7 kb of upstream and downstream, respectively, was injected into fertilized eggs to generate transgenic mice (upper panel). Digestion profile obtained by pulsed-field gel electrophoresis of BAC RP11-55M23 DNA (2µg) incubated with 0, 0.5, 1, 2 or 3 units of *Abs*I restriction enzyme (lower left panel). Validation of the purity of the *AbsI* fragment by PCR using oligonucleotides located in *USP24* (a), *BSND* (b) and *TMEM61* (c, transmembrane protein 61) genes (no amplification) or in *PCSK9* exons 1, 7-8 and 11 (lower center panel). The bar graph indicates the circulating hPCSK9 levels (µg/mL) in all transgenic lines (lower right panel). Error bars indicate standard error to the mean (SEM). ***, $p < 0.0005$ (Student's *t* test). The Tg copy number is indicated below the bar graph.

III.5.2 Tissue distribution of PCSK9 mRNA in the transgenic mouse lines

To verify whether hPCSK9 expression originating from the human Tg exhibited the expected profile, whole-mount ISH were performed in post-natal day 10 (P10) mice (Figure 31). Mouse (left panels) or human (right panels) cRNA probes were hybridized to control WT and *Pcsk9*$^{-/-}$

(Tg0) sections, and Tg1, Tg2, Tg3 and Tg4 sections. The fainter signals obtained with the human probe in WT mice or with the mouse probe in Tg1, Tg2, Tg3 and Tg4 sections reveal a partial cross-reactivity between human and mouse sequences. However, very similar hybridization patterns for WT or transgenic PCSK9 were obtained, especially between the mouse WT pattern and human Tg2 and Tg3 ones, in which PCSK9 mRNA expression was observed predominantly in liver and intestine, as expected.

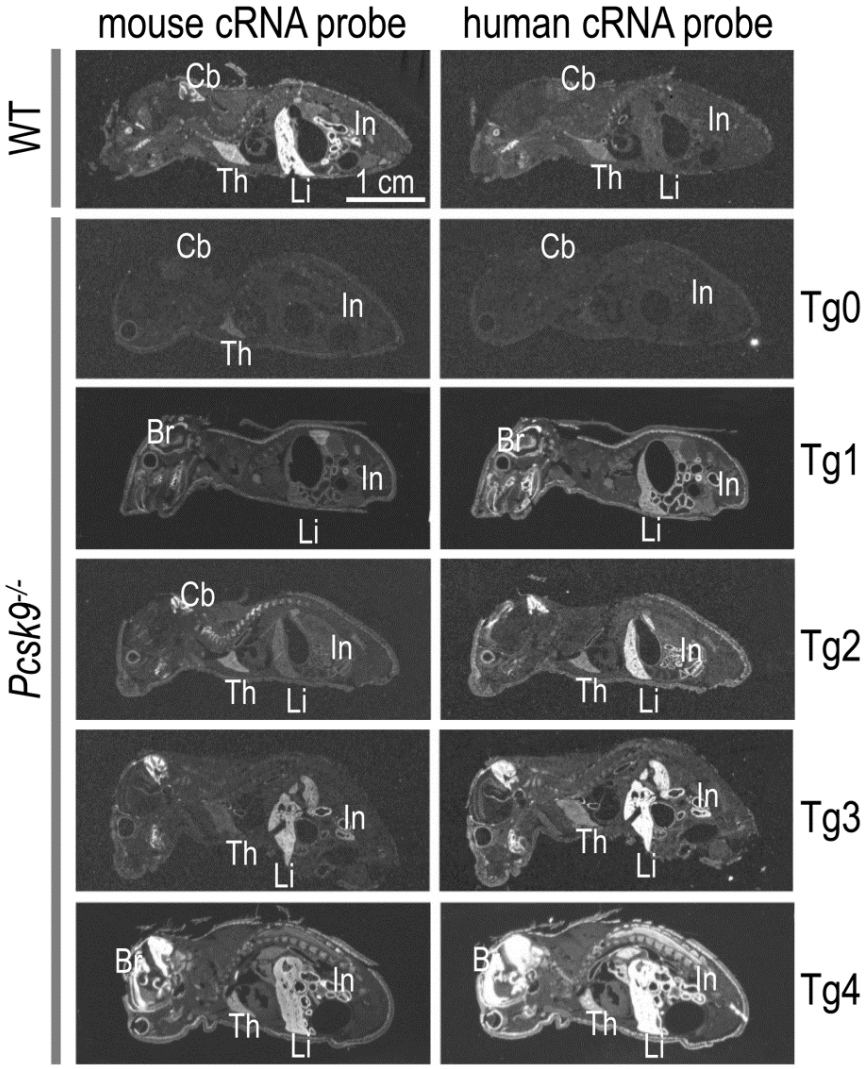

Figure 31. Tissue distribution of human PCSK9 mRNA in transgenic mice. Whole body sections from P10 WT (top panels), *Pcsk9*$^{-/-}$ (Tg0) and Tg1, Tg2, Tg3 and Tg4 mice were hybridized with mouse or human PCSK9 cRNA probes. Br, brain; Cb, cerebellum; In, intestine; Li, liver; Th, thymus.

III.5.3 PCSK9 and LDLR expression in transgenic livers

hPCSK9 and mLDLR mRNA levels were assessed in WT, Tg0 and the four transgenic lines in both male and female mice (Figures 32 A, B). The data are normalized to those of male Tg1 values, arbitrarily fixed to 1. Endogenous mPCSK9 mRNA was also measured in WT mice as an indication, although it cannot be quantitatively compared to hPCSK9 mRNA levels (Figure 32A). Interestingly, mouse and hPCSK9 mRNA levels were always higher in females than in males, with females exhibiting a higher variability. On average, hPCSK9 mRNA levels in male and female Tg2, Tg3 and Tg4 were 2.4-, 11-, and 35-fold higher than in Tg1, respectively. These values are in agreement with the Tg copy number (Figure 30, lower right panel), except for Tg3 that has 2 copies, like Tg2, but expresses 3-fold higher mRNA levels. mLDLR mRNA levels (Figure 32B) also tend to be higher in females than males. However, compared to WT mice, there were no significant changes in mLDLR mRNA levels across the lines, in agreement with the exclusive post-transcriptional impact of PCSK9 on the LDLR.

The hepatic mLDLR protein levels were analyzed by WB in the same mice. The highest levels of mLDLR were observed in the absence of PCSK9 (Tg0) and normalized to 100% (Figure 32C). Endogenous mPCSK9 reduced mLDLR to 14 and 22% (WT) in male (Figure 32C; left panel) and female (Figure 32C; right panel) mice, respectively. hPCSK9 in Tg lines reduced mLDLR to 66-65%, 27-30%, 33%, and 1-2% in Tg1, Tg2, Tg3 and Tg4, respectively. Surprisingly, although hPCSK9 mRNA levels in Tg2 and Tg3 lines differed by 4.4-fold, and the circulating levels of full length active PCSK9 were ~2-fold higher in Tg3 compared to Tg2 (Figure 32D, upper band), their mLDLR protein levels were similar.

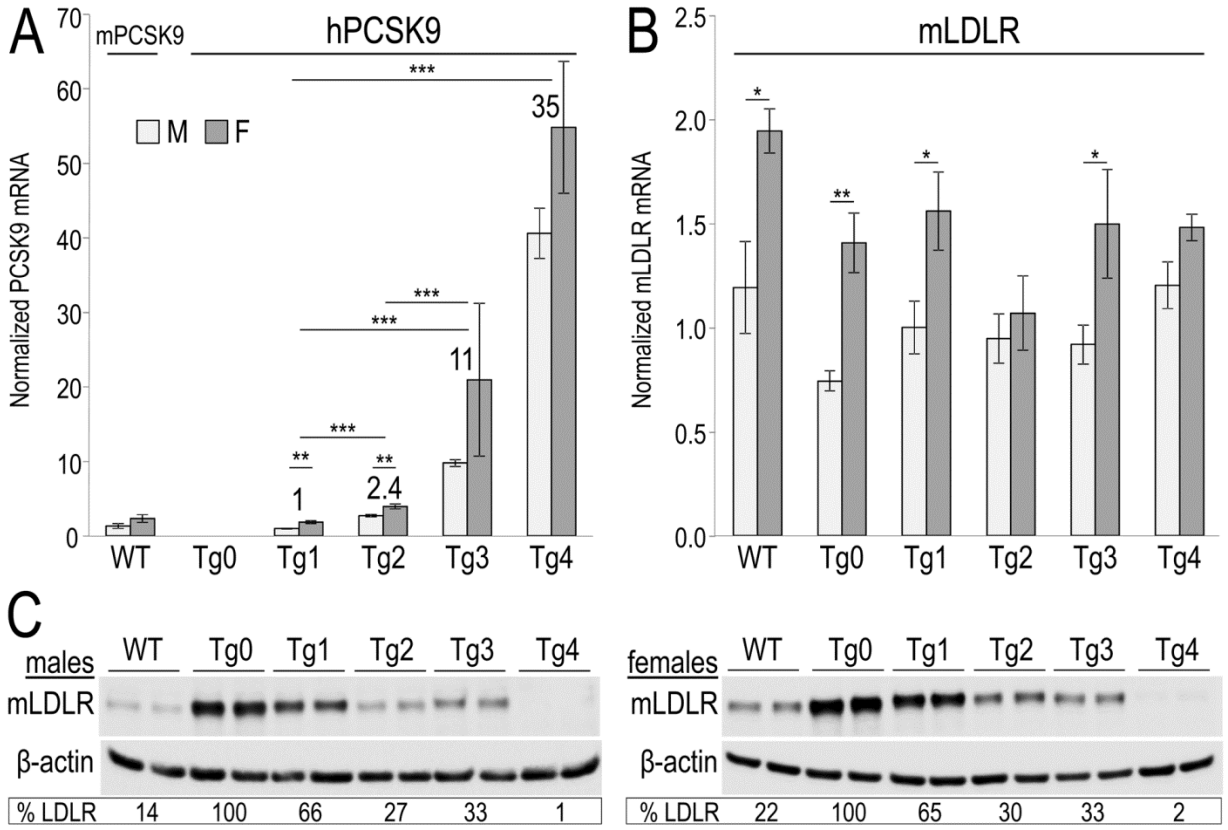

Figure 32. Human PCSK9 and mouse LDLR expression in transgenic livers. hPCSK9 (*A*) or mLDLR (*B*) mRNA levels in livers from male and female mice (n=4-8) were calibrated to HPRT mRNA levels and normalized to the male Tg1 value set to 1. Error bars indicate SEM. *, $p < 0.05$; **, $p < 0.005$; ***, $p < 0.0005$ (Student's *t* test). The indicated values are the average of male and female mRNA levels, each normalized to Tg1 of the same sex (not shown for females). Semi-quantitative WB analysis of liver LDLR protein levels calibrated to β-actin ones and normalized to Tg0 (100%) in male (left panel) and female (right panel) mice (*C*). The indicated % LDLR values represent the average quantification of the two lanes.

III.5.4 Plasma characteristics of transgenic mice

The levels of TC and apoB were measured in WT and *Ldlr*$^{-/-}$ male mice, as well as in *Ldlr*$^{-/-}$, Tg0, Tg1, Tg2, Tg3 and Tg4 mice lacking mPCSK9 (*Pcsk9*$^{-/-}$ background; Figure 33). TC levels were 3.5-fold higher in *Ldlr*$^{-/-}$ compared to WT mice. As expected, there was no difference between *Ldlr*$^{-/-}$ and *Ldlr*$^{-/-}$ *Pcsk9*$^{-/-}$ TC, confirming that PCSK9 controls LDLc in a LDLR-dependent manner (172). TC values increased gradually to reach 158 mg/dL in Tg4 mice. Although mLDLR was barely detected in liver extracts from Tg4 mice (Figure 32C), their TC levels did not reach the 253

and 238 mg/dL measured in *Ldlr*$^{-/-}$ and *Ldlr*$^{-/-}$ *Pcsk9*$^{-/-}$ mice, respectively. Notably, TC levels of Tg2 and Tg3 were very similar, as suggested by circulating PCSK9 levels and Tg copy numbers (Figure 30).

Circulating apoB levels were then measured by ELISA. Although 5 to 9 plasma samples of all lines were analysed simultaneously, a 1.3-fold increase only could be detected between *Ldlr*$^{-/-}$ and WT levels, indicating how poorly sensitive was this assay compared to TC measurement (3.5-fold increase). Globally, plasma apoB levels followed the TC ones, with two exceptions: *Ldlr*$^{-/-}$ *Pcsk9*$^{-/-}$ apoB values were similar to that of WT mice, and Tg4 values were equivalent to that of Tg3 and *Ldlr*$^{-/-}$ *Pcsk9*$^{-/-}$, again an indication of a poor sensitivity of the apoB ELISA.

The plasma hPCSK9 was then analysed by WB. PCSK9 was not detected in plasma from Tg0 and the same gradual increase in the bands intensity was seen in transgenic lines Tg1 to Tg4. The difference between Tg3 and Tg4 is striking, especially given the fact that the plasma of Tg4 has been diluted 1/5. We could observe the presence of both full and furin-cleaved PCSK9 (PCSK9-ΔN_{218}) (305), which demonstrates that the protein is properly processed (Figure 33).

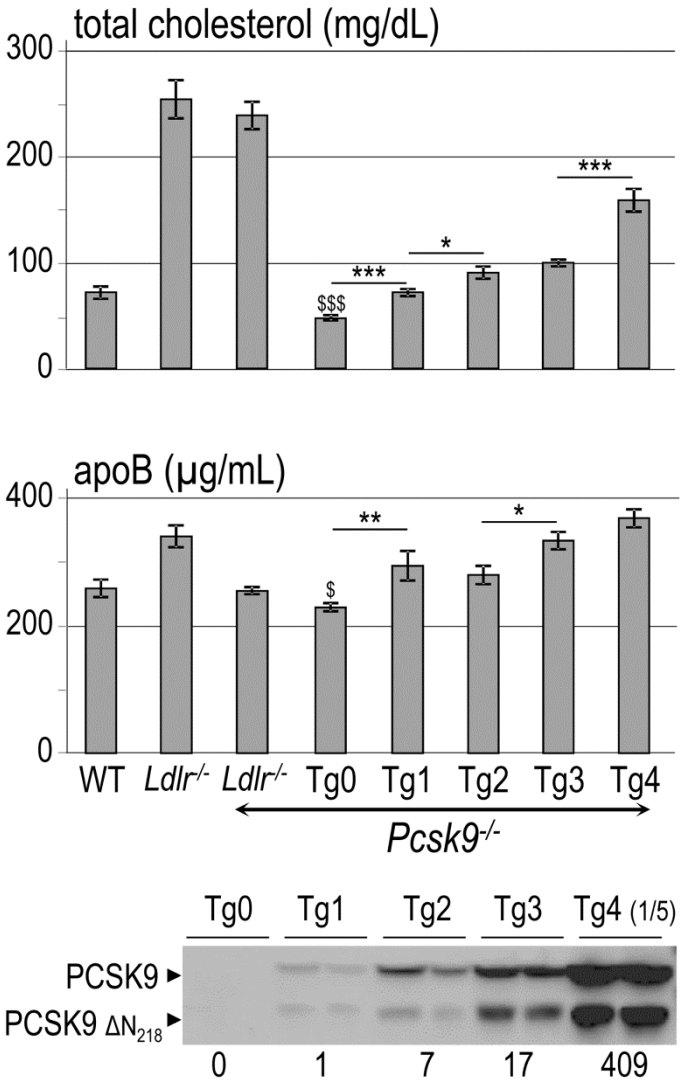

Figure 33. Transgenic mice plasma characteristics. TC and apoB levels were measured in plasma from WT, *Ldlr*$^{-/-}$, *Pcsk9*$^{-/-}$, *Pcsk9*$^{-/-}$*Ldlr*$^{-/-}$, and the four transgenic lines (Tg1, Tg2, Tg3 and Tg4; upper and center panels). Measures were performed in 5 to 9 mice per genotype. Error bars indicate SEM. *, $p < 0.05$; **, $p < 0.005$; ***, $p < 0.0005$ (Student's *t* test). $ replaces the * symbol for comparison to WT mice. Mouse plasma from Tg0 and the four transgenic mouse lines was also subjected to hPCSK9 WB (lower panel). The Blot is representative of three experiments.

III.5.5 Impact of a single injection of evolocumab in transgenic mice

We next assessed the ability of the four transgenic mouse lines to respond to 10 mg/kg of the commercially available PCSK9 mAb evolocumab, injected in the tail vein. TC levels were measured in mice plasma before the injection (virtually at day 0), 2 and 4 days post-injection, and the livers were collected at day 4. The data represent the difference in TC (ΔTC) between each transgenic mouse line and Tg0 (Figure 34).

We observed that TC was partially reduced 2 days post-injection and reached the Tg0 levels after 4 days in Tg1, Tg2 and Tg3. In contrast, TC in Tg4 was only transitorily reduced by ~1.5-fold at 2 days post-injection. This shows that evolocumab completely neutralizes hPCSK9 activity on the LDLR in Tg1, Tg2 and Tg3 lines, but not in Tg4, likely due to its huge levels of circulating hPCSK9.

The mLDLR protein levels in the liver were not significantly different in mice receiving vehicle only or mAb-injected Tg0. In Tg1 and Tg2, there was a significant 1.7-fold and 2.5-fold mLDLR increase upon injection of evolocumab, respectively. A similar 2.5-fold increase was found in Tg3. As expected, mLDLR levels could not be rescued in Tg4.

In conclusion, Tg1 responded properly to evolocumab, but its relatively low PCSK9 expression (~65% of the average human value) reduces the activity window of this inhibitor. Tg4 with 33-fold higher hPCSK9 levels than in human only poorly responded to evolocumab. In contrast, Tg2 and Tg3, which express ~2.5-fold higher levels of hPCSK9 than normal, showed similar and optimal response to evolocumab. Thus, both lines seem well suited for the screening of hPCSK9 inhibitors.

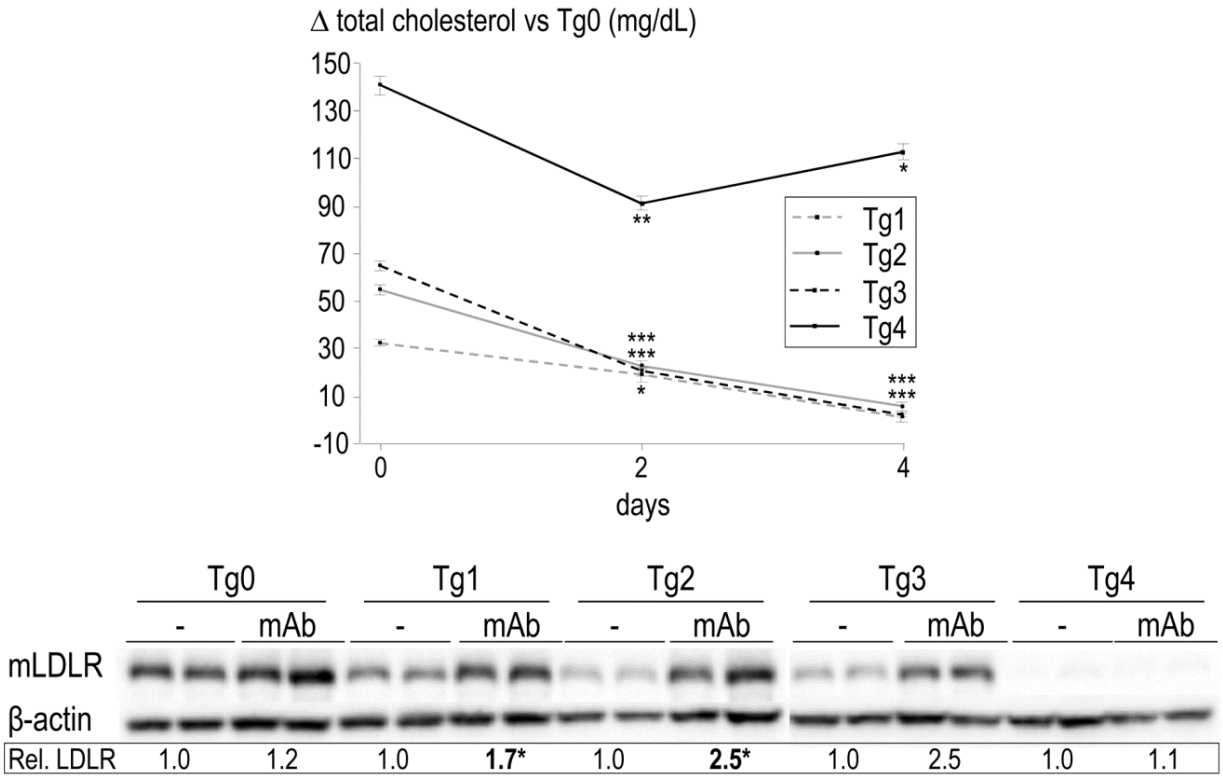

Figure 34. Impact of a single injection of evolocumab in transgenic mice. Plasma from control Tg0 and the four transgenic lines that received 10 mg/kg evolocumab was collected before injection (-10 days, represented as day 0) or 2 and 4 days post-injection. Cholesterol and apoB contents were analyzed and the data is represented as a difference to the levels of injected Tg0 mice (upper panels). Liver LDLR levels were analyzed by WB and calibrated to β-actin ones (lower panel). A representative blot is shown, and the averaged normalized LDLR values were obtained from 5 to 7 mice per group. Error bars indicate SEM. *, $p < 0.05$ (Student's *t* test compared to day 0).

III.5.6 A mouse model for the characterization of human PCSK9 inhibitors

We then compared the inhibitory effects of evolocumab and PKF8-mFc, a previously described sdAb directed against the CHRD of PCSK9 and fused to a mFc (1). Both Tg0 and Tg2 mice were injected in the tail vein with PBS or PBS containing the inhibitor (10 mg/kg) and bled at indicated time points in order to analyze their TC levels (Figure 35). Both inhibitors led to a maximal TC decrease 5 days post-injection. PKF8-mFc or evolocumab neutralized 58% or 116% of the TC increase resulting from hPCSK9 expression, respectively. Thus, evolocumab was twice more effective in reducing TC levels than PKF8-mFc. However, the cholesterol-lowering effect of the latter lasted at least 14 days instead of 10 days for evolocumab. Note that a two-way ANOVA comparing Tg2 mice injected with PBS or PKF8-mFc from day 3 to day 19 and Tg2 mice injected with PBS or evolocumab from day 3 to day 9 resulted in highly significant *p*-values of 3.61e-12 and 1.92e-11, respectively. A second injection of PKF8-mFc 24 days after the first one led to a slightly stronger TC decrease (-66%) 7 days later, while a second evolocumab injection resulted in a slightly reduced TC drop (-102%) 5 days later. Mice were euthanized before the reversibility of the TC drop and liver LDLR and plasma hPCSK9 were measured by ELISA.

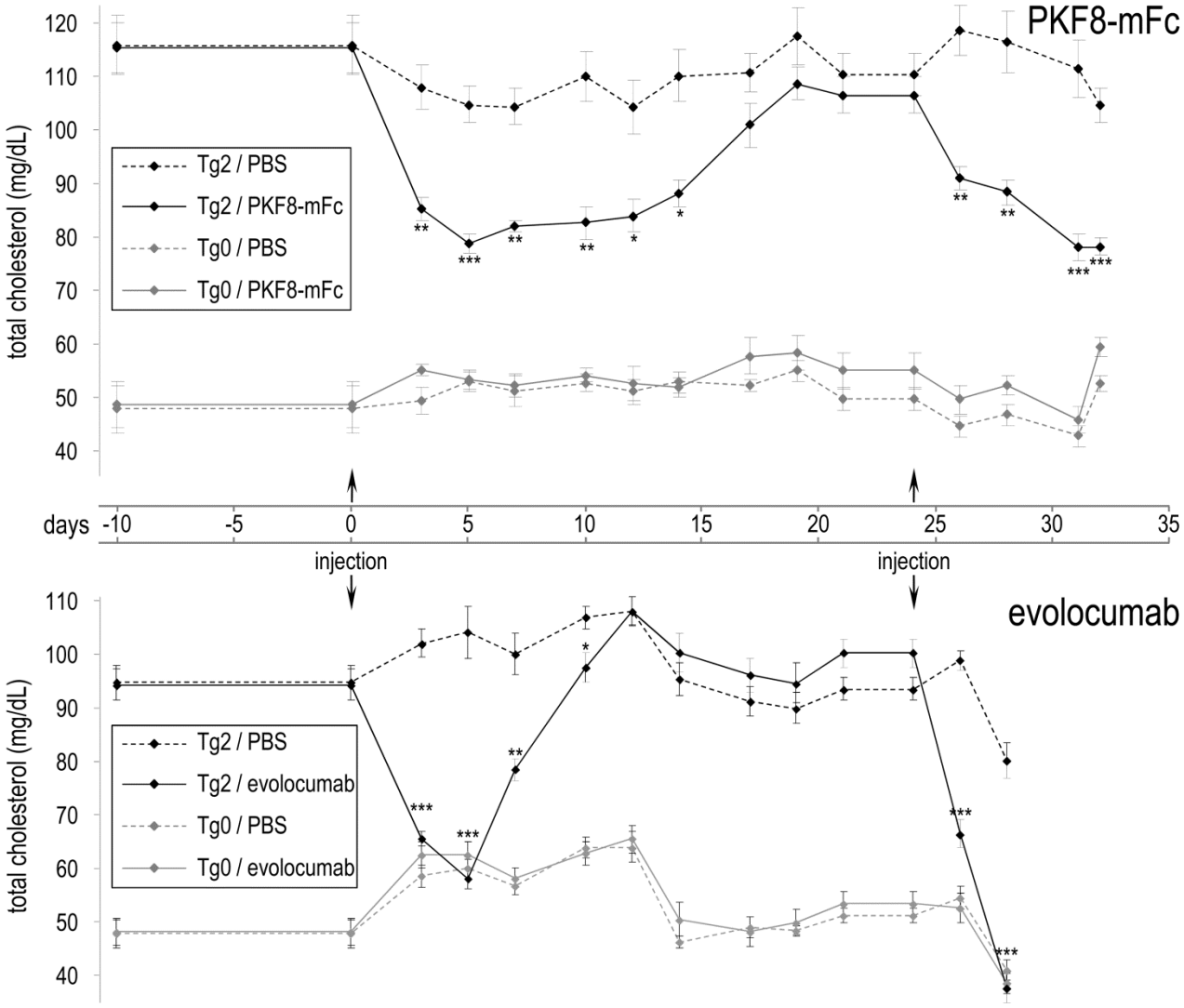

Figure 35. Long-term effect of two injections of PKF8-mFc or evolocumab. Plasma TC levels were measured before (10 days) and after two injections of 10mg/kg PFK8-mFc (upper panel), evolocumab (lower panel) or PBS. The first injection was performed at day 0 and the second at day 24. After each injection, blood was taken from the tail vein every two to three days in order to follow TC levels over time. Mice injected with PKF8-mFc or evolocumab were sacrificed at day 32 or 28, respectively. In each group, n= 7 to 8 mice. Error bars indicate SEM. *, $p < 0.05$; **, $p < 0.005$; ***, $p < 0.0005$ (Student's *t* test compared to Tg2 mice injected with PBS).

LDLR levels (100% in Tg0 littermates) indicated a 42% and 86% of LDLR recovery with PKF8-mFc or evolocumab, respectively, confirming the partial effect of PKF8-mFc (Figure 36A). Note that only non-significant variations of TC or mLDLR were observed among Tg0-injected mice or PBS-injected Tg2 mice, confirming the specificity for PCSK9 of both PKF8-mFc and evolocumab and that Tg0 is an adequate control mouse line. Unexpectedly, the plasma hPCSK9 profiles were very different (Figure 36B). hPCSK9 was unaffected by PKF8-mFc injection, whereas evolocumab injection promoted an accumulation of PCSK9 peaking at day 3, followed by a decrease to basal values at day 10, likely reflecting the clearance rate of circulating hPCSK9-evolocumab complexes. The non-accumulation of hPCSK9 in the plasma after PKF8-mFc injection indicated that the interaction of this sdAb with PCSK9 does not prevent PCSK9 binding to the LDLR, as shown previously (1). In order to determine whether the sdAb-PCSK9 complex can be internalized into cells, we treated Tg0 primary hepatocytes with media containing vehicle, PKF8-mFc (2 μM), hPCSK9 (0.08 μM) or both PKF8-mFc and PCSK9 pre-incubated at 37°C for 1h. Media were applied on cells kept on ice to prevent endocytosis or incubated at 37°C (Figure 36C). After a neutral or acidic wash, cells were lysed and analyzed for their hPCSK9 content. PCSK9 alone or in complex with PKF8-mFc bound primary hepatocytes on ice, but was not internalized since an acidic wash eliminated the PCSK9 signal. In contrast, the signal persisted in cells incubated at 37°C, indicating that PCSK9 was internalized independently of the 25-fold molar excess of PKF8-mFc. The LDLR content measured in protein extracts confirmed the partial inhibition achieved by PKF8-mFc on hPCSK9 activity.

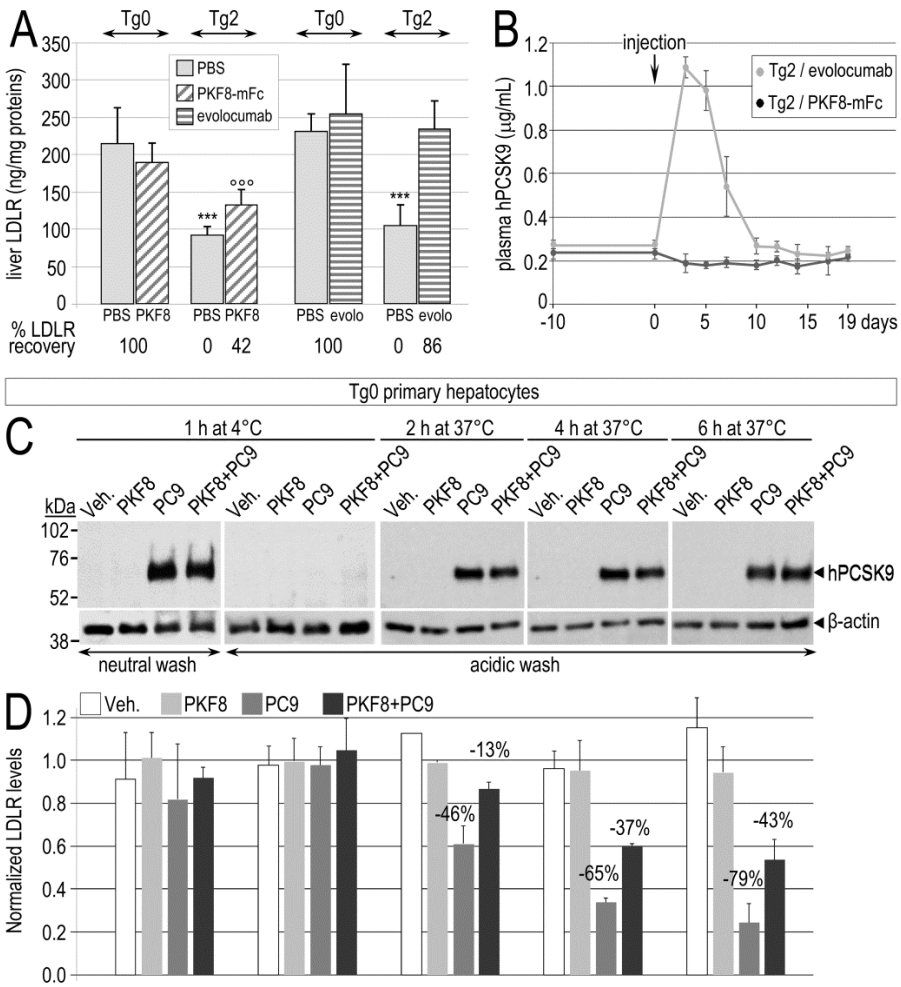

Figure 36. Comparison of PKF8-mFc and evolocumab activities in mice or primary hepatocytes. (*A*) Liver LDLR protein levels were measured by ELISA. LDLR recovery was set to 100% and 0% in Tg0 and Tg2 mice receiving PBS, respectively. ***, $p < 0.0005$ (Student's *t* test). The % LDLR recovery for each antibody is based on the 100% value given by Tg0 mice that received the antibody. °°°, $p < 0.0005$ (Student's *t* test). Average + SD; n = 6 to 8 mice per condition. (*B*) Circulating hPCSK9 levels (average ± SD) were assessed in the above mice before and after injection of PKF8-mFc or evolocumab. (*C*) Tg0 primary hepatocytes were incubated with vehicle (Veh.), PKF8-mFc (PKF8; 2 µM), PCSK9 (PC9; 0.08 µM), or a combination of both in the indicated conditions. After a neutral or acidic wash, proteins were extracted, and hPCSK9 binding or internalization was analyzed by WB (pool of 3 triplicates/well). (*D*) LDLR levels (average + SD) were measured by ELISA in two independent experiments at 37°C, each in triplicate. Data were first normalized to the vehicle value of the 2h incubation, and then normalized to the average obtained after 1h at 4°C and an acidic wash (no PCSK9 activity, one experiment in triplicate). LDLR % loss (PC9 versus Veh. or PKF8+PC9 versus PKF8 alone) are indicated.

III.6 Discussion

In this study, we report the generation of a new transgenic mouse model expressing the human *PCSK9* gene under the control of its own promoter in a mouse *Pcsk9*$^{-/-}$ background (Figure 30). Four transgenic mouse lines were obtained (Tg1 to Tg4) and *Pcsk9*$^{-/-}$ mice (Tg0) were used as control littermates. Circulating PCSK9 varied from 95 to 4,974 ng/mL, with 1 to 32 copies of the Tg per genome (Figure 30). The tissue distribution of hPCSK9 mRNA nicely reproduced that of mPCSK9 (Figure 31). Relative hepatic hPCSK9 mRNA levels varied from 1 to 35, in good agreement with the 52-fold ratio between lowest and highest expressions of the protein. In contrast and as expected, mLDLR mRNA levels were unaffected (Figure 32). Interestingly, both hPCSK9 and mLDLR mRNA levels were higher in females than in males. For hPCSK9 protein, this was also reported in human plasma (267). Although Tg2 and Tg3 exhibited the same Tg copy number of 2 and similar hPCSK9 protein levels (~365 ng/mL), a significant 4.4-fold difference was observed in hPCSK9 mRNA levels. Whether the stability or translation of hPCSK9 messengers transcribed from one of the two Tg copies in Tg2 or Tg3 is affected remains undetermined. In agreement with the ability of PCSK9 to trigger LDLR protein degradation, mLDLR levels assessed by WB were decreased by 35 to 98% in Tg1 to Tg4. In the same lines, TC was increased by 50 to 230%. Interestingly, TC levels in Tg4 (158 mg/dL) were considerably lower than those in *Ldlr*$^{-/-}$ (253 mg/dL) and *Ldlr*$^{-/-}$ *Pcsk9*$^{-/-}$ (238 mg/dL) mice, even though LDLR protein levels in Tg4 were barely detectable in liver. This reveals how key the few percent of remaining LDLR are. *In vivo*, PCSK9 was shown to target liver cell surface LDLR for degradation essentially via an extracellular pathway, thus leaving nascent LDLR intact. The latter may limit hypercholesterolemia by triggering intracellular apoB degradation as reported previously (615, 616). ApoB measurement by ELISA turned out to be poorly informative due to the very small window between lower and higher values. Importantly, although different mRNA levels led to similar hPCSK9 protein levels in Tg2 and Tg3, the protein exhibited the same apparent molecular weight and the same extent of cleavage by furin, confirming the integrity of hPCSK9 in these two lines (Figure 33).

All transgenic lines were treated with 10 mg/kg of evolocumab, which targets PCSK9 catalytic domain (Figure 34). The mAb completely neutralized hPCSK9 activity 4 days post-injection,

except in Tg4, in which the inhibitory effect was only partial and transient. At 4 days versus 10 days, TC dropped by 63, 67 and 74% in Tg1, Tg2 and Tg3, respectively. When first tested *in vivo* in WT mice, a single injection of evolocumab at 10 mg/kg was reported to lead to a 28% TC decrease 6 days later (189). We observed a higher efficacy in this study, likely due to the higher binding affinity of evolocumab for hPCSK9 (4 pM) compared to mPCSK9 (160 pM). In humans, an injection of 140 mg of evolocumab every 2 or 4 weeks leads to ~60% LDLc drop, well maintained for 2 to 4 years (435). For an average human body weight of 70 kg, the dose injected corresponds to only 2 mg/kg. However, this dose did not significantly decrease TC in our mice (see Appendix A2). Thus, although the TC decrease observed in our model was similar to the one seen in humans, the pharmacodynamics of evolocumab is different in mice and humans. Therefore, adjustments are needed when switching from mouse to human, as expected (617) .

We further studied the long-term effect of PKF8-mFc, a sdAb targeting the CHRD of PCSK9 and fused to a mFc, and evolocumab in the Tg2 mouse model (Figure 35). The TC-reducing effect of PKF8-mFc was ~2-fold lower (-58% versus -116%), but its duration was ~2-fold longer (14 days versus 7 days for evolocumab). The lower efficiency of PKF8-mFc may reside in its mechanism of action via binding to the CHRD, and not the catalytic domain of hPCSK9. Indeed, to date, no approach targeting the CHRD was able to prevent LDLR binding or to achieve complete PCSK9 inhibition. Even though the CHRD exhibits mutations leading to hypo- and hypercholesterolemia (64, 209, 618, 619), it is not directly involved in LDLR binding (179), and PCSK9 lacking this domain has the same affinity for LDLR (91). However, the latter truncated PCSK9-ΔCHRD is unable to induce LDLR degradation (179, 184). Whether the CHRD, which is a flexible region (173, 620, 621), recruits one or more proteins implicated in the targeting of the PCSK9-LDLR complex to the lysosomal pathway (190) remains to be proven. All three CHRD antibodies reported previously had partial inhibitory efficiencies. The first one, a human Fab, reduced LDL uptake in cell lines by ~50% (187). The second one, a mAb, recognizes the CHRD with an affinity of 4.1 nM and reduced LDLc levels by ~40% when injected at 10 mg/kg in cynomolgus monkeys (188). The third one is another sdAb that neutralized ~60% of hPCSK9 activity at 10 mg/kg, like PKF8-mFc. In addition, the natural annexin A2 that also interacts with the CHRD and inhibits PCSK9 activity in non-hepatic cells, led to a ~30% reduction only of PCSK9 activity upon

overexpression in HepG2 cells (229), again suggesting that CHRD targeting alone would not completely inhibit PCSK9 activity on the LDLR. While the present study does not identify the mechanism by which the sdAb only achieved a partial inhibition of PCSK9 activity towards the LDLR, our results point to an inhibitory effect post-internalization of the sdAb-PCSK9-LDLR complex. In evolocumab-treated mice, hPCSK9-mAb complexes can no longer bind the LDLR. It is thus no surprise to observe an accumulation of hPCSK9 in the plasma, with a peak around day 3, and a return to basal levels at day 10 (Figure 36B), a negative mirror image of the TC profile (Figure 33). In contrast, PKF8-mFc-treated mice showed unchanged plasma levels of PCSK9. PKF8-mFc which does not prevent PCSK9 binding to the LDLR (1), seems not to interfere with hPCSK9 internalization (Figure 36C). Whether PKF8-mFc partially prevents the interaction of trafficking interactors with the CHRD, or tends to dissociate from hPCSK9 in acidic compartments remains to be defined. The longer effect of PKF8-mFc (~85 kDa per dimer) observed in our study (14 days versus 10 days for evolocumab; ~144 kDa) may be due to a ~1.7-fold molar excess upon a 10 mg/kg treatment, or to a slower clearance due to distinct Fc domains. PKF8 was fused to an IgG2 mFc, whereas evolocumab is a human IgG2 that may be cleared more rapidly because of an immune reaction from mice towards the human antibody. However, the response to the second injection was as strong as the first response.

In conclusion, our transgenic mice offer a larger window of TC measurements due to its *Pcsk9*$^{-/-}$ background. Indeed, no persistent PCSK9 activity due to the endogenous protein will be detected once hPCSK9 is completely neutralized. We showed that TC decrease is reversible, allowing thus several assays with the same group of mice, and thus reducing the costs of an *in vivo* screening. Although very efficient mAbs to PCSK9 are already marketed, there is still a need for other approaches to inhibit PCSK9 because of their high costs that restrict their use to specific patients (444, 445). Thus, partial PCSK9 inhibition with sdAbs through CHRD targeting might be of interest since the total loss of PCSK9 was shown to lead to incomplete liver regeneration (172) and higher risk of HCV infection (296).

In this study, we generated four transgenic mouse lines expressing various levels of hPCSK9 under the control of its own promoter in a *Pcsk9*$^{-/-}$ background. hPCSK9 was detected in plasma as

mature and furin-cleaved forms. All lines reproduced the endogenous PCSK9 expression pattern with different intensities. The higher hPCSK9 expression is, the higher are TC levels and lower are hepatic endogenous LDLR levels. We compared the inhibitory potencies of two PCSK9 inhibitors, evolocumab and the sdAb PKF8-mFc, in the Tg2 line and control Tg0 littermates. Pharmacodynamics differences between these two inhibitors could be observed. hPCSK9 inhibition was reversible and was maintained upon a second injection. These mice constitute valuable tools in the discovery and study of novel agents reducing PCSK9 activity or expression, possibly leading to a better control of CVD events.

III.7 Additional information

III.7.1 Funding

This research work was supported by the CIHR grants Foundation Scheme 148363 and MOP 102741, a Pfizer Aspire 1 Cardiovasc Res award WI207162, the Canada Research Chair 231335, and a Fondation Leducq grant #13CVD03.

III.7.2 Acknowledgements

We are grateful to all the members of the Seidah laboratory for technical support. We would like to thank Manon Laprise for animal experimentation, Suzie Riverin for animal care, and Odile Neyret, Myriam Rondeau and Agnès Dumont for mouse genotyping and BAC copy numbers. Finally, we are very grateful to Dr. Robert Dufour (IRCM) for his generous gift of evolocumab.

III.7.3 Conflicts of interest

The authors declare that they have no competing interests.

III.7.4 Author contributions

RE generated the mouse model (Figure 30), evaluated their circulating PCSK9 (Figure 30 and Figure 36B) and liver LDLR levels (Figure 32C) and performed the primary hepatocytes assays (Figure 36C). **EW designed the BAC copy number determination experiment (Figure 30) and conducted the plasma measurements (Figure 33) as well as all injections experiments and their analysis (Figures 34 and 35).** JM performed the *in situ* hybridization analysis, AC the QPCRs and DSR and AR some ELISAs. **EW, RE, AP and NGS performed the experimental design and analyzed the data. EW wrote the manuscript under the guidance of AP.**

III.8 Chapter discussion

In this chapter, a complete characterization of new transgenic mice expressing hPCSK9 and their response to one or two injections of PCSK9 inhibitors were presented.

One of the limitations of the presented mouse model resides in the fact that the mouse is not entirely humanized. This drawback includes the fact that the FcRn are murine. Although human antibodies can bind both mouse and human FcRn, the affinity of human IgG1 for human FcRn is lower than that for mouse FcRn *in vitro* (519, 622). Half-life estimations in mouse models could thus be overestimated. The FcRn-mediated antibodies recycling being a key factor modulating antibodies clearance, these species differences can explain the poor predictability of human pharmacokinetics using mouse models. In order to counteract this issue, a homozygous mouse model for human FcRn was recently documented and showed a stronger correlation of human mAb clearance than WT mouse (623). This mouse model presents a net advantage in that it could be used earlier in the drug discovery process and decrease the need for time-consuming and expensive pre-clinical studies in non-human primates. In our mice, only mouse FcRn is present and PKF8-mFc contains a mFc (IgG2a) while evolocumab contains a human Fc (IgG2). Therefore, the differences in the pharmacokinetics of mouse and human have to be taken into consideration when comparing these two inhibitors. Besides, since the human FcRn does not bind mouse IgG2a (622), the administration of our sdAb fused to mFc in human would probably have a shorter half-life than in our tested mouse model.

As stated previously in sections I.4.1.2. and I.4.2.6., mAbs are known to be mainly cleared from circulation by two systems: the RES and the FcRn-mediated recycling. It can be hypothesized that sdAbs fused to a mFc would also be cleared by this system, although this is not yet documented in the literature. However, their elimination and thus their half-lives are probably different from mAbs because of their smaller size, even when fused to an Fc domain.

Another limitation is that although these transgenic mice are hypercholesterolemic, they do not entirely mimic human hypercholesterolemia. Although this is partly due to their distinct lipoprotein metabolism, we thought that this could be counteracted by using transgenic mice lacking one allele of *Ldlr*, i.e., hemizygous *Ldlr*$^{+/-}$. We developed such mice and they responded to evolocumab and PKF8-mFc as well as the mice that are homozygous for *Ldlr* in a pilot study (see Appendix A3). However, they did not show a higher difference between Tg0 and Tg2 mice since Tg0 control mice also needed to be *Ldlr* hemizygous. Therefore, we did not find that this mouse model brought a net advantage compared to the homozygous *Ldlr* mice.

Note that we investigated if evolocumab or PKF8-mFc modified the ratio of circulating furin-cleaved *versus* intact PCSK9 in the tested transgenic mice. Unlike what was mentioned by others (308), we did not see any differences in furin cleaved forms upon mice treatment with either PKF8-mFc or evolocumab when TC was the lowest (day 32 for PKF8-mFc and day 28 for evolocumab), suggesting that furin cleaves PCSK9 before its exit from hepatocytes, and hence such cleavage would not be sensitive to the presence of the circulating sdAb.

In a pilot study, we performed a dose-response assay for evolocumab that we injected at 2, 4 and 10 mg/kg. Surprisingly, 2 mg/kg evolocumab did not change the TC levels, although this dose corresponds approximately to the injection of evolocumab in human (140 mg for 70 kg). The dose of 4 mg/kg yielded a slight but significant TC decrease 4 days later, while the 10 mg/kg led to an important decrease as demonstrated in Chapter III. The sdAb-mFcs were always tested at 10 mg/kg. It would now be informative to attest their *in vivo* effects at lower concentrations. Note that P1.40-mFc and PKF8-mFc showed very similar *in vivo* TC-reducing potencies, as expected from their similar efficiencies in cell-based assays.

Future experiments that could be performed to better delineate the distinct mechanisms of PKF8-mFc and evolocumab include the comparison of the internalization of PCSK9 in presence of PKF8 alone or PKF8-mFc in Tg0 primary hepatocytes. It should also be verified that the complex PCSK9-PKF8-mFc enters cells by microscopic analysis of Tg0 primary hepatocytes incubated with such complex produced *in vitro*. Besides, the fate of PCSK9 and LDLR could be followed by

microscopy of various cellular compartments in the presence or absence of PKF8-mFc or evolocumab. This would allow us to know how the injection of PKF8-mFc yields a TC decrease of ~50% relative to control mice, even though it does not prevent the interaction to LDLR nor the internalization of PCSK9. One of the hypotheses is that it triggers the recycling of some LDLR instead of escorting them to lysosomal degradation, likely by partially preventing the fixation of a protein that usually escorts and directs the PCSK9-LDLR complex along this pathway. One other interesting experiment to be performed would be the concomitant injection of both PKF8-mFc and evolocumab. Although it could not increase the TC-reducing efficiency of evolocumab that is already maximal, it might potentiate its duration.

Note that we focused our experiments on the mouse line Tg2 because it expresses physiological levels of hPCSK9. As mentioned, Tg2 was similar to Tg3. The mouse lines Tg1 and Tg4 are too low and too high expressers of hPCSK9, respectively. Although their use as screening and study tools for PCSK9 inhibitors is limited, they could be used to study PCSK9 functions and its role in disease in those two “extreme” conditions.

IV. Chapter IV: Discussion and perspectives

The discovery of PCSK9 took place only 14 years ago. Since then, the knowledge advancement in understanding and inhibiting PCSK9 was very impressive. It is now clear that PCSK9 inhibition can help reducing LDLc levels in patients who are statin-intolerant or who are at high risk of developing CVD, thus reducing global CVD risk. This is an excellent example of a successful "bench to bedside" project.

In the two last Chapters II and III of this PhD thesis, we presented the development of sdAbs targeting hPCSK9. These sdAbs were characterized *in vitro*, in cell-based assays and *in vivo* in a newly elaborated humanized mouse model expressing hPCSK9 that was also characterized. They were shown to be efficient in increasing LDLR levels and decreasing TC levels. sdAbs were also compared to other PCSK9 inhibitors, including EGF-A mimicking peptides and the commercially available mAb evolocumab. This enabled us to demonstrate that sdAbs targeting the CHRD of PCSK9 decrease the TC levels by up to 60%, although PCSK9 could still bind LDLR. In contrast, evolocumab targets PCSK9 catalytic domain and reduces TC levels >100% compared to Tg0 mice. The presented work demonstrated that the newly developed mouse model can be used to study hPCSK9 inhibitors.

We selected four llama sdAbs, fused them to a mFc and demonstrated that *in vivo*, the sdAbs P1.40-mFc and PKF8-mFc had very similar effects, as predicted from our cell-based assays. The third selected sdAb P2.57-mFc had little to no *in vivo* effect in a preliminary study (see Appendix A4). The fourth one, PKE9-mFc was never tested *in vivo*. Although it can be predicted that it would have the same properties than P1.40-mFc and PKF8-mFc, it would be interesting to compare it in another *in vivo* injection assay. As a control it would also have been pertinent to use an unspecific sdAb fused to a mFc instead of PBS. However, we had no access to such molecule. The sdAb P2.57-mFc could arguably have been used as a negative control. However, we did not take that risk because despite its low potency in most of our assays, it was potent in some assays and had a nanomolar-range affinity to PCSK9. Note that it is quite surprising that three out of four selected sdAbs have such similar behaviors although they were selected from four distinct families based on phylogenetic analysis of the selected sdAbs. We thus concluded that the family from which the sdAbs come from has a limited importance on their efficacy.

The studies performed during this PhD thesis highlighted once more the importance of the CHRD of PCSK9 in LDLR degradation. However, its precise role is still unknown. Note that the studied sdAb-Fcs could be used to study the exact function(s) of the CHRD. As discussed previously, the CHRD might be the binding site of one or several protein(s) X that bring the PCSK9-LDLR complex to lysosomal degradation, as indicated on Figure 37. Several experiments could be imagined. As an example, cells could be incubated in presence or absence of PCSK9 with various candidates for protein(s) X either in presence or absence of P1.40 or PKF8 and the cellular LDLR levels subsequently measured by WB, ELISA or FACS. The cells in which the incubation with P1.40 or PKF8 would have no LDLR increase would then be likely to have been incubated with the potential protein X, allowing for its identification. Other techniques such as phage display or mass spectrometry could be used to pull down and identify the binding partners of PCSK9 after its incubation in presence or absence of the identified sdAbs. Once one or several protein(s) X will be identified, their specificity to PCSK9 would have to be verified by knockdown and knockout studies that should be performed both *in vitro* and *in vivo*.

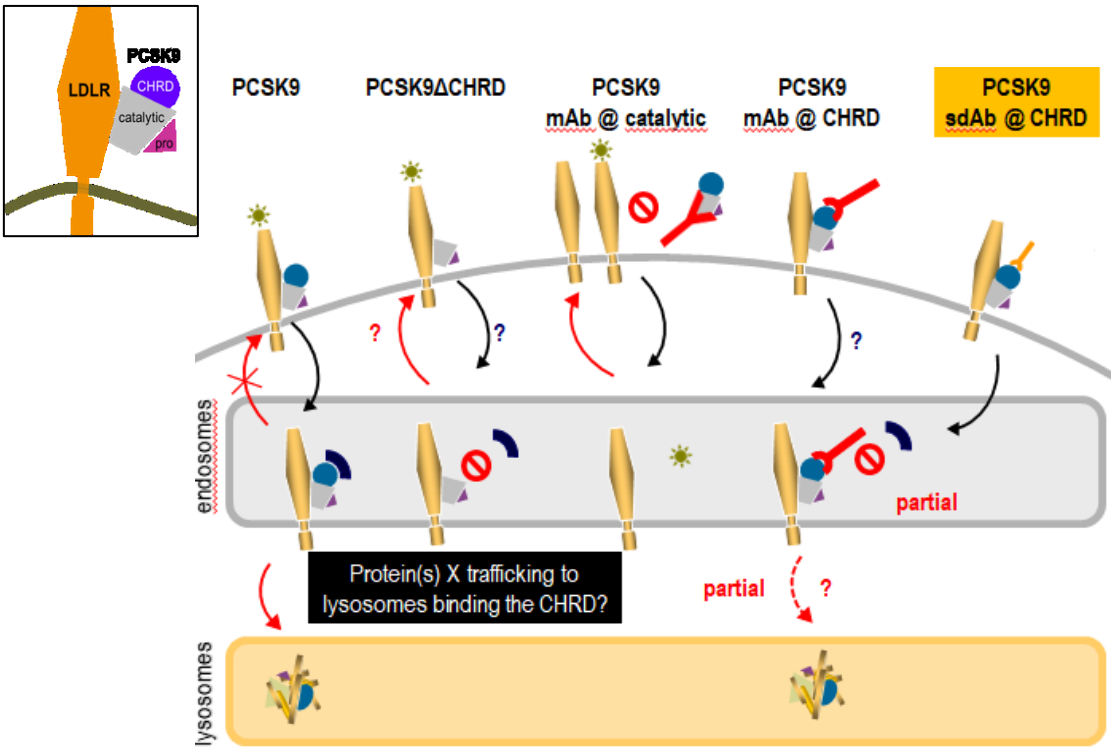

Figure 37. Scheme of potential mechanisms for the degradation of the PCSK9-LDLR complex. Five conditions are depicted from left to right in this figure. PCSK9 binds LDLR and the complex is internalized into endosomes, in which it is hypothesized that one or several protein(s) X might bind the PCSK9 CHRD in order to send the PCSK9-LDLR complex to lysosomal degradation. LDLR recycling is thus prevented. PCSK9 mutant lacking its CHRD (PCSK9ΔCHRD) does not get degraded, which is in favor of the protein X hypothesis. mAbs targeting the catalytic domain of PCSK9 prevent their binding to LDLR and enable LDLR recycling. mAbs or sdAbs targeting the CHRD of PCSK9 have shown partial decrease of LDLc and partial recycling of the LDLR compared to mAbs targeting the catalytic domain of PCSK9. This could be explained by the prevention of protein X to the CHRD due to the binding of mAbs or sdAbs in this region of PCSK9. The precise mechanisms of action of the PCSK9-LDLR trafficking and degradation remain to be discovered.

Ideally, it would be nice to have a set of sdAbs targeting each domain of PCSK9 in order to perform cell-based assays or to inject them in the characterized transgenic mice. This would allow observing the effect of each sdAb and subsequent understanding the role of each domain of PCSK9 in its various physiological roles. Since sdAbs apparently enter the cells, they could also be used to study the intracellular degradation pathway and its location in various tissues *in vivo* (186). We

could also label the tested sdAbs with a radioactive tracer to study the fate of PCSK9 and the role of extrahepatic PCSK9. This could be done on whole transgenic mice by using quantitative non-invasive imaging. As mentioned earlier, sdAbs have demonstrated advantageous imaging properties due to their fast clearance and subsequent high contrast imaging only a few hours following the injection of the sdAb coupled to a radioactive tracer. A phase 1 clinical trials recently showed that the use of anti-Human Epidermal growth factor Receptor 2 (HER2) sdAbs labeled with Gallium 68 (^{68}Ga) for PET/CT imaging enabled a safe and efficient assessment of HER2 in women patients with breast carcinoma (624). A similar study was recently reported in mice using Technetium 99m (^{99m}Tc)-labeled sdAbs for Single-Photon Emission Computed Tomography (SPECT) imaging (625).

Note that we focused our assays on the pharmacodynamics, which analyzes the effect of a drug on an organism. However, we did not study extensively the pharmacokinetics, which analyzes the effect of an organism on the drug. To that end, it would be appropriate to assess the concentrations of sdAb-Fc and evolocumab in mice plasma over time after injection. This could be achieved by WB using V5 antibodies for the sdAb-Fcs which are V5-tagged and using human IgG antibodies for evolocumab. Note that it will not be possible to compare the levels of inhibitors between each other, unless an antibody against a portion of the Fc domain that is conserved between mouse and human Fc would be used. Since we were limited by the maximal volume of ~100 µL of mice plasma to be taken each week, we could not perform these assays. Therefore, the long-term experiments would have to be repeated in order to use mouse plasma for pharmacokinetics studies.

The presented mouse model will very probably be helpful in the development of new PCSK9 inhibitors. Since the currently marketed mAbs are very efficient, this research field is challenging. New PCSK9 inhibitors will need to be as efficient as them but present additional advantages such as a less frequent administration or easier mode of administration. Since the siRNA “inclisiran” seems promising in terms of LDLc and PCSK9 reductions, and holds the important advantage of being able to be injected every 3 to 6 months, it can be predicted that if the ongoing phase 3 confirms these results, this drug will be the next one marketed as a PCSK9 inhibitor. Although it remains to be verified upon approval, their price can be expected to be competitive in comparison

to mAbs. Although not as efficient as targeting the catalytic domain of PCSK9, the work of this PhD thesis suggests that the CHRD is also a possible inhibitory target for PCSK9. Since the search of small molecules targeting PCSK9 have proven to be very difficult, notably because of the flat surface interaction between LDLR and PCSK9, it would be interesting to develop small molecules targeting PCSK9 CHRD. They might be easier to develop than the ones targeting the catalytic domain. Even if their efficiency would not be as high as mAbs, since they could potentially be orally available, they would present a net advantage over mAbs. We could imagine that they could be used in patients at moderate risk for CVD, instead of statin monotherapy for example, or to potentiate the effect of statins.

Although very advantageous, PCSK9 inhibition presents some limitations. First, it cannot be used in patients harboring homozygous mutations in LDLR. Second, it remains to be seen if the total absence of PCSK9 and the very low LDLc levels achieved by PCSK9 inhibition are totally safe. Although they seem safe so far, they might cause some issues as demonstrated by studies showing the protective role of PCSK9 in sepsis or HCV or liver regeneration (172, 286, 296). This data suggests that in cases where TC levels are adequate, the presence of PCSK9 is beneficial. Another open question is: why would we have kept these two proteins from an evolutionary point of view if they are "seemingly" dispensable? A relevant argument to this point is that the sedentary lifestyle and unlimited access to industrialized food appeared rapidly and relatively recently in developed countries, not leaving enough time for our genomes to adapt to these environmental modifications

It is possible that other PCs will become therapeutic targets to reduce CVD in the future, such as furin, PC5 or PC7. Further studies need to be performed in order to confirm these more or less early hypotheses. It is not unlikely that in the next decades we see other PCs inhibitors on the market in order to decrease CVD. Note that the PCs furin and PC5 were related to atherosclerosis. A large-scale association study identified a furin SNP as a novel risk locus for CVD (626). Given that furin and PC5 were detected in human atherosclerotic lesions (627, 628), they were proposed as therapeutic targets to reduce atherosclerosis and CVD (629), which was recently reviewed (630). Finally, genomic studies revealed that under certain conditions PC7 may regulate TG (157, 160) and small dense LDL (631).

Altogether, it can be foreseen that the work accomplished during this PhD project will enable research to be pursued in various fields, including the understanding of the role of each domain of PCSK9, and especially the CHRD in LDLR degradation, the *in vivo* function of PCSK9 in various tissues and diseases, as well as the research of innovative PCSK9 inhibitors. All this should contribute to decrease the frequency of CVD and to ameliorate the lifespan of hypercholesterolemic and FH patients. As a general conclusion, the work accomplished during this PhD project contributed to extend the knowledge of sdAbs by adding an application of this relatively new technology in the field of CVD study and treatment. It also brought a new mouse model that is now fully characterized and that is currently and will probably continue to be very useful in the research of new PCSK9 inhibitors of any kinds.

V. References list

1. Weider E, Susan-Resiga D, Essalmani R, Hamelin J, Asselin MC, Nimesh S, et al. Proprotein convertase subtilisin/kexin type 9 (PCSK9) single domain antibodies are potent inhibitors of low density lipoprotein receptor degradation. J Biol Chem. 2016;291(32):16659-71.

2. Zetterstrom R. The 1964 Nobel Prize for the discovery of the biosynthesis of cholesterol. Acta paediatrica (Oslo, Norway : 1992). 2009;98(7):1223-7.

3. Grundy SM. Cholesterol Metabolism in Man. West J Med. 1978;128(1):13-25.

4. Goldstein JL, Brown MS. Regulation of the mevalonate pathway. Nature. 1990;343(6257):425-30.

5. Cyster JG, Dang EV, Reboldi A, Yi T. 25-Hydroxycholesterols in innate and adaptive immunity. Nat Rev Immunol. 2014;14(11):731-43.

6. Dietschy JM. Regulation of cholesterol metabolism in man and in other species. Klinische Wochenschrift. 1984;62(8):338-45.

7. Ignatowski A. Influence of animal food on the organism of rabbits. Izvlest Imp Voyenno Med Akad. 1908;16:154.

8. Horton JD, Goldstein JL, Brown MS. SREBPs: activators of the complete program of cholesterol and fatty acid synthesis in the liver. J Clin Invest. 2002;109(9):1125-31.

9. Yokoyama C, Wang X, Briggs MR, Admon A, Wu J, Hua X, et al. SREBP-1, a basic-helix-loop-helix-leucine zipper protein that controls transcription of the low density lipoprotein receptor gene. Cell. 1993;75(1):187-97.

10. Hua X, Yokoyama C, Wu J, Briggs MR, Brown MS, Goldstein JL, et al. SREBP-2, a second basic-helix-loop-helix-leucine zipper protein that stimulates transcription by binding to a sterol regulatory element. Proc Natl Acad Sci U S A. 1993;90(24):11603-7.

11. Hua X, Nohturfft A, Goldstein JL, Brown MS. Sterol resistance in CHO cells traced to point mutation in SREBP cleavage-activating protein. Cell. 1996;87(3):415-26.

12. Korn BS, Shimomura I, Bashmakov Y, Hammer RE, Horton JD, Goldstein JL, et al. Blunted feedback suppression of SREBP processing by dietary cholesterol in transgenic mice expressing sterol-resistant SCAP(D443N). J Clin Invest. 1998;102(12):2050-60.

13. Matsuda M, Korn BS, Hammer RE, Moon YA, Komuro R, Horton JD, et al. SREBP cleavage-activating protein (SCAP) is required for increased lipid synthesis in liver induced by cholesterol deprivation and insulin elevation. Genes Dev. 2001;15(10):1206-16.

14. Wang X, Sato R, Brown MS, Hua X, Goldstein JL. SREBP-1, a membrane-bound transcription factor released by sterol-regulated proteolysis. Cell. 1994;77(1):53-62.

15. Sakai J, Duncan EA, Rawson RB, Hua X, Brown MS, Goldstein JL. Sterol-regulated release of SREBP-2 from cell membranes requires two sequential cleavages, one within a transmembrane segment. Cell. 1996;85(7):1037-46.

16. Rawson RB, Zelenski NG, Nijhawan D, Ye J, Sakai J, Hasan MT, et al. Complementation cloning of S2P, a gene encoding a putative metalloprotease required for intramembrane cleavage of SREBPs. Mol Cell. 1997;1(1):47-57.

17. Seidah NG, Mowla SJ, Hamelin J, Mamarbachi AM, Benjannet S, Toure BB, et al. Mammalian subtilisin/kexin isozyme SKI-1: A widely expressed proprotein convertase with a unique cleavage specificity and cellular localization. Proc Natl Acad Sci U S A. 1999;96(4):1321-6.

18. Peek C, Espenshade P. Sterol Regulatory Element Binding Proteins in Fungi: Hypoxic Transcription Factors Linked to Pathogenesis2010. 352-9.

19. Olson RE. Discovery of the lipoproteins, their role in fat transport and their significance as risk factors. J Nutr. 1998;128(2 Suppl):439s-43s.

20. Shen L, Lo CC, Woollett LA, Liu M. Apolipoprotein A-IV exerts its anorectic action through a PI3K/Akt signaling pathway in the hypothalamus. Biochem Biophys Res Commun. 2017.

21. Feingold KR GC. Introduction to Lipids and Lipoproteins 2015.

22. Masson CJ, Plat J, Mensink RP, Namiot A, Kisielewski W, Namiot Z, et al. Fatty Acid- and Cholesterol Transporter Protein Expression along the Human Intestinal Tract. PLoS One. 2010;5(4):e10380.

23. Altmann SW, Davis HR, Jr., Zhu LJ, Yao X, Hoos LM, Tetzloff G, et al. Niemann-Pick C1 Like 1 protein is critical for intestinal cholesterol absorption. Science. 2004;303(5661):1201-4.

24. Berge KE, Tian H, Graf GA, Yu L, Grishin NV, Schultz J, et al. Accumulation of dietary cholesterol in sitosterolemia caused by mutations in adjacent ABC transporters. Science. 2000;290(5497):1771-5.

25. Brown MS, Goldstein JL. Receptor-mediated control of cholesterol metabolism. Science. 1976;191(4223):150-4.

26. Goldstein JL, Brown MS, Anderson RG, Russell DW, Schneider WJ. Receptor-mediated endocytosis: concepts emerging from the LDL receptor system. Annu Rev Cell Biol. 1985;1:1-39.

27. Huang S, Henry L, Ho YK, Pownall HJ, Rudenko G. Mechanism of LDL binding and release probed by structure-based mutagenesis of the LDL receptor. J Lipid Res. 2010;51(2):297-308.

28. Linke M, Gordon RE, Brillard M, Lecaille F, Lalmanach G, Bromme D. Degradation of apolipoprotein B-100 by lysosomal cysteine cathepsins. Biol Chem. 2006;387(9):1295-303.

29. Hoeg JM, Demosky SJ, Jr., Pescovitz OH, Brewer HB, Jr. Cholesteryl ester storage disease and Wolman disease: phenotypic variants of lysosomal acid cholesteryl ester hydrolase deficiency. Am J Hum Genet. 1984;36(6):1190-203.

30. Rogers MA, Liu J, Song BL, Li BL, Chang CCY, Chang TY. Acyl-CoA:cholesterol acyltransferases (ACATs/SOATs): enzymes with multiple sterols as substrates and as activators. J Steroid Biochem Mol Biol. 2015;151:102-7.

31. Naureckiene S, Sleat DE, Lackland H, Fensom A, Vanier MT, Wattiaux R, et al. Identification of HE1 as the second gene of Niemann-Pick C disease. Science. 2000;290(5500):2298-301.

32. Kwon HJ, Abi-Mosleh L, Wang ML, Deisenhofer J, Goldstein JL, Brown MS, et al. Structure of N-terminal domain of NPC1 reveals distinct subdomains for binding and transfer of cholesterol. Cell. 2009;137(7):1213-24.

33. Urano Y, Watanabe H, Murphy SR, Shibuya Y, Geng Y, Peden AA, et al. Transport of LDL-derived cholesterol from the NPC1 compartment to the ER involves the trans-Golgi network and the SNARE protein complex. Proc Natl Acad Sci U S A. 2008;105(43):16513-8.

34. Fitzgerald ML, Mujawar Z, Tamehiro N. ABC transporters, atherosclerosis and inflammation. Atherosclerosis.211(2):361-70.

35. Cochain C, Zernecke A. Macrophages and immune cells in atherosclerosis: recent advances and novel concepts. Basic Res Cardiol. 2015;110(4):34.

36. Mahmood SS, Levy D, Vasan RS, Wang TJ. The Framingham Heart Study and the Epidemiology of Cardiovascular Diseases: A Historical Perspective. Lancet. 2014;383(9921):999-1008.

37. Hajar R. Framingham Contribution to Cardiovascular Disease. Heart Views : The Official Journal of the Gulf Heart Association. 2016;17(2):78-81.

38. Katsiki N, Perez-Martinez P, Mikhailidis DP. Homocysteine and non-cardiac vascular disease. Curr Pharm Des. 2017;23(22):3224-32.

39. Chen J, Budoff MJ, Reilly MP, Yang W, Rosas SE, Rahman M, et al. Coronary Artery Calcification and Risk of Cardiovascular Disease and Death Among Patients With Chronic Kidney Disease. JAMA cardiology. 2017;2(6):635-43.

40. Li Y, Zhong X, Cheng G, Zhao C, Zhang L, Hong Y, et al. Hs-CRP and all-cause, cardiovascular, and cancer mortality risk: A meta-analysis. Atherosclerosis. 2017;259:75-82.

41. Miller KA, Siscovick DS, Sheppard L, Shepherd K, Sullivan JH, Anderson GL, et al. Long-Term Exposure to Air Pollution and Incidence of Cardiovascular Events in Women. N Engl J Med. 2007;356(5):447-58.

42. Ward-Caviness CK, Neas LM, Blach C, Haynes CS, LaRocque-Abramson K, Grass E, et al. A genome-wide trans-ethnic interaction study links the PIGR-FCAMR locus to coronary atherosclerosis via interactions between genetic variants and residential exposure to traffic. PLoS One. 2017;12(3):e0173880.

43. Cholesterol Treatment Trialists C, Baigent C, Blackwell L, Emberson J, Holland LE, Reith C, et al. Efficacy and safety of more intensive lowering of LDL cholesterol: a meta-analysis of data from 170,000 participants in 26 randomised trials. Lancet. 2010;376(9753):1670-81.

44. Reddy VS, Bui QT, Jacobs JR, Begelman SM, Miller DP, French WJ. Relationship between serum low-density lipoprotein cholesterol and in-hospital mortality following acute myocardial infarction (the lipid paradox). Am J Cardiol. 2015;115(5):557-62.

45. Ravnskov U, Diamond DM, Hama R, Hamazaki T, Hammarskjöld B, Hynes N, et al. Lack of an association or an inverse association between low-density-lipoprotein cholesterol and mortality in the elderly: a systematic review. BMJ (Clinical research ed). 2016;6(6).

46. Renaud S, de Lorgeril M. Wine, alcohol, platelets, and the French paradox for coronary heart disease. Lancet. 1992;339(8808):1523-6.

47. Müller C. Xanthomata, Hypercholesterolemia, Angina Pectoris. Acta Med Scand. 1938;95(S89):75-84.

48. Wilkinson CF, Jr, Hand EA, Fliegelman MT. Essential familial hypercholesterolemia. Ann Intern Med. 1948;29(4):671-86.

49. Utermann G, Kindermann I, Kaffarnik H, Steinmetz A. Apolipoprotein E phenotypes and hyperlipidemia. Hum Genet. 1984;65(3):232-6.

50. Arca M, Zuliani G, Wilund K, Campagna F, Fellin R, Bertolini S, et al. Autosomal recessive hypercholesterolaemia in Sardinia, Italy, and mutations in ARH: a clinical and molecular genetic analysis. Lancet. 2002;359(9309):841-7.

51. He G, Gupta S, Yi M, Michaely P, Hobbs HH, Cohen JC. ARH is a modular adaptor protein that interacts with the LDL receptor, clathrin, and AP-2. J Biol Chem. 2002;277(46):44044-9.

52. Benn M, Watts GF, Tybjaerg-Hansen A, Nordestgaard BG. Mutations causative of familial hypercholesterolaemia: screening of 98 098 individuals from the Copenhagen General Population Study estimated a prevalence of 1 in 217. Eur Heart J. 2016;37(17):1384-94.

53. Meiner V, Landsberger D, Berkman N, Reshef A, Segal P, Seftel HC, et al. A common Lithuanian mutation causing familial hypercholesterolemia in Ashkenazi Jews. Am J Hum Genet. 1991;49(2):443-9.

54. Lehrman MA, Schneider WJ, Brown MS, Davis CG, Elhammer A, Russell DW, et al. The Lebanese allele at the low density lipoprotein receptor locus. Nonsense mutation produces truncated receptor that is retained in endoplasmic reticulum. J Biol Chem. 1987;262(1):401-10.

55. Davignon J, Roy M. Familial hypercholesterolemia in French-Canadians: taking advantage of the presence of a "founder effect". Am J Cardiol. 1993;72(10):6d-10d.

56. Hopkins PN, Toth PP, Ballantyne CM, Rader DJ. Familial hypercholesterolemias: prevalence, genetics, diagnosis and screening recommendations from the National Lipid Association Expert Panel on Familial Hypercholesterolemia. J Clin Lipidol. 2011;5(3 Suppl):S9-17.

57. Youngblom E, Pariani M, Knowles JW. Familial Hypercholesterolemia. GeneReviews1993.

58. Dey A, Aggarwal R, Dwivedi S. Cardiovascular profile of xanthelasma palpebrarum. BioMed Res Int. 2013;2013:932863.

59. Tsouli SG, Kiortsis DN, Argyropoulou MI, Mikhailidis DP, Elisaf MS. Pathogenesis, detection and treatment of Achilles tendon xanthomas. Eur J Clin Invest. 2005;35(4):236-44.

60. Perez de Isla L, Alonso R, Watts GF, Mata N, Saltijeral Cerezo A, Muniz O, et al. Attainment of LDL-Cholesterol Treatment Goals in Patients With Familial Hypercholesterolemia: 5-Year SAFEHEART Registry Follow-Up. J Am Coll Cardiol. 2016;67(11):1278-85.

61. Hobbs HH, Brown MS, Goldstein JL. Molecular genetics of the LDL receptor gene in familial hypercholesterolemia. Hum Mutat. 1992;1(6):445-66.

62. Hovingh GK, Kastelein JJ. Diagnosis and Management of Individuals With Heterozygous Familial Hypercholesterolemia: Too Late and Too Little. Circulation. 2016;134(10):710-2.

63. Seidah NG, Benjannet S, Wickham L, Marcinkiewicz J, Jasmin SB, Stifani S, et al. The secretory proprotein convertase neural apoptosis-regulated convertase 1 (NARC-1): liver regeneration and neuronal differentiation. Proc Natl Acad Sci U S A. 2003;100(3):928-33.

64. Abifadel M, Varret M, Rabes JP, Allard D, Ouguerram K, Devillers M, et al. Mutations in PCSK9 cause autosomal dominant hypercholesterolemia. Nat Genet. 2003;34(2):154-6.

65. Awan Z, Choi HY, Stitziel N, Ruel I, Bamimore MA, Husa R, et al. APOE p.Leu167del mutation in familial hypercholesterolemia. Atherosclerosis. 2013;231(2):218-22.

66. Wintjens R, Bozon D, Belabbas K, F MB, Girardet JP, Tounian P, et al. Global molecular analysis and APOE mutations in a cohort of autosomal dominant hypercholesterolemia patients in France. J Lipid Res. 2016;57(3):482-91.

67. Marduel M, Ouguerram K, Serre V, Bonnefont-Rousselot D, Marques-Pinheiro A, Berge KE, et al. Description of a large family with autosomal dominant hypercholesterolemia associated with the APOE p.Leu167del mutation. Hum Mutat. 2013;34(1):83-7.

68. Fouchier SW, Dallinga-Thie GM, Meijers JC, Zelcer N, Kastelein JJ, Defesche JC, et al. Mutations in STAP1 are associated with autosomal dominant hypercholesterolemia. Circ Res. 2014;115(6):552-5.

69. Day IN. FH4=STAP1. Another gene for familial hypercholesterolemia? Relevance to cascade testing and drug development? Circ Res. 2014;115(6):534-6.

70. Marques-Pinheiro A, Marduel M, Rabes JP, Devillers M, Villeger L, Allard D, et al. A fourth locus for autosomal dominant hypercholesterolemia maps at 16q22.1. Eur J Hum Genet : EJHG. 2010;18(11):1236-42.

71. Goldstein JL, Brown MS. Familial hypercholesterolemia: identification of a defect in the regulation of 3-hydroxy-3-methylglutaryl coenzyme A reductase activity associated with overproduction of cholesterol. Proc Natl Acad Sci U S A. 1973;70(10):2804-8.

72. Anderson RG, Goldstein JL, Brown MS. Localization of low density lipoprotein receptors on plasma membrane of normal human fibroblasts and their absence in cells from a familial hypercholesterolemia homozygote. Proc Natl Acad Sci U S A. 1976;73(7):2434-8.

73. Schneider WJ, Beisiegel U, Goldstein JL, Brown MS. Purification of the low density lipoprotein receptor, an acidic glycoprotein of 164,000 molecular weight. J Biol Chem. 1982;257(5):2664-73.

74. Yamamoto T, Davis CG, Brown MS, Schneider WJ, Casey ML, Goldstein JL, et al. The human LDL receptor: a cysteine-rich protein with multiple Alu sequences in its mRNA. Cell. 1984;39(1):27-38.

75. Sudhof TC, Goldstein JL, Brown MS, Russell DW. The LDL receptor gene: a mosaic of exons shared with different proteins. Science. 1985;228(4701):815-22.

76. Wasan KM, Brocks DR, Lee SD, Sachs-Barrable K, Thornton SJ. Impact of lipoproteins on the biological activity and disposition of hydrophobic drugs: implications for drug discovery. Nat Rev Drug Discov. 2008;7(1):84-99.

77. Russell DW, Schneider WJ, Yamamoto T, Luskey KL, Brown MS, Goldstein JL. Domain map of the LDL receptor: Sequence homology with the epidermal growth factor precursor. Cell. 1984;37(2):577-85.

78. Chen WJ, Goldstein JL, Brown MS. NPXY, a sequence often found in cytoplasmic tails, is required for coated pit-mediated internalization of the low density lipoprotein receptor. J Biol Chem. 1990;265(6):3116-23.

79. Van Driel IR, Brown MS, Goldstein JL. Stoichiometric binding of low density lipoprotein (LDL) and monoclonal antibodies to LDL receptors in a solid phase assay. J Biol Chem. 1989;264(16):9533-8.

80. Innerarity TL, Pitas RE, Mahley RW. Binding of arginine-rich (E) apoprotein after recombination with phospholipid vesicles to the low density lipoprotein receptors of fibroblasts. J Biol Chem. 1979;254(10):4186-90.

81. Brown MS, Goldstein JL. Familial hypercholesterolemia: A genetic defect in the low-density lipoprotein receptor. N Engl J Med. 1976;294(25):1386-90.

82. Lehrman MA. Mutation in LDL receptor: Alu-Alu recombination deletes exons encoding transmembrane and cytoplasmic domains. Science. 1985;227:140-6.

83. Hobbs HH, Leitersdorf E, Goldstein JL, Brown MS, Russell DW. Multiple crm- mutations in familial hypercholesterolemia. Evidence for 13 alleles, including four deletions. J Clin Invest. 1988;81(3):909-17.

84. Lehrman MA, Russell DW, Goldstein JL, Brown MS. Alu-Alu recombination deletes splice acceptor sites and produces secreted low density lipoprotein receptor in a subject with familial hypercholesterolemia. J Biol Chem. 1987;262(7):3354-61.

85. Hobbs HH. The LDL receptor locus in familial hypercholesterolemia: mutational analysis of a membrane protein. Annu Rev Genet. 1990;24:133-70.

86. Fokkema IF, Taschner PE, Schaafsma GC, Celli J, Laros JF, den Dunnen JT. LOVD v.2.0: the next generation in gene variant databases. Hum Mutat. 2011;32(5):557-63.

87. Sørensen S, Ranheim T, Bakken KS, Leren TP, Kulseth MA. Retention of Mutant Low Density Lipoprotein Receptor in Endoplasmic Reticulum (ER) Leads to ER Stress. J Biol Chem. 2006;281(1):468-76.

88. Ranheim T, Kulseth MA, Berge KE, Leren TP. Model system for phenotypic characterization of sequence variations in the LDL receptor gene. Clin Chem. 2006;52(8):1469-79.

89. Etxebarria A, Benito-Vicente A, Palacios L, Stef M, Cenarro A, Civeira F, et al. Functional Characterization and Classification of Frequent Low-Density Lipoprotein Receptor Variants. Human Mutation. 2015;36(1):129-41.

90. Koivisto UM, Hubbard AL, Mellman I. A novel cellular phenotype for familial hypercholesterolemia due to a defect in polarized targeting of LDL receptor. Cell. 2001;105(5):575-85.

91. Bottomley MJ, Cirillo A, Orsatti L, Ruggeri L, Fisher TS, Santoro JC, et al. Structural and Biochemical Characterization of the Wild Type PCSK9-EGF(AB) Complex and Natural Familial Hypercholesterolemia Mutants. J Biol Chem. 2009;284(2):1313-23.

92. Susan-Resiga D, Girard E, Kiss RS, Essalmani R, Hamelin J, Asselin MC, et al. A novel mechanism causing familial hypercholesterolemia: The proprotein convertase subtilisin/kexin type 9-resistant Arg410Ser LDL receptor mutation. J Biol Chem. 2016.

93. Innerarity TL, Mahley RW. Enhanced binding by cultured human fibroblasts of apo-E-containing lipoproteins as compared with low density lipoproteins. Biochemistry. 1978;17(8):1440-7.

94. Kane JP, Hardman DA, Paulus HE. Heterogeneity of apolipoprotein B: isolation of a new species from human chylomicrons. Proc Natl Acad Sci U S A. 1980;77(5):2465-9.

95. Anant S, Davidson NO. Molecular mechanisms of apolipoprotein B mRNA editing. Curr Opin Lipidol. 2001;12(2):159-65.

96. Kane JP. Apolipoprotein B: structural and metabolic heterogeneity. Annu Rev Physiol. 1983;45:637-50.

97. Knott TJ, Pease RJ, Powell LM, Wallis SC, Rall SC, Jr., Innerarity TL, et al. Complete protein sequence and identification of structural domains of human apolipoprotein B. Nature. 1986;323(6090):734-8.

98. Chen SH, Yang CY, Chen PF, Setzer D, Tanimura M, Li WH, et al. The complete cDNA and amino acid sequence of human apolipoprotein B-100. J Biol Chem. 1986;261(28):12918-21.

99. Yang CY, Chen SH, Gianturco SH, Bradley WA, Sparrow JT, Tanimura M, et al. Sequence, structure, receptor-binding domains and internal repeats of human apolipoprotein B-100. Nature. 1986;323(6090):738-42.

100. Blackhart BD, Ludwig EM, Pierotti VR, Caiati L, Onasch MA, Wallis SC, et al. Structure of the human apolipoprotein B gene. J Biol Chem. 1986;261(33):15364-7.

101. Walsh MT, Atkinson D. Solubilization of low-density lipoprotein with sodium deoxycholate and recombination of apoprotein B with dimyristoylphosphatidylcholine. Biochemistry. 1983;22(13):3170-8.

102. Boren J, Lee I, Zhu W, Arnold K, Taylor S, Innerarity TL. Identification of the low density lipoprotein receptor-binding site in apolipoprotein B100 and the modulation of its binding activity by the carboxyl terminus in familial defective apo-B100. J Clin Invest. 1998;101(5):1084-93.

103. Weisgraber KH, Rall SC, Jr. Human apolipoprotein B-100 heparin-binding sites. J Biol Chem. 1987;262(23):11097-103.

104. Camejo G, Olofsson SO, Lopez F, Carlsson P, Bondjers G. Identification of Apo B-100 segments mediating the interaction of low density lipoproteins with arterial proteoglycans. Arteriosclerosis. 1988;8(4):368-77.

105. Boren J, Olin K, Lee I, Chait A, Wight TN, Innerarity TL. Identification of the principal proteoglycan-binding site in LDL. A single-point mutation in apo-B100 severely affects

proteoglycan interaction without affecting LDL receptor binding. J Clin Invest. 1998;101(12):2658-64.

106. Whitfield AJ, Marais AD, Robertson K, Barrett PH, van Bockxmeer FM, Burnett JR. Four novel mutations in APOB causing heterozygous and homozygous familial hypobetalipoproteinemia. Hum Mutat. 2003;22(2):178.

107. Cefalu AB, Norata GD, Ghiglioni DG, Noto D, Uboldi P, Garlaschelli K, et al. Homozygous familial hypobetalipoproteinemia: two novel mutations in the splicing sites of apolipoprotein B gene and review of the literature. Atherosclerosis. 2015;239(1):209-17.

108. Soria LF, Ludwig EH, Clarke HR, Vega GL, Grundy SM, McCarthy BJ. Association between a specific apolipoprotein B mutation and familial defective apolipoprotein B-100. Proc Natl Acad Sci U S A. 1989;86(2):587-91.

109. Myant NB. Familial defective apolipoprotein B-100: a review, including some comparisons with familial hypercholesterolaemia. Atherosclerosis. 1993;104:1-18.

110. Fouchier SW, Defesche JC, Kastelein JJ, Sijbrands EJ. Familial defective apolipoprotein B versus familial hypercholesterolemia: an assessment of risk. Semin Vasc Med. 2004;4(3):259-64.

111. Innerarity TL. Familial defective apolipoprotein B-100: low density lipoproteins with abnormal receptor binding. Proc Natl Acad Sci USA. 1987;84:6919-23.

112. Myant NB. Estimation of the age of the ancestral arginine3500glutamine mutation in human apoB-100. Genomics. 1997;45:78-87.

113. Fernández-Higuero JA, Etxebarria A, Benito-Vicente A, Alves AC, Arrondo JLR, Ostolaza H, et al. Structural analysis of APOB variants, p.(Arg3527Gln), p.(Arg1164Thr) and p.(Gln4494del), causing Familial Hypercholesterolaemia provides novel insights into variant pathogenicity. Sci Rep. 2015;5.

114. Thomas ER, Atanur SS, Norsworthy PJ, Encheva V, Snijders AP, Game L, et al. Identification and biochemical analysis of a novel APOB mutation that causes autosomal dominant hypercholesterolemia. Mol Genet Genomic Med. 2013;1(3):155-61.

115. Rabes JP, Varret M, Devillers M, Aegerter P, Villeger L, Krempf M, et al. R3531C mutation in the apolipoprotein B gene is not sufficient to cause hypercholesterolemia. Arterioscler Thromb Vasc Biol. 2000;20(10):E76-82.

116. Chrétien M, Li CH. Isolation, purification, and characterization of γ-lipotropic hormone from sheep pituitary glands. Can J Biochem. 1967;45(7):1163-74.

117. Roberts JL, Seeburg PH, Shine J, Herbert E, Baxter JD, Goodman HM. Corticotropin and beta-endorphin: construction and analysis of recombinant DNA complementary to mRNA for the common precursor. Proc Natl Acad Sci U S A. 1979;76(5):2153-7.

118. Nakanishi S, Inoue A, Kita T, Nakamura M, Chang AC, Cohen SN, et al. Nucleotide sequence of cloned cDNA for bovine corticotropin-beta-lipotropin precursor. Nature. 1979;278(5703):423-7.

119. Chretien M, Benjannet S, Gossard F, Gianoulakis C, Crine P, Lis M, et al. From beta-lipotropin to beta-endorphin and 'pro-opio-melanocortin'. Can J Biochem. 1979;57(9):1111-21.

120. Lazure C, Seidah NG, Pélaprat D, Chrétien M. Proteases and posttranslational processing of prohormones: a review. Biochem Cell Biol. 1983;61(7):501-15.

121. Puente XS, Sanchez LM, Overall CM, Lopez-Otin C. Human and mouse proteases: a comparative genomic approach. Nat Rev Genet. 2003;4(7):544-58.

122. Davidson HW, Peshavaria M, Hutton JC. Proteolytic conversion of proinsulin into insulin. Identification of a Ca2+-dependent acidic endopeptidase in isolated insulin-secretory granules. Biochem J. 1987;246(2):279-86.

123. Mizuno K, Matsuo H. A novel protease from yeast with specificity towards paired basic residues. Nature. 1984;309(5968):558-60.

124. Fuller RS, Brake A, Thorner J. Yeast prohormone processing enzyme (KEX2 gene product) is a Ca2+-dependent serine protease. Proc Natl Acad Sci U S A. 1989;86(5):1434-8.

125. Thomas G, Thorne BA, Thomas L, Allen RG, Hruby DE, Fuller R, et al. Yeast KEX2 endopeptidase correctly cleaves a neuroendocrine prohormone in mammalian cells. Science. 1988;241(4862):226-30.

126. Siezen RJ, Leunissen JA. Subtilases: the superfamily of subtilisin-like serine proteases. Protein Sci. 1997;6(3):501-23.

127. Fuller RS, Brake AJ, Thorner J. Intracellular targeting and structural conservation of a prohormone-processing endoprotease. Science. 1989;246(4929):482-6.

128. Smeekens SP, Steiner DF. Identification of a human insulinoma cDNA encoding a novel mammalian protein structurally related to the yeast dibasic processing protease Kex2. J Biol Chem. 1990;265(6):2997-3000.

129. Seidah NG, Gaspar L, Mion P, Marcinkiewicz M, Mbikay M, Chretien M. cDNA sequence of two distinct pituitary proteins homologous to Kex2 and furin gene products: tissue-specific mRNAs encoding candidates for pro-hormone processing proteinases. DNA Cell Biol. 1990;9(6):415-24.

130. Smeekens SP, Avruch AS, LaMendola J, Chan SJ, Steiner DF. Identification of a cDNA encoding a second putative prohormone convertase related to PC2 in AtT20 cells and islets of Langerhans. Proc Natl Acad Sci USA. 1991;88(2):340-4.

131. Seidah NG. What lies ahead for the proprotein convertases? Ann N Y Acad Sci. 2011;1220:149-61.

132. Seidah NG, Prat A. The biology and therapeutic targeting of the proprotein convertases. Nat Rev Drug Discov. 2012;11(5):367-83.

133. Seidah NG, Sadr MS, Chretien M, Mbikay M. The multifaceted proprotein convertases: their unique, redundant, complementary, and opposite functions. J Biol Chem. 2013;288(30):21473-81.

134. Seidah NG GJ. Posttranslational processing of secretory proteins. Molecular Neuroendocrinology: From Genome to Physiology. 2016:171–94.

135. Seidah NG, Abifadel M, Prost S, Boileau C, Prat A. The Proprotein Convertases in Hypercholesterolemia and Cardiovascular Diseases: Emphasis on Proprotein Convertase Subtilisin/Kexin 9. Pharmacol Rev. 2017;69(1):33-52.

136. Scamuffa N, Calvo F, Chretien M, Seidah NG, Khatib AM. Proprotein convertases: lessons from knockouts. FASEB J. 2006;20(12):1954-63.

137. Creemers JW, Khatib AM. Knock-out mouse models of proprotein convertases: unique functions or redundancy? Front Biosci. 2008;13:4960-71.

138. Zhou A, Martin S, Lipkind G, LaMendola J, Steiner DF. Regulatory roles of the P domain of the subtilisin-like prohormone convertases. J Biol Chem. 1998;273(18):11107-14.

139. Marcinkiewicz M, Day R, Seidah NG, Chrétien M. Ontogeny of the prohormone convertases PC1 and PC2 in the mouse hypophysis and their colocalization with corticotropin and alpha-melanotropin. Proc Natl Acad Sci U S A. 1993;90(11):4922-6.

140. Steiner DF. The proprotein convertases. Curr Opin Chem Biol. 1998;2(1):31-9.

141. Zhu X, Zhou A, Dey A, Norrbom C, Carroll R, Zhang C, et al. Disruption of PC1/3 expression in mice causes dwarfism and multiple neuroendocrine peptide processing defects. Proc Natl Acad Sci U S A. 2002;99(16):10293-8.

142. Furuta M, Yano H, Zhou A, Rouille Y, Holst JJ, Carroll R, et al. Defective prohormone processing and altered pancreatic islet morphology in mice lacking active SPC2. Proc Natl Acad Sci U S A. 1997;94(13):6646-51.

143. Nakayama K, Kim WS, Torii S, Hosaka M, Nakagawa T, Ikemizu J, et al. Identification of the fourth member of the mammalian endoprotease family homologous to the yeast Kex2 protease. Its testis-specific expression. J Biol Chem. 1992;267(9):5897-900.

144. Seidah NG, Day R, Hamelin J, Gaspar A, Collard MW, Chretien M. Testicular expression of PC4 in the rat: molecular diversity of a novel germ cell-specific Kex2/subtilisin-like proprotein convertase. Mol Endocrinol. 1992;6(10):1559-70.

145. Mbikay M, Tadros H, Ishida N, Lerner CP, De Lamirande E, Chen A, et al. Impaired fertility in mice deficient for the testicular germ-cell protease PC4. Proc Natl Acad Sci U S A. 1997;94(13):6842-6.

146. Gyamera-Acheampong C, Tantibhedhyangkul J, Weerachatyanukul W, Tadros H, Xu H, Loo J-Wvd, et al. Sperm from Mice Genetically Deficient for the PCSK4 Proteinase Exhibit Accelerated Capacitation, Precocious Acrosome Reaction, Reduced Binding to Egg Zona Pellucida, and Impaired Fertilizing Ability1. Biol Reprod. 2006;74(4):666-73.

147. Seidah NG, Mayer G, Zaid A, Rousselet E, Nassoury N, Poirier S, et al. The activation and physiological functions of the proprotein convertases. Int J Biochem Cell Biol. 2008;40(6-7):1111-25.

148. Roebroek AJ, Umans L, Pauli IG, Robertson EJ, van Leuven F, Van de Ven WJ, et al. Failure of ventral closure and axial rotation in embryos lacking the proprotein convertase Furin. Development. 1998;125(24):4863-76.

149. Constam DB, Robertson EJ. Tissue-specific requirements for the proprotein convertase furin/SPC1 during embryonic turning and heart looping. Development. 2000;127(2):245-54.

150. Essalmani R, Zaid A, Marcinkiewicz J, Chamberland A, Pasquato A, Seidah NG, et al. In vivo functions of the proprotein convertase PC5/6 during mouse development: Gdf11 is a likely substrate. Proc Natl Acad Sci USA. 2008;105(15):5750-5.

151. Constam DB, Robertson EJ. SPC4/PACE4 regulates a TGFbeta signaling network during axis formation. Genes Dev. 2000;14(9):1146-55.

152. Li JP, Wang XB, Chen CZ, Xu X, Hong XM, Xu XP, et al. The association between paired basic amino acid cleaving enzyme 4 gene haplotype and diastolic blood pressure. Chin Med J. 2004;117(3):382-8.

153. Seidah NG, Hamelin J, Mamarbachi M, Dong W, Tardos H, Mbikay M, et al. cDNA structure, tissue distribution, and chromosomal localization of rat PC7, a novel mammalian proprotein convertase closest to yeast kexin-like proteinases. Proc Natl Acad Sci U S A. 1996;93(8):3388-93.

154. Wetsel WC, Rodriguiz RM, Guillemot J, Rousselet E, Essalmani R, Kim IH, et al. Disruption of the expression of the proprotein convertase PC7 reduces BDNF production and affects learning and memory in mice. Proc Natl Acad Sci U S A. 2013;110(43):17362-7.

155. Guillemot J, Canuel M, Essalmani R, Prat A, Seidah NG. Implication of the proprotein convertases in iron homeostasis: proprotein convertase 7 sheds human transferrin receptor 1 and furin activates hepcidin. Hepatology. 2013;57(6):2514-24.

156. Huang T, Huang J, Qi Q, Li Y, Bray GA, Rood J, et al. PCSK7 genotype modifies effect of a weight-loss diet on 2-year changes of insulin resistance: the POUNDS LOST trial. Diabetes care. 2015;38(3):439-44.

157. Kurano M, Tsukamoto K, Kamitsuji S, Kamatani N, Hara M, Ishikawa T, et al. Genome-wide association study of serum lipids confirms previously reported associations as well as new associations of common SNPs within PCSK7 gene with triglyceride. J Hum Genet. 2016;61(5):427-33.

158. Gombojav B, Lee SJ, Kho M, Song YM, Lee K, Sung J. Multiple susceptibility loci at chromosome 11q23.3 are associated with plasma triglyceride in East Asians. J Lipid Res. 2016;57(2):318-24.

159. Stickel F, Buch S, Zoller H, Hultcrantz R, Gallati S, Osterreicher C, et al. Evaluation of genome-wide loci of iron metabolism in hereditary hemochromatosis identifies PCSK7 as a host risk factor of liver cirrhosis. Hum Mol Gen. 2014;23(14):3883-90.

160. Peloso GM, Auer PL, Bis JC, Voorman A, Morrison AC, Stitziel NO, et al. Association of low-frequency and rare coding-sequence variants with blood lipids and coronary heart disease in 56,000 whites and blacks. Am J Hum Genet. 2014;94(2):223-32.

161. Cheng D, Espenshade PJ, Slaughter CA, Jaen JC, Brown MS, Goldstein JL. Secreted site-1 protease cleaves peptides corresponding to luminal loop of sterol regulatory element-binding proteins. J Biol Chem. 1999;274(32):22805-12.

162. Espenshade PJ, Cheng D, Goldstein JL, Brown MS. Autocatalytic processing of site-1 protease removes propeptide and permits cleavage of sterol regulatory element-binding proteins. J Biol Chem. 1999;274(32):22795-804.

163. Yang J, Goldstein JL, Hammer RE, Moon YA, Brown MS, Horton JD. Decreased lipid synthesis in livers of mice with disrupted Site-1 protease gene. Proc Natl Acad Sci U S A. 2001;98(24):13607-12.

164. Sanchez AJ, Vincent MJ, Nichol ST. Characterization of the glycoproteins of Crimean-Congo hemorrhagic fever virus. J Virol. 2002;76(14):7263-75.

165. Varret M, Rabes JP, Saint-Jore B, Cenarro A, Marinoni JC, Civeira F, et al. A third major locus for autosomal dominant hypercholesterolemia maps to 1p34.1-p32. Am J Hum Genet. 1999;64(5):1378-87.

166. Hunt SC, Hopkins PN, Bulka K, McDermott MT, Thorne TL, Wardell BB, et al. Genetic localization to chromosome 1p32 of the third locus for familial hypercholesterolemia in a Utah kindred. Arterioscler Thromb Vasc Biol. 2000;20(4):1089-93.

167. Maxwell KN, Soccio RE, Duncan EM, Sehayek E, Breslow JL. Novel putative SREBP and LXR target genes identified by microarray analysis in liver of cholesterol-fed mice. J Lipid Res. 2003;44(11):2109-19.

168. Benjannet S, Rhainds D, Essalmani R, Mayne J, Wickham L, Jin W, et al. NARC-1/PCSK9 and its natural mutants: zymogen cleavage and effects on the low density lipoprotein (LDL) receptor and LDL cholesterol. J Biol Chem. 2004;279(47):48865-75.

169. Maxwell KN, Breslow JL. Adenoviral-mediated expression of Pcsk9 in mice results in a low-density lipoprotein receptor knockout phenotype. Proc Natl Acad Sci USA. 2004;101(18):7100-5.

170. Park SW, Moon YA, Horton JD. Post-transcriptional regulation of low density lipoprotein receptor protein by proprotein convertase subtilisin/kexin type 9a in mouse liver. J Biol Chem. 2004;279(48):50630-8.

171. Rashid S, Curtis DE, Garuti R, Anderson NN, Bashmakov Y, Ho YK, et al. Decreased plasma cholesterol and hypersensitivity to statins in mice lacking Pcsk9. Proc Natl Acad Sci U S A. 2005;102(15):5374-9.

172. Zaid A, Roubtsova A, Essalmani R, Marcinkiewicz J, Chamberland A, Hamelin J, et al. Proprotein convertase subtilisin/kexin type 9 (PCSK9): hepatocyte-specific low-density lipoprotein receptor degradation and critical role in mouse liver regeneration. Hepatology. 2008;48(2):646-54.

173. Cunningham D, Danley DE, Geoghegan KF, Griffor MC, Hawkins JL, Subashi TA, et al. Structural and biophysical studies of PCSK9 and its mutants linked to familial hypercholesterolemia. Nat Struct Mol Biol. 2007;14(5):413-9.

174. Seidah NG, Awan Z, Chretien M, Mbikay M. PCSK9: a key modulator of cardiovascular health. Circ Res. 2014;114(6):1022-36.

175. Naureckiene S, Ma L, Sreekumar K, Purandare U, Lo CF, Huang Y, et al. Functional characterization of Narc 1, a novel proteinase related to proteinase K. Arch Biochem Biophys. 2003;420(1):55-67.

176. Benjannet S, Hamelin J, Chretien M, Seidah NG. Loss- and gain-of-function PCSK9 variants: cleavage specificity, dominant negative effects, and low density lipoprotein receptor (LDLR) degradation. J Biol Chem. 2012;287(40):33745-55.

177. Zhang DW, Lagace TA, Garuti R, Zhao Z, McDonald M, Horton JD, et al. Binding of proprotein convertase subtilisin/kexin type 9 to epidermal growth factor-like repeat A of low density lipoprotein receptor decreases receptor recycling and increases degradation. J Biol Chem. 2007;282(25):18602-12.

178. Lo Surdo P, Bottomley MJ, Calzetta A, Settembre EC, Cirillo A, Pandit S, et al. Mechanistic implications for LDL receptor degradation from the PCSK9/LDLR structure at neutral pH. EMBO Rep. 2011;12(12):1300-5.

179. Zhang DW, Garuti R, Tang WJ, Cohen JC, Hobbs HH. Structural requirements for PCSK9-mediated degradation of the low-density lipoprotein receptor. Proc Natl Acad Sci U S A. 2008;105(35):13045-50.

180. Saavedra YG, Day R, Seidah NG. The M2 module of the Cys-His-rich domain (CHRD) of PCSK9 protein is needed for the extracellular low-density lipoprotein receptor (LDLR) degradation pathway. J Biol Chem. 2012;287(52):43492-501.

181. Abifadel M, Guerin M, Benjannet S, Rabes JP, Le Goff W, Julia Z, et al. Identification and characterization of new gain-of-function mutations in the PCSK9 gene responsible for autosomal dominant hypercholesterolemia. Atherosclerosis. 2012;223(2):394-400.

182. Kosenko T, Golder M, Leblond G, Weng W, Lagace TA. Low density lipoprotein binds to proprotein convertase subtilisin/kexin type-9 (PCSK9) in human plasma and inhibits PCSK9-mediated low density lipoprotein receptor degradation. J Biol Chem. 2013;288(12):8279-88.

183. Kwon HJ, Lagace TA, McNutt MC, Horton JD, Deisenhofer J. Molecular basis for LDL receptor recognition by PCSK9. Proc Natl Acad Sci U S A. 2008;105(6):1820-5.

184. Nassoury N, Blasiole DA, Tebon Oler A, Benjannet S, Hamelin J, Poupon V, et al. The cellular trafficking of the secretory proprotein convertase PCSK9 and its dependence on the LDLR. Traffic. 2007;8(6):718-32.

185. Holla OL, Cameron J, Berge KE, Ranheim T, Leren TP. Degradation of the LDL receptors by PCSK9 is not mediated by a secreted protein acted upon by PCSK9 extracellularly. BMC Cell Biol. 2007;8:9.

186. Poirier S, Mayer G, Poupon V, McPherson PS, Desjardins R, Ly K, et al. Dissection of the endogenous cellular pathways of PCSK9-induced low density lipoprotein receptor degradation: evidence for an intracellular route. J Biol Chem. 2009;284(42):28856-64.

187. Ni YG, Condra JH, Orsatti L, Shen X, Di Marco S, Pandit S, et al. A proprotein convertase subtilisin-like/kexin type 9 (PCSK9) C-terminal domain antibody antigen-binding fragment inhibits PCSK9 internalization and restores low density lipoprotein uptake. J Biol Chem. 2010;285(17):12882-91.

188. Schiele F, Park J, Redemann N, Luippold G, Nar H. An antibody against the C-terminal domain of PCSK9 lowers LDL cholesterol levels in vivo. J Mol Biol. 2014;426(4):843-52.

189. Chan JC, Piper DE, Cao Q, Liu D, King C, Wang W, et al. A proprotein convertase subtilisin/kexin type 9 neutralizing antibody reduces serum cholesterol in mice and nonhuman primates. Proc Natl Acad Sci U S A. 2009;106(24):9820-5.

190. Butkinaree C, Canuel M, Essalmani R, Poirier S, Benjannet S, Asselin MC, et al. Amyloid Precursor-like Protein 2 and Sortilin Do Not Regulate the PCSK9 Convertase-mediated Low Density Lipoprotein Receptor Degradation but Interact with Each Other. J Biol Chem. 2015;290(30):18609-20.

191. Gauthier MS, Perusse JR, Awan Z, Bouchard A, Tessier S, Champagne J, et al. A semi-automated mass spectrometric immunoassay coupled to selected reaction monitoring (MSIA-SRM) reveals novel relationships between circulating PCSK9 and metabolic phenotypes in patient cohorts. Methods. 2015;81:66-73.

192. Tagliabracci VS, Wiley SE, Guo X, Kinch LN, Durrant E, Wen J, et al. A Single Kinase Generates the Majority of the Secreted Phosphoproteome. Cell. 2015;161(7):1619-32.

193. Yamamoto T, Lu C, Ryan RO. A two-step binding model of PCSK9 interaction with the low density lipoprotein receptor. J Biol Chem. 2011;286(7):5464-70.

194. Canuel M, Sun X, Asselin MC, Paramithiotis E, Prat A, Seidah NG. Proprotein convertase subtilisin/kexin type 9 (PCSK9) can mediate degradation of the low density lipoprotein receptor-related protein 1 (LRP-1). PLoS One. 2013;8(5):e64145.

195. Holla OL, Strom TB, Cameron J, Berge KE, Leren TP. A chimeric LDL receptor containing the cytoplasmic domain of the transferrin receptor is degraded by PCSK9. Mol Genet Metab. 2010;99(2):149-56.

196. Gustafsen C, Kjolby M, Nyegaard M, Mattheisen M, Lundhede J, Buttenschon H, et al. The hypercholesterolemia-risk gene SORT1 facilitates PCSK9 secretion. Cell Metab. 2014;19(2):310-8.

197. DeVay RM, Shelton DL, Liang H. Characterization of proprotein convertase subtilisin/kexin type 9 (PCSK9) trafficking reveals a novel lysosomal targeting mechanism via amyloid precursor-like protein 2 (APLP2). J Biol Chem. 2013;288(15):10805-18.

198. Chen XW, Wang H, Bajaj K, Zhang P, Meng ZX, Ma D, et al. SEC24A deficiency lowers plasma cholesterol through reduced PCSK9 secretion. Elife. 2013;2:e00444.

199. Poirier S, Mamarbachi M, Chen WT, Lee AS, Mayer G. GRP94 Regulates Circulating Cholesterol Levels through Blockade of PCSK9-Induced LDLR Degradation. Cell Rep. 2015;13(10):2064-71.

200. Timms KM, Wagner S, Samuels ME, Forbey K, Goldfine H, Jammulapati S, et al. A mutation in PCSK9 causing autosomal-dominant hypercholesterolemia in a Utah pedigree. Hum Genet. 2004;114(4):349-53.

201. Leren TP. Mutations in the PCSK9 gene in Norwegian subjects with autosomal dominant hypercholesterolemia. Clin Genet. 2004;65:419-22.

202. Abifadel M, Elbitar S, El Khoury P, Ghaleb Y, Chemaly M, Moussalli ML, et al. Living the PCSK9 adventure: from the identification of a new gene in familial hypercholesterolemia towards a potential new class of anticholesterol drugs. Curr Atheroscler Rep. 2014;16(9):439.

203. Abifadel M, Rabes JP, Devillers M, Munnich A, Erlich D, Junien C, et al. Mutations and polymorphisms in the proprotein convertase subtilisin kexin 9 (PCSK9) gene in cholesterol metabolism and disease. Hum Mutat. 2009;30(4):520-9.

204. Hopkins PN, Defesche J, Fouchier SW, Bruckert E, Luc G, Cariou B, et al. Characterization of Autosomal Dominant Hypercholesterolemia Caused by PCSK9 Gain of Function Mutations and Its Specific Treatment With Alirocumab, a PCSK9 Monoclonal Antibody. Circ Cardiovasc Genet. 2015;8(6):823-31.

205. Awan Z, Baass A, Genest J. Proprotein convertase subtilisin/kexin type 9 (PCSK9): lessons learned from patients with hypercholesterolemia. Clin Chem. 2014;60(11):1380-9.

206. Cohen J, Pertsemlidis A, Kotowski IK, Graham R, Garcia CK, Hobbs HH. Low LDL cholesterol in individuals of African descent resulting from frequent nonsense mutations in PCSK9. Nat Genet. 2005;37(2):161-5.

207. Cohen JC. Sequence variations in PCSK9, low LDL, and protection against coronary heart disease. N Engl J Med. 2006;354:1264-72.

208. Zhao Z, Tuakli-Wosornu Y, Lagace TA, Kinch L, Grishin NV, Horton JD, et al. Molecular characterization of loss-of-function mutations in PCSK9 and identification of a compound heterozygote. Am J Hum Genet. 2006;79(3):514-23.

209. Kotowski IK. A spectrum of PCSK9 alleles contributes to plasma levels of low-density lipoprotein cholesterol. Am J Hum Genet. 2006;78:410-22.

210. Verbeek R, Boyer M, Boekholdt SM, Hovingh GK, Kastelein JJ, Wareham N, et al. Carriers of the PCSK9 R46L Variant Are Characterized by an Antiatherogenic Lipoprotein Profile Assessed by Nuclear Magnetic Resonance Spectroscopy-Brief Report. Arterioscler Thromb Vasc Biol. 2017;37(1):43-8.

211. Saavedra YG, Dufour R, Davignon J, Baass A. PCSK9 R46L, lower LDL, and cardiovascular disease risk in familial hypercholesterolemia: a cross-sectional cohort study. Arterioscler Thromb Vasc Biol. 2014;34(12):2700-5.

212. Scartezini M, Hubbart C, Whittall RA, Cooper JA, Neil AH, Humphries SE. The PCSK9 gene R46L variant is associated with lower plasma lipid levels and cardiovascular risk in healthy U.K. men. Clin Sci. 2007;113(11):435-41.

213. Awan Z, Delvin EE, Levy E, Genest J, Davignon J, Seidah NG, et al. Regional distribution and metabolic effect of PCSK9 insLEU and R46L gene mutations and apoE genotype. Can J Cardiol. 2013;29(8):927-33.

214. Hooper AJ, Marais AD, Tanyanyiwa DM, Burnett JR. The C679X mutation in PCSK9 is present and lowers blood cholesterol in a Southern African population. Atherosclerosis. 2007;193(2):445-8.

215. Cariou B, Ouguerram K, Zair Y, Guerois R, Langhi C, Kourimate S, et al. PCSK9 dominant negative mutant results in increased LDL catabolic rate and familial hypobetalipoproteinemia. Arterioscler Thromb Vasc Biol. 2009;29.

216. Mayne J, Dewpura T, Raymond A, Bernier L, Cousins M, Ooi TC, et al. Novel loss-of-function PCSK9 variant is associated with low plasma LDL cholesterol in a French-Canadian family and with impaired processing and secretion in cell culture. Clin Chem. 2011;57(10):1415-23.

217. Lambert G, Krempf M, Costet P. PCSK9: a promising therapeutic target for dyslipidemias? Trends Endocrinol Metab : TEM. 2006;17(3):79-81.

218. Seidah NG, Prat A. The proprotein convertases are potential targets in the treatment of dyslipidemia. J Mol Med (Berlin, Germany). 2007;85(7):685-96.

219. Lakoski SG, Lagace TA, Cohen JC, Horton JD, Hobbs HH. Genetic and metabolic determinants of plasma PCSK9 levels. J Clin Endocrinol Metab. 2009;94(7):2537-43.

220. Baass A, Dubuc G, Tremblay M, Delvin EE, O'Loughlin J, Levy E, et al. Plasma PCSK9 is associated with age, sex, and multiple metabolic markers in a population-based sample of children and adolescents. Clin Chem. 2009;55.

221. Persson L, Cao G, Ståhle L, Sjöberg BG, Troutt JS, Konrad RJ, et al. Circulating Proprotein Convertase Subtilisin Kexin Type 9 Has a Diurnal Rhythm Synchronous With Cholesterol Synthesis and Is Reduced by Fasting in Humans. Arterioscler Thromb Vasc Biol. 2010;30(12):2666-72.

222. Persson L, Cao G, Stahle L, Sjoberg B, Troutt JS, Konrad RJ, et al. Circulating proprotein convertase subtilisin kexin type 9 has a diurnal rhythm synchronous with cholesterol synthesis and is reduced by fasting in humans. Arterioscler Thromb Vasc Biol. 2010;30.

223. Sun H, Samarghandi A, Zhang N, Yao Z, Xiong M, Teng BB. Proprotein convertase subtilisin/kexin type 9 interacts with apolipoprotein B and prevents its intracellular degradation, irrespective of the low-density lipoprotein receptor. Arterioscler Thromb Vasc Biol. 2012;32(7):1585-95.

224. Tavori H, Christian D, Minnier J, Plubell D, Shapiro MD, Yeang C, et al. PCSK9 Association With Lipoprotein(a). Circ Res. 2016;119(1):29-35.

225. Nekaies Y, Baudin B, Kelbousi S, Sakly M, Attia N. Plasma proprotein convertase subtilisin/kexin type 9 is associated with Lp(a) in type 2 diabetic patients. J Diabetes Complications. 2015;29(8):1165-70.

226. Romagnuolo R, Scipione CA, Boffa MB, Marcovina SM, Seidah NG, Koschinsky ML. Lipoprotein(a) catabolism is regulated by proprotein convertase subtilisin/kexin type 9 through the low density lipoprotein receptor. J Biol Chem. 2015;290(18):11649-62.

227. Mayer G, Poirier S, Seidah NG. Annexin A2 is a C-terminal PCSK9-binding protein that regulates endogenous low density lipoprotein receptor levels. J Biol Chem. 2008;283(46):31791-801.

228. Ly K, Saavedra YG, Canuel M, Routhier S, Desjardins R, Hamelin J, et al. Annexin A2 reduces PCSK9 protein levels via a translational mechanism and interacts with the M1 and M2 domains of PCSK9. J Biol Chem. 2014;289(25):17732-46.

229. Seidah NG, Poirier S, Denis M, Parker R, Miao B, Mapelli C, et al. Annexin A2 is a natural extrahepatic inhibitor of the PCSK9-induced LDL receptor degradation. PLoS One. 2012;7(7):e41865.

230. Fairoozy RH, Cooper J, White J, Giambartolomei C, Folkersen L, Wannamethee SG, et al. Identifying low density lipoprotein cholesterol associated variants in the Annexin A2 (ANXA2) gene. Atherosclerosis. 2017;261:60-8.

231. Parker RA, Garcia R, Ryan CS, Liu X, Shipkova P, Livanov V, et al. Bile acid and sterol metabolism with combined HMG-CoA reductase and PCSK9 suppression. J Lipid Res. 2013;54(9):2400-9.

232. Langhi C, Le May C, Gmyr V, Vandewalle B, Kerr-Conte J, Krempf M, et al. PCSK9 is expressed in pancreatic delta-cells and does not alter insulin secretion. Biochem Biophys Res Commun. 2009;390(4):1288-93.

233. Le May C, Berger JM, Lespine A, Pillot B, Prieur X, Letessier E, et al. Transintestinal cholesterol excretion is an active metabolic process modulated by PCSK9 and statin involving ABCB1. Arterioscler Thromb Vasc Biol. 2013;33(7):1484-93.

234. Roubtsova A, Chamberland A, Marcinkiewicz J, Essalmani R, Fazel A, Bergeron JJ, et al. PCSK9 deficiency unmasks a sex- and tissue-specific subcellular distribution of the LDL and VLDL receptors in mice. J Lipid Res. 2015;56(11):2133-42.

235. Robinson JG, Farnier M, Krempf M, Bergeron J, Luc G, Averna M, et al. Efficacy and Safety of Alirocumab in Reducing Lipids and Cardiovascular Events. N Engl J Med. 2015;372(16):1489-99.

236. Lagace TA, Curtis DE, Garuti R, McNutt MC, Park SW, Prather HB, et al. Secreted PCSK9 decreases the number of LDL receptors in hepatocytes and in livers of parabiotic mice. J Clin Invest. 2006;116(11):2995-3005.

237. Grefhorst A, McNutt MC, Lagace TA, Horton JD. Plasma PCSK9 preferentially reduces liver LDL receptors in mice. J Lipid Res. 2008;49(6):1303-11.

238. Roubtsova A, Munkonda MN, Awan Z, Marcinkiewicz J, Chamberland A, Lazure C, et al. Circulating proprotein convertase subtilisin/kexin 9 (PCSK9) regulates VLDLR protein and triglyceride accumulation in visceral adipose tissue. Arterioscler Thromb Vasc Biol. 2011;31(4):785-91.

239. Tavori H, Fan D, Blakemore JL, Yancey PG, Ding L, Linton MF, et al. Serum proprotein convertase subtilisin/kexin type 9 and cell surface low-density lipoprotein receptor: evidence for a reciprocal regulation. Circulation. 2013;127(24):2403-13.

240. Hogarth CA, Roy A, Ebert DL. Genomic evidence for the absence of a functional cholesteryl ester transfer protein gene in mice and rats. Comp Biochem Physiol B Biochem Mol Biol. 2003;135(2):219-29.

241. Yin W, Carballo-Jane E, McLaren DG, Mendoza VH, Gagen K, Geoghagen NS, et al. Plasma lipid profiling across species for the identification of optimal animal models of human dyslipidemia. J Lipid Res. 2012;53(1):51-65.

242. Al-Mashhadi RH, Sorensen CB, Kragh PM, Christoffersen C, Mortensen MB, Tolbod LP, et al. Familial hypercholesterolemia and atherosclerosis in cloned minipigs created by DNA transposition of a human PCSK9 gain-of-function mutant. Sci Transl Med. 2013;5(166):166ra1.

243. Roche-Molina M, Sanz-Rosa D, Cruz FM, Garcia-Prieto J, Lopez S, Abia R, et al. Induction of sustained hypercholesterolemia by single adeno-associated virus-mediated gene transfer of mutant hPCSK9. Arterioscler Thromb Vasc Biol. 2015;35(1):50-9.

244. Sirois F, Chretien M, Mbikay M. Comparing expression and activity of PCSK9 in SPRET/EiJ and C57BL/6J mouse strains shows lack of correlation with plasma cholesterol. Mol Genet Metab Rep. 2017;10:11-7.

245. Luo Y, Warren L, Xia D, Jensen H, Sand T, Petras S, et al. Function and distribution of circulating human PCSK9 expressed extrahepatically in transgenic mice. J Lipid Res. 2009;50(8):1581-8.

246. Herbert B, Patel D, Waddington SN, Eden ER, McAleenan A, Sun XM, et al. Increased secretion of lipoproteins in transgenic mice expressing human D374Y PCSK9 under physiological genetic control. Arterioscler Thromb Vasc Biol. 2010;30(7):1333-9.

247. Norata GD, Tavori H, Pirillo A, Fazio S, Catapano AL. Biology of proprotein convertase subtilisin kexin 9: beyond low-density lipoprotein cholesterol lowering. Cardiovasc Res. 2016;112(1):429-42.

248. Cariou B, Si-Tayeb K, Le May C. Role of PCSK9 beyond liver involvement. Curr Opin Lipidol. 2015;26(3):155-61.

249. Leblond F, Seidah NG, Precourt LP, Delvin E, Dominguez M, Levy E. Regulation of the proprotein convertase subtilisin/kexin type 9 in intestinal epithelial cells. Am J Physiol Gastrointest Liver. 2009;296(4):G805-15.

250. Levy E, Ben Djoudi Ouadda A, Spahis S, Sane AT, Garofalo C, Grenier E, et al. PCSK9 plays a significant role in cholesterol homeostasis and lipid transport in intestinal epithelial cells. Atherosclerosis. 2013;227(2):297-306.

251. Le May C, Kourimate S, Langhi C, Chetiveaux M, Jarry A, Comera C, et al. Proprotein convertase subtilisin kexin type 9 null mice are protected from postprandial triglyceridemia. Arterioscler Thromb Vasc Biol. 2009;29(5):684-90.

252. Rashid S, Tavori H, Brown PE, Linton MF, He J, Giunzioni I, et al. Proprotein convertase subtilisin kexin type 9 promotes intestinal overproduction of triglyceride-rich apolipoprotein B lipoproteins through both low-density lipoprotein receptor-dependent and -independent mechanisms. Circulation. 2014;130(5):431-41.

253. Mbikay M, Sirois F, Mayne J, Wang GS, Chen A, Dewpura T, et al. PCSK9-deficient mice exhibit impaired glucose tolerance and pancreatic islet abnormalities. FEBS Lett. 2010;584(4):701-6.

254. Schmidt RJ, Beyer TP, Bensch WR, Qian YW, Lin A, Kowala M, et al. Secreted proprotein convertase subtilisin/kexin type 9 reduces both hepatic and extrahepatic low-density lipoprotein receptors in vivo. Biochem Biophys Res Commun. 2008;370(4):634-40.

255. Soundararajan R, Pearce D, Hughey RP, Kleyman TR. Role of epithelial sodium channels and their regulators in hypertension. J Biol Chem. 2010;285(40):30363-9.

256. Sharotri V, Collier DM, Olson DR, Zhou R, Snyder PM. Regulation of epithelial sodium channel trafficking by proprotein convertase subtilisin/kexin type 9 (PCSK9). J Biol Chem. 2012;287(23):19266-74.

257. Berger JM, Vaillant N, Le May C, Calderon C, Bregeon J, Prieur X, et al. PCSK9-deficiency does not alter blood pressure and sodium balance in mouse models of hypertension. Atherosclerosis. 2015;239(1):252-9.

258. Cohen JC, Boerwinkle E, Mosley TH, Hobbs HH. Sequence variations in PCSK9, low LDL, and protection against coronary heart disease. N Engl J Med. 2006;354.

259. Poirier S, Prat A, Marcinkiewicz E, Paquin J, Chitramuthu BP, Baranowski D, et al. Implication of the proprotein convertase NARC-1/PCSK9 in the development of the nervous system. J Neurochem. 2006;98(3):838-50.

260. Rousselet E, Marcinkiewicz J, Kriz J, Zhou A, Hatten ME, Prat A, et al. PCSK9 reduces the protein levels of the LDL receptor in mouse brain during development and after ischemic stroke. J Lipid Res. 2011;52(7):1383-91.

261. Chen YQ, Troutt JS, Konrad RJ. PCSK9 is present in human cerebrospinal fluid and is maintained at remarkably constant concentrations throughout the course of the day. Lipids. 2014;49(5):445-55.

262. Poirier S, Mayer G, Benjannet S, Bergeron E, Marcinkiewicz J, Nassoury N, et al. The proprotein convertase PCSK9 induces the degradation of low density lipoprotein receptor (LDLR) and its closest family members VLDLR and ApoER2. J Biol Chem. 2008;283(4):2363-72.

263. Kysenius K, Muggalla P, Matlik K, Arumae U, Huttunen HJ. PCSK9 regulates neuronal apoptosis by adjusting ApoER2 levels and signaling. Cell Mol Life Sci : CMLS. 2012;69(11):1903-16.

264. Shan L, Pang L, Zhang R, Murgolo NJ, Lan H, Hedrick JA. PCSK9 binds to multiple receptors and can be functionally inhibited by an EGF-A peptide. Biochem Biophys Res Commun. 2008;375(1):69-73.

265. Haffner SM, Lehto S, Rönnemaa T, Pyörälä K, Laakso M. Mortality from Coronary Heart Disease in Subjects with Type 2 Diabetes and in Nondiabetic Subjects with and without Prior Myocardial Infarction. N Engl J Med. 1998;339(4):229-34.

266. Colhoun HM, Betteridge DJ, Durrington PN, Hitman GA, Neil HA, Livingstone SJ, et al. Primary prevention of cardiovascular disease with atorvastatin in type 2 diabetes in the

Collaborative Atorvastatin Diabetes Study (CARDS): multicentre randomised placebo-controlled trial. Lancet. 2004;364(9435):685-96.

267. Ruscica M, Macchi C, Morlotti B, Sirtori CR, Magni P. Statin therapy and related risk of new-onset type 2 diabetes mellitus. Eur J Intern Med. 2014;25(5):401-6.

268. Brault M, Ray J, Gomez YH, Mantzoros CS, Daskalopoulou SS. Statin treatment and new-onset diabetes: a review of proposed mechanisms. Metabolism. 2014;63(6):735-45.

269. Colbert JD, Stone JA. Statin use and the risk of incident diabetes mellitus: a review of the literature. Can J Cardiol. 2012;28(5):581-9.

270. Momtazi AA, Banach M, Pirro M, Stein EA, Sahebkar A. PCSK9 and diabetes: is there a link? Drug Discov Today. 2017;22(6):883-95.

271. Ferri N, Ruscica M. Proprotein convertase subtilisin/kexin type 9 (PCSK9) and metabolic syndrome: insights on insulin resistance, inflammation, and atherogenic dyslipidemia. Endocrine. 2016;54(3):588-601.

272. Ibarretxe D, Girona J, Plana N, Cabre A, Ferre R, Amigo N, et al. Circulating PCSK9 in patients with type 2 diabetes and related metabolic disorders. Clin Investig Arterioscler en arteriosclerosis : publicacion oficial de la Sociedad Espanola de Arteriosclerosis. 2016;28(2):71-8.

273. Cariou B, Le Bras M, Langhi C, Le May C, Guyomarc'h-Delasalle B, Krempf M, et al. Association between plasma PCSK9 and gamma-glutamyl transferase levels in diabetic patients. Atherosclerosis. 2010;211(2):700-2.

274. Brouwers MC, Troutt JS, van Greevenbroek MM, Ferreira I, Feskens EJ, van der Kallen CJ, et al. Plasma proprotein convertase subtilisin kexin type 9 is not altered in subjects with impaired glucose metabolism and type 2 diabetes mellitus, but its relationship with non-HDL cholesterol and apolipoprotein B may be modified by type 2 diabetes mellitus: The CODAM study. Atherosclerosis. 2011;217(1):263-7.

275. Awan Z, Dubuc G, Faraj M, Dufour R, Seidah NG, Davignon J, et al. The effect of insulin on circulating PCSK9 in postmenopausal obese women. Clin Biochem. 2014;47(12):1033-9.

276. Costet P, Cariou B, Lambert G, Lalanne F, Lardeux B, Jarnoux AL, et al. Hepatic PCSK9 expression is regulated by nutritional status via insulin and sterol regulatory element-binding protein 1c. J Biol Chem. 2006;281(10):6211-8.

277. Cariou B, Langhi C, Le Bras M, Bortolotti M, Lê K-A, Theytaz F, et al. Plasma PCSK9 concentrations during an oral fat load and after short term high-fat, high-fat high-protein and high-fructose diets. Nutr Metab. 2013;10(1):4.

278. Niesen M, Bedi M, Lopez D. Diabetes alters LDL receptor and PCSK9 expression in rat liver. Arch Biochem Biophys. 2008;470(2):111-5.

279. Denis M, Marcinkiewicz J, Zaid A, Gauthier D, Poirier S, Lazure C, et al. Gene inactivation of proprotein convertase subtilisin/kexin type 9 reduces atherosclerosis in mice. Circulation. 2012;125(7):894-901.

280. Tang ZH, Peng J, Ren Z, Yang J, Li TT, Li TH, et al. New role of PCSK9 in atherosclerotic inflammation promotion involving the TLR4/NF-kappaB pathway. Atherosclerosis. 2017;262:113-22.

281. Guella I, Asselta R, Ardissino D, Merlini PA, Peyvandi F, Kathiresan S, et al. Effects of PCSK9 genetic variants on plasma LDL cholesterol levels and risk of premature myocardial infarction in the Italian population. J Lipid Res. 2010;51(11):3342-9.

282. Gaieski DF, Edwards JM, Kallan MJ, Carr BG. Benchmarking the incidence and mortality of severe sepsis in the United States. Crit Care Med. 2013;41(5):1167-74.

283. dos Santos C, Marshall JC. Bridging lipid metabolism and innate host defense. Sci Transl Med. 2014;6(258):258fs41.

284. Walley KR, Thain KR, Russell JA, Reilly MP, Meyer NJ, Ferguson JF, et al. PCSK9 is a critical regulator of the innate immune response and septic shock outcome. Sci Transl Med. 2014;6(258):258ra143.

285. Boyd JH, Fjell CD, Russell JA, Sirounis D, Cirstea MS, Walley KR. Increased Plasma PCSK9 Levels Are Associated with Reduced Endotoxin Clearance and the Development of Acute Organ Failures during Sepsis. J Innate Immun. 2016;8(2):211-20.

286. Dwivedi DJ, Grin PM, Khan M, Prat A, Zhou J, Fox-Robichaud AE, et al. Differential Expression of PCSK9 Modulates Infection, Inflammation, and Coagulation in a Murine Model of Sepsis. Shock. 2016;46(6):672-80.

287. Topchiy E, Cirstea M, Kong HJ, Boyd JH, Wang Y, Russell JA, et al. Lipopolysaccharide Is Cleared from the Circulation by Hepatocytes via the Low Density Lipoprotein Receptor. PLoS One. 2016;11(5):e0155030.

288. Walley KR. Role of lipoproteins and proprotein convertase subtilisin/kexin type 9 in endotoxin clearance in sepsis. Curr Opin Crit Care. 2016;22(5):464-9.

289. Momtazi AA, Banach M, Sahebkar A. PCSK9 inhibitors in sepsis: a new potential indication? Expert Opin Investig Drugs. 2017;26(2):137-9.

290. Berger JM, Loza Valdes A, Gromada J, Anderson N, Horton JD. Inhibition of PCSK9 does not improve lipopolysaccharide-induced mortality in mice. J Lipid Res. 2017;58(8):1661-69.

291. Sun X, Essalmani R, Day R, Khatib AM, Seidah NG, Prat A. Proprotein convertase subtilisin/kexin type 9 deficiency reduces melanoma metastasis in liver. Neoplasia (New York, NY). 2012;14(12):1122-31.

292. Jonas MC, Costantini C, Puglielli L. PCSK9 is required for the disposal of non-acetylated intermediates of the nascent membrane protein BACE1. EMBO Rep. 2008;9(9):916-22.

293. Liu M, Wu G, Baysarowich J, Kavana M, Addona GH, Bierilo KK, et al. PCSK9 is not involved in the degradation of LDL receptors and BACE1 in the adult mouse brain. J Lipid Res. 2010;51(9):2611-8.

294. Benn M, Nordestgaard BG, Frikke-Schmidt R, Tybjaerg-Hansen A. Low LDL cholesterol, PCSK9 and HMGCR genetic variation, and risk of Alzheimer's disease and Parkinson's disease: Mendelian randomisation study. BMJ (Clinical research ed). 2017;357:j1648.

295. Khan AR, Riaz H, Farid T, Bolli R. Neurocognitive Risk With PCSK9 Inhibitors: Need for More Robust Evidence. J Am Coll Cardiol. 2017;69(19):2468-9.

296. Labonte P, Begley S, Guevin C, Asselin MC, Nassoury N, Mayer G, et al. PCSK9 impedes hepatitis C virus infection in vitro and modulates liver CD81 expression. Hepatology. 2009;50(1):17-24.

297. Le QT, Blanchet M, Seidah NG, Labonte P. Plasma Membrane Tetraspanin CD81 Complexes with Proprotein Convertase Subtilisin/Kexin Type 9 (PCSK9) and Low Density Lipoprotein Receptor (LDLR), and Its Levels Are Reduced by PCSK9. J Biol Chem. 2015;290(38):23385-400.

298. Meex SJ, Andreo U, Sparks JD, Fisher EA. Huh-7 or HepG2 cells: which is the better model for studying human apolipoprotein-B100 assembly and secretion? J Lipid Res. 2011;52(1):152-8.

299. Ramanathan A, Gusarova V, Stahl N, Gurnett-Bander A, Kyratsous CA. Alirocumab, a Therapeutic Human Antibody to PCSK9, Does Not Affect CD81 Levels or Hepatitis C Virus Entry and Replication into Hepatocytes. PLoS One. 2016;11(4):e0154498.

300. Bridge SH, Sheridan DA, Felmlee DJ, Crossey MM, Fenwick FI, Lanyon CV, et al. PCSK9, apolipoprotein E and lipoviral particles in chronic hepatitis C genotype 3: evidence for genotype-specific regulation of lipoprotein metabolism. J Hepatol. 2015;62(4):763-70.

301. Jeong HJ, Lee HS, Kim KS, Kim YK, Yoon D, Park SW. Sterol-dependent regulation of proprotein convertase subtilisin/kexin type 9 expression by sterol-regulatory element binding protein-2. J Lipid Res. 2008;49(2):399-409.

302. Lambert G, Jarnoux AL, Pineau T, Pape O, Chetiveaux M, Laboisse C, et al. Fasting induces hyperlipidemia in mice overexpressing PCSK9: lack of modulation of VLDL hepatic output by the LDLr. Endocrinology. 2006;147.

303. Alvarez ML, Khosroheidari M, Eddy E, Done SC. MicroRNA-27a decreases the level and efficiency of the LDL receptor and contributes to the dysregulation of cholesterol homeostasis. Atherosclerosis. 2015;242(2):595-604.

304. Irani S, Pan X, Peck BC, Iqbal J, Sethupathy P, Hussain MM. MicroRNA-30c Mimic Mitigates Hypercholesterolemia and Atherosclerosis in Mice. J Biol Chem. 2016;291(35):18397-409.

305. Benjannet S, Rhainds D, Hamelin J, Nassoury N, Seidah NG. The proprotein convertase (PC) PCSK9 is inactivated by furin and/or PC5/6A: functional consequences of natural mutations and post-translational modifications. J Biol Chem. 2006;281(41):30561-72.

306. Essalmani R, Susan-Resiga D, Chamberland A, Abifadel M, Creemers JW, Boileau C, et al. In vivo evidence that furin from hepatocytes inactivates PCSK9. J Biol Chem. 2011;286(6):4257-63.

307. Han B, Eacho PI, Knierman MD, Troutt JS, Konrad RJ, Yu X, et al. Isolation and characterization of the circulating truncated form of PCSK9. J Lipid Res. 2014;55(7):1505-14.

308. Schroeder KM, Beyer TP, Hansen RJ, Han B, Pickard RT, Wroblewski VJ, et al. Proteolytic cleavage of antigen extends the durability of an anti-PCSK9 monoclonal antibody. J Lipid Res. 2015;56(11):2124-32.

309. Ding K, McDonough SJ, Kullo IJ. Evidence for positive selection in the C-terminal domain of the cholesterol metabolism gene PCSK9 based on phylogenetic analysis in 14 primate species. PLoS One. 2007;2(10):e1098.

310. Cameron J, Holla OL, Berge KE, Kulseth MA, Ranheim T, Leren TP, et al. Investigations on the evolutionary conservation of PCSK9 reveal a functionally important protrusion. FEBS J. 2008;275(16):4121-33.

311. Prufer K, Racimo F, Patterson N, Jay F, Sankararaman S, Sawyer S, et al. The complete genome sequence of a Neanderthal from the Altai Mountains. Nature. 2014;505(7481):43-9.

312. Longuespee R, Couture F, Levesque C, Kwiatkowska A, Desjardins R, Gagnon S, et al. Implications of Proprotein Convertases in Ovarian Cancer Cell Proliferation and Tumor Progression: Insights for PACE4 as a Therapeutic Target. Transl Oncol. 2014;7(3):410-9.

313. Levesque C, Couture F, Kwiatkowska A, Desjardins R, Guerin B, Neugebauer WA, et al. PACE4 inhibitors and their peptidomimetic analogs block prostate cancer tumor progression through quiescence induction, increased apoptosis and impaired neovascularisation. Oncotarget. 2015;6(6):3680-93.

314. Malfait AM, Seymour AB, Gao F, Tortorella MD, Hellio Le Graverand-Gastineau MP, Wood LS, et al. A Role for PACE4 in Osteoarthritis Pain: Evidence from Human Genetic Association and Null Mutant Phenotype. Ann Rheum Dis. 2012;71(6):1042-8.

315. Miller RE, Lu Y, Tortorella MD, Malfait AM. Genetically Engineered Mouse Models Reveal the Importance of Proteases as Drug Targets in Osteoarthritis. Curr Rheumatol Rep. 2013;15(8):350.

316. Hawkins JL, Robbins MD, Warren LC, Xia D, Petras SF, Valentine JJ, et al. Pharmacologic inhibition of site 1 protease activity inhibits sterol regulatory element-binding protein processing and reduces lipogenic enzyme gene expression and lipid synthesis in cultured cells and experimental animals. J Pharm Exp Ther. 2008;326(3):801-8.

317. Pasquato A, Rochat C, Burri DJ, Pasqual G, la Torre JCd, Kunz S. Evaluation of the anti-arenaviral activity of the subtilisin kexin isozyme-1/site-1 protease inhibitor PF-429242. Virology. 2012;423(1):14-22.

318. Pasquato A, Kunz S. Novel drug discovery approaches for treating arenavirus infections. Expert Opin Drug Discov. 2016;11(4):383-93.

319. Blanchet M, Sureau C, Guevin C, Seidah NG, Labonte P. SKI-1/S1P inhibitor PF-429242 impairs the onset of HCV infection. Antiviral Res. 2015;115:94-104.

320. Uchida L, Urata S, Ulanday GEL, Takamatsu Y, Yasuda J, Morita K, et al. Suppressive Effects of the Site 1 Protease (S1P) Inhibitor, PF-429242, on Dengue Virus Propagation. Viruses. 2016;8(2):e46.

321. Gorski JP, Huffman NT, Vallejo J, Brotto L, Chittur SV, Breggia A, et al. Deletion of Mbtps1 (Pcsk8, S1p, Ski-1) Gene in Osteocytes Stimulates Soleus Muscle Regeneration and Increased Size and Contractile Force with Age. J Biol Chem. 2016;291(9):4308-22.

322. Senzer N, Barve M, Kuhn J, Melnyk A, Beitsch P, Lazar M, et al. Phase I Trial of "bi-shRNAi(furin)/GMCSF DNA/Autologous Tumor Cell" Vaccine (FANG) in Advanced Cancer. Mol Ther. 2012;20(3):679-86.

323. Peng M, Watanabe S, Chan KWK, He Q, Zhao Y, Zhang Z, et al. Luteolin restricts dengue virus replication through inhibition of the proprotein convertase furin. Antiviral Res. 2017;143:176-85.

324. Ozden S, Lucas-Hourani M, Ceccaldi PE, Basak A, Valentine M, Benjannet S, et al. Inhibition of Chikungunya virus infection in cultured human muscle cells by furin inhibitors: impairment of the maturation of the E2 surface glycoprotein. J Biol Chem. 2008;283(32):21899-908.

325. Wu C, Song Z, Liu H, Pan J, Jiang H, Liu C, et al. Inhibition of furin results in increased growth, invasiveness and cytokine production of synoviocytes from patients with rheumatoid arthritis. Joint, bone, spine : revue du rhumatisme. 2016;84(4):433-9.

326. Anderson TJ, Grégoire J, Pearson GJ, Barry AR, Couture P, Dawes M, et al. 2016 Canadian Cardiovascular Society Guidelines for the Management of Dyslipidemia for the Prevention of Cardiovascular Disease in the Adult. Can J Cardiol. 2016;32(11):1263-82.

327. Piepoli MF, Hoes AW, Agewall S, Albus C, Brotons C, Catapano AL, et al. 2016 European Guidelines on cardiovascular disease prevention in clinical practice: The Sixth Joint Task Force of the European Society of Cardiology and Other Societies on Cardiovascular Disease Prevention in Clinical Practice (constituted by representatives of 10 societies and by invited experts) Developed with the special contribution of the European Association for Cardiovascular Prevention and Rehabilitation (EACPR). Atherosclerosis. 2016;252:207-74.

328. Stone NJ, Robinson JG, Lichtenstein AH, Bairey Merz CN, Blum CB, Eckel RH, et al. 2013 ACC/AHA Guideline on the Treatment of Blood Cholesterol to Reduce Atherosclerotic Cardiovascular Risk in Adults: A Report of the American College of Cardiology/American Heart Association Task Force on Practice Guidelines. J Am Coll Cardiol. 2014;63(25, Part B):2889-934.

329. Waters DD, Boekholdt SM. An Evidence-Based Guide to Cholesterol-Lowering Guidelines. Can J Cardiol. 2017;33(3):343-9.

330. Grundy SM. Does Dietary Cholesterol Matter? Curr Atheroscler Rep. 2016;18(11):68.

331. Richard C, Couture P, Desroches S, Benjannet S, Seidah NG, Lichtenstein AH, et al. Effect of the Mediterranean diet with and without weight loss on surrogate markers of cholesterol homeostasis in men with the metabolic syndrome. Br J Nutr. 2012;107(5):705-11.

332. Richard C, Couture P, Desroches S, Charest A, Lamarche B. Effect of the Mediterranean diet with and without weight loss on cardiovascular risk factors in men with the metabolic syndrome. Nutr Metab Cardiovasc Dis. 2011;21(9):628-35.

333. Rudkowska I, Jones PJ. Functional foods for the prevention and treatment of cardiovascular diseases: cholesterol and beyond. Expert Rev Cardiovasc Ther. 2007;5(3):477-90.

334. Bjermo H, Iggman D, Kullberg J, Dahlman I, Johansson L, Persson L, et al. Effects of n-6 PUFAs compared with SFAs on liver fat, lipoproteins, and inflammation in abdominal obesity: a randomized controlled trial. Am J Clin Nutr. 2012;95.

335. Sabate J, Fraser GE, Burke K, Knutsen SF, Bennett H, Lindsted KD. Effects of walnuts on serum lipid levels and blood pressure in normal men. N Engl J Med. 1993;328(9):603-7.

336. Mathur S, Devaraj S, Grundy SM, Jialal I. Cocoa products decrease low density lipoprotein oxidative susceptibility but do not affect biomarkers of inflammation in humans. J Nutr. 2002;132(12):3663-7.

337. Browning JD, Horton JD. Fasting reduces plasma proprotein convertase, subtilisin/kexin type 9 and cholesterol biosynthesis in humans. J Lipid Res. 2010;51(11):3359-63.

338. Kraus WE, Houmard JA, Duscha BD, Knetzger KJ, Wharton MB, McCartney JS, et al. Effects of the Amount and Intensity of Exercise on Plasma Lipoproteins. N Engl J Med. 2002;347(19):1483-92.

339. Kamani CH, Gencer B, Montecucco F, Courvoisier D, Vuilleumier N, Meyer P, et al. Stairs instead of elevators at the workplace decreases PCSK9 levels in a healthy population. Eur J Clin Invest. 2015;45(10):1017-24.

340. Gandhi S, Chen S, Hong L, Sun K, Gong E, Li C, et al. Effect of Mobile Health Interventions on the Secondary Prevention of Cardiovascular Disease: Systematic Review and Meta-analysis. Can J Cardiol. 2017;33(2):219-31.

341. Schoeppe S, Alley S, Van Lippevelde W, Bray NA, Williams SL, Duncan MJ, et al. Efficacy of interventions that use apps to improve diet, physical activity and sedentary behaviour: a systematic review. Int J Behav Nutr Phys Act. 2016;13(1):127.

342. Katan MB, Grundy SM, Jones P, Law M, Miettinen T, Paoletti R. Efficacy and safety of plant stanols and sterols in the management of blood cholesterol levels. Mayo Clin Proc. 2003;78(8):965-78.

343. Sanclemente T, Marques-Lopes I, Puzo J, Garcia-Otin AL. Role of naturally-occurring plant sterols on intestinal cholesterol absorption and plasmatic levels. Journal of physiology and biochemistry. 2009;65(1):87-98.

344. Ikeda I, Tanabe Y, Sugano M. Effects of sitosterol and sitostanol on micellar solubility of cholesterol. J Nutr Sci Vitaminol. 1989;35(4):361-9.

345. Heinemann T, Kullak-Ublick GA, Pietruck B, von Bergmann K. Mechanisms of action of plant sterols on inhibition of cholesterol absorption. Eur J Clin Pharmacol. 1991;40(1):S59-S63.

346. Weststrate JA, Ayesh R, Bauer-Plank C, Drewitt PN. Safety evaluation of phytosterol esters. Part 4. Faecal concentrations of bile acids and neutral sterols in healthy normolipidaemic volunteers consuming a controlled diet either with or without a phytosterol ester-enriched margarine. Food Chem Toxicol : an international journal published for the British Industrial Biological Research Association. 1999;37(11):1063-71.

347. Plat J, Mensink RP. Plant stanol and sterol esters in the control of blood cholesterol levels: mechanism and safety aspects. Am J Cardiol. 2005;96(1a):15d-22d.

348. Calpe-Berdiel L, Escola-Gil JC, Blanco-Vaca F. New insights into the molecular actions of plant sterols and stanols in cholesterol metabolism. Atherosclerosis. 2009;203(1):18-31.

349. Jenkins DJ, Kendall CW, Marchie A, Faulkner DA, Wong JM, de Souza R, et al. Effects of a dietary portfolio of cholesterol-lowering foods vs lovastatin on serum lipids and C-reactive protein. J Am Med Assoc. 2003;290(4):502-10.

350. Garcia-Calvo M, Lisnock J, Bull HG, Hawes BE, Burnett DA, Braun MP, et al. The target of ezetimibe is Niemann-Pick C1-Like 1 (NPC1L1). Proc Natl Acad Sci U S A. 2005;102(23):8132-7.

351. Alrefai WA, Annaba F, Sarwar Z, Dwivedi A, Saksena S, Singla A, et al. Modulation of human Niemann-Pick C1-like 1 gene expression by sterol: role of sterol regulatory element binding protein 2. Am J Physiol Gastrointest Liver. 2007;292(1):G369-G76.

352. Davis HR, Jr., Zhu LJ, Hoos LM, Tetzloff G, Maguire M, Liu J, et al. Niemann-Pick C1 Like 1 (NPC1L1) is the intestinal phytosterol and cholesterol transporter and a key modulator of whole-body cholesterol homeostasis. J Biol Chem. 2004;279(32):33586-92.

353. Sudhop T, Lutjohann D, Kodal A, Igel M, Tribble DL, Shah S, et al. Inhibition of intestinal cholesterol absorption by ezetimibe in humans. Circulation. 2002;106(15):1943-8.

354. Dujovne CA, Ettinger MP, McNeer JF, Lipka LJ, LeBeaut AP, Suresh R, et al. Efficacy and safety of a potent new selective cholesterol absorption inhibitor, ezetimibe, in patients with primary hypercholesterolemia. Am J Cardiol. 2002;90(10):1092-7.

355. Investigators TMIGC. Inactivating Mutations in NPC1L1 and Protection from Coronary Heart Disease. N Engl J Med. 2014;371(22):2072-82.

356. Altmann SW, Davis HR, Jr., Yao X, Laverty M, Compton DS, Zhu LJ, et al. The identification of intestinal scavenger receptor class B, type I (SR-BI) by expression cloning and its role in cholesterol absorption. Biochim Biophys Acta. 2002;1580(1):77-93.

357. van Heek M, Farley C, Compton DS, Hoos L, Davis HR. Ezetimibe selectively inhibits intestinal cholesterol absorption in rodents in the presence and absence of exocrine pancreatic function. Br J Pharmacol. 2001;134(2):409-17.

358. Cannon CP, Blazing MA, Giugliano RP, McCagg A, White JA, Theroux P, et al. Ezetimibe Added to Statin Therapy after Acute Coronary Syndromes. N Engl J Med. 2015;372(25):2387-97.

359. Zhang Y, Liu J, Li S, Xu R-X, Sun J, Li J-J. Impact of currently prescribed lipid-lowering drugs on plasma PCSK9 concentration: single or in combination study in rats. Lipids Health Dis. 2014;13(1):35.

360. Jun Liu Y-LG, Rui-Xia Xu, and Jian-Jun Li. Rapid effects of different lipid-lowering drugs on PCSK9 in humans. Clin Lipidol. 2013;8(5):519-24.

361. Birjmohun RS, Hutten BA, Kastelein JJ, Stroes ES. Efficacy and safety of high-density lipoprotein cholesterol-increasing compounds: a meta-analysis of randomized controlled trials. J Am Coll Cardiol. 2005;45(2):185-97.

362. Shepherd J. Mechanism of action of fibrates. Postgrad Med J. 1993;69 Suppl 1:S34-41.

363. Staels B, Dallongeville J, Auwerx J, Schoonjans K, Leitersdorf E, Fruchart JC. Mechanism of action of fibrates on lipid and lipoprotein metabolism. Circulation. 1998;98(19):2088-93.

364. Ginsberg HN, Elam MB, Lovato LC, Crouse JR, 3rd, Leiter LA, Linz P, et al. Effects of combination lipid therapy in type 2 diabetes mellitus. N Engl J Med. 2010;362(17):1563-74.

365. Jun M, Foote C, Lv J, Neal B, Patel A, Nicholls SJ, et al. Effects of fibrates on cardiovascular outcomes: a systematic review and meta-analysis. Lancet.375(9729):1875-84.

366. Mayne J, Dewpura T, Raymond A, Cousins M, Chaplin A, Lahey KA, et al. Plasma PCSK9 levels are significantly modified by statins and fibrates in humans. Lipids Health Dis. 2008;7:22.

367. Alsheikh-Ali AA, Kuvin JT, Karas RH. Risk of adverse events with fibrates. Am J Cardiol. 2004;94(7):935-8.

368. Graham DJ, Staffa JA, Shatin D, Andrade SE, Schech SD, La Grenade L, et al. Incidence of hospitalized rhabdomyolysis in patients treated with lipid-lowering drugs. J Am Med Assoc. 2004;292(21):2585-90.

369. Lu Z, Kou W, Du B, Wu Y, Zhao S, Brusco OA, et al. Effect of Xuezhikang, an Extract From Red Yeast Chinese Rice, on Coronary Events in a Chinese Population With Previous Myocardial Infarction. Am J Cardiol. 2008;101(12):1689-93.

370. Li JJ, Lu ZL, Kou WR, Chen Z, Wu YF, Yu XH, et al. Impact of Xuezhikang on coronary events in hypertensive patients with previous myocardial infarction from the China Coronary Secondary Prevention Study (CCSPS). Ann Med. 2010;42(3):231-40.

371. Lei X, Chen J, Liu CX, Lin J, Lou J, Shang HC. Status and thoughts of Chinese patent medicines seeking approval in the US market. Chin J Integr Med. 2014;20(6):403-8.

372. Luiza Andreazza N, Vevert-Bizet C, Bourg-Heckly G, Sureau F, Jose Salvador M, Bonneau S. Berberine as a photosensitizing agent for antitumoral photodynamic therapy: Insights into its association to low density lipoproteins. Int J Pharm. 2016;510(1):240-9.

373. Cameron J, Ranheim T, Kulseth MA, Leren TP, Berge KE. Berberine decreases PCSK9 expression in HepG2 cells. Atherosclerosis. 2008;201(2):266-73.

374. Li H, Dong B, Park SW, Lee H-S, Chen W, Liu J. Hepatocyte Nuclear Factor 1α Plays a Critical Role in PCSK9 Gene Transcription and Regulation by the Natural Hypocholesterolemic Compound Berberine. J Biol Chem. 2009;284(42):28885-95.

375. Dong H, Zhao Y, Zhao L, Lu F. The Effects of Berberine on Blood Lipids: A Systemic Review and Meta-Analysis of Randomized Controlled Trials. Planta Med. 2013;79(06):437-46.

376. Endo A, Tsujita Y, Kuroda M, Tanzawa K. Inhibition of cholesterol synthesis in vitro and in vivo by ML-236A and ML-236B, competitive inhibitors of 3-hydroxy-3-methylglutaryl-coenzyme A reductase. Eur J Biochem. 1977;77(1):31-6.

377. Endo A. The discovery and development of HMG-CoA reductase inhibitors. 1992. Atheroscler Suppl. 2004;5(3):67-80.

378. Endo A. A gift from nature: the birth of the statins. Nat Med. 2008;14(10):1050-2.

379. LaRosa JC, Grundy SM, Waters DD, Shear C, Barter P, Fruchart J-C, et al. Intensive Lipid Lowering with Atorvastatin in Patients with Stable Coronary Disease. N Engl J Med. 2005;352(14):1425-35.

380. Stam-Slob MC, van der Graaf Y, Greving JP, Dorresteijn JA, Visseren FL. Cost-Effectiveness of Intensifying Lipid-Lowering Therapy With Statins Based on Individual Absolute Benefit in Coronary Artery Disease Patients. J Am Heart Assoc. 2017;6(2):e004648.

381. Hovingh GK, Gandra SR, McKendrick J, Dent R, Wieffer H, Catapano AL, et al. Identification and management of patients with statin-associated symptoms in clinical practice: A clinician survey. Atherosclerosis. 2016;245:111-7.

382. Mendes P, Robles PG, Mathur S. Statin-Induced Rhabdomyolysis: A Comprehensive Review of Case Reports. Physiother Can. 2014;66(2):124-32.

383. Antons KA, Williams CD, Baker SK, Phillips PS. Clinical perspectives of statin-induced rhabdomyolysis. Am J Med. 2006;119(5):400-9.

384. Backes JM, Ruisinger JF, Gibson CA, Moriarty PM. Statin-associated muscle symptoms-Managing the highly intolerant. J Clin Lipidol. 2017;11(1):24-33.

385. Dong B, Wu M, Li H, Kraemer FB, Adeli K, Seidah NG, et al. Strong induction of PCSK9 gene expression through HNF1alpha and SREBP2: mechanism for the resistance to LDL-cholesterol lowering effect of statins in dyslipidemic hamsters. J Lipid Res. 2010;51(6):1486-95.

386. Dubuc G, Chamberland A, Wassef H, Davignon J, Seidah NG, Bernier L, et al. Statins upregulate PCSK9, the gene encoding the proprotein convertase neural apoptosis-regulated convertase-1 implicated in familial hypercholesterolemia. Arterioscler Thromb Vasc Biol. 2004;24(8):1454-9.

387. Guo Y-L, Liu J, Xu R-X, Zhu C-G, Wu N-Q, Jiang L-X, et al. Short-Term Impact of Low-Dose Atorvastatin on Serum Proprotein Convertase Subtilisin/Kexin Type 9. Clin Drug Investig. 2013;33(12):877-83.

388. Berge KE, Ose L, Leren TP. Missense Mutations in the PCSK9 Gene Are Associated With Hypocholesterolemia and Possibly Increased Response to Statin Therapy. Arterioscler Thromb Vasc Biol. 2006;26(5):1094-100.

389. Thompson JF, Hyde CL, Wood LS, Paciga SA, Hinds DA, Cox DR, et al. Comprehensive Whole-Genome and Candidate Gene Analysis for Response to Statin Therapy in the Treating to New Targets (TNT) Cohort. Circ Cardiovasc Genet. 2009;2(2):173-81.

390. Barter PJ, Caulfield M, Eriksson M, Grundy SM, Kastelein JJ, Komajda M, et al. Effects of torcetrapib in patients at high risk for coronary events. N Engl J Med. 2007;357(21):2109-22.

391. Schwartz GG, Olsson AG, Abt M, Ballantyne CM, Barter PJ, Brumm J, et al. Effects of dalcetrapib in patients with a recent acute coronary syndrome. N Engl J Med. 2012;367(22):2089-99.

392. Eyvazian VA, Frishman WH. Evacetrapib: Another CETP Inhibitor for Dyslipidemia With No Clinical Benefit. Cardiol Rev. 2017;25(2):43-52.

393. Landray MJ, Reveal Collaborative G. Randomized Evaluation of the Effects of Anacetrapib through Lipid-modification (REVEAL)-A large-scale, randomized, placebo-controlled trial of the clinical effects of anacetrapib among people with established vascular disease: Trial design, recruitment, and baseline characteristics. Am Heart J. 2017;187:182-90.

394. Teramoto T, Daida H, Ikewaki K, Arai H, Maeda Y, Nakagomi M, et al. Lipid-modifying efficacy and tolerability of anacetrapib added to ongoing statin therapy in Japanese patients with dyslipidemia. Atherosclerosis. 2017;261:69-77.

395. Ballantyne CM, Shah S, Sapre A, Ashraf TB, Tobias SC, Sahin T, et al. A Multiregional, Randomized Evaluation of the Lipid-Modifying Efficacy and Tolerability of Anacetrapib Added to Ongoing Statin Therapy in Patients With Hypercholesterolemia or Low High-Density Lipoprotein Cholesterol. Am J Cardiol. 2017;120(4):569-576.

396. Grundy SM, Ahrens EH, Jr., Salen G. Interruption of the enterohepatic circulation of bile acids in man: comparative effects of cholestyramine and ileal exclusion on cholesterol metabolism. J Lab Clin Med. 1971;78(1):94-121.

397. Black DM. Gut-acting drugs for lowering cholesterol. Curr Atheroscler Rep. 2002;4(1):71-5.

398. Knapp HH, Schrott H, Ma P, Knopp R, Chin B, Gaziano JM, et al. Efficacy and safety of combination simvastatin and colesevelam in patients with primary hypercholesterolemia. Am J Med. 2001;110(5):352-60.

399. Bell DA, Hooper AJ, Watts GF, Burnett JR. Mipomersen and other therapies for the treatment of severe familial hypercholesterolemia. Vasc Health Risk Manag. 2012;8:651-9.

400. Stein EA, Raal FJ. New therapies for reducing low-density lipoprotein cholesterol. Endocrinol Metab Clin North Am. 2014;43(4):1007-33.

401. Raal FJ, Santos RD, Blom DJ, Marais AD, Charng MJ, Cromwell WC, et al. Mipomersen, an apolipoprotein B synthesis inhibitor, for lowering of LDL cholesterol concentrations in patients with homozygous familial hypercholesterolaemia: a randomised, double-blind, placebo-controlled trial. Lancet. 2010;375(9719):998-1006.

402. Rader DJ, Kastelein JJ. Lomitapide and mipomersen: two first-in-class drugs for reducing low-density lipoprotein cholesterol in patients with homozygous familial hypercholesterolemia. Circulation. 2014;129(9):1022-32.

403. Gaudet D, Alexander VJ, Baker BF, Brisson D, Tremblay K, Singleton W, et al. Antisense Inhibition of Apolipoprotein C-III in Patients with Hypertriglyceridemia. N Engl J Med. 2015;373(5):438-47.

404. Cuchel M, Bloedon LT, Szapary PO, Kolansky DM, Wolfe ML, Sarkis A, et al. Inhibition of microsomal triglyceride transfer protein in familial hypercholesterolemia. N Engl J Med. 2007;356(2):148-56.

405. Cuchel M, Meagher EA, du Toit Theron H, Blom DJ, Marais AD, Hegele RA, et al. Efficacy and safety of a microsomal triglyceride transfer protein inhibitor in patients with homozygous familial hypercholesterolaemia: a single-arm, open-label, phase 3 study. Lancet. 2013;381(9860):40-6.

406. Sacks FM, Stanesa M, Hegele RA. Severe hypertriglyceridemia with pancreatitis: thirteen years' treatment with lomitapide. JAMA Intern Med. 2014;174(3):443-7.

407. D'Erasmo L, Cefalu AB, Noto D, Giammanco A, Averna M, Pintus P, et al. Efficacy of Lomitapide in the Treatment of Familial Homozygous Hypercholesterolemia: Results of a Real-World Clinical Experience in Italy. Adv Ther. 2017;34(5);1200–10.

408. Gordon BR, Kelsey SF, Bilheimer DW, Brown DC, Dau PC, Gotto AM, Jr., et al. Treatment of refractory familial hypercholesterolemia by low-density lipoprotein apheresis using an automated dextran sulfate cellulose adsorption system. Am J Cardiol. 1992;70(11):1010-6.

409. Kroon AA, Aengevaeren WR, van der Werf T, Uijen GJ, Reiber JH, Bruschke AV, et al. LDL-Apheresis Atherosclerosis Regression Study (LAARS). Effect of aggressive versus conventional lipid lowering treatment on coronary atherosclerosis. Circulation. 1996;93(10):1826-35.

410. Mabuchi H, Koizumi J, Shimizu M, Kajinami K, Miyamoto S, Ueda K, et al. Long-term efficacy of low-density lipoprotein apheresis on coronary heart disease in familial hypercholesterolemia. Am J Cardiol. 1998;82(12):1489-95.

411. Kroon AA, van't Hof MA, Demacker PNM, Stalenhoef AFH. The rebound of lipoproteins after LDL-apheresis. Kinetics and estimation of mean lipoprotein levels. Atherosclerosis. 2000;152(2):519-26.

412. Yokoyama S, Hayashi R, Kikkawa T, Tani N, Takada S, Hatanaka K, et al. Specific sorbent of apolipoprotein B-containing lipoproteins for plasmapheresis. Characterization and experimental use in hypercholesterolemic rabbits. Arteriosclerosis. 1984;4(3):276-82.

413. Mabuchi H, Michishita I, Takeda M, Fujita H, Koizumi J, Takeda R, et al. A new low density lipoprotein apheresis system using two dextran sulfate cellulose columns in an automated column regenerating unit (LDL continuous apheresis). Atherosclerosis. 1987;68(1):19-25.

414. Sachais BS, Katz J, Ross J, Rader DJ. Long-term effects of LDL apheresis in patients with severe hypercholesterolemia. J Clin Apher. 2005;20(4):252-5.

415. Farmer JA. Nicotinic acid: a new look at an old drug. Curr Atheroscler Rep. 2009;11(2):87-92.

416. Carlson LA, Hamsten A, Asplund A. Pronounced lowering of serum levels of lipoprotein Lp(a) in hyperlipidaemic subjects treated with nicotinic acid. J Intern Med. 1989;226(4):271-6.

417. Taylor AJ, Sullenberger LE, Lee HJ, Lee JK, Grace KA. Arterial Biology for the Investigation of the Treatment Effects of Reducing Cholesterol (ARBITER) 2: a double-blind, placebo-

controlled study of extended-release niacin on atherosclerosis progression in secondary prevention patients treated with statins. Circulation. 2004;110(23):3512-7.

418. Creider JC, Hegele RA, Joy TR. Niacin: another look at an underutilized lipid-lowering medication. Nat Rev Endocrinol. 2012;8(9):517-28.

419. Khera AV, Qamar A, Reilly MP, Dunbar RL, Rader DJ. Effects of niacin, statin, and fenofibrate on circulating proprotein convertase subtilisin/kexin type 9 levels in patients with dyslipidemia. Am J Cardiol. 2015;115(2):178-82.

420. Burke AC, Huff MW. ATP-citrate lyase: genetics, molecular biology and therapeutic target for dyslipidemia. Curr Opin Lipidol. 2017;28(2):193-200.

421. Pinkosky SL, Filippov S, Srivastava RA, Hanselman JC, Bradshaw CD, Hurley TR, et al. AMP-activated protein kinase and ATP-citrate lyase are two distinct molecular targets for ETC-1002, a novel small molecule regulator of lipid and carbohydrate metabolism. J Lipid Res. 2013;54(1):134-51.

422. Ballantyne CM, Davidson MH, Macdougall DE, Bays HE, Dicarlo LA, Rosenberg NL, et al. Efficacy and safety of a novel dual modulator of adenosine triphosphate-citrate lyase and adenosine monophosphate-activated protein kinase in patients with hypercholesterolemia: results of a multicenter, randomized, double-blind, placebo-controlled, parallel-group trial. J Am Coll Cardiol. 2013;62(13):1154-62.

423. Thompson PD, Rubino J, Janik MJ, MacDougall DE, McBride SJ, Margulies JR, et al. Use of ETC-1002 to treat hypercholesterolemia in patients with statin intolerance. J Clin Lipidol. 2015;9(3):295-304.

424. Gutierrez MJ, Rosenberg NL, Macdougall DE, Hanselman JC, Margulies JR, Strange P, et al. Efficacy and safety of ETC-1002, a novel investigational low-density lipoprotein-cholesterol-lowering therapy for the treatment of patients with hypercholesterolemia and type 2 diabetes mellitus. Arterioscler Thromb Vasc Biol. 2014;34(3):676-83.

425. Thompson PD, MacDougall DE, Newton RS, Margulies JR, Hanselman JC, Orloff DG, et al. Treatment with ETC-1002 alone and in combination with ezetimibe lowers LDL cholesterol in hypercholesterolemic patients with or without statin intolerance. J Clin Lipidol. 2016;10(3):556-67.

426. Guo Y-L, Zhang W, Li J-J. PCSK9 and lipid lowering drugs. Clin Chim Acta. 2014;437:66-71.

427. Cui CJ, Li S, Li JJ. PCSK9 and its modulation. Clin Chim Acta. 2015;440:79-86.

428. Ferri N. Proprotein Convertase Subtilisin/Kexin Type 9: From the Discovery to the Development of New Therapies for Cardiovascular Diseases. Scientifica. 2012;2012:927352.

429. Burke AC, Dron JS, Hegele RA, Huff MW. PCSK9: Regulation and Target for Drug Development for Dyslipidemia. Annu Rev Pharmacol Toxicol. 2017;57(1): 223-44.

430. Seidah NG. The PCSK9 revolution and the potential of PCSK9-based therapies to reduce LDL-cholesterol. Glob Cardiol Sci Pract. 2015;2015(5):59.

431. Banerjee Y, Santos RD, Al-Rasadi K, Rizzo M. Targeting PCSK9 for therapeutic gains: Have we addressed all the concerns? Atherosclerosis. 2016;248:62-75.

432. Duff CJ, Scott MJ, Kirby IT, Hutchinson SE, Martin SL, Hooper NM. Antibody-mediated disruption of the interaction between PCSK9 and the low-density lipoprotein receptor. Biochem J. 2009;419(3):577-84.

433. Stein EA, Mellis S, Yancopoulos GD, Stahl N, Logan D, Smith WB, et al. Effect of a monoclonal antibody to PCSK9 on LDL cholesterol. N Engl J Med. 2012;366(12):1108-18.

434. Ito MK, Santos RD. PCSK9 Inhibition With Monoclonal Antibodies: Modern Management of Hypercholesterolemia. J Clin Pharmacol. 2017;57(1):7-32.

435. Koren MJ, Sabatine MS, Giugliano RP, Langslet G, Wiviott SD, Kassahun H, et al. Long-term Low-Density Lipoprotein Cholesterol-Lowering Efficacy, Persistence, and Safety of

Evolocumab in Treatment of Hypercholesterolemia: Results Up to 4 Years From the Open-Label OSLER-1 Extension Study. JAMA cardiology. 2017;2(6):598-607.

436. Sabatine MS, Giugliano RP, Keech AC, Honarpour N, Wiviott SD, Murphy SA, et al. Evolocumab and Clinical Outcomes in Patients with Cardiovascular Disease. N Engl J Med. 2017;376(18):1713-22.

437. Shah P, Glueck CJ, Goldenberg N, Min S, Mahida C, Schlam I, et al. Efficacy, safety, Low density lipoprotein cholesterol lowering, and calculated 10-year cardiovascular risk reduction of alirocumab and evolocumab in addition to maximal tolerated cholesterol lowering therapy: a post-commercialization study. Lipids Health Dis. 2017;16(1):19.

438. Lambert G, Thedrez A, Croyal M, Ramin-Mangata S, Couret D, Diotel N, et al. The complexity of lipoprotein (a) lowering by PCSK9 monoclonal antibodies. Clin Sci. 2017;131(4):261-8.

439. Ferri N, Corsini A, Sirtori CR, Ruscica M. Bococizumab for the treatment of hypercholesterolaemia. Expert Opin Biol Ther. 2017;17(2):237-43.

440. Kastelein JJ, Nissen SE, Rader DJ, Hovingh GK, Wang MD, Shen T, et al. Safety and efficacy of LY3015014, a monoclonal antibody to proprotein convertase subtilisin/kexin type 9 (PCSK9): a randomized, placebo-controlled Phase 2 study. Eur Heart J. 2016;37(17):1360-9.

441. Rashid H, Meredith IT, Nasis A. PCSK9 Monoclonal Antibodies in 2016: Current Status and Future Challenges. Heart Lung Circ. 2017;26(8):786-98.

442. Mazhar F, Haider N. Proprotein convertase subtilisin/kexin type 9 enzyme inhibitors: An emerging new therapeutic option for the treatment of dyslipidemia. J Pharmacol Pharmacother. 2016;7(4):190-3.

443. Mascitelli L, Goldstein MR. PCSK9 inhibition and the global diabetes epidemic. Diabetologia. 2017;60(4):751-2.

444. Garattini L, Padula A. Cholesterol-lowering drugs: science and marketing. J R Soc Med. 2017;110(2):57-64.

445. Toth PP, Danese M, Villa G, Qian Y, Beaubrun A, Lira A, et al. Estimated burden of cardiovascular disease and value-based price range for evolocumab in a high-risk, secondary-prevention population in the US payer context. J Med Econ. 2017:1-10.

446. Lipovsek D. Adnectins: engineered target-binding protein therapeutics. Protein Eng Des Sel. 2011;24(1-2):3-9.

447. Mitchell T, Chao G, Sitkoff D, Lo F, Monshizadegan H, Meyers D, et al. Pharmacologic profile of the Adnectin BMS-962476, a small protein biologic alternative to PCSK9 antibodies for low-density lipoprotein lowering. J Pharm Exp Ther. 2014;350(2):412-24.

448. Graham MJ, Lemonidis KM, Whipple CP, Subramaniam A, Monia BP, Crooke ST, et al. Antisense inhibition of proprotein convertase subtilisin/kexin type 9 reduces serum LDL in hyperlipidemic mice. J Lipid Res. 2007;48(4):763-7.

449. Yamamoto T, Harada-Shiba M, Nakatani M, Wada S, Yasuhara H, Narukawa K, et al. Cholesterol-lowering Action of BNA-based Antisense Oligonucleotides Targeting PCSK9 in Atherogenic Diet-induced Hypercholesterolemic Mice. Mol Ther Nucleic Acids. 2012;1:e22.

450. Gupta N, Fisker N, Asselin MC, Lindholm M, Rosenbohm C, Orum H, et al. A locked nucleic acid antisense oligonucleotide (LNA) silences PCSK9 and enhances LDLR expression in vitro and in vivo. PLoS One. 2010;5(5):e10682.

451. Lindholm MW, Elmen J, Fisker N, Hansen HF, Persson R, Moller MR, et al. PCSK9 LNA antisense oligonucleotides induce sustained reduction of LDL cholesterol in nonhuman primates. Mol Ther. 2012;20(2):376-81.

452. van Poelgeest EP, Hodges MR, Moerland M, Tessier Y, Levin AA, Persson R, et al. Antisense-mediated reduction of proprotein convertase subtilisin/kexin type 9 (PCSK9): a first-in-human randomized, placebo-controlled trial. Br J Clin Pharmacol. 2015;80(6):1350-61.

453. Frank-Kamenetsky M, Grefhorst A, Anderson NN, Racie TS, Bramlage B, Akinc A, et al. Therapeutic RNAi targeting PCSK9 acutely lowers plasma cholesterol in rodents and LDL cholesterol in nonhuman primates. Proc Natl Acad Sci U S A. 2008;105(33):11915-20.

454. Jayaraman M, Ansell SM, Mui BL, Tam YK, Chen J, Du X, et al. Maximizing the potency of siRNA lipid nanoparticles for hepatic gene silencing in vivo. Angew Chem Int Ed Engl. 2012;51(34):8529-33.

455. Suzuki Y, Hyodo K, Suzuki T, Tanaka Y, Kikuchi H, Ishihara H. Biodegradable lipid nanoparticles induce a prolonged RNA interference-mediated protein knockdown and show rapid hepatic clearance in mice and nonhuman primates. Int J Pharm. 2017;519(1-2):34-43.

456. Fitzgerald K, Frank-Kamenetsky M, Shulga-Morskaya S, Liebow A, Bettencourt BR, Sutherland JE, et al. Effect of an RNA interference drug on the synthesis of proprotein convertase subtilisin/kexin type 9 (PCSK9) and the concentration of serum LDL cholesterol in healthy volunteers: a randomised, single-blind, placebo-controlled, phase 1 trial. Lancet. 2014;383(9911):60-8.

457. Fitzgerald K, White S, Borodovsky A, Bettencourt BR, Strahs A, Clausen V, et al. A Highly Durable RNAi Therapeutic Inhibitor of PCSK9. N Engl J Med. 2017;376(1):41-51.

458. Ray KK, Landmesser U, Leiter LA, Kallend D, Dufour R, Karakas M, et al. Inclisiran in Patients at High Cardiovascular Risk with Elevated LDL Cholesterol. N Engl J Med. 2017;376(15):1430-40.

459. Ni YG, Di Marco S, Condra JH, Peterson LB, Wang W, Wang F, et al. A PCSK9-binding antibody that structurally mimics the EGF(A) domain of LDL-receptor reduces LDL cholesterol in vivo. J Lipid Res. 2011;52(1):78-86.

460. Zhang Y, Zhou L, Kong-Beltran M, Li W, Moran P, Wang J, et al. Calcium-independent inhibition of PCSK9 by affinity-improved variants of the LDL receptor EGF(A) domain. J Mol Biol. 2012;422(5):685-96.

461. Schroeder CI, Swedberg JE, Withka JM, Rosengren KJ, Akcan M, Clayton DJ, et al. Design and synthesis of truncated EGF-A peptides that restore LDL-R recycling in the presence of PCSK9 in vitro. Chem Biol. 2014;21(2):284-94.

462. Miyosawa K, Watanabe Y, Murakami K, Murakami T, Shibata H, Iwashita M, et al. New CETP inhibitor K-312 reduces PCSK9 expression: a potential effect on LDL cholesterol metabolism. Am J Physiol Endocrinol Metab. 2015;309(2):E177-90.

463. Petersen DN, Hawkins J, Ruangsiriluk W, Stevens KA, Maguire BA, O'Connell TN, et al. A Small-Molecule Anti-secretagogue of PCSK9 Targets the 80S Ribosome to Inhibit PCSK9 Protein Translation. Cell Chem Biol. 2016;23(11):1362-71.

464. Chackerian B, Remaley A. Vaccine strategies for lowering LDL by immunization against proprotein convertase subtilisin/kexin type 9. Curr Opin Lipidol. 2016;27(4):345-50.

465. Galabova G, Brunner S, Winsauer G, Juno C, Wanko B, Mairhofer A, et al. Peptide-based anti-PCSK9 vaccines - an approach for long-term LDLc management. PLoS One. 2014;9(12):e114469.

466. Crossey E, Amar MJ, Sampson M, Peabody J, Schiller JT, Chackerian B, et al. A cholesterol-lowering VLP vaccine that targets PCSK9. Vaccine. 2015;33(43):5747-55.

467. Chadwick AC, Musunuru K. Treatment of Dyslipidemia Using CRISPR/Cas9 Genome Editing. Curr Atheroscler Rep. 2017;19(7):32.

468. Ding Q, Strong A, Patel KM, Ng SL, Gosis BS, Regan SN, et al. Permanent alteration of PCSK9 with in vivo CRISPR-Cas9 genome editing. Circ Res. 2014;115(5):488-92.

469. Saavedra YG, Zhang J, Seidah NG. PCSK9 prosegment chimera as novel inhibitors of LDLR degradation. PLoS One. 2013;8(8):e72113.

470. Momtazi AA, Banach M, Pirro M, Stein EA, Sahebkar A. MicroRNAs: New Therapeutic Targets for Familial Hypercholesterolemia? Clin Rev Allergy Immunol. 2017.

471. Goedeke L, Wagschal A, Fernandez-Hernando C, Naar AM. miRNA regulation of LDL-cholesterol metabolism. Biochim Biophys Acta. 2016;1861(12 Pt B):2047-52.

472. Bai J, Na H, Hua X, Wei Y, Ye T, Zhang Y, et al. A retrospective study of NENs and miR-224 promotes apoptosis of BON-1 cells by targeting PCSK9 inhibition. Oncotarget. 2017;8(4):6929-39.

473. He M, Zhang W, Dong Y, Wang L, Fang T, Tang W, et al. Pro-inflammation NF-kappaB signaling triggers a positive feedback via enhancing cholesterol accumulation in liver cancer cells. J Exp Clin Cancer Res. 2017;36(1):15.

474. Sniderman A, Thanassoulis G, Couture P, Williams K, Alam A, Furberg CD. Is lower and lower better and better? A re-evaluation of the evidence from the Cholesterol Treatment Trialists' Collaboration meta-analysis for low-density lipoprotein lowering. J Clin Lipidol. 2012;6(4):303-9.

475. Mascitelli L, Goldstein MR. Statin-induced low low-density lipoprotein cholesterol level: is lower better? J Am Coll Cardiol. 2015;65(1):108-9.

476. Ishida T. Dawn of a New Era- The Far Lower, the Far Better Low-Density Lipoprotein Cholesterol Story in Japan. Circ J. 2016;80(9):1903-4.

477. Janeway CA Jr TP, Walport M, et al. . The Immune System in Health and Disease. Immunobiology. 2001.

478. Wang W, Singh S, Zeng DL, King K, Nema S. Antibody structure, instability, and formulation. J Pharm Sci. 2007;96(1):1-26.

479. Brekke OH, Sandlie I. Therapeutic antibodies for human diseases at the dawn of the twenty-first century. Nat Rev Drug Discov. 2003;2(1):52-62.

480. Brambell FWR, Hemmings WA, Morris IG. A Theoretical Model of [gamma]-Globulin Catabolism. Nature. 1964;203(4952):1352-5.

481. Brambell FW. The transmission of immunity from mother to young and the catabolism of immunoglobulins. Lancet. 1966;2:1087-93.

482. Brambell FW. The transmission of immune globulins from the mother to the foetal and newborn young. Proc Nutr Soc. 1969;28(1):35-41.

483. Rath T, Kuo TT, Baker K, Qiao S-W, Kobayashi K, Yoshida M, et al. The Immunologic Functions of the Neonatal Fc Receptor for IgG. J Clin Immunol. 2013;33(1):9-17.

484. Roopenian DC, Akilesh S. FcRn: the neonatal Fc receptor comes of age. Nat Rev Immunol. 2007;7(9):715-25.

485. Nimmerjahn F, Ravetch JV. Fcgamma receptors: old friends and new family members. Immunity. 2006;24(1):19-28.

486. Martins JP, Kennedy PJ, Santos HA, Barrias C, Sarmento B. A comprehensive review of the neonatal Fc receptor and its application in drug delivery. Pharmacol Ther. 2016;161:22-39.

487. Williams AF, Barclay AN. The immunoglobulin superfamily--domains for cell surface recognition. Annu Rev Immunol. 1988;6:381-405.

488. Rodewald R. pH-dependent binding of immunoglobulins to intestinal cells of the neonatal rat. The J Cell Biol. 1976;71(2):666-9.

489. Baker K, Qiao S-W, Kuo T, Kobayashi K, Yoshida M, Lencer WI, et al. Immune and non-immune functions of the (not so) neonatal Fc receptor, FcRn. Semin Immunopathol. 2009;31(2):223-36.

490. Rath T, Kuo TT, Baker K, Qiao SW, Kobayashi K, Yoshida M, et al. The immunologic functions of the neonatal Fc receptor for IgG. J Clin Immunol. 2013;33 Suppl 1:S9-17.

491. Challa DK, Velmurugan R, Ober RJ, Sally Ward E. FcRn: from molecular interactions to regulation of IgG pharmacokinetics and functions. Curr Top Microbiol Immunol. 2014;382:249-72.

492. Baker K, Rath T, Pyzik M, Blumberg RS. The Role of FcRn in Antigen Presentation. Front Immunol. 2014;5:408.

493. Abdiche YN, Yeung YA, Chaparro-Riggers J, Barman I, Strop P, Chin SM, et al. The neonatal Fc receptor (FcRn) binds independently to both sites of the IgG homodimer with identical affinity. Mabs. 2015;7(2):331-43.

494. Sand KM, Bern M, Nilsen J, Noordzij HT, Sandlie I, Andersen JT. Unraveling the Interaction between FcRn and Albumin: Opportunities for Design of Albumin-Based Therapeutics. Front Immunol. 2014;5:682.

495. Oganesyan V, Damschroder MM, Cook KE, Li Q, Gao C, Wu H, et al. Structural insights into neonatal Fc receptor-based recycling mechanisms. J Biol Chem. 2014;289(11):7812-24.

496. Kim J, Bronson CL, Hayton WL, Radmacher MD, Roopenian DC, Robinson JM, et al. Albumin turnover: FcRn-mediated recycling saves as much albumin from degradation as the liver produces. Am J Physiol Gastrointest Liver. 2006;290(2):G352-G60.

497. Junghans RP, Anderson CL. The protection receptor for IgG catabolism is the beta2-microglobulin-containing neonatal intestinal transport receptor. Proc Natl Acad Sci USA. 1996;93(11):5512-6.

498. Rath T, Baker K, Pyzik M, Blumberg RS. Regulation of Immune Responses by the Neonatal Fc Receptor and Its Therapeutic Implications. Front Immunol. 2015;5(664).

499. Popov S. The stoichiometry and affinity of the interaction of murine Fc fragments with the MHC class I-related receptor, FcRn. Mol Immunol. 1996;33:521-30.

500. Rath T, Baker K, Dumont JA, Peters RT, Jiang H, Qiao SW, et al. Fc-fusion proteins and FcRn: structural insights for longer-lasting and more effective therapeutics. Crit Rev Biotechnol. 2015;35(2):235-54.

501. Pridgen EM, Alexis F, Kuo TT, Levy-Nissenbaum E, Karnik R, Blumberg RS, et al. Transepithelial Transport of Fc-Targeted Nanoparticles by the Neonatal Fc Receptor for Oral Delivery. Sci Transl Med. 2013;5(213):213ra167.

502. Vllasaliu D, Alexander C, Garnett M, Eaton M, Stolnik S. Fc-mediated transport of nanoparticles across airway epithelial cell layers. J Control Release. 2012;158(3):479-86.

503. Capon DJ, Chamow SM, Mordenti J, Marsters SA, Gregory T, Mitsuya H, et al. Designing CD4 immunoadhesins for AIDS therapy. Nature. 1989;337(6207):525-31.

504. Moreland LW. Soluble tumor necrosis factor receptor (p75) fusion protein (enbrel) as a therapy for rheumatoid arthritis. Rheum Dis Clin North Am. 1998;24(3):579-91.

505. Strohl WR. Fusion Proteins for Half-Life Extension of Biologics as a Strategy to Make Biobetters. BioDrugs. 2015;29(4):215-39.

506. Lobo ED, Hansen RJ, Balthasar JP. Antibody pharmacokinetics and pharmacodynamics. J Pharm Sci. 2004;93(11):2645-68.

507. De Meyer T, Muyldermans S, Depicker A. Nanobody-based products as research and diagnostic tools. Trends Biotechnol. 2014;32(5):263-70.

508. Deeks ED. Certolizumab Pegol: A Review in Inflammatory Autoimmune Diseases. BioDrugs. 2016;30(6):607-17.

509. Holliger P, Prospero T, Winter G. "Diabodies": small bivalent and bispecific antibody fragments. Proc Natl Acad Sci U S A. 1993;90(14):6444-8.

510. Bird RE, Hardman KD, Jacobson JW, Johnson S, Kaufman BM, Lee SM, et al. Single-chain antigen-binding proteins. Science. 1988;242(4877):423-6.

511. Crivianu-Gaita V, Thompson M. Aptamers, antibody scFv, and antibody Fab' fragments: An overview and comparison of three of the most versatile biosensor biorecognition elements. Biosens Bioelectron. 2016;85:32-45.

512. Doria-Rose NA, Joyce MG. Strategies to guide the antibody affinity maturation process. Curr Opin Virol. 2015;11:137-47.

513. Winau F, Winau R. Emil von Behring and serum therapy. Microbes Infect. 2002;4(2):185-8.

514. Winau F, Westphal O, Winau R. Paul Ehrlich--in search of the magic bullet. Microbes Infect. 2004;6(8):786-9.

515. Kohler G, Milstein C. Continuous cultures of fused cells secreting antibody of predefined specificity. Nature. 1975;256(5517):495-7.

516. Alkan SS. Monoclonal antibodies: the story of a discovery that revolutionized science and medicine. Nat Rev Immunol. 2004;4(2):153-6.

517. Emmons C, Hunsicker LG. Muromonab-CD3 (Orthoclone OKT3): the first monoclonal antibody approved for therapeutic use. Iowa Med. 1987;77(2):78-82.

518. Schroff RW, Foon KA, Beatty SM, Oldham RK, Morgan AC, Jr. Human anti-murine immunoglobulin responses in patients receiving monoclonal antibody therapy. Cancer Res. 1985;45(2):879-85.

519. Andersen JT, Daba MB, Berntzen G, Michaelsen TE, Sandlie I. Cross-species binding analyses of mouse and human neonatal Fc receptor show dramatic differences in immunoglobulin G and albumin binding. J Biol Chem. 2010;285(7):4826-36.

520. Morrison SL, Johnson MJ, Herzenberg LA, Oi VT. Chimeric human antibody molecules: mouse antigen-binding domains with human constant region domains. Proc Natl Acad Sci U S A. 1984;81(21):6851-5.

521. Popma JJ, Satler LF. Early and late clinical outcome following coronary angioplasty performed with platelet glycoprotein IIb/IIIa receptor inhibition: the EPIC Trial results. J Invasive Cardiol. 1994;6 Suppl A:19A-28A; discussion 45A-50A.

522. Jones PT, Dear PH, Foote J, Neuberger MS, Winter G. Replacing the complementarity-determining regions in a human antibody with those from a mouse. Nature. 1986;321(6069):522-5.

523. Carter P, Presta L, Gorman CM, Ridgway JB, Henner D, Wong WL, et al. Humanization of an anti-p185HER2 antibody for human cancer therapy. Proc Natl Acad Sci U S A. 1992;89(10):4285-9.

524. Presta LG, Lahr SJ, Shields RL, Porter JP, Gorman CM, Fendly BM, et al. Humanization of an antibody directed against IgE. J Immunol. 1993;151(5):2623-32.

525. Wu H, Nie Y, Huse WD, Watkins JD. Humanization of a murine monoclonal antibody by simultaneous optimization of framework and CDR residues. J Mol Biol. 1999;294(1):151-62.

526. Vincenti F, Nashan B, Light S. Daclizumab: outcome of phase III trials and mechanism of action. Double Therapy and the Triple Therapy Study Groups. Transplant Proc. 1998;30(5):2155-8.

527. Hwang WY, Foote J. Immunogenicity of engineered antibodies. Methods. 2005;36(1):3-10.

528. Foltz IN, Karow M, Wasserman SM. Evolution and Emergence of Therapeutic Monoclonal Antibodies: What Cardiologists Need to Know. Circulation. 2013;127(22):2222-30.

529. Steinitz M, Klein E. Human monoclonal antibodies produced by immortalization with Epstein-Barr virus. Immunol Today. 1981;2(2):38-9.

530. Skerra A, Pluckthun A. Assembly of a functional immunoglobulin Fv fragment in Escherichia coli. Science. 1988;240(4855):1038-41.

531. Better M, Chang CP, Robinson RR, Horwitz AH. Escherichia coli secretion of an active chimeric antibody fragment. Science. 1988;240(4855):1041-3.

532. McCafferty J, Griffiths AD, Winter G, Chiswell DJ. Phage antibodies: filamentous phage displaying antibody variable domains. Nature. 1990;348(6301):552-4.

533. Bazan J, Całkosiński I, Gamian A. Phage display—A powerful technique for immunotherapy: 1. Introduction and potential of therapeutic applications. Hum Vaccin Immunother. 2012;8(12):1817-28.

534. Chan CE, Lim AP, MacAry PA, Hanson BJ. The role of phage display in therapeutic antibody discovery. Int Immunol. 2014;26(12):649-57.

535. Irving RA, Coia G, Roberts A, Nuttall SD, Hudson PJ. Ribosome display and affinity maturation: from antibodies to single V-domains and steps towards cancer therapeutics. J Immunol Methods. 2001;248(1-2):31-45.

536. Green LL. Antibody engineering via genetic engineering of the mouse: XenoMouse strains are a vehicle for the facile generation of therapeutic human monoclonal antibodies. J Immunol Methods. 1999;231(1-2):11-23.

537. Foltz IN, Gunasekaran K, King CT. Discovery and bio-optimization of human antibody therapeutics using the XenoMouse(R) transgenic mouse platform. Immunol Rev. 2016;270(1):51-64.

538. Lorenz HM. Technology evaluation: adalimumab, Abbott laboratories. Curr Opin Mol Ther. 2002;4(2):185-90.

539. Cai H. Risk Evaluation and Mitigation Strategy for Approved Therapeutic Antibodies. MOJ Immunol. 2014;1(5).

540. Cai H. Therapeutic Monoclonal Antibodies Approved by FDA in 2016. MOJ Immunol. 2017;5(1).

541. Nelson AL, Dhimolea E, Reichert JM. Development trends for human monoclonal antibody therapeutics. Nat Rev Drug Discov. 2010;9(10):767-74.

542. Ecker DM, Jones SD, Levine HL. The therapeutic monoclonal antibody market. Mabs. 2015;7(1):9-14.

543. Mould DR, Sweeney KR. The pharmacokinetics and pharmacodynamics of monoclonal antibodies--mechanistic modeling applied to drug development. Current opinion in drug discovery & development. 2007;10(1):84-96.

544. Tabrizi MA, Tseng CM, Roskos LK. Elimination mechanisms of therapeutic monoclonal antibodies. Drug Discov Today. 2006;11(1-2):81-8.

545. Datta-Mannan A, Lu J, Witcher DR, Leung D, Tang Y, Wroblewski VJ. The interplay of non-specific binding, target-mediated clearance and FcRn interactions on the pharmacokinetics of humanized antibodies. Mabs. 2015;7(6):1084-93.

546. Seligmann M, Danon F, Hurez D, Mihaesco E, Preud'homme JL. Alpha-chain disease: a new immunoglobulin abnormality. Science. 1968;162(3860):1396-7.

547. Lecuit M, Abachin E, Martin A, Poyart C, Pochart P, Suarez F, et al. Immunoproliferative small intestinal disease associated with Campylobacter jejuni. N Engl J Med. 2004;350(3):239-48.

548. Wahner-Roedler DL, Witzig TE, Loehrer LL, Kyle RA. Gamma-heavy chain disease: review of 23 cases. Medicine (Baltimore). 2003;82(4):236-50.

549. Wahner-Roedler DL KR. Mu-heavy chain disease: presentation as a benign monoclonal gammopathy. Am J Hematol. 1992;40(1);56-60.

550. Hamers-Casterman C, Atarhouch T, Muyldermans S, Robinson G, Hamers C, Songa EB, et al. Naturally occurring antibodies devoid of light chains. Nature. 1993;363(6428):446-8.

551. Achour I, Cavelier P, Tichit M, Bouchier C, Lafaye P, Rougeon F. Tetrameric and homodimeric camelid IgGs originate from the same IgH locus. J Immunol. 2008;181(3):2001-9.

552. Desmyter A, Transue TR, Ghahroudi MA, Thi MH, Poortmans F, Hamers R, et al. Crystal structure of a camel single-domain VH antibody fragment in complex with lysozyme. Nat Struct Biol. 1996;3(9):803-11.

553. Greenberg AS, Avila D, Hughes M, Hughes A, McKinney EC, Flajnik MF. A new antigen receptor gene family that undergoes rearrangement and extensive somatic diversification in sharks. Nature. 1995;374(6518):168-73.

554. Stanfield RL, Dooley H, Flajnik MF, Wilson IA. Crystal structure of a shark single-domain antibody V region in complex with lysozyme. Science. 2004;305(5691):1770-3.

555. Kovaleva M, Ferguson L, Steven J, Porter A, Barelle C. Shark variable new antigen receptor biologics - a novel technology platform for therapeutic drug development. Expert Opin Biol Ther. 2014;14(10):1527-39.

556. Muyldermans S. Nanobodies: natural single-domain antibodies. Annu Rev Biochem. 2013;82:775-97.

557. Desmyter A, Spinelli S, Roussel A, Cambillau C. Camelid nanobodies: killing two birds with one stone. Curr Opin Struct Biol. 2015;32:1-8.

558. Davies J, Riechmann L. Antibody VH domains as small recognition units. Biotechnology. 1995;13(5):475-9.

559. Arbabi Ghahroudi M, Desmyter A, Wyns L, Hamers R, Muyldermans S. Selection and identification of single domain antibody fragments from camel heavy-chain antibodies. FEBS Lett. 1997;414(3):521-6.

560. van der Linden R, de Geus B, Stok W, Bos W, van Wassenaar D, Verrips T, et al. Induction of immune responses and molecular cloning of the heavy chain antibody repertoire of Lama glama. J Immunol Methods. 2000;240(1-2):185-95.

561. van der Linden RH, Frenken LG, de Geus B, Harmsen MM, Ruuls RC, Stok W, et al. Comparison of physical chemical properties of llama VHH antibody fragments and mouse monoclonal antibodies. Biochim Biophys Acta. 1999;1431(1):37-46.

562. Fridy PC, Li Y, Keegan S, Thompson MK, Nudelman I, Scheid JF, et al. A robust pipeline for rapid production of versatile nanobody repertoires. Nat Methods. 2014;11(12):1253-60.

563. Comor L, Dolinska S, Bhide K, Pulzova L, Jimenez-Munguia I, Bencurova E, et al. Joining the in vitro immunization of alpaca lymphocytes and phage display: rapid and cost effective pipeline for sdAb synthesis. Microb Cell Fact. 2017;16(1):13.

564. Arbabi-Ghahroudi M, Tanha J, MacKenzie R. Prokaryotic expression of antibodies. Cancer Metastasis Rev. 2005;24(4):501-19.

565. Sarker SA, Jakel M, Sultana S, Alam NH, Bardhan PK, Chisti MJ, et al. Anti-rotavirus protein reduces stool output in infants with diarrhea: a randomized placebo-controlled trial. Gastroenterology. 2013;145(4):740-8.e8.

566. De Meyer T, Laukens B, Nolf J, Van Lerberge E, De Rycke R, De Beuckelaer A, et al. Comparison of VHH-Fc antibody production in Arabidopsis thaliana, Nicotiana benthamiana and Pichia pastoris. Plant Biotechnol J. 2015;13(7):938-47.

567. Koide S. Engineering of recombinant crystallization chaperones. Curr Opin Struct Biol. 2009;19(4):449-57.

568. Helma J, Cardoso MC, Muyldermans S, Leonhardt H. Nanobodies and recombinant binders in cell biology. The J Cell Biol. 2015;209(5):633-44.

569. Dmitriev OY, Lutsenko S, Muyldermans S. Nanobodies as Probes for Protein Dynamics in Vitro and in Cells. J Biol Chem. 2016;291(8):3767-75.

570. Wesolowski J, Alzogaray V, Reyelt J, Unger M, Juarez K, Urrutia M, et al. Single domain antibodies: promising experimental and therapeutic tools in infection and immunity. Med Microbiol Immun. 2009;198(3):157-74.

571. Van Heeke G, Allosery K, De Brabandere V, De Smedt T, Detalle L, de Fougerolles A. Nanobodies(R) as inhaled biotherapeutics for lung diseases. Pharmacol Ther. 2017;169:47-56.

572. Vincke C, Loris R, Saerens D, Martinez-Rodriguez S, Muyldermans S, Conrath K. General strategy to humanize a camelid single-domain antibody and identification of a universal humanized nanobody scaffold. J Biol Chem. 2009;284(5):3273-84.

573. Cortez-Retamozo V, Lauwereys M, Hassanzadeh Gh G, Gobert M, Conrath K, Muyldermans S, et al. Efficient tumor targeting by single-domain antibody fragments of camels. Int J Cancer. 2002;98(3):456-62.

574. Peyvandi F, Scully M, Kremer Hovinga JA, Knobl P, Cataland S, De Beuf K, et al. Caplacizumab reduces the frequency of major thromboembolic events, exacerbations and death in patients with acquired thrombotic thrombocytopenic purpura. J Thromb Haemost. 2017;15(7):1448-52.

575. Peyvandi F, Scully M, Kremer Hovinga JA, Cataland S, Knöbl P, Wu H, et al. Caplacizumab for Acquired Thrombotic Thrombocytopenic Purpura. N Engl J Med. 2016;374(6):511-22.

576. Holz JB. The TITAN trial - Assessing the efficacy and safety of an anti-von Willebrand factor Nanobody in patients with acquired thrombotic thrombocytopenic purpura. Transfus Apher Sci. 2012;46(3):343-6.

577. Kratz F, Elsadek B. Clinical impact of serum proteins on drug delivery. J Control Release. 2012;161(2):429-45.

578. Elsadek B, Kratz F. Impact of albumin on drug delivery--new applications on the horizon. J Control Release. 2012;157(1):4-28.

579. Van Roy M, Ververken C, Beirnaert E, Hoefman S, Kolkman J, Vierboom M, et al. The preclinical pharmacology of the high affinity anti-IL-6R Nanobody (R) ALX-0061 supports its clinical development in rheumatoid arthritis. Arthritis Res Ther. 2015;17:s13075-015-0651-0.

580. Detalle L, Stohr T, Palomo C, Piedra PA, Gilbert BE, Mas V, et al. Generation and Characterization of ALX-0171, a Potent Novel Therapeutic Nanobody for the Treatment of Respiratory Syncytial Virus Infection. Antimicrob Agents Chemother. 2016;60(1):6-13.

581. Jahnichen S, Blanchetot C, Maussang D, Gonzalez-Pajuelo M, Chow KY, Bosch L, et al. CXCR4 nanobodies (VHH-based single variable domains) potently inhibit chemotaxis and HIV-1 replication and mobilize stem cells. Proc Natl Acad Sci U S A. 2010;107(47):20565-70.

582. Papadopoulos KP, Isaacs R, Bilic S, Kentsch K, Huet HA, Hofmann M, et al. Unexpected hepatotoxicity in a phase I study of TAS266, a novel tetravalent agonistic Nanobody(R) targeting the DR5 receptor. Cancer Chemother Pharmacol. 2015;75(5):887-95.

583. Maxwell KN, Breslow JL. Adenoviral-mediated expression of Pcsk9 in mice results in a low-density lipoprotein receptor knockout phenotype. Proc Natl Acad Sci U S A. 2004;101(18):7100-5.

584. Kotowski IK, Pertsemlidis A, Luke A, Cooper RS, Vega GL, Cohen JC, et al. A spectrum of PCSK9 alleles contributes to plasma levels of low-density lipoprotein cholesterol. Am J Hum Genet. 2006;78(3):410-22.

585. Seidah NG. PCSK9 as a therapeutic target of dyslipidemia. Expert Opin Ther Targets. 2009;13(1):19-28.

586. Stein EA, Raal F. Reduction of low-density lipoprotein cholesterol by monoclonal antibody inhibition of PCSK9. Annu Rev Med. 2014;65:417-31.

587. McLaughlin P, Grillo-Lopez AJ, Link BK, Levy R, Czuczman MS, Williams ME, et al. Rituximab chimeric anti-CD20 monoclonal antibody therapy for relapsed indolent lymphoma: half of patients respond to a four-dose treatment program. J Clin Oncol. 1998;16(8):2825-33.

588. Lundin J, Kimby E, Bjorkholm M, Broliden PA, Celsing F, Hjalmar V, et al. Phase II trial of subcutaneous anti-CD52 monoclonal antibody alemtuzumab (Campath-1H) as first-line treatment for patients with B-cell chronic lymphocytic leukemia (B-CLL). Blood. 2002;100(3):768-73.

589. Cobleigh MA, Vogel CL, Tripathy D, Robert NJ, Scholl S, Fehrenbacher L, et al. Multinational study of the efficacy and safety of humanized anti-HER2 monoclonal antibody in women who have HER2-overexpressing metastatic breast cancer that has progressed after chemotherapy for metastatic disease. J Clin Oncol. 1999;17(9):2639-48.

590. Shrank WH, Barlow JF, Brennan TA. New Therapies in the Treatment of High Cholesterol: An Argument to Return to Goal-Based Lipid Guidelines. J Am Med Assoc. 2015;314(14):1443-4.

591. Genest J, McPherson R, Frohlich J, Anderson T, Campbell N, Carpentier A, et al. 2009 Canadian Cardiovascular Society/Canadian guidelines for the diagnosis and treatment of dyslipidemia and prevention of cardiovascular disease in the adult - 2009 recommendations. Can J Cardiol. 2009;25(10):567-79.

592. Bartunek J, Barbato E, Heyndrickx G, Vanderheyden M, Wijns W, Holz JB. Novel antiplatelet agents: ALX-0081, a Nanobody directed towards von Willebrand factor. J Cardiovasc Transl Res. 2013;6(3):355-63.

593. Benjannet S, Saavedra YG, Hamelin J, Asselin MC, Essalmani R, Pasquato A, et al. Effects of the prosegment and pH on the activity of PCSK9: evidence for additional processing events. J Biol Chem. 2010;285(52):40965-78.

594. Hussack G, Arbabi-Ghahroudi M, van Faassen H, Songer JG, Ng KK, MacKenzie R, et al. Neutralization of Clostridium difficile toxin A with single-domain antibodies targeting the cell receptor binding domain. J Biol Chem. 2011;286(11):8961-76.

595. Schippers IJ, Moshage H, Roelofsen H, Muller M, Heymans HS, Ruiters M, et al. Immortalized human hepatocytes as a tool for the study of hepatocytic (de-)differentiation. Cell Biol Toxicol. 1997;13(4-5):375-86.

596. Maclean J, Koekemoer M, Olivier AJ, Stewart D, Hitzeroth, II, Rademacher T, et al. Optimization of human papillomavirus type 16 (HPV-16) L1 expression in plants: comparison of the suitability of different HPV-16 L1 gene variants and different cell-compartment localization. J Gen Virol. 2007;88(Pt 5):1460-9.

597. Voinnet O, Rivas S, Mestre P, Baulcombe D. An enhanced transient expression system in plants based on suppression of gene silencing by the p19 protein of tomato bushy stunt virus. Plant J : for cell and molecular biology. 2003;33(5):949-56.

598. Powers DB, Amersdorfer P, Poul M, Nielsen UB, Shalaby MR, Adams GP, et al. Expression of single-chain Fv-Fc fusions in Pichia pastoris. J Immunol Methods. 2001;251(1-2):123-35.

599. Pedersen NB, Wang S, Narimatsu Y, Yang Z, Halim A, Schjoldager KT, et al. Low density lipoprotein receptor class A repeats are O-glycosylated in linker regions. J Biol Chem. 2014;289(25):17312-24.

600. Pelham HR. Evidence that luminal ER proteins are sorted from secreted proteins in a post-ER compartment. EMBO J. 1988;7(4):913-8.

601. Marcinkiewicz M, Ramla D, Seidah NG, Chretien M. Developmental expression of the prohormone convertases PC1 and PC2 in mouse pancreatic islets. Endocrinology. 1994;135(4):1651-60.

602. Huang Y, Ballinger DG, Stokowski R, Beilharz E, Robinson JG, Liu S, et al. Exploring the interaction between SNP genotype and postmenopausal hormone therapy effects on stroke risk. Genome Med. 2012;4(7):57.

603. Grunberg J, Knogler K, Waibel R, Novak-Hofer I. High-yield production of recombinant antibody fragments in HEK-293 cells using sodium butyrate. BioTechniques. 2003;34(5):968-72.

604. Zhu J, Declercq J, Roucourt B, Ghassabeh GH, Meulemans S, Kinne J, et al. Generation and characterization of non-competitive furin-inhibiting nanobodies. Biochem J. 2012;448(1):73-82.

605. Nie Q, Jia D, Yang H, Feng Y, Fan Q, Shi Q, et al. Conjugation to 10 kDa Linear PEG Extends Serum Half-Life and Preserves the Receptor-Binding Ability of mmTRAIL with Minimal Stimulation of PEG-Specific Antibodies. Mol Pharm. 2017;14(2):502-12.

606. Sleep D, Cameron J, Evans LR. Albumin as a versatile platform for drug half-life extension. Biochim Biophys Acta. 2013;1830(12):5526-34.

607. Kelley B. Industrialization of mAb production technology: the bioprocessing industry at a crossroads. Mabs. 2009;1(5):443-52.

608. Shaughnessy AF. Monoclonal antibodies: magic bullets with a hefty price tag. BMJ (Clinical research ed). 2012;345.

609. Soran H, Dent R, Durrington P. Evidence-based goals in LDL-C reduction. Clin Res Cardiol. 2017;106(4):237-48.

610. Egan BM, Li J, White K, Fleming DO, Connell K, Hernandez GT, et al. 2013 ACC/AHA Cholesterol Guideline and Implications for Healthy People 2020 Cardiovascular Disease Prevention Goals. J Am Heart Assoc. 2016;5(8):e003558.

611. Elbitar S, Khoury PE, Ghaleb Y, Rabes JP, Varret M, Seidah NG, et al. Proprotein convertase subtilisin / kexin 9 (PCSK9) inhibitors and the future of dyslipidemia therapy: an updated patent review (2011-2015). Expert Opin Ther Pat. 2016;26(12):1377-92.

612. Essalmani R, Hamelin J, Marcinkiewicz J, Chamberland A, Mbikay M, Chretien M, et al. Deletion of the gene encoding proprotein convertase 5/6 causes early embryonic lethality in the mouse. Mol Cell Biol . 2006;26(1):354-61.

613. Dubuc G, Tremblay M, Pare G, Jacques H, Hamelin J, Benjannet S, et al. A new method for measurement of total plasma PCSK9: clinical applications. J Lipid Res. 2010;51(1):140-9.

614. Essalmani R, Susan-Resiga D, Chamberland A, Asselin MC, Canuel M, Constam D, et al. Furin is the primary in vivo convertase of angiopoietin-like 3 and endothelial lipase in hepatocytes. J Biol Chem. 2013;288(37):26410-8.

615. Larsson SL, Skogsberg J, Björkegren J. The Low Density Lipoprotein Receptor Prevents Secretion of Dense ApoB100-containing Lipoproteins from the Liver. J Biol Chem. 2004;279(2):831-6.

616. Blasiole DA, Oler AT, Attie AD. Regulation of ApoB Secretion by the Low Density Lipoprotein Receptor Requires Exit from the Endoplasmic Reticulum and Interaction with ApoE or ApoB. J Biol Chem. 2008;283(17):11374-81.

617. Wang J, Iyer S, Fielder PJ, Davis JD, Deng R. Projecting human pharmacokinetics of monoclonal antibodies from nonclinical data: comparative evaluation of prediction approaches in early drug development. Biopharm Drug Disposition. 2016;37(2):51-65.

618. Cameron J, Holla ØL, Laerdahl JK, Kulseth MA, Berge KE, Leren TP. Mutation S462P in the PCSK9 gene reduces secretion of mutant PCSK9 without affecting the autocatalytic cleavage. Atherosclerosis.203(1):161-5.

619. Allard D, Amsellem S, Abifadel M, Trillard M, Devillers M, Luc G, et al. Novel mutations of the PCSK9 gene cause variable phenotype of autosomal dominant hypercholesterolemia. Hum Mutat. 2005;26(5):497.

620. Hampton EN, Knuth MW, Li J, Harris JL, Lesley SA, Spraggon G. The self-inhibited structure of full-length PCSK9 at 1.9 A reveals structural homology with resistin within the C-terminal domain. Proc Natl Acad Sci U S A. 2007;104(37):14604-9.

621. Piper DE, Jackson S, Liu Q, Romanow WG, Shetterly S, Thibault ST, et al. The crystal structure of PCSK9: a regulator of plasma LDL-cholesterol. Structure. 2007;15(5):545-52.

622. Ober RJ, Radu CG, Ghetie V, Ward ES. Differences in promiscuity for antibody–FcRn interactions across species: implications for therapeutic antibodies. Int Immunol. 2001;13(12):1551-9.

623. Avery LB, Wang M, Kavosi MS, Joyce A, Kurz JC, Fan YY, et al. Utility of a human FcRn transgenic mouse model in drug discovery for early assessment and prediction of human pharmacokinetics of monoclonal antibodies. Mabs. 2016;8(6):1064-78.

624. Keyaerts M, Xavier C, Heemskerk J, Devoogdt N, Everaert H, Ackaert C, et al. Phase I Study of 68Ga-HER2-Nanobody for PET/CT Assessment of HER2 Expression in Breast Carcinoma. J Nucl Med : official publication, Society of Nuclear Medicine. 2016;57(1):27-33.

625. Katrijn Broos MK, Quentin Lecocq, Dries Renmans, Tham Nguyen, David Escors, Adrian Liston, Geert Raes, Karine Breckpot, Nick Devoogdt. Non-invasive assessment of murine PD-L1 levels in syngeneic tumor models by nuclear imaging with nanobody tracers. Oncotarget. 2017;8(26):41932-46.

626. Deloukas P, Kanoni S, Willenborg C, Farrall M, Assimes TL, Thompson JR, et al. Large-scale association analysis identifies new risk loci for coronary artery disease. Nat Genet. 2013;45(1):25-33.

627. Stawowy P, Kallisch H, Borges Pereira Stawowy N, Stibenz D, Veinot JP, Gräfe M, et al. Immunohistochemical localization of subtilisin/kexin-like proprotein convertases in human atherosclerosis. Virchows Archiv. 2005;446(4):351-9.

628. Stawowy P, Kappert K. The Molecular Biology of Furin-Like Proprotein Convertases in Vascular Remodelling. Methods Mol Biol (Clifton, NJ). 2011;768:191-206.

629. Stawowy P, Fleck E. Proprotein convertases furin and PC5: targeting atherosclerosis and restenosis at multiple levels. J Mol Med (Berlin, Germany). 2005;83(11):865-75.

630. Ren K, Jiang T, Zheng XL, Zhao GJ. Proprotein convertase furin/PCSK3 and atherosclerosis: New insights and potential therapeutic targets. Atherosclerosis. 2017;262:163-70.

631. Hoogeveen RC, Gaubatz JW, Sun W, Dodge RC, Crosby JR, Jiang J, et al. Small dense low-density lipoprotein-cholesterol concentrations predict risk for coronary heart disease: the Atherosclerosis Risk In Communities (ARIC) study. Arterioscler Thromb Vasc Biol. 2014;34(5):1069-77.

VI. Appendices

Appendix A1. FACS analysis of cell surface LDLR in HepG2 cells incubated in presence of PCSK9 and various concentrations of sdAb-mFcs. HepG2 cells were incubated for 4h in the absence (Ctl (-)) or presence (Ctl (+)) of 15 µg/ml WT PCSK9 mixed with 0-1.2 µM sdAb as indicated. Cells were then detached and cell surface LDLR fluorescently labelled and measured by FACS. Error bars represent standard deviation. *, $p < 0.05$, **, $p < 0.005$, ***, $p < 0.0005$, ****, $p < 0.00005$ (Student's *t* test). The data shown here are representative of two to three independent experiments.

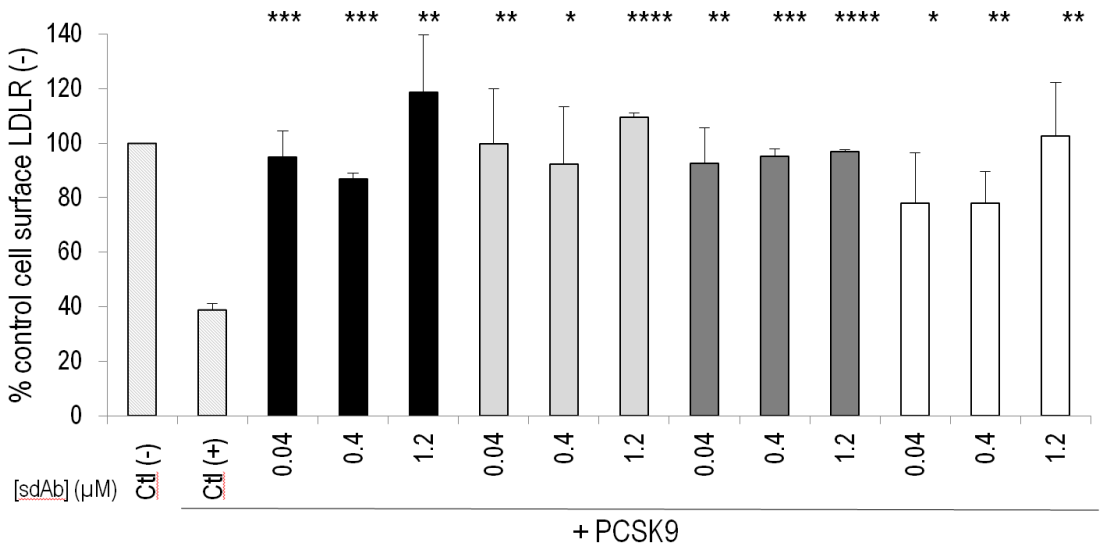

Appendix A2. Pilot study: injection of Tg2 mice with various doses of evolocumab. Total cholesterol levels were measured in mice plasma before and after injection of 2, 4 or 10 mg/kg evolocumab. Error bars represent SEM.

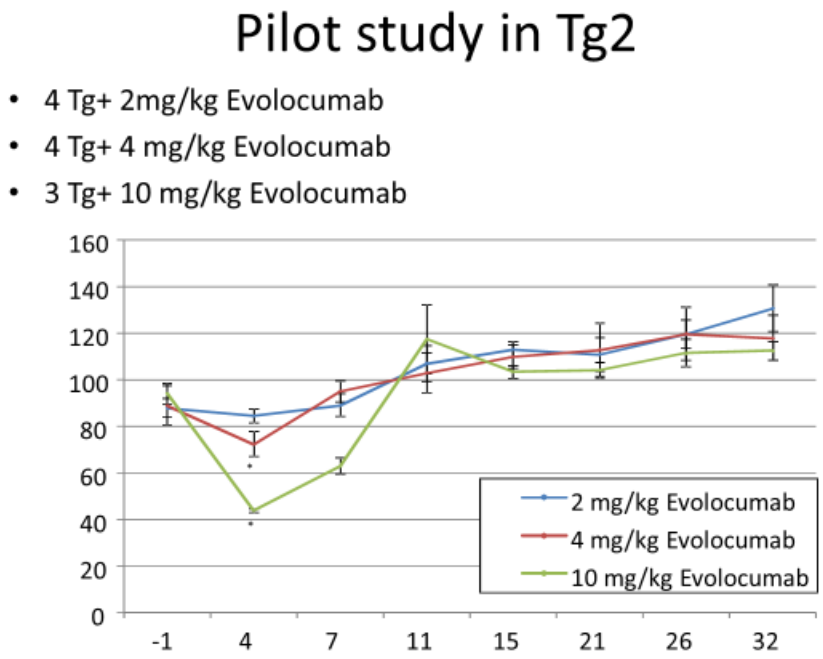

Appendix A3. Pilot study: injection of Tg2 Ldlr$^{+/-}$ mice with PKF8-mFc and evolocumab. Total cholesterol levels were measured in mice plasma before and after injection of either PKF8-mFc or evolocumab. Error bars represent SEM. *, $p < 0.05$, **, $p < 0.005$, (Student's *t* test).

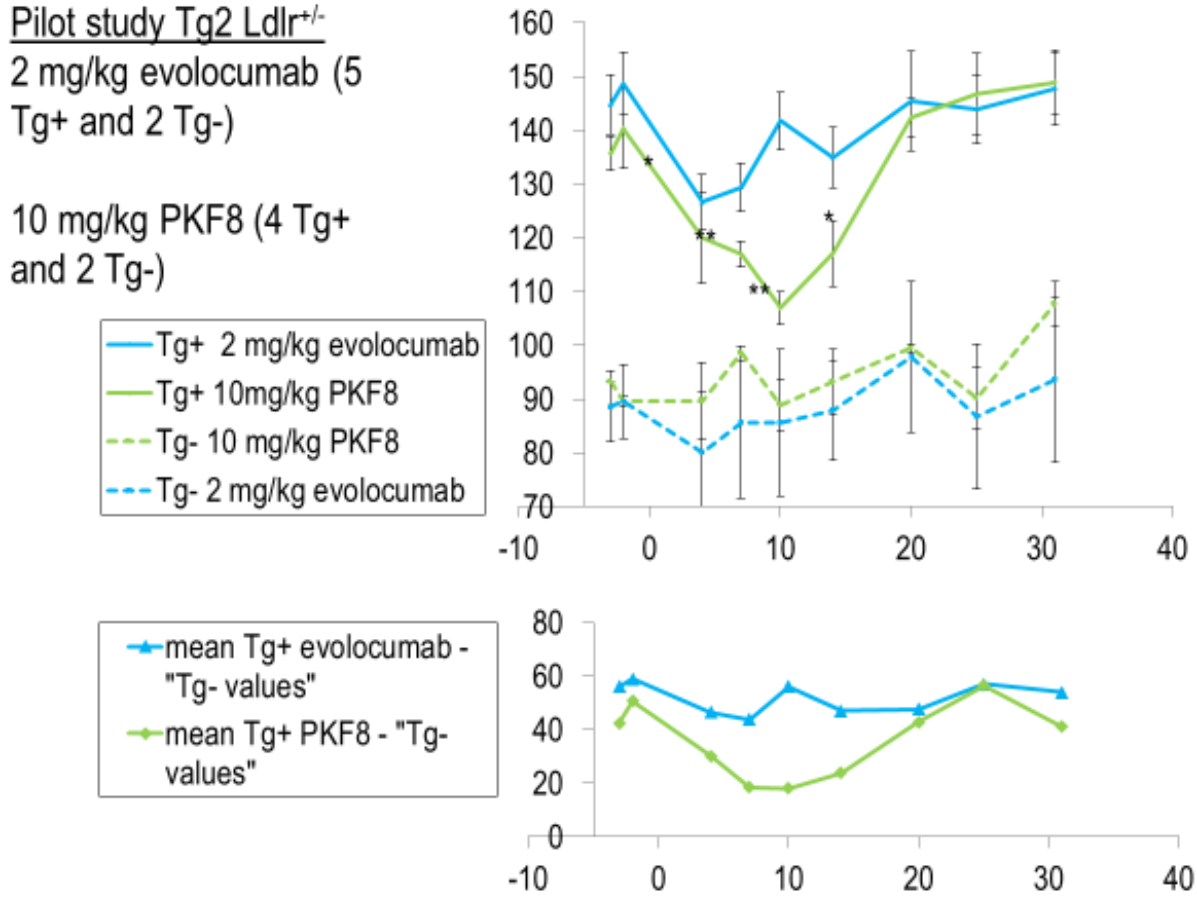

Appendix A4. Pilot study: injection of Tg0 and Tg2 mice with P1.40-mFc and P2.57-mFc. 3 mice per group were injected with 10 mg/kg P1.40-mFc or P2.57-mFc. Blood was collected 10 days before the injections and 1h and 4 days post-injection. apoB levels were determined by ELISA (upper table). Livers were collected 4 days post-injection, lysed and subjected to WB using mLDLR and β-actin antibodies (lower pannel).

Time before (-) or after (+) injection	- 10 days		+ 1h		+ 96h		
Mouse genotype	Tg2	Tg0	Tg2	Tg0	Tg2	Tg0	
apoB plasma concentration (ng/ml)	136	77	119	83	97	65	P1.40
	121	80	133	71	114	88	P2.57